

UNIVERSITY
OF TASMANIA

**Synthesis and characterisation of
aurothiosulfate-selective magnetic ion
exchange resins**

By Elijah Michael Marshall BSc(Hons)

Submitted in the fulfilment of the requirements of the degree of

Doctor of Philosophy

School of Chemistry, University of Tasmania, September 2010

Declaration

To the best of my knowledge, this thesis contains no material which has been accepted for a degree or diploma by the University or any other institution, except by way of background information and duly acknowledged in the thesis, and to the best of my knowledge and belief no material previously published or written by another person except where due acknowledgement is made in the text of the thesis, nor does the thesis contain any material that infringes copyright



30/8/10

Elijah Marshall

Statement of Access

This thesis is not to be made available for loan or copying for two years following the date this statement was signed. Following that time the thesis may be reproduced, archived, and communicated in any material form in whole or in part by the University of Tasmania or its agents, and may be made available for loan and copying in accordance with the Copyright Act 1968.



30/8/10

Elijah Marshall

Acknowledgements

Firstly, I would like thank my parents, Michael and Liz Marshall for starting me on this course many years ago. I never dreamed I'd end up like this. I would also like to thank Lee and John Anderson for the many years of kindness and support that made this rough journey a little smoother.

I like to thank my supervisors, Dr Greg Dicinoski and Prof Paul Haddad for many hours of labour and support over the years this PhD has taken. I would also like to thank them for their faith in my ability to complete this work, even when I thought it was pointless.

I would also like to thank the tireless researchers of the Document Delivery Service of the Library at the University of Tasmania, the brilliant minds and bottomless knowledge of the Central Science Laboratory and the support and kindness of the School of Chemistry.

Special thanks are required for Mr Murray Frith, for maintenance of mental health and Prof Brian Yates, for always having time to listen and for excellent advice and guidance.

I would also like to acknowledge the support and assistance of the members of the ACROSS group, for always having that one piece of information that cracked the impenetrable wall and allowed progress to continue.

I would like to acknowledge the contribution to this thesis made by the brewers and winemakers of Australia, for without them, sanity would have fled long ago. I would also like to thank the many authors who provided a small volume of imagination that I could hide away in when things got rough, especially John Scalzi, Neil Gaiman, Douglas Adams, Terry Pratchett and J.R.R. Tolkien.

I would like to dedicate this work to my wife, Rachel Anderson, for without her, it would never have happened and I'd always be wondering whether I could. I guess I can.

Abstract

A series of novel ion-exchange resins was prepared based upon the commercial Magnetic Ion Exchange (MIEXTM) substrate produced by Orica Watercare for the selective adsorption and removal of aurothiosulfate from ammoniacal thiosulfate leach liquors. Gold adsorption by these resins was ascertained using bottle-roll tests both from water and from a synthetic thiosulfate leach solution. Elution of aurothiosulfate from these resins was examined using a variety of eluents and used to narrow the set of prospective resins.

A common synthetic method was utilised, based upon amination using primary, secondary and tertiary amines of the terminal epoxide group present on the MIEXTM substrate using an aqueous solvent. The weak-base resins formed were then dried and solvated in dimethylformamide, followed by alkylation employing a variety of alkyl halides to form quaternary ammonium moieties. Several structurally-related derivatives of imidazole, piperidine, piperazine and diethylamine were prepared with ion-exchange capacities ranging between 0.5 and 1.5mmol/g, dependent on the steric nature of the amine.

The strong-base functionalised resins formed by initial amination and alkylation of weak-base groups were then characterised by ion-exchange capacity determination, elemental analysis and attenuated-total-reflectance infrared spectroscopy with results from each of the techniques being comparable. The resin substrate was also characterised using BET surface area analysis and scanning electron microscopy, with surface areas ranging between 40-47m²/g.

The performance of the resins was compared using a synthetic thiosulfate leach solution (pH~10.5) containing gold (20ppm), copper (200ppm), ammonia (1.3M) and thiosulfate (0.1M), with resin gold loadings of aurothiosulfate ranging between 14 and 124g/kg.

Elution studies were performed using acidic thiourea, basic thiocyanate and concentrated nitrate solutions, with all resins showing efficient elution of aurothiosulfate utilising one or more of the elution regimes, with typical efficiencies in the range of 30 to 75% elution.

The performance of a subset of resins was assessed by the sequential addition of small amounts of trithionate to assess the selective nature of the resins against a significant competitor ion. The best performing resins retained over 75% of the previously adsorbed aurothiosulfate when exposed to 10mM trithionate. Resins were also assessed for their permanent binding of the aurothiosulfate complex by repeated uptake/elution/regeneration studies utilising basic thiocyanate elution, followed by regeneration with ferric nitrate. The optimal resins tested eluted 63-78% aurothiosulfate over 5 cycles. Resins completing this testing were then destructively analysed for aurothiosulfate retained between elution cycles, with optimum resins retaining less than 1mg Au over 5 cycles.

The following alkylamine functionalised ion-exchange resins were determined to be viable industrial candidates, including *N*-methyl-piperidine, *N,N*-dimethyl-piperazine, methyl-diethylamine and piperidine-ethanol-based resins. Of these, *N*-methyl-piperidine showed the most selective uptake of aurothiosulfate from leach solution, coupled with the most efficient elution using the regime tested and is the most likely candidate for further study.

Table of Contents

Declarationii

Statement of Access.....ii

Acknowledgements.....iii

Abstractiv

Table of Contentsvi

List of Abbreviationsxii

List of Figuresxiii

List of Tables.....xvi

1 Introduction and Literature Review..... 1

1.1 History of gold extraction..... 1

1.1.1 Pre-cyanide..... 1

1.2 Cyanidation 5

1.2.1 History 5

1.2.2 Mechanism..... 6

1.2.3 Adsorption/solution concentration 7

1.2.4 Issues with cyanidation 16

1.3 Thiosulfate leaching 18

1.3.1 History 19

1.3.2 Mechanism..... 19

1.3.3 Problems 23

1.4	Ion-exchange resins	27
1.4.1	Cyanide-selective resins	27
1.4.2	Thiosulfate-selective resins.....	28
1.4.3	Resin-in-pulp/resin-in-leach.....	33
1.5	MIEX substrate	35
1.6	Conclusions	36
1.6.1	Research aims	37
1.7	References.....	39
2	General Experimental	48
2.1	Introduction	48
2.2	General synthetic procedure and equipment.....	48
2.2.1	Reagent purity and sources.....	48
2.2.2	Resin drying and preparation.....	48
2.2.3	Epoxide capacity testing of resins	49
2.2.4	Ion-exchange capacity testing of resins both via manual and auto-titration	50
2.2.5	Infra-red instrumentation and methods.....	51
2.2.6	Atomic absorption spectrophotometric instrumentation, optimisation and methods.....	51
2.2.7	Trithionate synthesis and characterisation (Ion-exchange and photometric)	57
2.2.8	Gold leach preparation	61
2.2.9	Gold uptake methods.....	65
2.2.10	Gold elution methods	66
2.2.11	Gold selectivity testing via trithionate competition	69

2.2.12	Gold saturation testing	70
2.2.13	Resin microanalysis preparation and testing	71
2.2.14	Resin destruction testing	71
2.3	References.....	72
3	Resin Synthesis and Characterisation	75
3.1	Introduction	75
3.2	Resin synthesis	76
3.2.1	Single step resin synthesis and variations	76
3.2.2	Multi-step resin synthesis, including variations	79
3.2.3	Resin backbone IR vibrations	79
3.2.4	Elemental Analysis	80
3.2.5	Trimethylamine (TMA)	80
3.2.6	Triethylamine (TEA).....	81
3.2.7	Tributylamine (TBA)	82
3.2.8	Diethanolamine (DAM)	83
3.2.9	Diethylamine (DEA).....	83
3.2.10	2-Piperidine-methanol (2PM)	84
3.2.11	Piperidine-ethanol (PET)	84
3.2.12	Piperidine (PIP).....	85
3.2.13	N-methyl piperidine (NIP)	86
3.2.14	Piperazine (PAZ)	86
3.2.15	N-methyl piperazine (NAZ).....	87

3.2.16	Quinuclidine (QNU)	88
3.2.17	Imidazole (IMZ)	89
3.2.18	Methyl-imidazole (MIM)	90
3.2.19	Ethyl-imidazole (EIM)	91
3.2.20	1-propyl-imidazole (1PIM)	92
3.2.21	2-propyl-imidazole (2PIM)	93
3.2.22	Benzyl-imidazole (BIM)	94
3.2.23	Methyl-piperidine (MIP).....	95
3.2.24	N,N dimethyl-piperazine (MAZ)	96
3.2.25	Methyl 2 piperidine methanol (M2PM)	98
3.2.26	Methyl-diethylamine (MDM)	99
3.2.27	1-propyl-diethylamine (1PDM)	100
3.3	Resin characterisation	100
3.3.1	Surface area and porosimetry analysis	101
3.3.2	Scanning electron microscopy	102
3.3.3	Particle size analysis	103
3.4	Conclusions	106
3.5	References.....	107
4	Screening of resins	108
4.1	Introduction	108
4.2	Gold uptake testing of resins	108
4.2.1	Gold uptake results in varying matrices.....	109

4.3	Gold elution testing of resins	119
4.3.1	Elution using acidic thiourea	120
4.3.2	Elution using basic thiocyanate.....	124
4.3.3	Elution using nitrate	127
4.3.4	Conclusions	130
4.4	References.....	133
5	Further resin evaluation.....	135
5.1	Introduction	135
5.1.1	Trithionate competition testing results	135
5.1.2	Gold saturation testing results.....	140
5.2	Resin cycling results	143
5.2.1	Basic thiocyanate elution cycling results	144
5.3	Kinetic studies	148
5.3.1	Resin preparation and temperature selection.....	148
5.3.2	Results, analysis and discussion	148
5.4	Thermodynamic studies.....	152
5.5	Conclusions	155
5.5.1	Resin cycling results	155
5.5.2	Kinetics and thermodynamics studies	157
5.5.3	Resin selection	158
5.6	References.....	159
6	Conclusions	160

6.1	Introduction	160
6.2	Resin recommendations and proposals.....	160
6.2.1	Problematic resin syntheses	160
6.2.2	Possible correlations between structural characteristics of resins and performance	162
6.2.3	Selection of optimal resin systems from uptake/elution/regeneration testing and kinetic experimentation.....	162
6.3	Possible further work and development.....	167
6.3.1	Optimisation of the synthetic method.....	167
6.3.2	Resin strengthening and use in actual leach environments	167
6.3.3	Development and optimisation of elution/regeneration process	167
6.3.4	Development of single solvent synthetic method	168
6.3.5	Integration of MIEX-Au resins into working RIP/RIL process	169
6.4	References.....	170
Appendix A	Resin correlation table	A-1
Appendix B	Elution performances of all resins	B-1
Appendix C	Scanning electron micrographs of resin beads	C-1

List of Abbreviations

1PDM	1-propyl-diethylamine	MAZ	N,N-dimethyl-piperazine
1PIM	1-propyl-imidazole	MDM	Methyl-diethylamine
2PIM	2-propyl-imidazole	meq_x	milliequivalents of component x
2PM	2-piperidine methanol	mg	milligrams
AARL	Anglo-American Research Laboratories	MIBK	Methyl isobutyl ketone
AAS	Atomic absorption spectrophotometry	MIEX	Magnetic Ion Exchange resin
ATR	Attenuated total reflectance infrared spectroscopy	MIM	Methyl imidazole
BET	Brunauer, Emmet, Teller surface area analysis	MIP	N-methyl-piperidine
BIM	Benzyl imidazole	mmol	millimoles
CCD	Charge-coupled device	NAZ	N-methyl-piperazine
CIC	Carbon-in-columns	NIP	N-methyl-piperidine
CIL	Carbon-in-leach	nm	nanometres
CIP	Carbon-in-pulp	oz	ounces
DBBP	di-n-butyl phosphonate	PAZ	Piperazine
DEA	Diethylamine	PET	Piperidine ethanol
DEM	Diethanolamine	PIP	Piperidine
DMF	dimethylformamide	ppm	parts per million
EA	Elemental analysis	QNU	Quinuclidine
EIM	Ethyl imidazole	RIL	Resin-in-leach
eq_x	Equivalents of component x	RIP	Resin-in-pulp
ESEM	Environmental Scanning Electron Microscope	SEM	Scanning electron microscope/microscopy
g	grams	SX	Solvent extration
HCN	Hydrogen cyanide	TBA	Tributylamine
IMZ	Imidazole	TBP	Tri-n-butyl phosphate
IR	Infra-red spectroscopy	TEA	Triethylamine
M2PM	Methyl-2-piperidine methanol	TMA	Trimethylamine
		WAD	Weak-acid dissociable cyanide complexes

List of Figures

Figure 1.1 Hybridisation of gold(I) orbitals ^{96, 97}	20
Figure 1.2 E_h -pH diagram for the $\text{Au-NH}_3\text{-S}_2\text{O}_3^{2-}\text{-H}_2\text{O}$ system ¹⁰³	22
Figure 1.3 Schematic of gold dissolution in ammoniacal thiosulfate leach solutions ¹⁰⁵	23
Figure 1.4 Mintek Grootvlei resin-in-pulp plant ⁷	34
Figure 2.2 Comparison of 5% HCl and ammoniacal thiosulfate leach matrix effects at 242.8nm... 54	
Figure 3.1 Particle size analysis of MIEX-DOC resin	104
Figure 3.2 Particle size analysis of unfunctionalised resin	104
Figure 3.3 EIM overall view of resins	105
Figure 3.4 MIEX Dry 1 overall view	105
Figure 3.5 MIEX Dry 2 overall view	105
Figure 3.6 MIEX Dry 3 overall view	105
Figure 3.7 MIEX Dry 4 overall view	105
Figure 3.8 MIEX Dry 5 overall view	105
Figure 4.1 Gold uptake over 24 h for initial resins at room temperature (~23°C)	110
Figure 4.2 Gold uptake over 24 h for extended resins at 30°C	111
Figure 4.3 Gold uptake for extended resins at 30°C	113
Figure 4.4 Trithionate production over 24 hours for synthetic leach solutions	114
Figure 4.5 Polythionate production in blank solution.....	115
Figure 4.6 Gold uptake in synthetic leach at room temperature	116
Figure 4.11 Basic thiocyanate elution profile 2.....	126
Figure 4.12 2M sodium nitrate elution for imidazole resins at room temperature	128
Figure 5.1 Trithionate analysis of synthetic leach solution.....	137
Figure 5.2 Trithionate competition testing results 1	138
Figure 5.3 Trithionate competition testing results 2	138

Figure 5.5 Aurothiosulfate uptake results for selected resins at 30°C	142
Figure 5.6 MIP 5 cycle elution profile	145
Figure 5.7 Plot of $\ln [Au]$ vs time (min) for resins studied	150
Figure 5.8 Plot of $\ln [Au]$ vs time (min) for N-methyl-piperidine (MIP)	150
Figure 5.9 Plot of $1/[Au]_t - 1/[Au]_0$ vs time (min) for selected resins.....	151
Figure 5.10 Plot of $1/[Au]_t - 1/[Au]_0$ vs time (min) for N-methyl-piperidine (MIP).....	151
Figure 5.11 Initial enthalpy of adsorption results for MIM, BIM and EIM	152
Figure 5.12 Enthalpy of adsorption results for PET and TEA	153
Figure 5.13 Enthalpy of adsorption results for MAZ, MIP and MDM	153
Figure B 1 PET Elution performance over 5 cycles.....	B-1
Figure B 2 BIM Elution performance over 5 cycles	B-1
Figure B 3 EIM Elution performance over 5 cycles	B-2
Figure B 4 TEA Elution performance over 5 cycles.....	B-2
Figure B 5 MIM Elution performance over 5 cycles	B-3
Figure B 6 QNU Elution performance over 5 cycles	B-3
Figure B 7 1PDM Elution performance over 5 cycles.....	B-4
Figure B 8 MAZ Elution performance over 5 cycles	B-4
Figure B 9 MDM Elution performance over 5 cycles	B-5
Figure B 10 MIP Elution performance over 5 cycles	B-5
Figure C 1 EIM overall view of resins	C-1
Figure C 2 MIEX Drying 1 overall view	C-1
Figure C 3 MIEX Drying 2 overall view	C-1
Figure C 4 MIEX Drying 3 overall view	C-1
Figure C 5 MIEX Drying 4 overall view	C-1
Figure C 6 MIEX Drying 5 overall view	C-1
Figure C 7 EIM detail of bead surface	C-2

Figure C 8 MIEX Drying 1 detail..... C-2

Figure C 9 MIEX Drying 2 detail of bead surface..... C-2

Figure C 10 MIEX Drying 3 detail of bead surface..... C-2

Figure C 11 MIEX Drying 4 large bead..... C-2

Figure C 12 MIEX Drying 5 large bead..... C-2

Figure C 13 EIM cracked conjoined bead..... C-3

Figure C 14 MIEX Drying 1 cracked bead C-3

Figure C 15 MIEX Drying 3 cracked bead C-3

Figure C 16 MIEX Drying 4 cracked bead C-3

Figure C 17 MIEX Drying 5 bead fragments C-3

Figure C 18 MIEX Drying 5 bead fragments C-3

List of Tables

Table 1-1 Stability constants for gold complexes ⁸⁶	21
Table 1-2 Basic functional group structures	39
Table 2-1 Gold detection parameters for Varian AAS instrumentation	52
Table 2-2 Preparation of gold standards in 5% HCl matrix	52
Table 2-3 Au standards in ammoniacal thiosulfate leach	53
Table 2-4 Calibration factors for [Au] in ammoniacal leach matrices.....	55
Table 2-5 Preparation of polythionate standards.....	61
Table 2-6 Development of thiosulfate leaching ³⁶	63
Table 2-8 Sampling intervals for bottle roll tests	66
Table 2-9 Sampling and trithionate addition procedure	70
Table 2-10 Sampling intervals for aurothiosulfate saturation testing	71
Table 3-1 Resin functionalisation mixture with cyclohexanol	77
Table 3-2 Resin functionalisation mixture without cyclohexanol.....	77
Table 3-3 BET surface area data for repeated drying of resins.....	102
Table 3-4 Resin ion-exchange summary	106
Table 4-4 Leach gold uptake mass balance summary 1.....	117
Table 4-5 Standard bottle roll artificial leach concentrations and molar ratios.....	117
Table 4-7 Elution results for imidazole and methyl-diethylamine resins	122
Table 4-8 Elution results for ring and cage alkylamines	124
Table 4-9 Basic thiocyanate elution results 1	126
Table 4-10 Basic thiocyanate elution results 2	127
Table 4-12 2M nitrate elution results for alkylamine resins.....	130
Table 5-2 Gold mass balance calculations for selected resins at 30°C	142
Table 5-3 Gold mass balance calculations for selected resins at 30°C	143

Table 5-5 Resin digestion results	147
Table 5-6 Resin gold stoichiometry at 50°C	154
Table 5-7 Resin enthalpy calculation results.....	155
Table 5-8 Maximum elution of adsorbed aurothiosulfate.....	156
Table 5-9 Minimum retention of adsorbed aurothiosulfate after 5 uptake/elution cycles	157
Table 6-1 Selection of industrially applicable resins	165

1 Introduction and Literature Review

1.1 History of gold extraction

1.1.1 Pre-cyanide

Along with copper, silver, platinum, arsenic, tin, zinc and bismuth, gold is one of the few metals able to be found in its natural state¹. As such, it has had a long history of use and abuse by mankind. Due to its softness and malleability, gold was one of the first metals to be worked with tools and due to its lustre and colour it was used for jewellery and ornamentation from the Chalcolithic or Copper Age onwards. Artifacts appear around 4000BC in the Balkans such as those found in the Varna Necropolis² which was considered to be one of the oldest metal-using cultures in the world. Egyptian use of gold was restricted to the nobility, with one notable lover of the metal being the Pharaoh Hatshepsut. From 1470 to 1458BC, this impressive woman forged trade networks, commissioned major building projects, was fond of gilding her face with a mixture of silver and gold and was responsible for the construction of two granite obelisks 100 feet high in Karnak. These massive monuments to Amon Re, the god of Thebes, were originally to be made of gold, however they were constructed in granite with gold peaks³. Most of the gold in biblical and Ancient Egyptian times was mined from the southern Egyptian region of Nubia, taking its name from nub, the Egyptian word for gold. Mining techniques in Nubia were a combination of alluvial and underground methods, with the Turin papyrus from 1150BC showing “bekhen-stone” quarrying centred on Wadi Hammamat and the gold mines at Bir Umm Fawakhir^{4,5}. Bekhen-stone is a grey-green metagraywacke siltstone and mudstone and was used for ornamental sculpture, with Wadi Hammamat being the only source⁵. Occupational health and safety were not concerns, with reports from the Greek historian and doctor Diodorus around 60BC of the horrific conditions suffered by the slave labourers at the time³. The same author in his *Bibliotheca historica* describes the use of fire-setting, or heating the rock face with fire followed by quench

fragmentation to liberate the entrained gold from the quartz. This technique also liberated arsenic, slowly poisoning any who inhaled the vapours³.

Several legends surround the acquisition of gold. El Dorado, the touch of King Midas and Blackbeard's gold are all additions to the tales surrounding the metal, however one of the most well-known legends concerning gold is that of Jason and the Argonauts. According to Appolonius Rhodius, a 3rd Century Alexandrian BC poet, Pelias, the half-brother of Aeson, the rightful king of Iolcus wanted to dispose of Aeson's son, Jason⁶. Jason was set the task of retrieving the Golden Fleece, the fleece of the winged ram, Chrysomallos. After many misadventures, Jason arrived in Colchis⁶, on the Black Sea in modern Georgia. At the time, gold was extracted from alluvial placer deposits by rubbing oils into fleeces then immersing them in streambeds⁷ and may be fleece referred to in the legend⁸.

Gold as coinage was first used by Egyptian Pharaohs around 2700BC, however these were not used for commerce. According to the histories of Herodotus, the people of Lydia, now in modern Turkey, were the first to issue gold coinage for general circulation around 560BC⁹.

Roman gold mining and extraction methods were used across Europe with the best examples being illustrated at the Bronze Age Dolaucothi gold mines in Britain. Mining practices were advanced for the time, using Archimedes screws, water wheels, fire-setting and hydraulic mining^{7, 8}. Despite the advanced technology, conditions for the slave mine workers had not improved⁸. According to *Naturalis Historia* by Pliny the Elder, the use of mercury for the amalgamation and refining of gold was known and used at the time¹⁰. Mining activity in Europe collapsed along with the Roman Empire until a revival in the 11th Century in Central Europe in the Harz Mountains⁷. The publication of *De re metallica* by Georg Bauer, better known as Georgius Agricola, in 1556 gave a history of mining, metallurgical and assaying practice through to the 16th Century⁸.

Following the Spanish *conquistador* era of expansion into Mexico in the early 1500s, expansion by the Spanish into Peru, Bolivia and Columbia in the 1550s brought the end of the Inca Empire. Along with 'civilisation', the Spanish brought European metallurgical practices for gold extraction, however the most commonly used extraction methods at the time were primitive, cheap and labour-intensive⁷, allowing for South American gold to be sold cheaper in Europe, including the cost of transportation. A curiosity of the Columbian gold ore at the time was the inclusion of platinum, unknown to Spanish and European metallurgists. The first European reference to platinum is in 1557 in the writings of Julius Caesar Scaliger, an Italian humanist as an unknown noble metal found between Darién and Mexico 'which no fire or Spanish artifice has been able to liquefy.'¹¹ The included platinum was considered an impurity ('platina' in Spanish is 'little silver') and the Spanish treasury ordered this 'unripe' gold to be discarded into the sea¹¹.

Gold fever was common in the 1800s with several gold rushes in California, South America, New Zealand and Australia. The California gold rush began on January 24, 1848 following the discovery of gold in the American River at Sutter's Mill by James W. Marshall¹². Gold grades were so high in the initial part of the rush that gravity separation techniques were as simple as tossing sands and gravels in a blanket⁷. Panning techniques were common but were soon replaced by larger scale techniques such as 'cradles', 'rockers', and 'long toms'⁷ however, once surface alluvial deposits were exhausted, underground mining was implemented. Similar deposits were discovered in Alaska, Colorado, Montana, Idaho, Nevada and South Dakota in the United States and in British Columbia in Canada⁷. The Australian gold rush began in 1851 with the discovery by Edward Hammond Hargreaves of gold near Bathurst, New South Wales¹². Due to little water being available, gravity methods of separation such as those listed in California were not suitable for use⁷. The major gold exploration success of the 1800s was the discovery of gold in the Witwatersrand basin of South Africa in 1886⁷ and despite the gold

rushes of Yukon and Nome, Alaska in 1897 and 1898 respectively, underground mining became the foremost method of ore extraction.

Hydrometallurgical methods were not known at the time and despite advances in gravity and amalgamation technologies, the difficulty for gravity methods to extract fine gold from ores or sulfide associated gold prompted the development of technologies capable of extracting gold from these ores. The discovery of chlorine by Carl Wilhelm Scheele in 1774 and the subsequent development of a chlorination process by Plattner in 1848¹³ allowed the extraction of gold by flowing chlorine over gold ores, forming water-soluble gold chloride. The addition of ferrous sulfate, hydrogen sulfide or charcoal then precipitated the dissolved gold, making it available for smelting. This process was used in the United States, South Africa and Australia as a supplement to gravity concentration or treatment of sulfide-rich ores⁷. In early pyrometallurgy, several techniques dominated the recovery of gold. From its discovery, gold-rich mercury was retorted to remove mercury and the resultant sponge gold was then smelted with fluxes for bullion production⁷. Likewise, gravity concentrates containing magnetite, ilmenite, chromite and other heavy metals were smelted with potash (potassium carbonate), borax (sodium borate) and nitre (potassium nitrate) for contaminant removal.

Throughout the 19th Century, pyrometallurgical methods were used to treat various high-grade auriferous silver, lead and copper ores including using direct fusion in a bath of lead, direct smelting with lead-rich fluxes, and smelting with fluxes for matte formation followed by resmelting with lead-rich fluxes^{7, 14}. In each case, the precious metals formed lead-gold-silver alloys in a similar manner to fire assaying. The products were then cupelled for lead removal leaving a precious metal alloy. This was then treated by one of the following methods

- Nitric acid dissolution of silver leaving gold residue

- Formation of silver sulfide by smelting with sulfur, pyrite or a mixture of antimony sulfide, sulfur and litharge to produce silver sulfide and gold-silver alloy. This was then treated as above.
- Chlorination to remove silver as insoluble silver chloride and removing gold as soluble gold chloride
- Electrolytic refining in a potassium cyanide bath

These processes dominated gold refining in Germany, Hungary and central Europe¹⁴.

1.2 Cyanidation

Since its development in 1887, the use of aerated cyanide solutions has become the most popular and widespread method for the hydrometallurgical extraction of gold from ore-bodies worldwide.

1.2.1 History

The dissolution of gold in cyanide solutions was investigated by Elsner in 1846¹⁵, despite observations being reported by previous researchers such as Scheele in 1793¹⁶ and patents on the use of cyanide baths for electroplating being held by Elkington⁷. The cyanide process for gold extraction was patented between 1887 and 1888 by MacArthur and the Forrest brothers¹⁷, and was rapidly developed into a commercial process that was first used at the Crown Mine in New Zealand in 1889¹⁸. The development of the cyanidation process was instrumental in the exploitation of the deeper, lower-grade Witwatersrand ores, as the gold was present as fine-grained particles within the host rock. Cyanidation coupled with zinc cementation, also known as the Merrill-Crowe process, increased yields from this area from less than 300,000oz in 1888 to more than 3 million oz in 1898¹⁹, and several reviews have been published on the hydrometallurgy of gold in South Africa¹⁹⁻²¹.

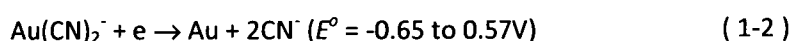
1.2.2 Mechanism

Elsner developed the equation shown in Equation (1-1)¹⁵, however this equation infers that the site of anodic reaction is identical to that of cathodic reaction. Despite this, Elsner's equation is still quoted in modern texts today²².

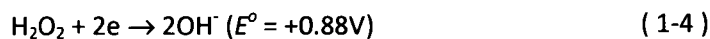
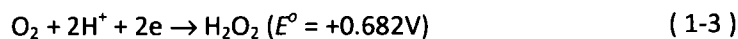


A more accurate representation of the reaction between alkaline cyanide solutions and metallic gold is given by Equations (1-2) to (1-6)⁷.

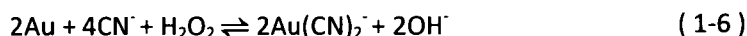
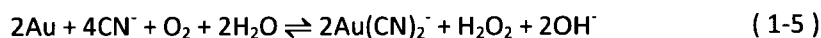
Anodic half reaction



Cathodic reactions



Overall reactions



Several factors influence the rate of gold lixiviation by alkaline cyanide, namely cyanide and oxygen concentration, temperature, solution pH, gold surface area exposure, agitation, gold purity and the presence of other ions in solution. Increased cyanide and oxygen concentration²³ in solution increase the rate at which gold is dissolved, as does increasing temperature up to a maximum of 85°C⁷. A decrease in pH slows the rate of gold lixiviation as more of the cyanide ions will be volatilised from the solution as HCN as opposed to forming aurocyanide complexes²⁴. Studies have shown that HCN will not leach gold at rates fast enough to competitive with CN⁻²⁴. The dissolution rate of gold is directly proportional to the surface area exposed in solution, therefore a finely ground ore will result in an increase in the rate of gold dissolution. However, cyanide concentration in solution decreases as other cyanide-consuming mineral components are made more accessible to the leaching solution²². There is a pronounced increase in the rate of gold

dissolution both from impurities in the gold grains and other ions in solution, especially lead and mercury^{25, 26}. The presence of sulfide minerals has the effect of either increasing or slowing the rate of gold dissolution through the formation of galvanic interactions. Chalcopyrite and chalcocite slow and cease gold dissolution respectively, whereas other sulfides increase the rate of dissolution²⁷. Further discussion regarding mineralogies that affect the rate of dissolution of gold will be covered in Section 1.2.4.2, while more detailed analyses on the mechanistic interpretation of silver, lead, sulfide and carbonaceous matter may be found in the literature²⁸.

1.2.3 Adsorption/solution concentration

Once dissolution of gold has occurred, the volume of solution and therefore the concentration of gold in the solution needs to be increased to allow for efficient recovery of the precious metal. Various methods have been developed for achieving this and a brief discussion of the more common is detailed in this section.

1.2.3.1 *Precipitation – Merrill Crowe process*

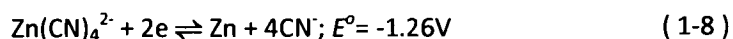
Precious metal recovery from solution via the addition of zinc dust has been in use since the late 1800s. First patented by Salman and Pritchard, in 1897 it was applied to the Homestake operation at Lead, South Dakota by C.W. Merrill²⁹. Refinement of the process using T.B Crowe's application of a vacuum deaerator in 1916²⁹ saw the Merrill-Crowe process as it became known gain application worldwide. The Merrill-Crowe process has developed into a highly efficient gold recovery process, reporting recoveries from solution usually >98% and occasionally as high as 99.5%⁷. The anodic, cathodic and overall reactions are given in Equations (1-7 to (1-10 and although at first glance simplification of the equation is possible through elimination of 4CN^- from both sides of the equation, this implies the site of gold cementation and zinc dissolution are identical. Literature has suggested that these processes may not occur with close physical proximity^{7, 29}. The cementation reaction proceeds via the following steps in cyanide solution:

- Mass transport of Au(I) cyanide and free cyanide species to the zinc surface from bulk solution
- Adsorption of Au(I) cyanide and free cyanide species to zinc surface
- Electron transfer between Au(I) and zinc along with simultaneous dissociation of Au(I) cyanide and formation of zinc cyanide
- Desorption of zinc cyanide species from zinc surface
- Mass transfer of zinc cyanide species into bulk solution

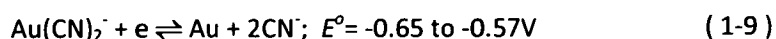
Confirmation of the mass transport mechanism has been reported in the literature³⁰ with one report of lower gold concentrations (80g/L Au) forming a porous gold product around the metallic zinc, while higher gold concentrations (640g/L Au) form a dense, non-porous product³¹. Increases in temperature increase the rate of zinc dissolution and hydrogen evolution along with a commensurate decrease in gold recovery³¹. It has also been found that the cyanide concentration has little effect on the precipitation rate unless it falls below a threshold dependent on solution pH and gold concentration³⁰⁻³². Addition of lead has been shown to reduce zinc consumption and increase gold cementation efficiency³⁰.

33

Anodic reactions



Cathodic reaction



Overall reactions



1.2.3.2 Solvent extraction

Solvent extraction (SX) has been applied industrially for the separation of gold, platinum group and base metals³⁴ and forms the basis for an established analytical technique for assaying low gold concentrations using methyl-iso-butyl ketone(MIBK)³⁵. Solvent

extraction uses suitable liquid organic extractants to selectively remove gold from aqueous solutions. Commonly this is performed by the dissolution of a chemical species containing a gold-selective functional group in a water-immiscible organic solvent, such as kerosene. Gold recovery from the loaded extractant is achieved either directly by precipitation or electrolysis, or indirectly by stripping the gold from solvent back into an aqueous phase for other recovery methods.

A major disadvantage of solvent extraction is that it must be applied either to clarified solutions or the solvent must be contained and separated from solid components of an unclarified leach solution or slurry due to production of a crud layer at the aqueous-organic interface. This causes a loss of extraction efficiency and limits the application of solvent extraction in industry. Solvent extraction systems can be grouped into two categories, being extraction by ion solvation and extraction by ion-exchange.

1.2.3.2.1 Ion solvation

Ion solvation solvent extraction of gold involves the replacement of the water of solvation around a metal ion in solution with an extractant molecule, thereby enabling partition into the organic phase. Suitable extractants contain either phosphorus or oxygen and current literature suggests that gold complexes are extracted as ion-pairs, i.e.

$M^{n+}[Au(CN)_2]_n$, in a similar manner to adsorption onto activated carbon³³. Ethers such as glycol dibutyl ether have been shown to have good selectivity for gold over platinum group and base metals³⁶, combined with low flash point and vapour pressure, however its water solubility results in losses of gold to the aqueous phase³⁶. Molecules with phosphorus-containing functional groups have also shown efficacy in extraction of gold from alkaline cyanide solutions^{37, 38}. Examples such as tri-*n*-butyl phosphate (TBP) and di-*n*-butyl phosphonate (DBBP) have been used, however due to their high densities, phase separation is poor, resulting in inadequate mixing. As such, these extractants are

commonly used with an amine to reduce their density. A scheme generating 99.99% pure gold using TBP has been proposed, showing selectivity for gold over nickel, cobalt, iron and zinc but not copper or silver. This process includes a scrubbing step to remove co-extracted copper and silver producing a gold-bearing organic phase suitable for electrowinning or direct reduction³⁹.

1.2.3.2.2 Ion exchange

Solvent extraction by ion-exchange occurs in a similar manner to ion-exchange using resins in that metal ions or complexes are adsorbed onto specific sites by virtue of selectivity based on the charge and steric size of the site. Due to gold cyanide complexes being anionic, primary, secondary and tertiary amines and quaternary ammonium species have been employed. Quaternary amines are the most gold-selective and hardest to elute, due to their strong-base pK_a values. Increased ease of elution and decreased gold selectivity follows the trend of decreased nitrogen substitution, i.e. tertiary > secondary > primary amines. Tertiary amines such as tridecylamine and trioctylamine have shown great promise as extractants due to selectivity for univalent ions such as $\text{Au}(\text{CN})_2^-$ over polyvalent ions such as $\text{Cu}(\text{CN})_4^{3-}$ ³⁸. Coupled with ease of elution, these trialkylamines are also promising candidates for the synthesis of gold selective ion-exchange resins. Further developments in the field have included a strong-base guanidine-based extractant, LIX 79 from the Cognis Corp., Tucson, Arizona. As the pK_a of the trialkyl-guanidine functional group used is 11.5, in more acidic solutions, the gold cyanide selective trialkyl-guanidinium functional group formed provides a strong-base-like ability to adsorb gold cyanide coupled with the ease of elution of weak-base functionalities⁴⁰⁻⁴³. Further, literature suggests that ion-exchange solvent extraction utilising a mixture of nitrogen-containing Primene JMT and phosphorus-containing Cyanex 923 can be used to preferentially transport gold cyanide across membranes⁴⁴. The Minataur process developed by Mintek for the extraction of gold chloride from chlorination leaching has

also been compared favourably with electrowinning and other solvent extraction processes.⁴⁵

1.2.3.3 *Electrowinning*

Electrowinning is the process whereby an electrolytic reaction in aqueous solution produces gold loaded electrodes or cell sludges according to Equations (1-11)to (1-13).

Cathodic reaction



Anodic reactions



Metal deposition occurs between -0.7V and -1.1V⁴⁶ with the reaction proceeding via adsorption of gold cyanide at the cathode with the subsequent reduction of the metal ion. This is followed by dissociation of the aurocyanide complex and desorption of the cyanide ion. This process is summarised by Equations (1-14) to (1-16).

Adsorption



Dissociation



At high overpotentials, electron transfer is likely to be direct, bypassing the formation of the intermediate gold(I) cyanide species. This difference causes distinct changes in the deposited gold product. Low cathodic potentials produce gold formations that are very dense and solid whereas higher potentials produce a fluffy, porous deposit which is more likely to end up as cell sludge. Formation of a sludge may be beneficial to removal of other metals such as mercury, whereas a high-density product is generally of higher purity, reducing the requirement for downstream processing.

1.2.3.4 Carbon adsorption

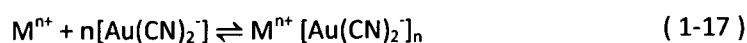
Adsorption of gold cyanide complexes onto activated carbon has become the most widely utilised method of solution concentration and purification in the gold metallurgy industry, due to its ease of gold adsorption, elution and carbon regeneration.

1.2.3.4.1 History

The patent for adsorption of gold cyanide onto activated carbon as an industrial process was granted to John MacArthur, Robert and William Forrest in 1888¹⁷ and was considered as an alternative to Merrill-Crowe precipitation in the Witwatersrand⁷. However, at the time, no technologies existed for the elution of the adsorbed gold complex, leaving no alternative but to combust the carbon and smelt the resultant ash. Further development of carbon as an adsorbent for gold cyanide complexes saw the development of a carbon-in-pulp adsorption process at the San Andreas de Copan plant in Honduras in 1949⁷ with the loaded carbon being sent to a smelter for combustion and smelting. A patent was granted by the United States to Frank McQuiston Jr. and Thomas Chapman for a carbon-in-pulp technique⁴⁷ for adsorption of gold cyanide from leach solutions. At the same time Zadra, Salisbury and Ross at the US Bureau of Mines worked to develop a process for recycling the carbon by elution of the adsorbed gold cyanide complexes⁴⁸⁻⁵⁰. The eluted gold complexes were then electrowon onto steel wool cathodes. Initial attempts at elution used a caustic sodium sulfide solution, however this failed to elute the adsorbed silver.

1.2.3.4.2 Mechanism

Several studies have shown that gold cyanide complexes adsorb onto activated carbon via the formation of an ion pair formed according to Equation (1-17)⁵¹⁻⁵⁴.



Further evidence is provided by chemical analyses, establishing that the oxidation state of gold on carbon is +1⁵⁵, with detailed experimental evidence being available in the literature^{51, 55, 56}. The rate of adsorption of gold onto activated carbon decreases with increased temperature as the process is exothermic⁵⁶, hence allowing elution of the adsorbed gold by raising the temperature. Both the equilibrium loading capacity and the rate of gold adsorption increase with increased solution gold concentration with typical loading rates of 10-100 g Au/hr/t carbon and equilibrium loadings of 5-10 kg Au/t carbon being achieved⁷. Further, both the loading rate and capacity decrease with increased cyanide concentration and is attributed to increased competition of free cyanide species for adsorption sites on the carbon⁵⁷.

1.2.3.4.3 Elution

As stated in Section 1.2.1, initial recovery methods from activated carbon involved combustion of the carbon and smelting of the ash to release the adsorbed gold. Development of the Zadra elution process^{48, 49} allowed the recycling of the adsorbent, thereby reducing the cost of carbon adsorption and making the process viable for industrial application. Additional elution regimes were developed and include the introduction of pressure as a modification to the Zadra technique, the Anglo-American Research Laboratories (AARL) elution regime and the incorporation of organic solvents and solvent distillation.

The Zadra process utilises a 1-2% sodium hydroxide/0.1% sodium cyanide solution at 95° with flow rates of 1-2 bed volumes/h. The process takes 36-72 h to elute the gold to a low residual loading (<100 g/t)^{48, 50}. However, by increasing temperature to 135-140°C and the pressure to 400-500kPa, a decrease the elution time to 8-14 hours at a flow-rate of 2 bed volumes/h can be achieved⁷. By comparison, the AARL regime utilises a pre-wash of dilute mineral acids followed by precious metal liberation using 3% cyanide and 1-2% sodium

hydroxide for 30 minutes^{7, 58}. This is then followed by elution using 6-10 bed volumes of deionised water at 110-120°C, taking advantage of the exothermic nature of gold adsorption for elution. Modification of the elution process using organic solvents has shown to be successful, with aqueous acetonitrile eluting gold cyanide in less than 8 hours at 25-70°C⁵⁹. Isopropanol, ethanol and ethylene glycol have also been reported as eluting agents for gold cyanide from activated carbon with 20% v/v isopropanol eluting >98% adsorbed gold in under 1 h at 80°C, however ethylene glycol was indicated as the most suitable eluent due to lower flammable hazards⁶⁰. Solvent distillation involves packing the gold cyanide-loaded carbon into a column, refluxing the solvent of choice through the column and collecting the eluted gold complexes. The Micron procedure involves the use of a sodium cyanide/sodium hydroxide solution as a pretreatment, followed by reflux with organic condensate⁶¹. Elution rates of 95% in 1 h with acetonitrile using reflux distillation exceeded the 90% in 6 h for both the methanol and AARL elution regimes⁶¹. Further research has indicated that the effectiveness of organic modifiers for the elution of gold from activated carbon is the order of acetonitrile > methyl ethyl ketone ≥ acetone >> dimethylformamide > ethanol⁵⁹.

1.2.3.4.4 Carbon-in-pulp/carbon-in-leach

The carbon-in-pulp (CIP) technology is a refinement of carbon adsorption of gold cyanide whereby carbon pellets or beads are introduced into the process slurry after leaching to allow for the adsorption of the gold complexes. The carbon is then pumped counter-current to the process stream with fresh carbon being introduced at the end of the process and transferred either in batches or continuously at a slower rate to the process stream. The gold concentration in solution decreases as the gold cyanide complex is adsorbed onto the carbon surface with the gold concentration in solution approaching pre-equilibrium and the counter-current flow ensures that gold complexes in the process stream encounter carbon with remaining capacity for adsorption. Carbon with the highest

loading of gold is removed from the start of the process whereas carbon with the lowest loading and highest activity occurs in the last stage, passing a barren solution to waste.

Retention of carbon between stages is via the use of interstage screens set to retain carbon but allow the passage of the leach slurry. This sets a lower limit on the carbon particle size that can be used in these processes, which can affect the rate of adsorption of the gold cyanide complex. Attempts have been made to develop an activated carbon that can be separated from the leach solution without the use of screens via magnetic separation and show both the ability to be magnetically separated from the leach solution and better adsorption rates due to smaller particle size⁶².

Carbon-in-leach (CIL) technology allows leaching and adsorption to be performed simultaneously in the same series of tanks. This process offers some advantages over CIP in lower capital costs over requiring separate leaching and adsorption tanks and can significantly improve the gold extraction in cases where the ore contains constituents that adsorb gold from the leach solution. This condition is known as 'preg-robbing' whereby the gold complexes are permanently lost to tailings or 'preg-borrowing' when the gold is liberated again later in the recovery process. The advantage in this situation is that the carbon competes with the preg-robbing or preg-borrowing constituents and preferentially adsorbs the gold complexes from solution. CIL does have some disadvantages over CIP, including a larger carbon inventory being required, in-plant gold inventory is higher and carbon attrition is greater and therefore carbon losses to tailings are higher. All of these cause operating costs to rise.

1.2.3.4.5 Carbon adsorption from non-cyanide solutions

The recovery of gold from non-cyanide solutions is an important consideration in the development of alternative leaching schemes as the chemistry of adsorption differs from

that studied for cyanide. The ability of activated carbon to adsorb gold complexes follows the sequence AuCl_4^- (as $\text{Au}_{(\text{s})}$) $>$ $\text{Au}(\text{CN})_2^-$ $>$ $\text{Au}(\text{SCN})_2^-$ $>$ $\text{Au}(\text{CS}(\text{NH}_2)_2)_2^+$ $>$ $\text{Au}(\text{S}_2\text{O}_3)_2^{3-}$ ⁵⁶.

The gold thiourea complex, $\text{Au}(\text{CS}(\text{NH}_2)_2)_2^+$, is thought to adsorb onto activated carbon without undergoing any chemical change with the mechanism believed to occur via formation and adsorption of an ion-pair⁶³, similar to that for gold cyanide. Elution of gold thiourea from activated carbon is usually performed using cyanide or sulfide eluents, whilst sodium hydroxide, sulfuric acid and hydrochloric acid have been shown to be ineffective⁶³.

Gold thiocyanate, $\text{Au}(\text{SCN})_2^-$, has been successfully adsorbed onto activated carbon and elution efficiencies of 95% have been achieved using 120g/L thiourea in 0.1-0.2M NaOH at 145-150°C⁶⁴. Further results were obtained in this study on the elution of silver thiocyanate complexes and at low concentrations, it is possible to sequentially elute silver thiocyanate followed by gold⁶⁴.

The adsorption of aurothiosulfate, $\text{Au}(\text{S}_2\text{O}_3)_2^{3-}$, onto activated carbon will be discussed in Section 1.3.3.2.

1.2.4 Issues with cyanidation

Despite the success at which cyanide has been applied to the lixiviation of gold from a variety of ore types, there are several issues related to its use, storage and disposal.

1.2.4.1 Toxicity of cyanide

One of the major environmental concerns with the use of cyanide as a lixiviant for gold is its toxicity. Hydrogen cyanide and all cyano-compounds that liberate free cyanide are highly toxic to almost all forms of fauna^{65, 66}. According to World Health Organisation guidelines for drinking water, 0.07mg/L cyanide is 'of health significance.'⁶⁷ Three forms of cyanide are measured in mine waste solutions, these being free cyanides, weak-acid-

dissociable cyanides and total cyanides. Of these, free cyanide is not persistent in the tailings environment but degrades through a variety of mechanisms to less toxic chemicals⁶⁶. Wildlife deaths have been associated with the use of tailings dams for the storage and remediation of cyanide wastes from processing despite several attempts at prevention^{66, 68}. These deaths have been due to the accumulation of weak-acid dissociable (WAD) cyanide complexes in the storage facilities. WAD cyanide concentrations below 50mg/L are deemed appropriate for wildlife protection⁶⁹, however toxicity levels vary between species and are shown to be unrelated to body size but related to diet⁶⁸. Cyanide has also been released from several tailings storage facilities worldwide, however one of the most publicised occurred on the 30th January 2000 at Baia Mare, Romania. This release was caused by a combination of rapid water influx from melting snow and heavy rains, poor tailings storage facility design and management, and a lack of planning in the event of accidental release^{66, 70-72}. This resulted in the release of around 100,000 cubic metres of tailings containing around 50 to 100 tonnes of cyanide along with copper and other heavy metals^{66, 72}.

1.2.4.2 *Refractory ore-types*

Whilst cyanidation is effective at the lixiviation of gold from most ore types, there are several types of ore that do not efficiently leach gold with cyanidation alone. These ore types are known as refractory ores and fall into one or more of the following categories⁷³:

- Pyritic ore – finely grained gold present in a pyrite matrix prevents access to cyanide during leaching and displays preg-borrowing behaviour in cyanide-deficient solutions⁷⁴
- Copper-rich ore – presence of copper in mineralogies leaches in preference to gold, increasing reagent consumption and show preg-borrowing behaviour⁷⁵

- Telluride-rich ore - Presence of gold telluride minerals reduces rate of gold leaching, increasing time taken for complete lixiviation¹⁴
- Carbonaceous ore – fine-grained organic particles compete with the adsorbent of choice in removal of gold cyanide from solution⁷⁶

Historically, most of these forms of refractory behaviour were mitigated by some form of oxidative pre-treatment such as roasting, to increase the effectiveness of cyanidation⁷.

This form of pre-treatment has disadvantages in terms of increased cost for entrapment and treatment of the by-products of the roasting process. As an alternative to pyrometallurgical oxidation of ores, bacterial oxidation of sulfide ores involves the use of mesophilic bacteria such as *Thiobacillus ferrooxidans*, *Thiobacillus thiooxidans* and *Leptospirillum ferrooxidans*^{77, 78}. These bacterial cultures oxidise the sulfide mineralogies that entrap the gold, allowing lixiviation to occur and increase the efficiencies of the cyanidation process. Notable examples of biological oxidation plants include the Ashanti (Ghana)^{7, 79}, Youanmi^{80, 81}, Wiluna^{80, 81} and Beaconsfield^{81, 82} (Australia.) Ashanti and Wiluna utilise the BIOX™ process from Gold Fields Inc⁷⁹, whereas Youanmi and Beaconsfield utilises the BacTech process from Mintek^{79, 81, 82}, with differences between the two processes related to the culture of thermophilic sulfur- and iron-oxidising bacteria used⁸³.

1.3 Thiosulfate leaching

One of the viable alternatives to the use of cyanide in gold lixiviation is the thiosulfate ion, $S_2O_3^{2-}$. Thiosulfate leaching has been a major focus as an alternative to cyanide leaching due to concerns over the environmental hazards inherent in the use of cyanide and the costs involved in waste treatment. This field has been extensively reviewed by many authors⁸⁴⁻⁹², however a large amount of knowledge has recently been contributed to the field.

1.3.1 History

Gold dissolution in oxidising thiosulfate solutions has been observed for some time^{87, 93} and the dissolution reaction was first used as the Patera process for the dissolution of silver⁹⁴. Until recently, thiosulfate was only of interest for treating refractory ore types such as those listed in Section 1.2.4.2. Thiosulfate, unlike cyanide, reacts only marginally with preg-robbing and preg-borrowing constituents of the leach. Thiosulfate solutions have been demonstrated to dissolve gold using a complex system involving an oxidant and an effective oxidant stabiliser. Despite considerable success, the major drawback to an effective thiosulfate-based process is the high reagent consumption due to thiosulfate oxidation and the lack of an effective aurothiosulfate removal mechanism from the leach solution.

1.3.2 Mechanism

Thiosulfate is a divalent, unidentate type 'A' soft ligand which binds via the terminal sulfur atom to low-spin d^8 (Pt(II), Pd(II) and Au(III)) and d^{10} (Au(I), Ag(I), Cu(I) and Hg(II)) metal ions, forming strong σ -bonds with the metal ion stabilised by $p\pi$ - $d\pi$ back-bonding⁹⁵. Formation of the linear gold(I) complex is via hybridisation of the $5d_{z^2}$ and vacant 6s orbitals, forming two hybrid orbitals with axes of electron density lying along the xy plane and z axis. Presence of the electron pair in the ψ_1 hybrid orbital will create less repulsion between the electron pair and the ligands, stabilising the overall complex. Further hybridisation of the ψ_2 hybrid orbital with $6p_z$ orbital will form two linear hybrid orbitals allowing overlap with the ligand orbitals and thereby give a linear complex^{96, 97}. This is illustrated in Figure 1.1.

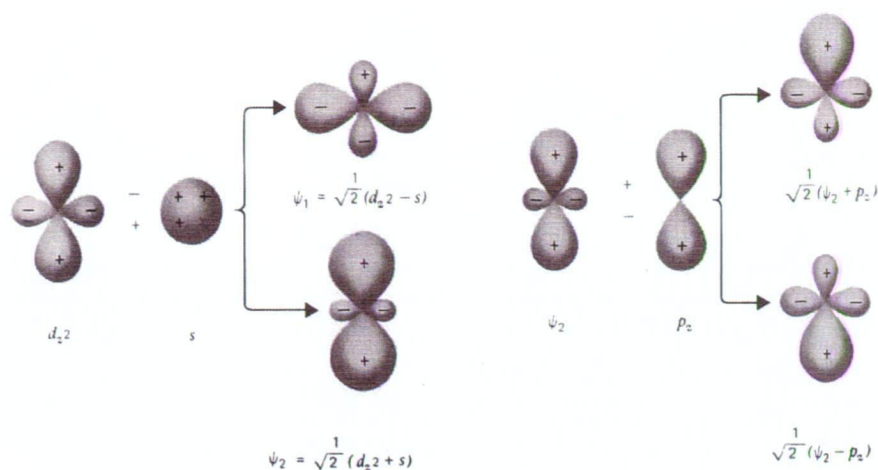
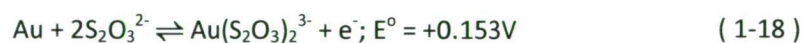
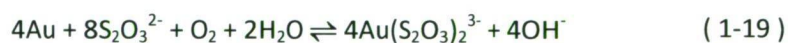


Figure 1.1 Hybridisation of gold(I) orbitals^{96, 97}

Gold forms a stable complex with thiosulfate in aqueous solution via Equation (1-18) below.

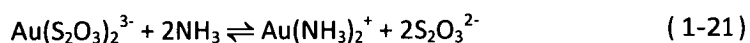


Gold dissolves in an alkaline thiosulfate solution using dissolved oxygen as the oxidant to form the Au(I) complex via Equation (1-19), however the rate of reaction is slow in the absence of a suitable catalyst.



The use of copper has been shown to be effective as a catalyst in combination with ammonia as the stabiliser^{85, 98} in concentrations around 10^{-3} to 10^{-4}M ⁸⁶. The activation energy of the reaction rises from 15.54 kJ/mol⁹⁹ in the presence of copper and ammonia to 27.99kJ/mol in the absence of both. Other oxidants have been proposed, such as ferric oxalate¹⁰⁰⁻¹⁰², however it has been suggested that Fe(III) species are unsuitable as oxidants in these thiosulfate leach systems due to instability of the complexes above pH 8⁷. One reported process uses high temperature (>90°C) and 10 to 100psi oxygen in a closed system to achieve high gold dissolution rates. Sulfite is added in this process to stabilise thiosulfate and convert any higher polythionate species to thiosulfate prior to

gold recovery. This process reports >80% gold recovery with thiosulfate and sodium sulfite consumption levels of 7 to 10 kg/t and 1 to 2 kg/t respectively¹⁰². The use of peroxide has also been proposed, however this reagent oxidises thiosulfate very rapidly and is difficult to stabilise⁷. Copper forms a tetra-amine complex according to (1-20) and as gold forms stable ammonia complexes, competition occurs between thiosulfate and ammonia species according to Equation (1-21).



As indicated in Table 1-1, both the stability constants and the standard potentials are very similar, hence there is a lack of certainty as to which gold complex predominates in leach solutions.

Table 1-1 Stability constants for gold complexes⁸⁶

Gold Species	Log K*	Standard Potential
$\text{Au}(\text{NH}_3)_2^+$	26	0.16V
$\text{Au}(\text{S}_2\text{O}_3)_2^{3-}$	26.5	0.15V

*At 25°C , ionic strength 1.0

E_h -pH diagrams for the $\text{Au-NH}_3\text{-S}_2\text{O}_3^{2-}\text{-H}_2\text{O}$ system¹⁰³ and the Au(0/I/III)-NH_3 system²⁸ have been published and suggest that leaching occurs over a wide range of pH values. The E_h -pH diagram for the $\text{Au-NH}_3\text{-S}_2\text{O}_3^{2-}\text{-H}_2\text{O}$ system is illustrated in Figure 1.2¹⁰³.

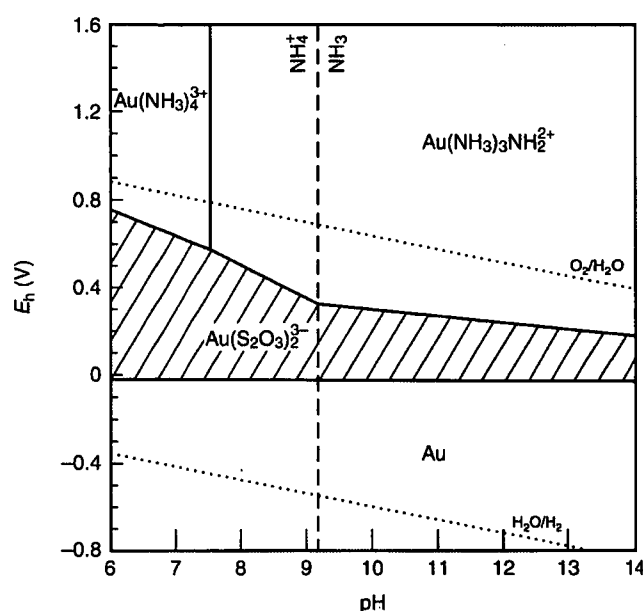
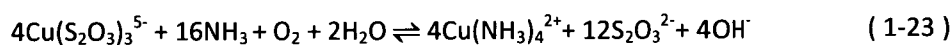
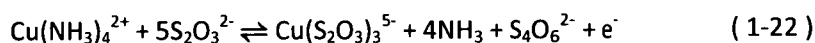
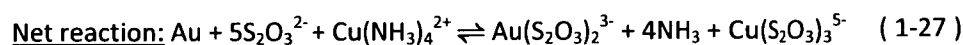
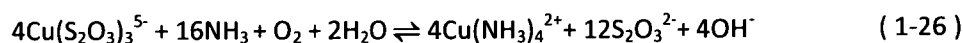
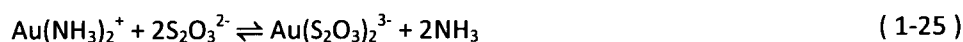
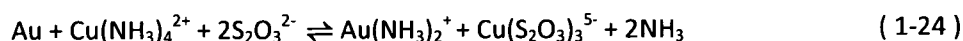


Figure 1.2 E_h -pH diagram for the Au-NH₃-S₂O₃²⁻-H₂O system¹⁰³

A complete understanding of the mechanism of gold dissolution and the catalytic action of Cu(II) is currently under research^{103, 104}, however the major reduction reaction is thought to occur via Equation (1-22) with regeneration of the Cu(II) oxidant via Equation (1-23).



The overall reaction for the dissolution of gold in an ammoniacal thiosulfate leach solution is therefore thought to occur according to Equations (1-24) to (1-27).



The presence of excess ammonia in this system is essential for the stabilisation of the Cu(II) in solution as the $\text{Cu}(\text{NH}_3)_2^+$ complex ion and prevention of both the formation of

$\text{Cu}(\text{OH})_2$ and passivation of the gold surface by preferential adsorption of sulfur species⁷.

A graphical summary of the dissolution reactions is given in Figure 1.3¹⁰⁵.

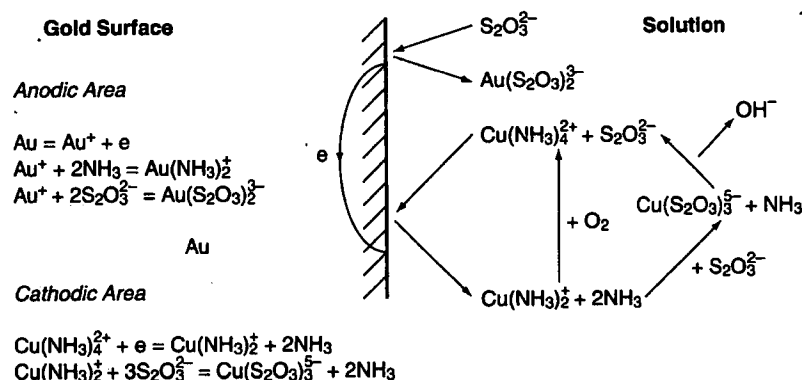


Figure 1.3 Schematic of gold dissolution in ammoniacal thiosulfate leach solutions¹⁰⁵

The development of the rotating electrochemical quartz crystal microbalance¹⁰⁶ has allowed an insight into the electrochemical interactions present at the surface of gold particles, including the interactions between sulfide minerals as well as acting as a sensor for the determination of thiosulfate concentration in leach solutions¹⁰⁷. Use of the rotating electrochemical quartz crystal microbalance has confirmed the cathodic half-reaction for the reduction of Cu(II) occurs in the potential region where gold is oxidised; however ammonia is required to allow the oxidation of gold to take place at an appreciable rate¹⁰⁸. The concentration of Cu(II) was also shown to affect the gold oxidation half-reaction with a decrease in Cu(II) concentration slowing the gold oxidation rate. Increased temperature and thiosulfate concentration were also shown to increase the gold oxidation rate.

1.3.3 Problems

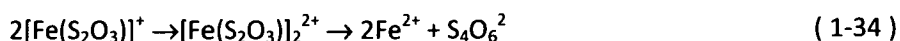
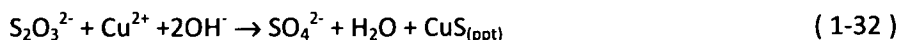
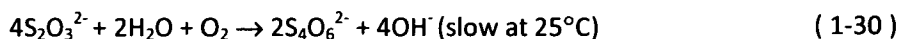
Despite continued success in the use of thiosulfate for the lixiviation of gold, there are a few problems that prevent wide-spread acceptance and utilisation of this technology. The major issues relate to rapid thiosulfate degradation in the presence of copper and

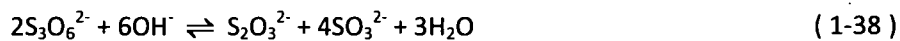
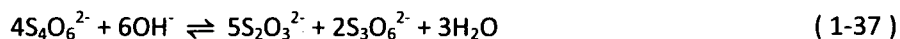
ammonia and although gold dissolution is quite rapid, a lack of a viable adsorption mechanism prevents the ammoniacal thiosulfate process from being fully utilised.

1.3.3.1 Thiosulfate degradation

In leach solutions, thiosulfate degrades via a variety of oxidation and association reactions. Formation of intermediates such as trithionate ($S_3O_6^{2-}$), tetrathionate ($S_4O_6^{2-}$), other polythionates ($S_xO_6^{2-}$ where $x=5, 6, 7$) or polysulfides (S_x^{2-}) is common, as is complete oxidation to sulfate (SO_4^{2-}) and in some cases to elemental sulfur^{87, 103, 104}. pH is an important factor in the degradation of thiosulfate, due to an increase in the rate of degradation in acidic media¹⁰⁹. Both trithionate and tetrathionate have been shown to have a detrimental effect on the recovery of aurothiosulfate by ion-exchange media^{110, 111} through displacement of the adsorbed aurothiosulfate complexes, despite showing negligible ability to lixiviate gold¹¹². Tetrathionate, $S_4O_6^{2-}$, has been shown to have a greater detrimental effect than trithionate in solution, preferentially adsorbing to Purolite A500C (Purolite; quaternary ammonium; 1.15mmol/g capacity).^{102, 113} Initial results published in the same paper suggest that despite contamination of trithionate stock with tetrathionate, little difference was shown between gold loading isotherms for trithionate/tetrathionate and tetrathionate alone, suggesting the major competing species for aurothiosulfate on these resins is tetrathionate.^{102, 113} These results should be compared with later published research showing that in alkaline leach solutions at pH 10.4, polythionate production was focussed on trithionate, not tetrathionate¹¹⁴. Hence, due to the alkaline synthetic leach solutions used, the focus of polythionate competition with aurothiosulfate in this thesis is on trithionate due to the increased production of this polythionate over tetrathionate, despite the latter being shown to have a greater detrimental effect on aurothiosulfate adsorption.

Some mineralogies and metal ions cause breakdown of thiosulfate, with Fe(III) being a catalyst for degradation through the formation of the $[\text{Fe}(\text{S}_2\text{O}_3)]_2^{2+}$ complex by dimerisation of $[\text{Fe}(\text{S}_2\text{O}_3)]^+$ followed by intramolecular electron transfer. The Fe(III) is then reduced to Fe(II) and thiosulfate dimerises to form tetrathionate¹¹⁵ as illustrated in (1-34). Many iron mineralogies such as pyrite and haematite along with most tectosilicates (SiO_2) and rutile group minerals (TiO_2) will also catalyse the degradation of thiosulfate to tetrathionate¹¹⁶ and in the presence of light, tectosilicates and Fe_2O_3 act as semiconductors, further increasing the degradation of thiosulfate^{116, 117}. Various metal species either catalyse the further oxidation or reduction of thiosulfate with arsenic, antimony and tin catalysing the formation of polythionates, in particular pentathionate and zinc and aluminium result in the formation of sulfides^{116, 118}. Mercury and silver also precipitate from solution as sulfides, however an excess of thiosulfate causes complexation of these minerals, negating the precipitation effect but adding the mercury and silver thiosulfate complexes as competitors for aurothiosulfate on ion-exchange sites¹¹⁸. Thiosulfate is also consumed by peroxides, phosphines, polysulfides, permanganates, chromates, halogens and their oxyanions. In addition, certain microfauna, microflora and fungi can very slowly digest thiosulfate¹¹⁶. Some of the thiosulfate degradation reactions are given in Equations (1-28) to (1-42).





The use of Cu(II) as a catalyst for thiosulfate leaching also has some inherent problems. Copper and ammonia will be present in the barren waste material and can present an environmental hazard for final waste treatment and disposal^{102, 119}. Copper can also cause precipitation of the dissolved gold when the concentration of dissolved oxygen in solution is low^{102, 119}. Finally, copper complexes adsorb onto both resin ion-exchange sites or activated carbon adsorption sites and will co-elute and be recovered in the elution step and therefore be present in the final product produced by electrowinning or precipitation¹⁰². This necessitates further smelting and refining to remove the entrained copper. Therefore, research has been focussed on the use of a thiosulfate leaching system without copper or ammonia. These processes have been described in Section 1.3.2 and have utilised ferric oxalate¹⁰⁰⁻¹⁰², peroxides⁷ and an over-pressure of oxygen¹⁰² as oxidants for the oxidation of gold in solution. Each of these has further issues regarding contamination of the final product by co-elution of the metal complex, inability to stabilise the oxidant species and increased polythionate formation respectively.

1.3.3.2 *Viability of activated carbon as an adsorption mechanism*

Initial results in the literature have shown that activated carbon achieved a 95% gold recovery after 6 hours at 25°C with an ammoniacal thiosulfate leach of a Dominican gold ore containing 15.8mg/L gold^{120, 121}. However, further research in the area has shown

unequivocally that aurothiosulfate is not adsorbed onto activated carbon to any appreciable degree and that activated carbon is a poor adsorbent for this leach system^{102,}

112, 122, 123

1.4 Ion-exchange resins

Ion exchange resins for the adsorption of gold complexes fall into one of two categories, dependent on the type of amine used for functionalisation. Alkylamines such as trimethylamine form Type 1 resins, where as hydroxyalkylamines form Type 2 resins. Based upon whether the functionalisation reagent is a primary/secondary or tertiary amine will determine whether the resin formed will be weak- or strong-base respectively.

The use of ion-exchange resins for the recovery of dissolved gold in leach solutions is a well-proven technology recovering gold at several processing plants around the world including the resin-in-pulp plant at Muruntau¹²⁴ (Tashkent, Uzbekistan) and the resin-in-leach plant at Penjom¹²⁵ (Pahang, Malaysia). Early process research was performed in the US, South Africa, Romania and the former USSR, with the latter being the site of the first resin-in-pulp (RIP) plant at Murantau (Tashkent, Uzbekistan) in the 1970s¹²⁴. The decision to use resin in this particular case was influenced by the company having experience in the uranium extraction industry. Commercial resins were unable to compete with activated carbon as an adsorption system in most mineral systems due to poor selectivity, mechanical degradation of the beads and complex elution/regeneration schemes. However, further research has addressed many of these issues.

1.4.1 Cyanide-selective resins

Metal cyanide complex adsorption is achieved with both strong- and weak-base resins with strong-base resins showing high loading capacities and fast loading rates but poorer selectivity (due to base metal adsorption) and difficult elution. Weak-base resins show greater selectivity for precious metal cyanide complexes; however this is at the cost of

slower loading rates and lower loading capacity (25-50% of strong-base capacity)¹²⁴. Selectivity for gold cyanide has been achieved utilising a strong-base tributylamine functional group and commercialised as the Minix ion-exchange resin by the Dow Chemical Company¹²⁶ and using a guanidine functionality marketed as the AuRIX-100 resin by Cognis Australia^{42, 127}. Further research into gold selective functional groups has shown the efficacy of the highly sterically hindered NOTREN resin in the selective adsorption of gold cyanide from ammonium cyanide leach solutions¹²⁸. Further research has developed a chitosan-coated magnetic nanoparticles and shown successful adsorption of tetrachloroaurate, AuCl_4^- , complexes¹²⁹. Research has also been reported into the adsorption of gold thiocyanate onto various strong-base quaternary ammonium and weak-base pyridine ion-exchange media showing 99% adsorption of gold thiocyanate from solution with no recomplexation of the gold ion by the resin functional groups being proven by Raman infra-red spectroscopy¹³⁰.

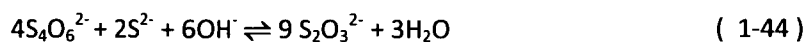
1.4.2 Thiosulfate-selective resins

An initial patent on the adsorption of gold from thiosulfate solutions utilised quaternary ammonium functional groups embedded in a poly-urethane matrix with a water-immiscible solvent, such as 1-octanol, improving the loading characteristics of the resins¹³¹. In this particular patent claim, aurothiosulfate was eluted from the resin using sodium or ammonium thiocyanate or more rapidly with dimethylformamide, acidic thiourea, zinc cyanide or sodium benzoate¹³¹.

Further research focussed on the comparison between Amberlite IRA-400(Rohm and Haas; quaternary ammonium; 3.8mmol/g capacity), Dowex 1(Dow Chemical Company; quaternary ammonium; 1.98mmol/g capacity) and Eichrom Strong Anion Exchange (Eichrom Technologies LLC; quaternary ammonium; 1.2mmol/g capacity) resins and activated carbon(Calgon Carbon Corp.)¹²³. The best results in this particular work were obtained using the strong-base Amberlite IRA-400 resin at ambient temperature and pH

9. Elution performance was somewhat unsuccessful with 76% elution using 5M NaCl over 24 hours. The copper selectivity of the resin was not examined in this work.

Weak-base ion-exchange resins such as Amberlite IRA-743 (Rohm&Haas; Weak-base polyamine; 0.6 mmol/g capacity) have been tested for recovery of gold from thiosulfate solutions¹³². A recent patent describes the recovery of aurothiosulfate using a wide variety of strong-base ion-exchange resins from resin-in-pulp and resin-in-leach processes with a single weak-base resin reported as applicable to these processes¹³³. The use of thiosulfate leaching and resin-in-pulp technology was used to treat carbonaceous, preg-robbing ores of the Goldstrike mine in Nevada¹³⁴. An initial pre-treatment of pressure oxidation followed by cooling and leaching using dilute liquors consisting of 0.03-0.05 M thiosulfate, 0.5-1.6mM Cu(II), and 7-100mM NH₃ with pH ranging from 7-9¹³³⁻¹³⁵. The leach solution was then contacted with resins in a Pachuca tank followed by screening to remove the loaded resin. Several resins are suggested as being suitable for the process, including the Type 1 resins Dowex M-41 and MSA-1 (Dow Chemicals), Amberlite IRA-900C and IRA-904 (Rohm&Haas) and the Type 2 resins Dowex M-42 and MSA-2 and Amberlite IRA-910. The resin contact stage was then followed by multistage stripping where copper and gold were eluted sequentially. Copper elution was achieved using 5-6 bed volumes of ammoniacal ammonium thiosulfate or oxygenated ammonia with ammonium thiosulfate buffer. The oxygenated ammonia was preferred as it enabled the recycling of the eluent as leach liquor¹³⁴. Gold was eluted from the resin using 5-6 bed volumes of ammonium, potassium or calcium thiocyanate. Resin regeneration was performed in this instance by flushing the resin with a solution of up to 8 bed volumes of either trithionate or tetrathionate. This eluted the thiocyanate from the resin with the adsorbed polythionates being oxidised to thiosulfate by flushing the resins with a solution of sodium hydrogen sulfide. This converted the adsorbed polythionates to thiosulfate according to Equations (1-43) and (1-44).



Further research utilised a macroporous strong-base resin to treat an ammoniacal thiosulfate leach liquor containing both copper and gold¹³⁴. The Purolite A-500C resin (Purolite; quaternary ammonium; 1.15mmol/g capacity) displayed good copper elution with 99.95% being eluted over 2 hours using 4 bed volumes of an ammoniacal thiosulfate eluent containing 150g/L thiosulfate. Flushing with a polythionate eluent containing either ~200g/L trithionate or ~40g/L trithionate with ~80g/L tetrathionate for 4 hours resulted in >99% elution of the adsorbed gold. The disadvantage of this system is the requirement for two elution stages with different reagents required for both.

Further research describes the use of Purolite A-500/2788 resin in a complete thiosulfate leaching regime, including pressure oxidation, thiosulfate leaching, resin adsorption and elution and electrowinning of the recovered gold^{136, 137}. Gold recoveries are reported to >95% within 24 hours. Leach conditions are considered very mild, making this an ideal process for adaptation to existing resin-in-pulp technologies. Of note is the utilisation of a previously patented elution system¹³⁸ utilising a combination of sulfite and another anionic species, such as nitrate or chloride for the elution of adsorbed aurothiosulfate. This elution system has been shown to decrease the volume and concentration of eluent required to elute the adsorbed aurothiosulfate from the resin. Previous work required the use of 2M ammonium nitrate for elution within 10 bed volumes¹¹¹, whereas the addition of 0.1M sodium sulfite to 1M ammonium nitrate allows complete elution within 5 bed volumes^{114, 137, 138}. This research also demonstrates the successful use of trithionate in combination with sulfite for the elution of aurothiosulfate, however the disadvantage of utilising trithionate is the requirement of resin regeneration with sulfide to convert the adsorbed trithionate to thiosulfate¹³⁷. A detailed study into the comparative uptake of copper and gold from ammoniacal thiosulfate solutions compared 3 weak-base and 8

strong-base ion-exchange resins of both Type 1 and Type 2 functionality¹³⁹. Results obtained showed that weak-base resins exhibit both slower adsorption rates and lower adsorption capacities than strong-base resins and that the adsorption of copper complexes follows a similar trend to that for aurothiosulfate¹³⁹. In both cases, adsorption was shown to follow a Freundlich isotherm and the presence of copper caused instability in the ammoniacal thiosulfate leach solutions studied, limiting the range of leaching conditions available¹³⁹. Elution was shown to be rapid and efficient using a 2M Na₂SO₃/1M NH₃ eluent.

A series of Russian ion-exchange polymers was utilised for the recovery of gold from an oxidised arsenopyrite flotation concentrate¹²². The thiosulfate leach contained equimolar amounts of 0.5g/L sodium thiosulfate and ammonia with high levels of arsenic (4.8%) and iron (7.1%) being present from the feedstock. The trimethylammonium strong-base polymer (AV-17-10-P; 4.4mmol/g capacity; TOKEM, Kemerovo, Russia) was shown to adsorb 94% of the gold at pH 6 and 85% at pH 11. Elution was performed using 0.5M thiourea in 0.5M sulfuric acid at ambient temperature with 92.7% of the eluted gold being removed in 1 hour and 120mL of the eluent. Initial research detailed a comparison between commercial carbon adsorbents and a series of Russian ion-exchange polymers with the carbon adsorbents comparing unfavourably with the ion-exchange media¹⁴⁰. Further research has compared the adsorption of silver from thiosulfate leach solutions onto both activated carbon and ion-exchange media, however recommendations in this case are for a trimethylammonium strong base polymer (AV-17-10-P; 4.4mmol/g capacity; TOKEM, Kemerovo, Russia) and an anthracite-derived carbon adsorbent¹⁴¹.

Equilibrium studies involving a set of commercially available ion-exchange resins were performed at pH 9.5 and 22°C¹⁴². The equilibrium isotherms generated using simple solutions of aurothiosulfate showed that strong-base resins were preferable to weak-base

resins for this application. Loadings were efficient, even at very low gold concentrations and the higher capacities of the strong-base resins made them more tolerant to low levels of competing anions. However, Minix, a strong-base resin with excellent gold cyanide selectivity showed similar loading characteristics to the weak-base resins tested¹⁴².

Amberjet 4200 (Rohm & Haas; quaternary ammonium; 3.7mmol/g capacity) was shown to be the best performing resin and was used to recover gold from a thiosulfate leach pulp containing 0.05M thiosulfate, 0.2M ammonia and 10ppm gold and copper at pH 9.5. Copper concentration in the leach rose as the aurothiosulfate displaced the copper complexes from the resin functional groups. A thiosulfate eluent rapidly displaced copper. The elution of the adsorbed gold could be performed either by thiocyanate or by 2M ammonium nitrate^{111, 142} with preference expressed for the use of nitrate as an eluent due to the requirement of regenerating the resins with ferric sulfate, thus leaving the resin in sulfate form.

Gold is not the only thiosulfate complex to adsorb onto resin surfaces with research showing that lead, copper, zinc and silver all adsorb onto strong-base resins from ammoniacal thiosulfate leach liquors^{111, 143}. The presence of these other complexes reduces a resins ability to adsorb aurothiosulfate and will contaminate the gold product when the resin undergoes elution. Copper thiosulfate has been shown to be displaced by aurothiosulfate¹¹¹ and the proposed affinity order for adsorption of thiosulfate complexes for strong-base resins was reported as $Au > Pb \gg Ag > Cu \gg Zn$.

The major products of thiosulfate oxidation such as trithionate, $S_3O_6^{2-}$, have been shown to thermodynamically displace aurothiosulfate from strong base resins^{111, 114}. Despite being kinetically slower to adsorb, the increasing concentration of these species in a leach solution sets an upper limit on the time feasible for gold adsorption. This is also of importance in intensive leaching systems where increased thiosulfate consumption will be

occurring and therefore large concentrations of polythionates will be generated. Research has shown that sulfide will eliminate trithionate from the leach solution, however this is at the cost of precipitating gold sulfide¹³⁴. Oxidation of thiosulfate must therefore be minimised to retain thiosulfate for leaching and also allow efficient gold recovery. How this is performed and still allow the use of oxidants for gold lixiviation remains to be seen.

A patent for the use of a guanidine functionalised polystyrene resin has been granted to Henkel Australia (Cognis Australia as of August 1999) and is commercialised under the Aurix tradename¹⁴⁴. The patent has shown the recovery of gold from liquors containing 25-200mM of thiosulfate and >50mM ammonia. The guanidine functionality is present in its protonated form due to the high pK_a of the functional group and as such behaves in a similar manner to strong-base ion-exchange media. The patent describes the elution of the adsorbed gold species by pH differential ($pH > 11$) with sodium cyanide or sodium benzoate as additives to facilitate elution. Further work has compared carbon-in-solution and resin-in-solution using the AuRIX100 resin¹⁴⁵ showing that the resin-in-pulp process has lower capital and operating costs and is competitive with the carbon-in-solution method tested.

1.4.3 Resin-in-pulp/resin-in-leach

Resin-in-pulp/resin-in-leach (RIP/RIL) systems are operated in a similar configuration to CIP/CIL systems already mentioned, with resin concentrations higher than in CIP/CIL systems with volume concentrations ranging from 5-15% or 1-20 g/L. The schematic of the Mintek-Grootvlei RIP plant is given in Figure 1.4.

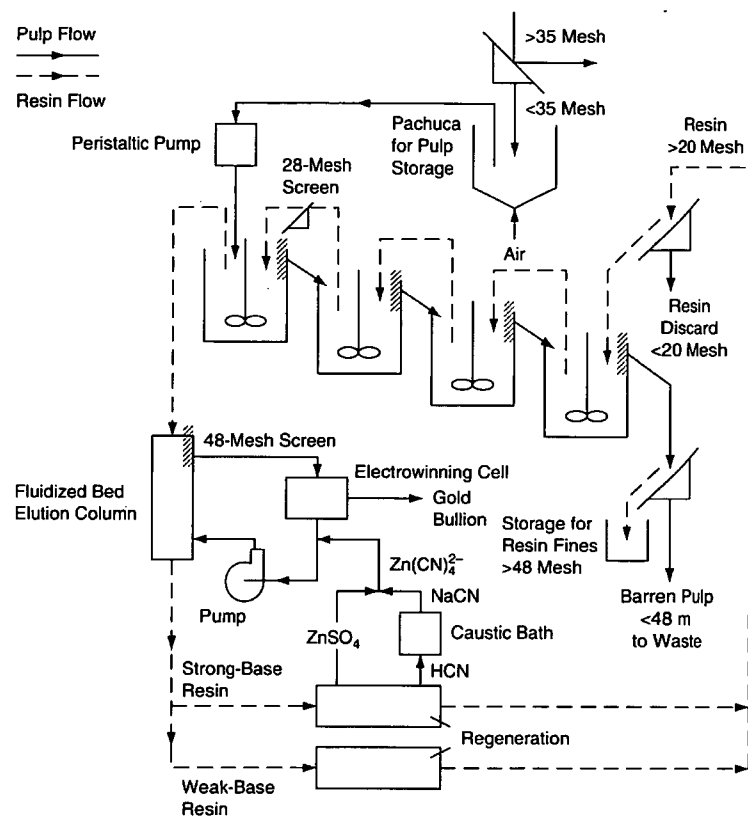


Figure 1.4 Mintek Grootvlei resin-in-pulp plant⁷

The preferred arrangement for these adsorption stages are for air-agitated, Pachuca-type tanks which keep the resin and slurry well-mixed with air-lifting for resin/slurry transfer between tanks and for static sieve bend screens to separate the resin from the slurry¹¹⁰. As with carbon particles, resin particle size affects screening and as commercially available resins have smaller particle sized when compared with carbon, must be able to function and separate smaller resin beads from the pulp solution. Advances in pulp preparation, such as the development of high-efficiency screening for slurry separation of fine particle sizes and inter-screening technology have made it possible to screen efficiently at the smaller particle sizes required for RIP/RIL operations. Typically, 0.5mm screens are required to separate the largest available resin beads (0.8-1.2mm) from slurry although the development of larger beads, foams, fibres and other materials is continuing¹⁹.

Mintek has continued to further the understanding and commercialisation of RIP processes with the development of the MINRIP process, based on the Dowex MINIX strong-base resin. This process has been used successfully at the Penjom mine in Pahang, Malaysia for the treatment of a highly carbonaceous preg-robbing ore¹²⁵. The resin functionality is based around a tributylamine functional group attached to a styrene-divinylbenzene gel resin bead. Elution is performed by flushing with acidic thiourea solution with gold recovery by electrowinning^{125, 146}.

1.5 MIEX substrate

The Magnetic Ion-EXchange, or MIEX^(R), resin was originally developed in collaboration between Orica Watercare, the CSIRO and the South Australian Water Corporation during the 1980s. Patents on the application of a magnetic resin for ion-exchange¹⁴⁷ were granted to the American Cyanamid Company, New York for the invention of magnetic phenol and aniline-based resins. Further patents were granted in 1980 for the suspension polymerisation of tertiary nitrogen containing vinyl monomers with styrene/pyridine or styrene/silane copolymers and divinylbenzene crosslinkers¹⁴⁸. An Australian patent on a water treatment process followed in 1995¹⁴⁹, based on the suspension polymerisation preparation of magnetic ion-exchange beads¹⁵⁰ utilising a variety of monomers suitable for further functionalisation.

Further development led to initial production of the first MIEX resin at Deer Park, Australia in August, 2000. This resin was designed for the removal of dissolved organic components from drinking water and was designated MIEX-DOC, where DOC stands for Dissolved Organic Carbon, the target analyte for this resin system. Once production of the MIEX resin had commenced, more resin was available for application in a variety of locations and industries.

Initial applications of the MIEX resin were for the intended purpose of DOC removal from potable water, with the first large-scale water treatment plant going into production at Wanneroo, Western Australia in 2001¹⁵¹, treating 112 ML/day. Further plants were established in the US with a 1 mega gallon/day plant at Vallejo, California in 2004, Kangaroo Island in South Australia in 2005, with the largest plant in the world being the 9 mega gallon/day plant at St. Cloud, Florida going online in March, 2008. Research into removal of various contaminants include trihalomethane and haloacetic acid¹⁵², natural organic matter¹⁵³, As(V) and Cr(VI)¹⁵⁴ and nitrate/sulfate/bromide¹⁵⁵.

1.6 Conclusions

Ammoniacal thiosulfate leaching has been shown to be an effective alternative for the lixiviation of gold from refractory ore types, both with refractory ore types and in areas of sensitive environmental impact. However, the major disadvantage preventing the widespread use of thiosulfate in an industrial capacity is the lack of a viable solution concentration and recovery method. Methods such as carbon adsorption and precipitation are not easily applicable and the requirement of clarification of leach liquors adds a further processing cost when solvent exchange is attempted.

Ion-exchange resins provide a viable method of adsorbing aurothiosulfate from ammoniacal leach liquor; however this method is not without disadvantages. They have been shown to be susceptible to competitive adsorption of undesired anions. Both base metal thiosulfate complexes such as copper thiosulfate and leach degradation products such as trithionate and tetrathionate both adsorb onto ion-exchange resins either competitively with or in preference to aurothiosulfate. Sequential elution of copper and gold is seen to be cost prohibitive in industrial applications, whereas the elution and destruction of adsorbed polythionate species both limit leaching timeframes and complicates an already costly process.

Further disadvantages are illustrated in the use of resin beads in a resin-in-pulp system. Resins used in this system are required to be robust, due to the corrosive and abrasive nature of the leaching system. As such, resin beads used in these systems are large, placing a limit both on the kinetics of gold adsorption and the ability of the leaching process to transport larger particles through leaching and elution to regeneration and recycling. Smaller particle sizes would allow more rapid uptake and elution of aurothiosulfate along with regeneration of the resin beads for further gold adsorption. This complicates the leaching process, as smaller bead sizes require finer screening for removal and finer milling of feedstock to allow for adequate separation of loaded resin beads from the leach process. Further, smaller particles are more sensitive to attrition from the abrasive environment of the leaching process.

A magnetic removal method would allow the simpler recovery of loaded resin beads from the leach process and also allow retention of finer attrition particles from the leach process, recovering the adsorbed aurothiosulfate complex before disposal. The MIEX^(R) resin system has been optimised for the adsorption of dissolved organic carbon from potable water, however the magnetic recovery method is applicable to the removal of resins and finer magnetic particles from leach solutions.

1.6.1 Research aims

The main objectives of this project are:

- Preparation of a series of resins with a range of different ion-exchange moieties on the MIEX^(R) backbone
- Measurement of the rate and degree of gold adsorption onto these resins
- Establishment of the relationship between resin capacity and gold adsorption onto these resins
- Examine the effects of polythionates on gold sorption

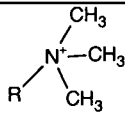
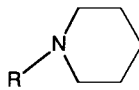
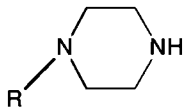
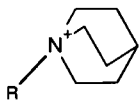
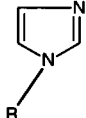
- Develop a series of systems for elution of gold from the resin products
- Compare the best performing resins under industrial conditions.

The ideal resin from these objectives is one that is highly selective for aurothiosulfate over both the copper thiosulfate complexes and polythionate species present in a synthetic leach solution, allows a rapid and large uptake of aurothiosulfate from a synthetic leach solution, allows for rapid and efficient elution of the adsorbed aurothiosulfate complex and retains a minimum of aurothiosulfate after elution.

With these aims in mind, this work will attempt to synthesise and characterise several aurothiosulfate-selective functional groups and attach them to the MIEXTM substrate, with fundamental functional group structures detailed in Table 1-2. These will then be tested in a variety of methods to establish their fitness for industrial application. Instrumental and analytical techniques and optimisations are described in Chapter 2. Resin synthesis and characterisation will be addressed in Chapter 3, including optimisation of the resin synthetic method, characterisation of the functional groups present by ion-exchange capacity testing, resin infra-red spectroscopic and elemental analyses and characterisation of the resin substrate by surface area analysis and scanning electron microscopy. This will be followed in Chapter 4 by initial screening of viable resin systems by aurothiosulfate adsorption testing in both pure water and synthetic leach solutions and testing of several elution regimes to ascertain potential of the trial resin systems. Chapter 5 details the further testing undertaken to ascertain the performance of viable resins in simulated industrial scenarios by repeated adsorption/elution/regeneration tests, competitive testing for the selectivity of the functional group for aurothiosulfate over trithionate and the kinetics and thermodynamics of the adsorption of aurothiosulfate onto the ion-exchange resins tested. Chapter 6 will assess the results of

the previous chapter and recommend a set of suitable resins for industrial trial along with further research required to prepare the resins for industrial application.

Table 1-2 Basic functional group structures

Resin	Structure
Trialkylamine	
Piperidine	
Piperazine	
Quinuclidine	
Imidazole	

1.7 References

1. Klein, C.; Hurlbut, C. S., *Manual of Mineralogy*. 21 ed.; John Wiley and Sons: New York, 1993; Vol. 1, p 681.
2. Bachmann, H.-G.; Tsintsov, Z., Placer Gold in SW Bulgaria: Past and Present. *Gold Bulletin* **2003**, 36, (4), 138-143.
3. Bernstein, P. L., *The Power of Gold: The History of an Obsession*. John Wiley and Sons Inc.: New York, 2000.
4. Meyer, C., Bir Umm Fawakhir: Insights into ancient Egyptian mining. *Journal of the Minerals, Metals and Materials Society* **1997**, 49, (3), 64-67.
5. Harrell, J. A.; Brown, V. M., The World's Oldest Surviving Geological Map: The 1150BC Turin Papyrus from Egypt. *The Journal of Geology* **1992**, 100, (1), 3-18.
6. Clare, R. J., *The path of the Argo : language, imagery, and narrative in the Argonautica of Apollonius Rhodius*. Cambridge University Press: Cambridge, U.K., 2002; Vol. 1, p 301.
7. Marsden, J.; House, I., *The Chemistry of Gold Extraction*. Second Edition ed.; Society for Mining, Metallurgy and Exploration 2006; p 650.

8. Agricola, G.; Hoover, H. C.; Hoover, L. H., *De re metallica*. Dover Publications: New York, 1556 - Translated 1950; Vol. 1.
9. Cahill, N.; Kroll, J. H., New Archaic coin finds at Sardis. *American Journal of Archaeology* **2005**, 109, (4), 613.
10. Pliny the Elder; Rackham, H., *Naturalis Historia*. Heinemann: London, 1938; Vol. 9.
11. Weeks, M. E., *Discovery of the Elements*. 5th ed.; Journal of Chemical Education: Easton, Pa., 1948; Vol. 1.
12. Monaghan, J., *Australians and the gold rush : California and down under, 1849-1854*. University of California Press: Berkeley, 1966; Vol. 1, p 317.
13. Plattner, C. F., Die Probierkunst mit dem Lötrohr *Die Probierkunst mit dem Lötrohr* **1835**, 570.
14. Schnabel, C., *Handbook of Metallurgy*. Macmillan: London, 1921; Vol. 1, p 936-1134.
15. Elsner, L., *Jnl. f. Prak. Chem.* **1846**, 37, 441-446.
16. Habashi, F., *Principles of Extractive Metallurgy*. Gordon and Breach: New York, 1970; Vol. 2.
17. Macarthur, J. S.; Forrest, R. W.; Forrest, W. Improvements in Obtaining Gold and Silver from Ores and Other Compounds British patent 14174, 1888.
18. Shoemaker, R. S., Gold: Quid non mort alia pectora cogis, auri sacra fames. In *Precious Metals: Mining, Extraction and Processing*, Kudryk, V., Ed. SME-AIME: Littleton, CO, 1984; Vol. 2, pp 4-10.
19. Stanley, G. G., *The Extractive Metallurgy of Gold in South Africa*. South African Institute of Mining and Metallurgy: Johannesburg, 1987.
20. King, A., *Gold Metallurgy on the Witwatersrand*. Transvaal Chamber of Mines: Johannesburg, 1949.
21. Adamson, R. J., *Gold Metallurgy in South Africa*. Chamber of Mines of South Africa: Johannesburg, 1972; p 452.
22. Marsden, J.; House, I., *The Chemistry of Gold Extraction*. First Edition ed.; Ellis Horwood: New York, 1992; p 597.
23. Cathro, K. J.; Koch, D. F. A., The Anodic Dissolution of Gold in Cyanide Solutions. *Journal of The Electrochemical Society* **1964**, 111, (12), 1416-1420.
24. Perry, R.; Browner, R. E.; Dunnei, R.; Stoitis, N., Low pH cyanidation of gold. *Minerals Engineering* **1999**, 12, (12), 1431-1440.
25. Lapidus, G., Unsteady-state model for gold cyanidation on a rotating disk. *Hydrometallurgy* **1995**, 39, (1-3), 251-263.
26. Wadsworth, M. E.; Zhu, X., Kinetics of enhanced gold dissolution: Activation by dissolved lead. *Innovations in Natural Resource Processing, Proceedings of the Jan D. Miller Symposium, Salt Lake City, UT, United States, Feb. 28-Mar. 2, 2005* **2005**, 3-19.
27. Aghamirian, M. M.; Yen, W. T., Mechanisms of galvanic interactions between gold and sulfide minerals in cyanide solution. *Minerals Engineering* **2005**, 18, (4), 393-407.
28. Senanayake, G., A review of effects of silver, lead, sulfide and carbonaceous matter on gold cyanidation and mechanistic interpretation. *Hydrometallurgy* **2008**, 90, (1), 46-73.
29. Chi, G.; Fuerstenau, M. C.; Marsden, J. O., Study of Merrill-Crowe processing. Part I: Solubility of zinc in alkaline cyanide solution. *International Journal of Mineral Processing* **1997**, 49, (3-4), 171-183.
30. Nicol, M. J.; Schalch, E.; Balestra, P.; Hedegus, H., A modern study of the kinetics and mechanism of the cementation of gold. *Journal of the South African Institute of Mining & Metallurgy* **1979**, 79, (7), 191-198.
31. Paul, R. L.; Howarth, D. In *Cementation of gold onto zinc from concentrated aurocyanide solutions*, Gold 100: Proceedings of the International Conference on Gold, Johannesburg, South Africa, 1986; Fivaz, C. E., Ed. South African Institute of Mining and Metallurgy: Johannesburg, South Africa, 1986; pp 157-172.

32. Leblanc, R., Precipitation of gold from cyanide solution by zinc dust-the influence of certain factors and impurities. *Canadian Mining Journal* **1942**, 63, 371-9.
33. Nicol, M. J.; Fleming, C. A.; Paul, R. L., *The chemistry of the Extraction of Gold*. South African Institute of Mining and Metallurgy: Johannesburg, South Africa, 1987; Vol. 2, p 831-905.
34. Barnes, J. E.; Edwards, J. D., Solvent extraction at Inco's Acton precious metal refinery. *Chemistry & Industry (London, United Kingdom)* **1982**, (5), 151-5.
35. Haswell, S. J. E., *Atomic Absorption Spectrophotometry - Theory, Design and Applications*. 1 ed.; Elsevier: Amsterdam, 1991; Vol. 5, p 560.
36. Thomas, J. A.; Phillips, W. A.; Farais, A., The refining of gold by a leach-solvent extraction process. *1st International Symposium on Precious Metals Recovery* **1984**.
37. Mooiman, M. B.; Miller, J. D., Soluble losses in the extraction of gold from alkaline cyanide solutions by modified amines. *Hydrometallurgy* **1986**, 16, (3), 245-261.
38. Wan, R. Y.; Miller, J. D., Research and development activities for the recovery of gold from alkaline cyanide solutions. *Mineral Processing & Extractive Metallurgy Review* **1990**, 6, 143-190.
39. Adams, M. D., On-site gold refining of cyanide liquors by solvent extraction. *Minerals Engineering* **2003**, 16, (4), 369-373.
40. Valenzuela, J. L.; Aguayo, S.; Parga, J. R.; Lewis, R. G., Gold solvent extraction from alkaline cyanide solutions, using LIX 79 extractant. *Hydrometallurgy 2003, Proceedings of the International Symposium honoring Professor Ian M. Ritchie, 5th, Vancouver, BC, Canada, Aug. 24-27, 2003* **2003**, 1, 881-889.
41. Virnig, M. J.; MacKenzie, J. M. W. In *Extractants for the Recovery of Gold*, 3rd International Gold Symposium, Lima, Peru, May 5-8, 1998; Lima, Peru, 1998; p 17 pp.
42. Virnig, M. J.; MacKenzie, J. M. W.; Adamson, C., The Use of Guanidine-based Extractants for the Recovery of Gold. In *Hidden Wealth*, South African Institute of Mining and Metallurgy: Johannesburg, South Africa, 1996; pp 151-156.
43. Kordosky, G. A.; Sierakoski, J. M.; Virnig, M. J.; Mattison, P. L., Gold solvent extraction from typical cyanide leach solutions. *Hydrometallurgy* **1992**, 30, (1-3), 291-305.
44. Alguacil, F. J.; Alonso, M., Transport of Au(CN)₂⁻ across a supported liquid membrane using mixtures of amine Primene JMT and phosphine oxide Cyanex 923. *Hydrometallurgy* **2004**, 74, (1-2), 157-163.
45. Feather, A.; Sole, K. C.; Bryson, L. J., Gold refining by solvent extraction - the Minataur Process. *Journal of the South African Institute of Mining & Metallurgy* **1997**, 97, (4), 169-173.
46. Bockris, J. O. M.; Reddy, A. K. N., *Modern Electrochemistry*. Plenum: New York, 1970; Vol. 2, p 623-1432.
47. Mcquiston Jr., F. W., Chapman, Thomas G. Recovery of gold or silver. U.S. patent US2545239, 1951.
48. Zadra, J. B., *A process for the recovery of gold from activated carbon by leaching and electrolysis. Report of Investigations 4672*. U.S. Bureau of Mines: Washington D.C., 1950; Vol. 4672.
49. Zadra, J. B. Process for extracting gold and silver. U.S. patent US2579531, 1951.
50. Zadra, J. B.; Engel, A. K.; Heinen, H. J., *Process for recovering gold and silver from activated carbon by leaching and electrolysis. Report of Investigations 4843*. U.S. Bureau of Mines: Washington D.C., 1952; Vol. 4843.
51. McDougall, G. J.; Hancock, R. D.; Nicol, M. J.; Wellington, O. L.; Copperthwaite, R. G., The mechanism for the adsorption of gold cyanide onto activated carbon. *Journal of the South African Institute of Mining & Metallurgy* **1980**, 80, (80), 344-356.
52. Adams, M. D.; McDougall, G. J.; Hancock, R. D., Models for the absorption of aurocyanide onto activated carbon. Part II: Extraction of aurocyanide ion pairs by polymeric adsorbents. *Hydrometallurgy* **1987**, 18, (2), 139-54.

53. Adams, M. D.; McDougall, G. J.; Hancock, R. D., Models for the adsorption of aurocyanide onto activated carbon. Part III: Comparison between the extraction of aurocyanide by activated carbon, polymeric adsorbents and 1-pentanol. *Hydrometallurgy* **1987**, 19, (1), 95-115.
54. McDougall, G. J.; Adams, M. D.; Hancock, R. D., Models for the adsorption of aurocyanide onto activated carbon. Part I: Solvent extraction of aurocyanide ion pairs by 1-pentanol. *Hydrometallurgy* **1987**, 18, (2), 125-38.
55. Ibrado, A. S.; Fuerstenau, D. W., Adsorption of the cyano complexes of silver(I), copper(I), mercury(II), cadmium (II), and zinc(II) on activated carbon. *Minerals & Metallurgical Processing* **1989**, 6, (1), 23-8.
56. McDougall, G. J.; Hancock, R. D., Gold complexes and activated carbon. *Gold Bulletin* **1981**, 14, (4), 138-153.
57. Fleming, C. A.; Nicol, M. J., The absorption of gold cyanide onto activated carbon. III. Factors influencing the rate of loading and the equilibrium capacity. *Journal of the South African Institute of Mining & Metallurgy* **1984**, 84, (4), 85-93.
58. Davidson, R. J.; Duncanson, D., The elution of gold from activated carbon using deionized water. *Journal of the South African Institute of Mining & Metallurgy* **1977**, 77, (12), 254-61.
59. Muir, D. M.; Hinchliffe, W.; Tsuchida, N.; Ruane, M., Solvent elution of gold from C.I.P. carbon. *Hydrometallurgy* **1985**, 14, (1), 47-65.
60. Ubaldini, S.; Massidda, R.; Vegliò, F.; Belochini, F., Gold stripping by hydro-alcoholic solutions from activated carbon: Experimental results and data analysis by a semi-empirical model. *Hydrometallurgy* **2006**, 81, 40-44.
61. Muir, D. M.; Hinchliffe, W. D.; Griffin, A., Elution of gold from carbon by the micron solvent distillation procedure. *Hydrometallurgy* **1985**, 14, (2), 151-169.
62. Miller, J. D.; Munoz, G. A.; Duyvesteyn, S., Design and synthesis of powdered magnetic activated carbons for aurodicyanide anion adsorption from alkaline cyanide leaching solutions. *Fundamentals and Applications of Anion Separations, [Proceedings of the Symposium "Fundamentals and Applications of Anion Separations" held during the American Chemical Society National Meeting]*, **2004**, 277-291.
63. Fleming, C. A., The recovery of gold from thiourea leach liquors with activated carbon. *Proceedings of International Symposium on Gold Metallurgy* **1987**, 259-277.
64. Kononova, O. N.; Kholmogorov, A. G.; Danilenko, N. V.; Kachin, S. V.; Kononov, Y. S.; Dmitrieva, Z. V., Sorption of gold and silver on carbon adsorbents from thiocyanate solutions. *Carbon* **2005**, 43, (1), 17-22.
65. Souren, A., Living with Cyanide *Geochemical News* **2000**, 105, (4), 16-26.
66. *Cyanide management: A series on best practice environmental management in mining* Department of Environment: Canberra, 2003.
67. *Guidelines for drinking-water quality [electronic resource]: incorporating 1st and 2nd addenda, Vol.1, Recommendations. – 3rd ed.* World Health Organisation: Geneva, 2008.
68. Donato, D. B.; Nichols, O.; Possingham, H.; Moore, M.; Ricci, P. F.; Noller, B. N., A critical review of the effects of gold cyanide-bearing tailings solutions on wildlife. *Environment International* **2007**, 33, (7), 974-984.
69. *Tailings storage facilities at Australian gold mines. Submission to the senate environment, recreation, communication and the arts reference committee.* Minerals Council of Australia: Melbourne, 1996.
70. Cyanide spill link to Aussie goldminer. *The Australian* 23/3/2000, 2000, p 28.
71. Röggl, G., UN report on cyanide spill warns of risk. *The Lancet* **2000**, 355, (9214), 1530-1530.
72. Csagoly, P., *The Cyanide Spill at Baia Mare, Romania: Before, during and after.* The Regional Environmental Center for Central and Eastern Europe: 2000.

73. Bhappu, R. B., Hydrometallurgical Processing of Precious Metal Ores. In *Gold: Advances in Precious Metal Recovery*, Arbiter, N.; Han, K. N., Eds. Gordon and Breach Science Publishers: New York, 1990; pp 66-80.
74. Rees, K. L.; van Deventer, J. S. J., Preg-robbing phenomena in the cyanidation of sulphide gold ores. *Hydrometallurgy* **2000**, 58, (1), 61-80.
75. Sarwar, M.; Naeem, S., Adsorption studies of gold on copper sulphide. *Hydrometallurgy* **1994**, 36, (3), 385-391.
76. Urban, M. R.; Urban, J.; Lloyd, P. J. D., Adsorption of gold from cyanide solutions onto constituents of the reef, and its role in reducing the efficiency of the gold-recovery process. *Journal of the South African Institute of Mining & Metallurgy* **1973**, 73, (11), 385-94.
77. Jordan, M. A.; McGinness, S.; Phillips, C. V., Acidophilic bacteria--their potential mining and environmental applications. *Minerals Engineering* **1996**, 9, (2), 169-181.
78. Olson, G. J., Microbial oxidation of gold ores and gold bioleaching. *FEMS Microbiology Letters* **1994**, 119, (1-2), 1-6.
79. Ndlovu, S., Biohydrometallurgy for sustainable development in the African minerals industry. *Hydrometallurgy* **2008**, 91, (1-4), 20-27.
80. Climo, M.; Watling, H. R.; Van Bronswijk, W., Biooxidation as pre-treatment for a telluride-rich refractory gold concentrate. *Minerals Engineering* **2000**, 13, (12), 1219-1229.
81. Brierley, J. A.; Brierley, C. L., Present and future commercial applications of biohydrometallurgy. *Hydrometallurgy* **2001**, 59, (2-3), 233-239.
82. Holder, R., Beaconsfield Gold Mine - Ironing Out the Bugs. *Ninth Mill Operators' Conference* **2007**, 185-193.
83. Brierley, J. A., A perspective on developments in biohydrometallurgy. *Hydrometallurgy* **2008**, 94, (1-4), 2-7.
84. Ritchie, I. M.; Nicol, M. J.; Staunton, W. P. In *Are there realistic alternatives to cyanide as a lixiviant for gold at the present time?*, Cyanide: Social, Industrial and Economic Aspects. Proceedings of a Symposium held at the Annual Meeting of TMS, New Orleans, Louisiana, USA, Feb. 12-15, 2001; Young, C. A.; Twidwell, L. G.; Anderson, C. B., Eds. The Minerals, Metals & Materials Society, Warrendale, PA, USA: New Orleans, Louisiana, USA, 2001; pp 427-440.
85. Grosse, A. C.; Dicoski, G. W.; Shaw, M. J.; Haddad, P. R., Leaching and recovery of gold using ammoniacal thiosulfate leach liquors (a review). *Hydrometallurgy* **2003**, 69, 1-21.
86. Muir, D. M.; Aylmore, M. G., Thiosulphate as an alternative to cyanide for gold processing-issues and impediments. *Transactions of the Institutions of Mining and Metallurgy, Section C: Mineral Processing and Extractive Metallurgy* **2004**, 113, (1), C2-C12.
87. Aylmore, M. G.; Muir, D. M., Thiosulfate leaching of Gold - A Review. *Miner. Eng.* **2001**, 14, (2), 135-174.
88. Nicol, M. J.; O'Malley, G., Recovering Gold from Thiosulfate Leach Pulps via Ion Exchange. *JOM* **2002**, (October), 44-46.
89. Hiskey, J. B.; Atluri, V. P., Dissolution chemistry of gold and silver in different lixiviants. *Mineral Processing & Extractive Metallurgy Review* **1988**, 4, (1), 95-134.
90. La Brooy, S. R.; Linge, H. G.; Walker, G. S., Review of Gold Extraction from Ores. *Minerals Engineering* **1994**, 7, (10), 1213-1241.
91. Sparrow, G. J.; Woodcock, J. T., Cyanide and other lixiviant leaching systems for gold with some practical applications. *Mineral Processing & Extractive Metallurgy Review* **1995**, 14, 193-247.
92. Senanayake, G., Gold leaching in non-cyanide lixiviant systems: critical issues on fundamentals and applications. *Minerals Engineering* **2004**, 17, (6), 785-801.
93. Gundiler, I. H.; Goering, P. D. In *Thiosulfate leaching of gold from copper-bearing ores.*, SME Annual Meeting, Reno, Nevada, February 15-18, 1993, 1993; SME: Reno, Nevada, 1993; pp Paper #93-281.

94. Gowland, W., *The Metallurgy of the Non-Ferrous Metals*. 4th Edition ed.; Charles Griffin & Co.: London, 1930; Vol. 1, p pp. 378-381; 415-418.
95. Livingstone, S. E., Metal Complexes of Ligands Containing Sulphur, Selenium or Tellurium as Donor Atoms. *Quarterly Reviews* **1965**, 19, 386-397.
96. Cotton, F. A.; Wilkinson, G., *Advanced Inorganic Chemistry*. 5th ed.; John Wiley & Sons: New York, 1988; p 1455.
97. Puddephatt, R. J., *The chemistry of gold*. Elsevier Scientific Pub. Co.: Amsterdam, 1978; p x, 274.
98. Breuer, P. L.; Jeffrey, M. I., A review of the chemistry, electrochemistry and kinetics of the gold thiosulfate leaching process. *Hydrometallurgy 2003, Proceedings of the International Symposium honoring Professor Ian M. Ritchie, 5th, Vancouver, BC, Canada, Aug. 24-27, 2003* **2003**, 1, 139-154.
99. Jiang, T.; Chen, J.; Xu, S., A Kinetic Study of Gold Leaching with Thiosulfate. In *Hydrometallurgy: Fundamentals, Technology & Innovations.*, 1993; Vol. Chapter 7, pp 119-126.
100. Chandra, I.; Jeffrey, M. I., A fundamental study of ferric oxalate for dissolving gold in thiosulfate solutions. *Hydrometallurgy* **2005**, 77, (3-4), 191-201.
101. Jeffrey, M. I.; Chandra, I.; Ritchie, I. M.; Hope, G. A.; Watling, K.; Woods, R., Innovations in gold leaching research and development. *Innovations in Natural Resource Processing, Proceedings of the Jan D. Miller Symposium, Salt Lake City, UT, United States, Feb. 28-Mar. 2, 2005* **2005**, 207-222.
102. Ji, J.; Fleming, C.; West-Sells, P. G.; Hackl, R. P., A novel thiosulfate system for leaching gold without the use of copper and ammonia. *Hydrometallurgy 2003, Proceedings of the International Symposium honoring Professor Ian M. Ritchie, 5th, Vancouver, BC, Canada, Aug. 24-27, 2003* **2003**, 1, 227-244.
103. Senanayake, G.; Perera, W. N.; Nicol, M. J., Thermodynamic studies of the gold(III)/(I)/(0) redox system in ammonia-thiosulphate solutions at 25 Deg. *Hydrometallurgy 2003, Proceedings of the International Symposium honoring Professor Ian M. Ritchie, 5th, Aug. 24-27, 2003* **2003**, 1, 155-168.
104. Lam, A. E. a. D., D.B., The importance of the Cu(II) catalyst in the thiosulfate leaching of gold. *Hydrometallurgy 2003, Proceedings of the International Symposium honoring Professor Ian M. Ritchie, 5th, Aug. 24-27, 2003* **2003**, 1, 195-211.
105. Aylmore, M. G.; Muir, D. M., Thermodynamic analysis of gold leaching by ammoniacal thiosulfate using Eh/pH and speciation diagrams. *Minerals and Metallurgical Processing* **2001**, 18, (4), 221-227.
106. Jeffrey, M. I.; Zheng, J.; Ritchie, I. M., The development of a rotating electrochemical quartz crystal microbalance for the study of leaching and deposition of minerals. *Measurement Science and Technology* **2000**, 11, (5), 560-567.
107. Breuer, P. L.; Jeffrey, M. I.; Tan, E. H. K.; Bott, A. W., The electrochemical quartz crystal microbalance as a sensor in the gold thiosulfate leaching process. *Journal of Applied Electrochemistry* **2002**, 32, 1167-1174.
108. Breuer, P. L.; Jeffrey, M. I., An electrochemical study of gold leaching in thiosulphate solutions containing copper and ammonia. *Hydrometallurgy* **2002**, 65, (2-3), 145-157.
109. Li, J.; Miller, J. D.; Wan, R. Y.; Le Vier, M. In *The ammoniacal thiosulfate system for precious metal recovery.*, Proceedings of the XIX International Mineral Processing Congress (IMPC), San Francisco, CA, USA, Oct. 22-27, 1995, 1995; SME, Littleton, CO, USA: San Francisco, CA, USA, 1995; pp 37-42.
110. Fleming, C. A., The Potential Role of Anion Exchange Resins in the Gold Industry. *EPD Congress 1998* **1998**, 1, 95-117.
111. O'Malley, G. P. The Elution of Gold from Anion Exchange Resins. International patent WO 01/23626 A1, 5 April 2001, 2001.

112. Aylmore, M. G., Treatment of a Refractory Gold-Copper Sulfide Concentrate by Copper Ammoniacal Thiosulfate Leaching. *Miner. Eng.* **2001**, 14, (6), 615-637.
113. West-Sells, P. G.; Ji, J.; Hackl, R. P., A process for counteracting the detrimental effect of tetrathionate on resin gold adsorption from thiosulfate leachates. *Hydrometallurgy 2003, Proceedings of the International Symposium honoring Professor Ian M. Ritchie, 5th, Vancouver, BC, Canada, Aug. 24-27, 2003* **2003**, 1, 245-256.
114. Jeffrey, M. I.; Brunt, S. D., The quantification of thiosulfate and polythionates in gold leach solutions and on anion exchange resins. *Hydrometallurgy* **2007**, 89, (1-2), 52-60.
115. Williamson, M. A.; Rimstidt, J. D., The rate of decomposition of the ferric-thiosulfate complex in acidic aqueous solutions. *Geochim. Cosmochim. Acta* **1993**, 57, (15), 3555-61.
116. Xu, Y.; Schoonen, M. A. A., The stability of thiosulfate in the presence of pyrite in low-temperature aqueous solutions. *Geochim. Cosmochim. Acta* **1995**, 59, (22), 4605-4622.
117. Benedetti, M.; Boulegue, J., Mechanism of gold transfer and deposition in a supergene environment. *Geochim. Cosmochim. Acta* **1991**, 55, (6), 1539-1547.
118. Bean, S. L., Thiosulfates. In *Kirk-Othmer Encyclopedia of Chemical Technology*, 4th Edition ed.; Kroschwitz, J. I., Ed. John Wiley and Sons: New York, 1997; Vol. 24, pp 51-68.
119. Breuer, P. L.; Jeffrey, M. I., The reduction of copper(II) and the oxidation of thiosulfate and oxysulfur anions in gold leaching solutions. *Hydrometallurgy* **2003**, 70, (1-3), 163-173.
120. Abbruzzese, C.; Fornari, P.; Massidda, R.; Veglio, F.; Ubaldini, S., Thiosulfate leaching for gold hydrometallurgy. *Hydrometallurgy* **1995**, 39, 265-276.
121. Meggiolaro, V.; Niccolini, G.; Miniussi, G.; Stefanelli, N.; Trivellini, E.; Llinas, R.; Ramirez, I.; Baccelle Scudeler, L.; Omenetto, P.; Primon, S.; Visona, D.; Abbruzzese, C.; Fornari, P.; Massidda, R.; Piga, L.; Ubaldini, S.; Ball, S.; Monhemius, A. J., Multidisciplinary approach to metallogenic models and types of primary gold concentration in the Cretaceous arc terranes of the Dominican Republic. *Trans. Inst. Min. Metall. Section B (Applied Earth Science)* **2000**, 109, (May-Aug), B95 - B104.
122. Kononova, O. N.; Kholmogorov, A. G.; Kononov, Y. S.; Pashkov, G. L.; Kachin, S. V.; Zotova, S. V., Sorption recovery of gold from thiosulfate solutions after leaching of products of chemical preparation of hard concentrates. *Hydrometallurgy* **2001**, 59, 115-123.
123. Mohansingh, R. Adsorption of Gold from Gold Copper Ammonium Thiosulfate complex onto Activated Carbon and Ion Exchange Resins. Master of Science, University of Nevada, Reno, Reno, Nevada, 2000.
124. Fleming, C. A.; Cromberge, G., The elution of aurocyanide from strong- and weak-base resins. *Journal of the South African Institute of Mining & Metallurgy* **1984**, 84, (9), 269-80.
125. Lewis, G. V., Increased recovery from preg-robbing gold ore at Penjom gold mine. *Proceedings Randol Gold and Silver Forum 1999* **1999**, 1, 105-108.
126. Kotze, M. H.; Green, B. R.; Steinbach, G., Progress in the Development of the Minix Gold-selective Strong-base Resin. In *Hydrometallurgy: Fundamentals, Technology and Innovation.*, Hiskey, J. B.; Warren, J. W., Eds. Society for Mining, Metallurgy and Exploration: Littleton, Colorado, USA, 1993.
127. Fisher, G. T.; Lewis, R. G.; Virnig, M. J.; MacKenzie, J. M. W.; Davis, M. R. *Cognis Aurix 100 Resin for Gold Extraction*; Cognis Australia Ptd Ltd: 2000.
128. Dicinoski, G. W., Novel Resins for the Selective Extraction of Gold from Copper Rich Ores. *S. Afr. J. Chem.* **2000**, 53, (1), 33-43.
129. Chang, Y.-C.; Chen, D.-H., Recovery of Gold(III) Ions by a Chitosan-coated Magnetic Nano-adsorbent. *Gold Bulletin* **2006**, 39, 98-102.
130. Krinitsyn, D.; Kononova, O.; Krylov, A.; Maznyak, N.; Kholmogorov, A., Recovery of Gold(I) thiocyanate complexes by some anion-exchangers. *Russian Journal of Physical Chemistry A, Focus on Chemistry* **2008**, 82, (3), 429-433.
131. Jay, W. H. Process for Recovery of Gold and/or Silver. WO 99/13116, 18 March, 1999, 1999.

132. Marchbank, A. R.; Thomas, K. G.; Dreisinger, D.; Fleming, C. Gold recovery from refractory ores by pressure oxidation and thiosulfate leaching. US Patent 5,536,297, Patent Application Date: 10 Feb. 1995 Patent publication Date : 16 July 1996, 1996.
133. Thomas, K. G.; Fleming, C.; Marchbank, A. R.; Dreisinger, D. Gold recovery from refractory carbonaceous ores by pressure oxidation, thiosulfate leaching and resin-in-pulp adsorption. US 5,785,736, 28 July 1998 Submitted 16 July 1996, 1998.
134. Fleming, C. A.; McMullen, J.; Thomas, K. G.; Wells, J. A., Recent Advances in the Development of an alternative to the cyanidation process: Thiosulfate leaching and resin in pulp. *Minerals & Metallurgical Processing* **2002**, 20, (1), 1-9.
135. Fleming, C. A.; McMullen, J.; Thomas, K. G.; Wells, J. A. In *Recent advances in the development of an alternative to the cyanidation process - based on thiosulfate leaching and resin in pulp*, SME Annual Meeting (2001), Denver, Colorado, February 26-28, 2001; SME: Denver, Colorado, 2001; pp {1-11} Preprint.
136. Jeffrey, M.; Heath, J.; Hewitt, D.; Brunt, S.; Dai, X. In *A thiosulfate process for recovering gold from refractory ores which encompasses pressure oxidation, leaching, resin adsorption, elution, and electrowinning*, Hydrometallurgy 2008: Proceedings of the 6th International Symposium, Phoenix, AZ, 2008; Phoenix, AZ, 2008; pp 791-800.
137. Jeffrey, M. I.; Hewitt, D. M.; Dai, X.; Brunt, S. D., Ion exchange adsorption and elution for recovering gold thiosulfate from leach solutions. *Hydrometallurgy* **2010**, 100, (3-4), 136-143.
138. Jeffrey, M. I. Recovery of metals from ion-exchange resins. International patent WO 2007/137325 A1, 20070522., 2007.
139. Zhang, H. G.; Dreisinger, D. B., The adsorption of gold and copper onto ion-exchange resins from ammoniacal thiosulfate solutions. *Hydrometallurgy* **2002**, 66, (1-3), 67-76.
140. Kholmogorov, A. G.; Kononova, O. N.; Pashkov, G. L.; Kononov, Y. S., Sorption recovery of gold thiosulphate complexes. *Chinese J. Chem. Eng.* **2002**, 10, (1), 123-127.
141. Kononova, O. N.; Kholmogorov, A. G.; Danilenko, N. V.; Goryaeva, N. G.; Shatnykh, K. A.; Kachin, S. V., Recovery of silver from thiosulfate and thiocyanate leach solutions by adsorption on anion exchange resins and activated carbon. *Hydrometallurgy* **2007**, 88, (1-4), 189-195.
142. O'Malley, G. P.; Nicol, M. J. In *Recovery of gold from thiosulfate solutions and pulps with ion-exchange resins.*, Cyanide: Social, Industrial and Economic Aspects. Proceedings of a Symposium held at the Annual Meeting of TMS, New Orleans, LA, February 12-15th, 2001; Young, C. A.; Twidwell, L. G.; Anderson, C. B., Eds. TMS, Warrendale, PA, USA: New Orleans, LA, 2001; pp 469-483.
143. Fagan, P. A.; Paull, B.; Haddad, P. R.; Dunne, R.; Kamar, H., Ion chromatographic analysis of cyanate in gold processing samples containing large concentrations of copper(I) and other metallo-cyanide complexes. *J. Chromatogr.* **1997**, 770, 175-183.
144. Virnig, M. J.; Sierakoski, J. M. Ammonium thiosulfate complex of gold or silver and an amine. U.S. patent 6,197,214, March 6th, 2001.
145. Davis, M. R.; MacKenzie, M. W.; Virnig, M. J., An Engineering Cost Study: CIS vs RIS with Aurix 100. *Randol Gold and Silver Forum '99* **1999**, 189-195.
146. Green, B. R.; Kotze, M. H.; Wyethe, J. P., Developments in ion exchange: The Mintek perspective. *Journal of Metals* **2002**, 10, (1), 37-44.
147. Herckenhoff, E. C. Ion exchange processes with magnetic ion exchange resins. 1953.
148. Lubbock, F. J.; Eldridge, R. J.; Mok, C. C. K. PROCESS FOR COMPOSITE POLYMER BEADS. 12/11/1980 1980.
149. Bursill, D. B. D., Mary ; Morran, James Young ; Nguyen, Hung Van ; Pearce, Veronica Laurel Water treatment process. 8th September, 1995.
150. Ballard, M. J.; Eldridge, R. J.; Bates, J. S. Polymer beads and method for preparation thereof. 1999.

151. Cadee, K.; O'Leary, B.; Smith, P., World's First Magnetic Ion Exchange Water Treatment Plant to be Installed in Western Australia. *Proceedings of AWWA Annual Conference* **2000**.
152. Singer, P. C.; Bilyk, K., Enhanced coagulation using a magnetic ion exchange resin. *Water Research* **2002**, 36, (16), 4009-4022.
153. Fearing, D. A.; Banks, J.; Guyetand, S.; Eroles, C. M.; Jefferson, B.; Wilson, D.; Hillis, P.; Campbell, A. T.; Parsons, S. A., Combination of ferric and MIEX (R) for the treatment of a humic rich water. *Water Research* **2004**, 38, (10), 2551-2558.
154. Jha, A. K.; Bose, A.; Downey, J. P., Removal of As(V) and Cr(VI) ions from aqueous solution using a continuous, hybrid field-gradient magnetic separation device. *Separation Science and Technology* **2006**, 41, (15), 3297-3312.
155. Humbert, H.; Gallard, H.; Jacquemet, V.; Croue, J. P., Combination of coagulation and ion exchange for the reduction of UF fouling properties of a high DOC content surface water. *Water Research* **2007**, 41, (17), 3803-3811.

2 General Experimental

2.1 Introduction

Multiple common analyses were performed throughout this work. Standard methodologies were followed as described in this chapter with variations noted in the text.

2.2 General synthetic procedure and equipment

2.2.1 Reagent purity and sources

All reagents were AR grade or better. Individual grades of reagents are listed when that reagent is first used. MilliQ (Millipore, Bedford, MA; 18.2M Ω) water was used for all experiments and for glassware rinsing.

The bis(thiosulfato)gold(I) complex, $\text{Au}(\text{S}_2\text{O}_3)_2^{3-}$, and its sodium salt, $\text{Na}_3[\text{Au}(\text{S}_2\text{O}_3)_2^{3-}]$ will be designated as aurothiosulfate and sodium aurothiosulfate throughout this work.

2.2.2 Resin drying and preparation

Due to the nature of the confidentiality agreement covering this project, all resins had to be supplied by ORICA Watercare and required a preparative step before use. This treatment typically involved the removal of resin synthesis by-products. The major by-product was residual particulate activated carbon, used in the resin synthesis to adsorb residual reagents. As such, if this particular by-product was left in the resin it was also very effective in the removal of the amines being used in the functionalisation of the MIEX matrix, thereby decreasing the degree of substitution and the final capacity. The residual particulate activated carbon was removed from a sample of the resin by either stirring on a magnetic stirrer or shaking in a 1L polyethylene bottle with MilliQ water, followed by magnetic separation of the resin and decantation of the supernatant, containing the particulate activated carbon. This was repeated until the liquor ran clear and contained no observable particulate activated carbon.

Dry resin was required for various processes, such as alkylation or resin dry mass determination, and this was achieved by slurrying the resin with ethanol, followed by phase separation and drying under vacuum in a vacuum oven at 35°C overnight. This process ensured minimal resin degradation due to epoxide ring opening. Resins were deemed to be dry when they had reached a constant mass and no odour of ethanol was detectable. Dried samples of resins were then stored in sealed polycarbonate tubes until required for further applications.

2.2.3 Epoxide capacity testing of resins

The amount of available epoxide groups present on the resin provides an indication of the upper limit to the ion-exchange capacity once the resin is functionalised. This procedure was also used as an estimation of unfunctionalised resin degradation. Resins were analysed by a modified hydrochloric acid-dioxane-argentometric method¹.

Concentrated hydrochloric acid (1.60mL; HCl; 32%; *Ajax Finechem*) was added to 100mL of dioxane. This mixture was then stored in a dark bottle with a Teflon screw cap until use. A ferric indicator solution was prepared by the addition of 78g of ferric nitrate ($\text{Fe}(\text{NO}_3)_3 \cdot 9\text{H}_2\text{O}$; >98%; *Chem Supply*) to 250mL of water followed by the addition of 50mL of aerated 30 weight% nitric acid (345mL concentrated nitric acid into 690mL of water).

Approximately 1g of resin, equivalent to 4mmol of epoxide, was added to a 500mL conical flask and reacted with 25mL of the [HCl]/dioxane solution at 30°C for 15 min to convert any epoxide present to a chlorhydrin group. MilliQ water (50mL), 5mL of the 30 weight% nitric acid and 3mL of the ferric indicator were then added. 0.50mL 0.05M NH_4SCN was added from a burette and the resulting solution was then titrated against 0.1M AgNO_3 until the red colour had clearly discharged. 10.00mL of nitrobenzene was then added and the flask stoppered and shaken for 15 sec. A second titration was then performed with 0.05M

NH₄SCN until the pink colour reappeared. A blank titration was performed and the epoxide content was then calculated by Equation 2-1:

$$\text{epoxide content}/100g = \frac{(V_b M - v_b m) - (V_s M - v_s m)}{10W} \quad (2-1)$$

where V_b is the titre of the AgNO₃ solution for the blank, v_b is the titre of the NH₄SCN solution for the blank, M is the molarity of the AgNO₃ solution, m is the molarity of the NH₄SCN solution, V_s is the titre of the AgNO₃ solution for the sample, v_s is the titre of the NH₄SCN solution for the sample and W is the weight of the resin.

2.2.4 Ion-exchange capacity testing of resins both via manual and auto-titration

Approximately 10mL of wet resin was loaded into an IEX column (25mL capacity, 10mL diameter) with a porosity #3 sintered-glass frit at the base and allowed to settle for 5 to 10 min. The resin was then conditioned by passing 50mL of 1M NaCl through the column at a flow-rate of 1.00mL min⁻¹. The resins were then washed with MilliQ until no chloride was detected in the effluent by a silver nitrate precipitation visual test. This was later amended to 50mL at 1mL min⁻¹. The column was then washed with 50mL of a 1M sodium nitrate solution (NaNO₃; >98%; *Griffin and George*) at a flow-rate of 1.00mL min⁻¹ and the effluent collected for chloride analysis via argentometric titration.

2.2.4.1 Argentometric titration

A chromate indicator was prepared by the addition of 0.1448g anhydrous sodium chromate (Na₂CrO₄; 98%; *BDH*) to 20.00mL of water and the resultant yellow solution was then stored in a brown glass bottle.

The silver nitrate solution was prepared by drying silver nitrate (AgNO₃; 99+%; *Aldrich*) in an oven at 116°C for one hour and dissolving 1.6996g (10.00mmol) in 1.000L of MilliQ water. This yielded a solution containing 0.010M AgNO₃, which was then stored in a brown glass bottle to prevent degradation of this light-sensitive reagent.

Chapter 2 – General Experimental

For manual titration, 10.00mL of the chloride-containing nitrate effluent was titrated against the 0.010M AgNO_3 using 15 drops of the chromate indicator to the red endpoint. This process was repeated in triplicate to allow for a statistical analysis.

This argentometric titration was also performed using a Metrohm 809 Titrando autotitrator equipped with a Ag Titrode silver electrode coupled to Tiamo version 1.2 Build 41 software.

For this application, 5.00mL of the nitrate effluent was added to approximately 40mL of MilliQ water and titrated against the 0.010M AgNO_3 solution, with 3 replicates being performed for statistical analysis.

2.2.5 Infra-red instrumentation and methods

All infra-red (IR) analyses were performed on a Bruker IFS66 FTIR instrument coupled to a Pike Technologies MIRacle™ ATR attachment. The ATR attachment used a ZnSe crystal and employed OPUS 4.2 for spectra acquisition and OPUS 6.5 for spectral processing. Once spectra had been obtained an extended ATR correction was applied using an angle of ATR incidence of 45° and one ATR reflection. The mean refractive index of the sample was 1.5. Initial scan rates were set at 32 scans per sample with a 4cm^{-1} resolution. This was increased to 128 scans per sample with a 4cm^{-1} resolution for later spectra.

2.2.6 Atomic absorption spectrophotometric instrumentation, optimisation and methods

2.2.6.1 AAS instrumentation

All atomic absorption spectrophotometric (AAS) analysis was performed on a Varian SpectrAA 800 atomic absorption spectrophotometer coupled to Varian SpectrAA 880 version 3 software. Hollow cathode lamps used throughout were Photron P821 and S&J Juniper & Co no. 4121 single element gold lamps.

2.2.6.2 Preparation of AAS standards

The operational parameters for the AAS determination of gold are provided in Table 2-1.

Table 2-1 Gold detection parameters for Varian AAS instrumentation

AAS Wavelength (nm)	Linear range (ppm)
242.8	0.1-30
267.6	0.2-60

As the Au(I) concentration used (0-20ppm) falls within the linear range for both wavelengths, the wavelength with the lower limit of detection was chosen (242.8nm). All samples were analysed directly by this method, with dilution factors being applied when response fell outside that of the calibration curve. Samples were compared to a set of standard solutions containing $[\text{AuCl}_4]^-$ in 5% HCl. In a typical preparation, the quantities of reagents used are given in Table 2-2.

Table 2-2 Preparation of gold standards in 5% HCl matrix

Au standard (mL)	32 % HCl solution (mL)	Final volume (mL)	Final [Au] (ppm)
0.1	10	100	1.014
0.125	5	50	2.535
0.25	5	50	5.070
0.5	5	50	10.14
1	5	50	20.28
1.25	5	50	25.35

These standards were stored in sealed polypropylene bottles in a dark, cool place to prevent degradation. These standards were used for a maximum of two months provided no degradation was noticed in comparison to previous standards analyses. The instrument zero and blank solutions were either MilliQ water or a leach blank. The burner was flushed with 0.1% nitric acid between measurements.

A set of gold leach standards were prepared from a batch of barren (or gold-free) leach solution synthesised as per the method described in Section 2.2.8. This was followed by the addition of a small amount of aurothiosulfate ($\text{Na}_3[\text{Au}(\text{S}_2\text{O}_3)_2] \cdot 2\text{H}_2\text{O}$; 0.01337g; 25.39 μmol ; 99.9%; *Alfa Aesar*) to 50.00mL of the barren leach. Individual standards were then prepared by serial dilution according to Table 2-3 to produce the working gold standards.

Table 2-3 Au standards in ammoniacal thiosulfate leach

100ppm [Au] (ml)	Total volume (ml)	Final [Au] (ppm)
5*	50	1
25 [#]	50	10
25 [*]	50	20
20	50	40
25	50	50

*Prepared by dilution of 5ppm standard; [#] Prepared by dilution of 10ppm standard;

^{*} Prepared by dilution of 20ppm standard

2.2.6.3 Validation of AAS standards

It is essential in this work to have gold standards that remain stable for long periods of time. Due to the significant and uncertain rate of decomposition of the leach liquor, this precludes making standards in artificial leach liquor. Making large amounts of artificial leach liquor standards would allow simpler and more accurate measurement of gold concentration, however frequent preparation of aurothiosulfate standards would consume large quantities of the gold complex. A comparison between $[\text{AuCl}_4]^-$ standards and the response of aurothiosulfate in an ammoniacal leach matrix shows a linear response, as illustrated by Figure 2.1 and Figure 2.2 along with linear best fit equations.

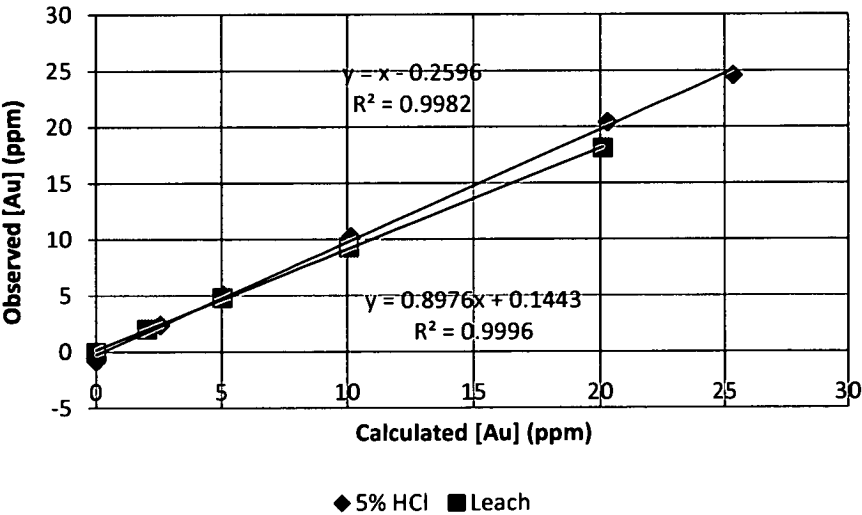


Figure 2.1 Comparison of 5% HCl and ammoniacal thiosulfate leach matrix effects at 267.6nm

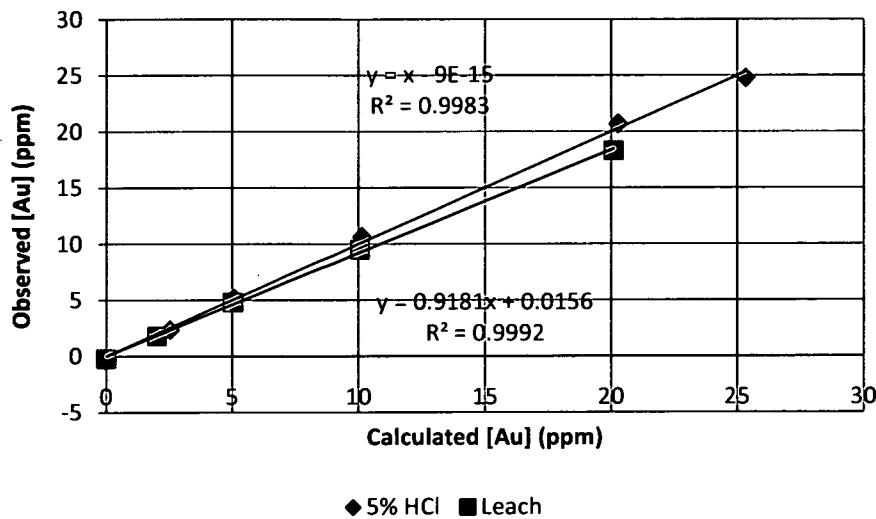


Figure 2.2 Comparison of 5% HCl and ammoniacal thiosulfate leach matrix effects at 242.8nm

The ammoniacal thiosulfate matrix shows a diminished slope of correlation in comparison to 5% HCl at both wavelengths with a least-squares fit of greater than 0.99.

Rearrangement of the linear best-fit equations forms Equation (2-2).

$$[Au]_{CORRECTED}^T = (M_w \cdot [Au]_{MATRIX}^T - E_w) \tag{2-2}$$

Table 2-4 contains calculated values for the variables M_w and E_w , the correlation coefficient and the zero correction respectively . Gold concentrations in an ammoniacal leach matrix should be scaled according to these linear factors. In practice, linear scaling factors were obtained for each bottle roll and elution experiment by comparison between the calculated and observed values for the gold concentration in either the Time Zero sample for the bottle roll experiments or a 25ppm aurothiosulfate standard made in the eluent used for that experiment.

Table 2-4 Calibration factors for [Au] in ammoniacal leach matrices

Solution Matrix	Wavelength (nm)	Correlation coefficient (M_w)	Zero Correction (E_w) (ppm)
Leach	242.8	1.0892	0.0156
Leach	267.6	1.1141	0.1443

The amount of gold present on the resin was calculated by difference, taking into account the small amounts of gold removed by sampling aliquots. The formula for conversion of bottle roll solution gold concentrations into resin gold loadings is given by Equation (2-3) below.

$$[Au]_R = \left[\frac{V_{t_0} \cdot [Au]_S^{t_0} - V_t \cdot [Au]_S^t - \sum_{N=t_0}^{t-1} A_N \cdot [Au]_S^N}{M_R} \right] \quad (2-3)$$

where $V_t = V_{t_0} - \sum_{N=t_0}^{t-1} A_N$ and

t_0 = Time zero for resin insertion into the synthetic leach

t = Elapsed time since t_0 in minutes at fixed intervals

$[Au]_R^t$ = Gold concentration on resin at time t in ppm

$[Au]_S^t$ = Gold concentration in solution at time t in ppm

V_t = Volume of synthetic leach remaining at time t in litres

A_N = Volume of aliquot taken at time t in litres

M_R = Mass of anhydrous resin sample in grams

N = Time step of Sigma function

2.2.6.4 Quantification of errors associated with AAS measurements

Quantification of errors associated with AAS measurements were performed using the method of least-squares² whereby a line of best fit described by Equation (2-4) was drawn through the calibration points on a plot of absorbance versus concentration.

$$y = mx + b \quad (2-4)$$

The standard deviation in absorbance, s_y , was then calculated according to Equation (2-5)

$$s_y = \sqrt{\frac{\sum(d_i^2)}{n-2}} \quad (2-5)$$

where d_i is the vertical deviation of the absorbance reading and n is the number of degrees of freedom.

The standard deviation of the slope and intercept were then calculated according to Equations (2-6) and (2-7)

$$s_m^2 = \frac{s_y^2 m}{D} \quad (2-6)$$

$$s_b^2 = \frac{s_y^2 \sum(x_i^2)}{D} \quad (2-7)$$

$$D = \begin{vmatrix} \sum(x_i^2) & \sum x_i \\ \sum x_i & n \end{vmatrix} \quad (2-8)$$

where s_m is an estimate of the standard deviation of the slope, s_b is an estimate of the standard deviation of the intercept and D is given by Equation (2-8).

Quantification of the error associated with the calibration curves was performed using Equation (2-9)

$$s_x = \frac{s_y}{|m|} \sqrt{\frac{1}{k} + \frac{x^2 n}{D} + \frac{\sum(x_i^2)}{D} - \frac{2x \sum x_i}{D}} \quad (2-9)$$

Where $|m|$ is the absolute value of the slope, n is the number of data points and k is the number of replicate measurements of the unknown.

Addition or subtraction and multiplication or division of the errors associated with a measurement were calculated by Equations (2-10) and (2-11)

$$s_w = \sqrt{(s_a)^2 + (s_b)^2} \quad (2-10)$$

$$s_w = \sqrt{\left(\frac{s_a}{a}\right)^2 + \left(\frac{s_b}{b}\right)^2} \quad (2-11)$$

where $w = a + b$ for Equation (2-10) and $w = a/b$ for Equation (2-11) and s_w , s_a and s_b are the

standard deviations in w , a and b respectively.

All errors reported throughout this thesis are standard deviations.

2.2.7 Trithionate synthesis and characterisation (Ion-exchange and photometric)

Sodium trithionate ($\text{Na}_2\text{S}_3\text{O}_6 \cdot 3\text{H}_2\text{O}$) has been shown to be the major competing species in an ammoniacal thiosulfate leach³. This reagent is unavailable commercially, however it can be synthesised readily from sodium or potassium thiosulfate using a method modified from Kelly and Wood⁴.

Sodium thiosulfate pentahydrate ($\text{Na}_2\text{S}_2\text{O}_3 \cdot 5\text{H}_2\text{O}$; 150g; 99%; *Chem Supply*) was dissolved in 90.0mL of MilliQ water in a 500mL three-necked round bottomed flask on a magnetic stirrer and chilled in an ice/salt bath to approximately 1°C.

Chilled (-4°C) 30% (w/v) hydrogen peroxide (H_2O_2 ; 140mL; 30%; *Ajax*) was then added with stirring from a 250mL dropping funnel. During this process, rate of addition of peroxide was such that the temperature of the solution was maintained below 20°C. After addition had been completed, stirring was ceased and the vessel maintained below 1°C for 1-2 h. Sodium sulfate was observed to precipitate during this period and was removed by vacuum filtration using a Büchner flask through a Whatman No. 1 filter paper.

The recovered sodium sulfate was washed with 100mL of chilled (-4°C) ethanol which was added to the filtrate. The sodium sulfate was then discarded and the filtrate transferred to a 2L beaker and mixed with 250mL of ice-cold ethanol and maintained at ~0° for 1 h to further precipitate residual sodium sulfate. This was also removed by vacuum filtration and washed on the filter with 200mL ice-cold ethanol which was added to the filtrate. The washed precipitate was then discarded.

The filtrate was then added to 1L of ice-cold ethanol in a 5L beaker, stirred thoroughly and left at 3°C for 1-2 h. The precipitate formed at this stage was sodium trithionate and was

recovered by filtration under vacuum and washed with 50mL of ice-cold ethanol, 50mL of acetone and followed by drying in a vacuum dessicator over phosphorus pentoxide under vacuum. This process yielded 29.88g of sodium thiosulfate which was labelled as Crop 1. Upon standing, further precipitation occurred following filtration. This product was covered and washed as above, yielding 13.29g of product which was labelled as Crop 2.

2.2.7.1 Analysis of polythionates by cyanolytic colourimetry

Analysis of both crops was performed by a cyanolytic colourimetric method published by Kelly and Wood⁴. In this method, the various polythionates were reacted with potassium cyanide to form potassium thiocyanate. This was then reacted with ferric nitrate, forming the dark-red ferric thiocyanate complex. This complex was then analysed spectrophotometrically against a set of known standards to yield the concentrations of the various polythionates in the sample.

The required reagents were prepared as follows:-

Buffer: 50mL of 0.2M NaH_2PO_4 was added to 39mL of 0.2M NaOH

Ferric nitrate reagent: 151.72g of $\text{Fe}(\text{NO}_3)_3 \cdot 9\text{H}_2\text{O}$ was dissolved in 112mL 70% of perchloric acid and made to 250.00mL with MilliQ water.

Potassium cyanide: 0.65216g of KCN was dissolved in of 100.00mL MilliQ water to give a final concentration of 0.1001M.

Copper sulfate: 2.49738g $\text{CuSO}_4 \cdot 5\text{H}_2\text{O}$ was dissolved in 100.00mL MilliQ water to give a final concentration of 0.1000M.

All analyses were performed in 25.00mL volumetric flasks. The sample to be analysed was added to approximately 4mL of buffer in the flask and MilliQ water was added to give a total

Chapter 2 – General Experimental

volume of approximately 10mL. Three replicate sets of samples were treated separately as indicated below:-

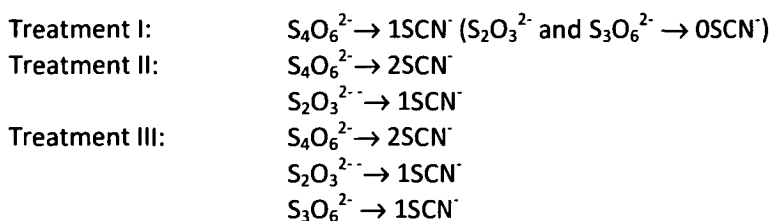
Treatment 1: The samples were cooled to between 5-10°C in an ice bath and 5mL of chilled KCN at an equivalent temperature was added with rapid stirring and the mixtures left at 5-10°C for 20 min.

Treatment 2: As per treatment I, however 1.5mL of the CuSO₄ solution was added after 5 min and the mixtures left at 5-10°C for 10-15 min.

Treatment 3: 5.00mL of the KCN solution was added with rapid mixing followed by heating in a boiling water bath for 45 min. After cooling, 1.5mL of the CuSO₄ solution was added and the solution left at room temperature for 10-15 min.

An aliquot of ferric nitrate reagent (3.00mL) was then added to each flask with continuous agitation and the flasks allowed to equilibrate to room temperature. After making up the flasks volumes of all flasks to 25.00mL with MilliQ water, the solutions were then analysed spectrophotometrically at 460nm using quartz cuvettes against a set of 1-10µM standards made using potassium thiocyanate as per Treatments I and II above.

In each of the treatments above, the various thionate species react differently to yield different amounts of thiocyanate. For each treatment, the amount of thiocyanate produced is:-



Therefore the concentration of the various species is given by Equations (2-12) to (2-14) below.

$$[\text{Tetrathionate}] = \text{Treatment I} \quad (2-12)$$

$$[\text{Thiosulfate}] = \text{Treatment II} - 2[\text{Tetrathionate}] \quad (2-13)$$

$$[\text{Trithionate}] = \text{Treatment III} - \text{Treatment II} \quad (2-14)$$

Linear calibration curves were produced using potassium thiocyanate ($r^2 = 0.995$ or greater) and used to quantify each crop for polythionate content.

Crop 1 was assayed to contain 88.6% trithionate, 11.3% tetrathionate with the remainder being sulfate while Crop 2 was assayed to contain 86.8% trithionate, 13.1% tetrathionate with the remainder being sulfate.

2.2.7.2 Analysis of polythionates by ion chromatography

Analysis of polythionates was also performed by an ion chromatographic method as described in Jeffrey, *et. al*⁵.

Polythionate ions were separated using a Dionex (Sunnyvale, CA, USA) ICS-3000 ion chromatography system consisting of an AS50 autosampler, an ICS-3000DP dual pump in single pump mode, an ICS-3000DC dual column and detector thermal compartment and an AD20 variable wavelength UV-visible absorbance detector, coupled to Chromeleon version 6.70 SP1 Build 1843 software. Dionex AS16 and AG16 analytical and guard columns were used at 25°C for all separations with an eluent consisting of 150mM sodium perchlorate at a flowrate of 1mL/min. This eluent was prepared by neutralisation of perchloric acid (HClO_4 ; 25.00mL; 70%; Sigma-Aldrich) with sodium hydroxide (NaOH ; 12.00g; 98%; *BDH*) and dilution with MilliQ water to 2.00L. The pH of the resultant solution was adjusted to 7.3 to prevent polythionate breakdown in acidic solutions. All analytes were detected using UV detection at 200nm.

Samples were prepared for polythionate analysis by an initial 1:10 dilution of the leach solution in a 5% ethylenediamine solution ($\text{NH}_2\text{CH}_2\text{CH}_2\text{NH}_2$; 99%; *Ajax*.) This was to ensure

that the copper thiosulfate complex present would not mask the trithionate peak as suggested in the literature⁵

Standards were prepared by serial dilution of 50mM thiosulfate, trithionate and tetrathionate solutions. These were prepared by dissolution of sodium thiosulfate pentahydrate ($\text{Na}_2\text{S}_2\text{O}_3 \cdot 5\text{H}_2\text{O}$; 0.6305g; 99%; *Chem Supply*), sodium trithionate trihydrate ($\text{Na}_2\text{S}_3\text{O}_6 \cdot 3\text{H}_2\text{O}$; 0.7884g; 88.6%; synthesised in-house) and sodium tetrathionate dehydrate ($\text{Na}_2\text{S}_4\text{O}_6 \cdot 2\text{H}_2\text{O}$; 0.7671g; $\geq 98\%$; Sigma-Aldrich) in 50mL of MilliQ water. Typical standard preparations are given in Table 2-5.

Table 2-5 Preparation of polythionate standards

Polythionate standard (mL)	Final volume (mL)	Final [polythionate] (mM)
0.05	1	2.5
0.1	1	5
0.2	1	10
0.4	1	20
0.5	1	25

Standards were refrigerated to $\sim 4^\circ\text{C}$ when not in use to prevent polythionate degradation.

2.2.8 Gold leach preparation

The aurothiosulfate leach preparation was intended to be representative of those currently used in industry and were employed in all bottle roll tests. Although gold concentrations in industry are approximately 10ppm, double this was used to facilitate AAS analysis. The concentrations of leach reagents vary widely as reported in the literature, however a summary table is given in Table 2-6.

Chapter 2 – General Experimental

Ref#	Year	Ore type	[S ₂ O ₃ ²⁻]	Cation	[Cu]	Anion	[NH ₃]	[NH ₄ ⁺]	Ion	pH	Temp (°C)	Au%	Time (h)	Notes
6	1991	High Cu sulfide	1	Na	1 g/L	SO ₄	2	0.1-0.4	SO ₄		40 - 50	95.6	37623	
7	1992	Sulfide concentrate (<200mesh)	0.2	NH ₄	3.0 g/L		3	1-1.6	SO ₄	10.2	60	97	2	
8	1992	Oxidised Nevada ore	0.2	Na	1.0 mM		0.09			10.35	Amb	83	48	
9	1992	Cu sulfide concentrate	1		0.1		1			1	20	95		
10	1992	Sulfide Au concentrate	0.2-0.3		3 g/L		~2-4	1.4-2.2	SO ₄	10-10.5	60	>95	2	
11	1993	Sulfide concentrate (<300mesh)	0.7	NH ₄	4 g/L		1	0.4-2.0	SO ₄		20 - 60	96.3	14	
12	1993	Fine Cu ore	0.5	NH ₄	10-100mM	SO ₄	0.25			10.1	25	81.8	6	
13	1993	Cuprous ore	4-15%		0.02		0.5			7-10.8	50		4	
14	1994	Bio-oxidised C/S	0.05-0.2	Na/NH ₄	1.0 mM	SO ₄	0.1			9.2-10	Amb	64.7	72	1
15	1995	Cretaceous ore	2	Na	0.1	SO ₄	4			8.5-10.5	25-60	80	3	
16	1996	Oxidised C/S	0.025-0.1	NH ₄	50-100ppm	SO ₄	>7mM			7-8.7	40-55	81.2	4	
17	1996	Oxidised pyrite concentrate	~0.5		4 g/L	SO ₄	0.3-0.6				Amb	91.2	2	
18	1996	Bio-oxidised pyrite	0.13	NH ₄	0.5 g/L		pH 10			9.5-10	20	84.2	288	2
19	1996	Copper sulfide	0.4	Na/NH ₄	1.9 g/L		0.2			11	Amb	90	24	
20	1997	Bio-oxidised C/S	0.1	NH ₄	0.5 mM		0.1			9	Amb	66	2784	1
21	1997	Low grade C/S	0.1	NH ₄	0.5 mM		0.1				Amb		~6 months	1
22	1998	Autoclaved C/S	0.01-0.1	NH ₄	10-100ppm	SO ₄	>7mM			7-8.7	45-55	85	1	3
23	1998	Refractory Cu sulfide	0.5	NH ₄			6			10.2	Amb	95-97	24	
24	1999	Pyrite/chalcopyrite	0.3	NH ₄	0.05		6			10.2	Amb	72	1200	1
25	2000	Refractory C/S ore	0.05	NH ₄	0.03		0.1			7.5-8	40-60	81-92	8	
26	2000	Limonitic barite	2		6.4 g/L		4				25	80		
3	2001	Blended calcined ore	0.05							8-9.5	25-35		24	
27	2001	Autoclaved C/S	0.4	Na	4.0 g/L	SO ₄	1.87				Amb	90-100	7	2
28	2001	Sulfide concentrate	0.2	NH ₄	0.08	SO ₄	3	1	SO ₄	10.2	50	>95	3	
28	2001	Copper concentrate	0.7	NH ₄	2.0 g/L	SO ₄	2	0.2-0.4	SO ₄	10.2	50	95.9	1.5	
29	2001	Au-Cu sulfide concentrate	0.8	Na	0.05	SO ₄	4			10.2	Amb	96	96	
30	2001	Sulfide ore (Nevada)	0.1	Na	0		0			9	60	81	6	

Chapter 2 – General Experimental

31	2002	Silicate ore (Hishikari)	0.3	NH ₄	30 mM	SO ₄	1	9.5	Amb		
32	2002	Sulfide concentrate (Chile)	0.3	NH ₄	50 mM	SO ₄	>0.2	10	25	94	15
33	2002	Goldstrike preg-robbing ore	0.05	NH ₄	0.5 mM	SO ₄	0.1	7.5-8	40–60	86.7	8
34	2002	Fine silicate ore	0.05	NH ₄	0.1 mM	SO ₄	0.5	9.5	Amb	94	12
35	2002	Fine Cu-Pb-Zn concentrate	0.5	NH ₄	10 g/L	SO ₄	0	6-7	70	99	1

Table 2-6 Development of thiosulfate leaching³⁶

Notes: All concentrations in mol/L unless stated otherwise

Au%: percentage of embedded gold in solution; g/L: grams per litre; ppm :parts per million (mg/L) ; Amb: ambient

1: Heap leach; 2: Column leach; 3: Resin-in-leach

The concentrations of the various reagents used in the leach are detailed in

Table 2-7.

Table 2-7 Standard Bottle Roll Artificial Leach Liquor Concentrations

Reagent	Formula	Concentration	ppm
Ammonia	NH_4OH	1.00M	
Ammonium chloride	NH_4Cl	0.100M	
Ammonium thiosulfate	$(\text{NH}_4)_2\text{S}_2\text{O}_3$	0.100M	
Cupric sulfate	$\text{CuSO}_4 \cdot 5\text{H}_2\text{O}$	3.149mM	200
Sodium aurothiosulfate	$\text{Na}_3[\text{Au}(\text{S}_2\text{O}_3)_2] \cdot 2\text{H}_2\text{O}$	0.101mM	20

The leach liquor was made freshly prior to each bottle roll test, allowing a resin:leach ratio of 1g:100mL. The leach was made according to the following sequence to prevent precipitation of the various copper salts and to minimise the oxidation of the thiosulfate prior to use:-

Ammonia solution was added to the appropriate volumetric flask and made up to ~50% of the total volume with MilliQ water.

Ammonium chloride was added and shaken to dissolve.

Copper sulfate was then washed in with approximately 50mL of MilliQ water. A white copper precipitate was often noticed, which redissolved with shaking.

Ammonium thiosulfate was added and the solution shaken gently to aid dissolution.

Sodium aurothiosulfate was then added. The resultant solution was then made up to the final volume with MilliQ water.

A 10.00mL aliquot of this leach solution was retained for AAS analysis as the time zero (t_0) sample.

2.2.9 Gold uptake methods

Once the ion-exchange capacity of the resins had been determined as per section 2.2.4, it was necessary to determine the ability of the resins to uptake aurothiosulfate. This was performed both in water and in leach as described below

2.2.9.1 Gold uptake from water

Aurothiosulfate uptake was first determined in MilliQ water, to ensure that the resins would uptake the target analyte without interference from other leach species.

A small amount of sodium aurothiosulfate ($\text{Na}_3[\text{Au}(\text{S}_2\text{O}_3)_2] \cdot 2\text{H}_2\text{O}$; 0.0998g; 18.96mmol) was dissolved in 2L of MilliQ water yielding a final gold concentration of 18.7ppm. A mass of dry resin (1.000g) was then rehydrated with ~10mL of MilliQ water for 30 min. The excess water was removed by magnetic separation and the resins rinsed into 500mL polypropylene bottles with ~20mL aliquots of the aurothiosulfate solution to be used. A 10.00mL portion of the solution was taken as the Time Zero (t_0) sample. The bottle was then capped leaving ~20mL headspace above the solution. The bottles were placed into an orbital shaker and agitated at 200rpm for 24 h. The bottles were kept out of direct sunlight but were under constant indoor fluorescent light for the duration of the experiment. The solutions were only open to air during sampling for an equivalent time for each bottle, as indicated by Table 2-8.

Table 2-8 Sampling intervals for bottle roll tests

Sample	1	2	3	4	5	6	7	8	9	10
Minutes	30	60	90	120	180	240	360	480	720	1440
Hours	0.5	1	1.5	2	3	4	6	8	12	24

In order to sample the solution, each bottle was removed from the orbital shaker and the resin magnetically separated from the solution by the application of strong magnets to the outside of the bottle. The sampling time was recorded, the bottle opened and 10.00mL of the solution was removed and decanted into an acid-washed glass vial. The vial was then sealed with an air-tight polyethylene cap and the bottle re-sealed and returned to the orbital shaker to allow resuspension of the resin. The vial was then stored in a dark, cool place until AAS analysis was able to be performed as per Section 2.2.6.

2.2.9.2 Gold uptake methods in synthetic leach solution

Once aurothiosulfate uptake had been confirmed in MilliQ water, it was then repeated in a synthetic leach solution to ascertain the interaction and competition of other species within the leach.

A synthetic leach solution was prepared as per Section 2.2.8 and a similar process was adhered to as described in Section 2.2.9.1.

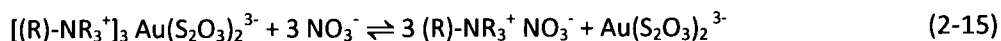
2.2.10 Gold elution methods

Once gold has been adsorbed onto the resin, it must then be removed. There are three possible mechanisms for attempting this, namely modification of the resin, modification of the gold species and ion-exchange interaction. Since all resins used in the study contain quaternary ammonium functional groups it was not possible to change the charge on the functional group through pH gradients. Modification of the aurothiosulfate species was achieved using acidic thiourea³⁶, while ion-exchange selectivity as a method of removal of

the adsorbed aurothiosulfate species was attempted using 2M sodium nitrate and alkaline thiocyanate solutions.

2.2.10.1 Gold elution using sodium nitrate

High concentrations of nitrate have been shown to remove the aurothiosulfate species from ion-exchange resins in leach systems³⁷. The mechanism for this removal is understood to be simple ion-exchange competition. The nitrate ion has a lesser ion-exchange selectivity coefficient for the quaternary ammonium functional groups on the resin than the previously adsorbed aurothiosulfate complex, however as it is in a much greater concentration than the aurothiosulfate complex, it will be preferentially adsorbed and therefore displace the adsorbed aurothiosulfate complex. The reaction proceeds via the Equation (2-15)



where (R) is the stationary (2-16) substituent.

A known mass of resin was loaded with aurothiosulfate from a synthetic leach solution. A 10.00mL sample of the leach was taken before and after resin contact for AAS analysis. These samples were analysed to allow a gold mass balance to be calculated according to Equation 2-8 where the concentration of gold in the leach is in parts per million.

$$mass\ Au_{resin} = \frac{[Au]_{To} - [Au]_{final}}{Volume\ of\ leach} \quad (2-16)$$

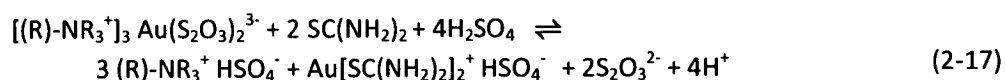
The aurothiosulfate loaded resin was then slurry-packed into an IEX column (~25mL capacity, ~10mL diameter) with a porosity #3 sintered-glass frit at the base and allowed to settle for 5-10 min . 2M sodium nitrate eluent solution (NaNO₃; >98%; Griffin and George) was prepared by dissolution of 169.99g of sodium nitrate in 2L of water. This solution was then allowed to flow through the system at 1mL min⁻¹ and the column effluent collected at 2

minute intervals into acid-washed glass vials and sealed with air-tight polyethylene stoppers for AAS analysis.

2.2.10.2 Gold elution using acidic thiourea

The second method whereby aurothiosulfate can be removed from the resin involves alteration of the gold complex from aurothiosulfate to gold thiourea.

The resin was loaded with aurothiosulfate and eluted in a similar manner to Section 2.2.10.1 and takes place according to Equation (2-17)



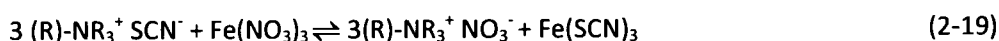
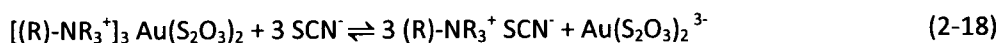
where (R) is the stationary phase and R is an alkyl substituent.

The acidic thiourea eluent was then prepared by the dissolution of 12.506g of concentrated sulfuric acid (H₂SO₄; 98%) and 18.031g of thiourea ((NH₂)₂CS; 99%; Ajax) into 100mL of water. This was then made up to 500mL giving a final concentration of 0.474M thiourea in 0.255M sulfuric acid and stored in a polyethylene bottle until use. The eluent was then passed through the packed resin at 1mL min⁻¹ and fractions collected at 10 minute intervals for 50 min. The sampling rate and elution time were both increased if necessary. The fractions collected were then analysed by AAS for gold concentration, diluting with eluent where necessary to bring the concentration of the gold within the linear range of the detector. A 25ppm standard of gold was also made in acidic thiourea eluent to allow for quantification of any matrix effects during AAS analysis.

2.2.10.3 Gold elution using basic thiocyanate followed by ferric nitrate

Thiocyanate has been shown to remove aurothiosulfate from ion-exchange resins³⁸. The adsorbed thiocyanate eluent ions are removed and the resin regenerated by elution with ferric chloride³⁸.

The resin was loaded with aurothiosulfate and eluted in a similar manner to Section 2.2.10.1 and occurs according to the elution and regeneration Equations (2-18) and (2-19).



where (R) is the stationary phase and R is an alkyl substituent.

A thiocyanate eluent was then prepared by the dissolution of potassium thiocyanate (KSCN; 405.3g; 98%, *Byproducts and Chemicals Pty Ltd*) and sodium hydroxide (NaOH; 49.99g; 98%: *BDH*) into 5.00L MilliQ water. This eluent was then passed through the packed IEX columns at 1 mL min^{-1} for 250 min with fractions collected into acid-washed glass vials every 5 min. The fractions collected were then analysed by AAS for gold concentration, diluting with thiocyanate eluent where necessary to bring the gold concentration within the linear range of the detector. A 10 and 20ppm gold standard was made up in the thiocyanate eluent to allow for quantification of any matrix effects during AAS analysis.

Following elution of the gold complex from the resin, it was then necessary to regenerate the resin by passing a ferric nitrate eluent through the column at 1 mL min^{-1} . This ferric nitrate eluent was prepared by the dissolution of 90.96g of ferric nitrate ($Fe(NO_3)_3 \cdot 9H_2O$;) in 1.00L of MilliQ water, giving a final concentration of 0.200M Fe^{3+} . The resins were deemed to be qualitatively regenerated when no more dark-red coloured ferric thiocyanate was observed in the column effluent.

2.2.11 Gold selectivity testing via trithionate competition

Trithionate has been determined to be a major competitor for aurothiosulfate adsorption from the leach solutions³⁹. The major source of trithionate in a leach solution is the decomposition of thiosulfate. A study into trithionate competition on the resin surface was

thus deemed necessary, to allow a timeframe for leach decomposition and hence resin contact

The leach composition employed was similar to that detailed in Section 2.2.8. A known mass of resin was loaded with aurothiosulfate from a synthetic leach solution. A 0.05M solution of sodium trithionate was prepared from sodium trithionate whose synthesis is described in Section 2.2.7. A 5.00mL aliquot of the leach solution was taken before and after aurothiosulfate uptake for AAS analysis to allow for gold mass balance calculations. The sampling and addition regime is described in Table 2-9, giving a final concentration of trithionate in the leach of approximately 10mM. This does not include trithionate that was formed from breakdown of leach components. A trithionate concentration of 10mM was determined to be equivalent to the level present in the leach after 12h in leach⁴⁰.

Table 2-9 Sampling and trithionate addition procedure

Sample	1	2	3	4	5	6	7	8	9	10
Minutes	30	60	90	120	150	180	210	240	270	300
Hours	0.5	1	1.5	2	2.5	3	3.5	4	4.5	5
Volume leach removed (mL)	5	5	5	5	5	5	5	5	5	5
Volume trithionate added (mL)	5	5	5	5	5	5	5	5	5	5

2.2.12 Gold saturation testing

Total aurothiosulfate loading capacity of the resin is an important factor to consider in industrial leach systems. Higher total gold capacities are preferable in that they allow the resin-in-pulp or resin-in-leach system to operate with a lower resin load.

A known mass of dry resin (2.500g) was contacted with 250mL of a 100ppm solution of sodium aurothiosulfate ($\text{Na}_3[\text{Au}(\text{S}_2\text{O}_3)_2] \cdot 2\text{H}_2\text{O}$) in a 250mL glass jar suspended in a thermostatically controlled water bath. The resin was then stirred with polyethylene anchor

stirrers at 330rpm and allowed to equilibrate for 24 h. The resin was magnetically separated from the solution and a 5.00mL aliquot of the solution was taken for AAS analysis.

This was repeated at time intervals of according to Table 2-10.

Table 2-10 Sampling intervals for aurothiosulfate saturation testing

Sample	1	2	3	4	5	6	7	8	9	10
Minutes	30	60	90	120	180	240	360	480	720	1440
Hours	0.5	1	1.5	2	3	4	6	8	12	24

2.2.13 Resin microanalysis preparation and testing

Resins were prepared for microanalysis by weighing out ~10mg of resin dried as per Section 2.2.2. This was then crushed in an agate mortar and pestle and submitted for microanalysis.

2.2.14 Resin destruction testing

Resins were tested for adsorbed gold by charring a known mass of aurothiosulfate loaded resin in 20mL of hot concentrated sulfuric acid (H₂SO₄; 98%; Merck). Concentrated nitric acid (~20mL; HNO₃; 69%; Merck) was then added dropwise until the solution had clarified. Small amounts of hydrogen peroxide (H₂O₂; 30%; Ajax) were added if sulfide precipitates resulted to oxidise sulfides to sulfate. Hydrochloric acid (5.00mL) was also added to ensure gold dissolution. The resultant solution was then made up to 100mL and analysed by AAS for gold concentration. A 25ppm gold chloride standard was made in identical acid concentrations to allow for quantification of matrix effects by comparison to the 25ppm gold standard.

2.3 References

1. Burge, R. E.; Bradford, P. G., *Analytical Chemistry of Polymers, Part I*. Third ed.; Interscience Publishers, Inc.: New York, 1966; Vol. XII.
2. Harris, D. C., *Quantitative chemical analysis*. 6th ed.; W.H. Freeman: New York, 2003.
3. O'Malley, G. P.; Nicol, M. J. In *Recovery of gold from thiosulfate solutions and pulps with ion-exchange resins.*, Cyanide: Social, Industrial and Economic Aspects. Proceedings of a Symposium held at the Annual Meeting of TMS, New Orleans, LA, February 12-15th, 2001; Young, C. A.; Twidwell, L. G.; Anderson, C. B., Eds. TMS, Warrendale, PA, USA: New Orleans, LA, 2001; pp 469-483.
4. Kelly, D. P.; Wood, A. P., Synthesis and determination of thiosulfate and polythionates. *Methods in Enzymology* **1994**, 243, 475-501.
5. Jeffrey, M. I.; Brunt, S. D., The quantification of thiosulfate and polythionates in gold leach solutions and on anion exchange resins. *Hydrometallurgy* **2007**, 89, (1-2), 52-60.
6. Hu, J.; Gong, Q. In *Substitution of Sulfate for Sulfite During Extraction of Gold by Thiosulfate Solution.*, Randol Gold Forum, Cairns, Queensland., 16-19 April, 1991, 1991; Randol International Ltd. (USA): Cairns, Queensland., 1991; pp 333-336.
7. Cao, C.; Hu, J.; Gong, Q., Leaching Gold by Low Concentration Thiosulfate Solution. *Transactions of the Nonferrous Metals Society of China* ISSN: 1003-6326 **1992**, 2, (4), 21-25.
8. Langhans, J. W. J.; Lei, K. P. V.; Carnahan, T. G., Copper-catalysed thiosulfate leaching of low-grade gold ores. *Hydrometallurgy* **1992**, 29, 191-203.
9. Jiang, T.; Xu, S.; Chen, J. In *Gold and Silver extraction by Ammoniacal Thiosulfate Catalytical Leaching at Ambient Temperature.*, Proceedings of the First International Conference on Modern Process Mineralogy and Mineral Processing, no idea., 1992; no idea., 1992; pp 648-653.
10. Cao, C.; Hu, J.; Gong, Q. In *Leaching Gold by Low Concentration Thiosulfate Solution.*, Randol Gold Forum, Vancouver, 1992; Randol International; Golden, Colo.: Vancouver, 1992; pp 293-298.
11. Gong, Q.; Hu, J.; Cao, C., Kinetics of Gold Leaching From Sulfide Gold Concentrates With Thiosulfate Solution. *Trans. Nonferrous Met. Soc. China* **1993**, 3, (4), 30-36.
12. Gundiler, I. H.; Goering, P. D. In *Thiosulfate leaching of gold from copper-bearing ores.*, SME Annual Meeting, Reno, Nevada, February 15-18, 1993, 1993; SME: Reno, Nevada, 1993; pp Paper #93-281.
13. Jiang, T.; Chen, J.; Xu, S., A Kinetic Study of Gold Leaching with Thiosulfate. In *Hydrometallurgy: Fundamentals, Technology & Innovations.*, 1993; Vol. Chapter 7, pp 119-126.
14. Wan, R., -Y. ; LeVier, K. M.; Clayton, R. B. Hydrometallurgical process for the recovery of precious metal values from precious metal ores with thiosulfate lixiviant. US 5354359, 11 Oct., 1994
15. Abbruzzese, C.; Fornari, P.; Massidda, R.; Veglio, F.; Ubaldini, S., Thiosulfate leaching for gold hydrometallurgy. *Hydrometallurgy* **1995**, 39, 265-276.
16. Marchbank, A. R.; Thomas, K. G.; Dreisinger, D.; Fleming, C. Gold recovery from refractory ores by pressure oxidation and thiosulfate leaching. US Patent 5,536,297, Patent Application Date: 10 Feb. 1995 Patent publication Date : 16 July 1996, 1996.
17. Panayotov, V. T. In *A technology for thiosulfate leaching of Au and Ag from pyrite concentrate.*, Changing scopes in Mineral Processing: Proceedings of the 6th International Mineral Processing Symposium, Kusadasi, Turkey, Sept. 24-26, 1996, 1996; Kernal, M., et al., Ed. Kusadasi, Turkey, 1996; pp 563-566.
18. Groudev, S. N.; Spasova, I. I.; Ivanov, I. M., Two-stage microbial leaching of a refractory gold-bearing pyrite ore. *Miner. Eng.* **1996**, 9, (7), 707-713.

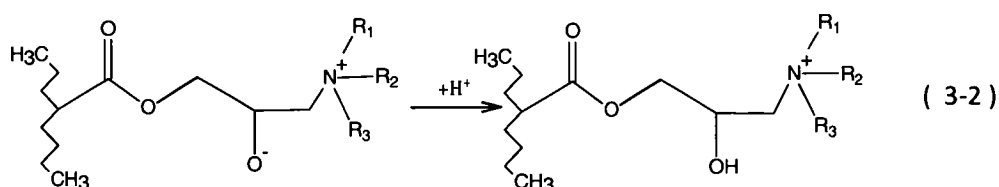
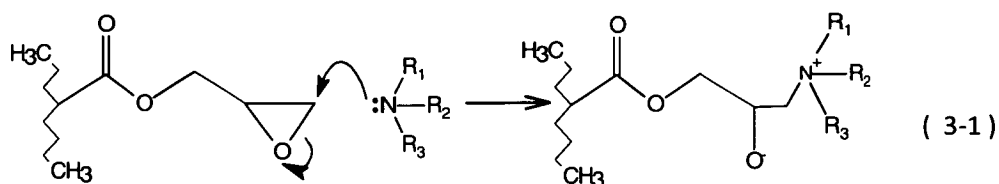
19. Yen, W. T.; Stogran, K.; Fujita, T., Gold extraction from a copper bearing ore by thiosulfate leaching. *Resources Treatment Technology* **1996**, 43, (2), 83-87.
20. Wan, R. Y.; Brierley, J. A., Thiosulfate leaching following biooxidation pretreatment for gold recovery from refractory carbonaceous-sulfidic ore. *Min. Eng. - Littleton* **1997**, 49, (8), 76-88.
21. Wan, R. Y. In *Importance of Solution Chemistry for Thiosulfate Leaching of Gold*, World Gold '97 Conference, Singapore, 1-3 September, 1997, 1997; Australasian Institute of Mining and Metallurgy, Carlton, VIC: Singapore, 1997; pp 159-162.
22. Thomas, K. G.; Fleming, C.; Marchbank, A. R.; Dreisinger, D. Gold recovery from refractory carbonaceous ores by pressure oxidation, thiosulfate leaching and resin-in-pulp adsorption. US 5,785,736, 28 July 1998 Submitted 16 July 1996, 1998.
23. Yen, W. T.; Aghamirian, M. M.; Deschenes, G.; Theben, S. In *Gold Extraction from Mild Refractory Ore using Ammonium Thiosulfate.*, International Symposium on Gold Recovery, May 1998, 1998; Yen, W. T., Ed. Unpublished.: 1998; p 11.
24. Yen, W. T.; Guo, H.; Deschenes, G. In *Development in Percolation Leaching with Ammonium Thiosulfate For Gold Extraction of a Mild Refractory Ore.*, EPD Congress 1999, San Diego, CA, USA, Feb 28- Mar 4, 1999; Mishra, B., Ed. The Minerals, Metals and Materials Society, Warrendale, PA, USA: San Diego, CA, USA, 1999; pp 441-455.
25. Fleming, C. A.; McMullen, J.; Thomas, K. G.; Wells, J. A. In *Recent advances in the development of an alternative to the cyanidation process - based on thiosulfate leaching and resin in pulp*, SME Annual Meeting (2001), Denver, Colorado, February 26-28, 2001; SME: Denver, Colorado, 2001; pp {1-11} Preprint.
26. Meggiolaro, V.; Niccolini, G.; Miniussi, G.; Stefanelli, N.; Trivellin, E.; Llinas, R.; Ramirez, I.; Baccelle Scudeler, L.; Omenetto, P.; Primon, S.; Visona, D.; Abbruzzese, C.; Fornari, P.; Massidda, R.; Piga, L.; Ubaldini, S.; Ball, S.; Monhemius, A. J., Multidisciplinary approach to metallogenic models and types of primary gold concentration in the Cretaceous arc terranes of the Dominican Republic. *Trans. Inst. Min. Metall. Section B (Applied Earth Science)* **2000**, 109, (May-Aug), B95 - B104.
27. Schmitz, P. A.; Duyvesteyn, S.; Johnson, W. P.; Enloe, L.; McMullen, J., Ammoniacal thiosulfate and sodium cyanide leaching of preg-robbing Goldstrike ore carbonaceous matter. *Hydrometallurgy* **2001**, 60, 25-40.
28. Chen, J.; Zhang, Y.; Lu, K.; Gong, Q.; Zhu, G., Studies on environmentally friendly leaching processes in China. *Chinese J. of Chem. Eng.* **2001**, 9, (1), 5-11.
29. Aylmore, M. G., Treatment of a Refractory Gold-Copper Sulfide Concentrate by Copper Ammoniacal Thiosulfate Leaching. *Miner. Eng.* **2001**, 14, (6), 615-637.
30. Ji, J.; Fleming, C. A.; West-Sells, P. G.; Hackl, R. P. Method for Thiosulfate Leaching of Precious-Metal Containing Materials. WO 01/88212 A2, 22 November 2001, 2001.
31. Arima, H.; Fujita, T.; Yen, W. T., Gold cementation from ammonium thiosulfate solution by zinc, copper and aluminium powders. *Mater. Trans* **2002**, 43, (3), 485-493.
32. Navarro, P.; Vargas, C.; Villarroel, A.; Alguacil, F. J., On the use of ammoniacal/ammonium thiosulphate for gold extraction from a concentrate. *Hydrometallurgy* **2002**, 65, (1), 37-42.
33. Fleming, C. A.; McMullen, J.; Thomas, K. G.; Wells, J. A., Recent Advances in the Development of an alternative to the cyanidation process: Thiosulfate leaching and resin in pulp. *Minerals & Metallurgical Processing* **2002**, 20, (1), 1-9.
34. Arima, H.; Fujita, T.; Yen, W. In *Thermodynamic Evaluation on Gold Oxidation and Reduction Mechanisms in Ammonium Thiosulfate Solution*, SME Annual Meeting 2002, Phoenix, Arizona, Feb. 25-27, 2002; SME: Phoenix, Arizona, 2002; pp 1-13.
35. Ficeriova, J.; Balaz, P.; Boldizarova, E.; Jelen, S., Thiosulfate leaching of gold from a mechanically activated CuPbZn concentrate. *Hydrometallurgy* **2002**, 67, 37-43.

36. Grosse, A. C. The development of Resin Sorbents for Gold in Ammoniacal Thiosulfate Leach Liquors. PhD, University of Tasmania, Hobart 2006.
37. O'Malley, G. P. The Elution of Gold from Anion Exchange Resins. WO 01/23626 A1, 5 April 2001, 2001.
38. Fleming, C. A. Regeneration of Thiocyanate Resins. US4608176, August 6, 1986, 1986.
39. Zhang, H. G.; Dreisinger, D. B., The adsorption of gold and copper onto ion-exchange resins from ammoniacal thiosulfate solutions. *Hydrometallurgy* **2002**, 66, (1-3), 67-76.
40. O'Reilly, J. W. Chromatographic and Electromigrative Determination of Sulfur-Oxygen Anions in Gold Thiosulfate Leach Solutions. PhD, University of Tasmania, Hobart, 2003.

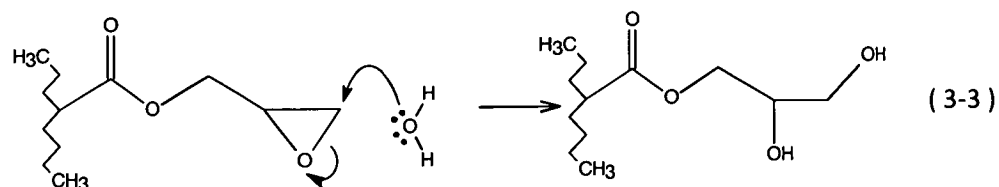
3 Resin Synthesis and Characterisation

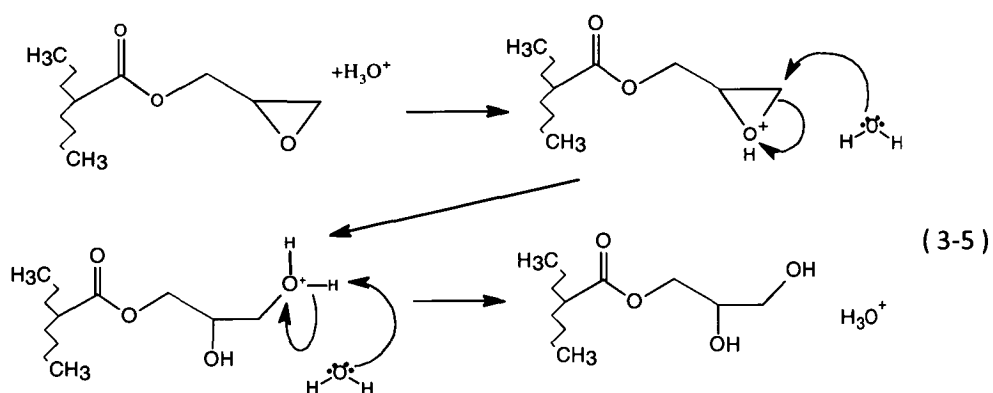
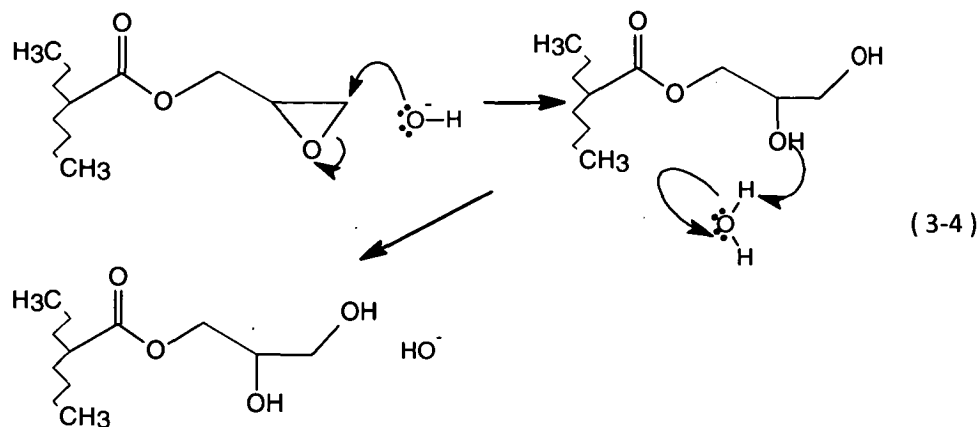
3.1 Introduction

Resin synthesis was performed via the S_N2 addition of an amine to an epoxide present on the resin substrate as indicated in Equations (3-1) and (3-2).



Epoxide ring opening during the storage of unfunctionalised resin was a major problem as it meant with time there was a decrease in the amount of amine that could be attached to the resin substrate. The mechanism by which the epoxide ring opening reaction is performed is described in Equation (3-3) below. This reaction can be catalysed by the presence of trace acid or trace base as shown in Equations (3-4) and (3-5). In the case of Equation (3-3), the ring opening is via S_N2 addition of the hydroxide followed by scavenging of a proton from the solvent, whereas in Equation (3-4) the ring opening is via S_N1 addition of the nucleophile to the protonated epoxide.





The degree of ring opening present was quantified by determining the total epoxide content of fresh resin supplied by Orica Watercare, together with that of resin that had been stored in equivalent conditions in Hobart. These determinations were performed as described in Section 2.2.3. Once characterisation of the total epoxide content had been performed, suitable resins were able to be selected for functionalisation. Resins that showed less than 1.5 mmol/g of available epoxide were found to be unsuitable for functionalisation with the larger amines expected to be selective for the aurothiosulfate complex.

3.2 Resin synthesis

3.2.1 Single step resin synthesis and variations

Initial information provided by Orica Watercare contained the following resin

functionalisation procedure, based on 5 g of resin. This was then adjusted according to the

resin amount required for each characterisation or functionalisation. The masses of reagents used are detailed in Table 3-1 and Table 3-2.

Table 3-1 Resin functionalisation mixture with cyclohexanol

Reagent	Formula	Percentage (% w/v)	Mass(g)	Moles	Molecular weight
MIEX resin		21.6	5		
Cyclohexanol	C ₆ H ₅ OH	10	2.314	0.09984	100.1602
Water	H ₂ O	57.7	13.35		
Trimethylamine hydrochloride	(CH ₃) ₃ N.HCl	10.7	2.476	0.02591	95.572

Table 3-2 Resin functionalisation mixture without cyclohexanol

Reagent	Formula	Percentage (%w/v)	Mass(g)	Moles	Molecular weight
MIEX resin		31.6	5		
Water	H ₂ O	57.7	13.35		
Trimethylamine hydrochloride	(CH ₃) ₃ N.HCl	10.7	2.476	0.02591	95.572

3.2.1.1 Bottle resin reactor synthesis

Initial resin synthesis methodology used a 50 mL Schott reagent bottle to contain the resin functionalisation solution. The reagent bottle was heated by immersion in a paraffin oil bath on a magnetic stirrer with the resin being circulated by the oscillating magnetic field from the stirrer-hotplate. No magnetic stirrer bar was required as the resin was satisfactorily circulated by the magnetic field. Due to the magnetic nature of the resin, use of a magnetic stirrer bar actually decreased resin functionalisation by binding resin beads to the bar and thereby decreasing the level of suspension of the resin and hence access of the functionalisation solution.

3.2.1.2 Resin reactor setup and characterisation

A further refinement to the resin functionalisation procedure was to employ a resin reactor comprising a 500 mL, flanged, five-necked flask coupled to a Liebig condenser, a

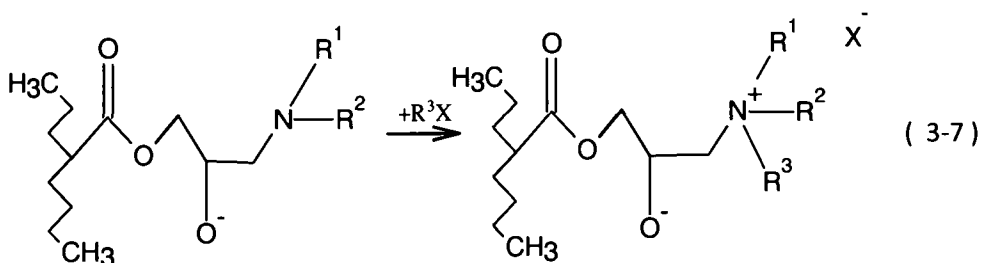
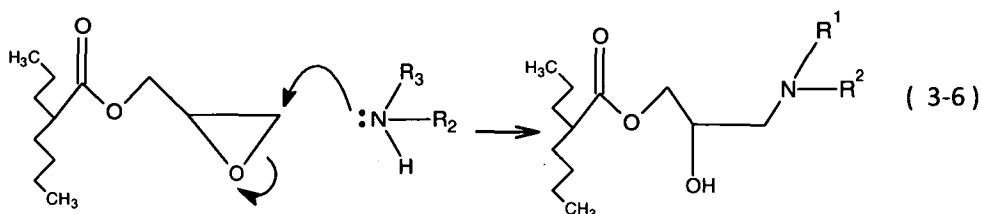
thermometer adapter and an overhead stirrer fitted with a glass stirrer gland. The stirrer used with this reactor was equipped with a two-bladed Teflon stirrer head. The remaining vacant ports on the flask were stoppered for the duration of the resin synthesis. The resin reactor was then suspended in either a paraffin or silicon oil bath that was situated on a lab jack. This apparatus was labelled as Resin Reactor 1.

A second resin reactor was developed employing either a 250mL or 500mL three-necked, round-bottomed flask suspended in an oil bath that was situated on a lab jack. A glass stirrer shaft was then placed inside a large-bore Liebig condenser and attached to an overhead stirrer. The condenser and stirrer were set into the middle port of the resin reactor. One of the remaining ports contained a thermometer adapter, while the other was stoppered for these syntheses. This apparatus was labelled as Resin Reactor 2.

Dried resin was decanted from a measuring cylinder into the resin reactor along with the required amount of water. The resin was then allowed to hydrate and swell for 30 min with the reactor being stirred at 300 rpm. This rate was applied throughout all resin functionalisation experiments. The stoichiometric amount of the amine hydrochloride was then added to a small amount of water and heated to aid dissolution. If the amine was able to be used as the free base, this was used neat in place of the amine hydrochloride. The resin reactor was then heated, the amine solution added and all ports on the reactor were sealed. The resins were allowed to react at temperature, followed by removal of the flask from the oil bath to allow for cooling. Once the reactor was cool to touch, the resins were recovered by magnetic separation from the functionalisation mixture and rinsed. Each rinse was allowed to stand for 5 min to allow solvent to penetrate the porous structure of the resin beads. The resins were then sampled for ion-exchange functionality as per Section 2.2.4.

3.2.2 Multi-step resin synthesis, including variations

Multi-step resin synthesis was performed to attach various alkyl groups to secondary and tertiary amines to create quaternary ammonium species, as per Equations (3-6) and (3-7).



A small amount of previously functionalised and dried resin was decanted from a glass weigh boat into a resin reactor. The only modifications made to the resin reactors were to include the addition of a nitrogen purge adapter and a 100 mL pressure-equalising dropping funnel to two of the vacant ports on Resin Reactor 1. When employing Resin Reactor 2, the vacant port was fitted with a 100 mL pressure-equalising dropping funnel coupled to a nitrogen purge adapter.

3.2.3 Resin backbone IR vibrations

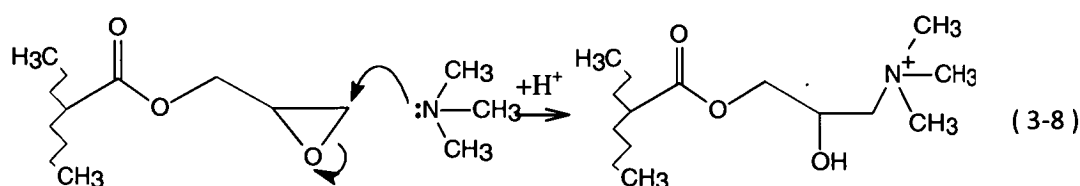
ATR infrared analysis of blank and unfunctionalised MIEG was performed as per Section 2.2.5 and each synthesis displays their characteristic vibrations. The analysis was performed on both unfunctionalised resin and on resins that had all epoxide groups converted to vicinal diols.

IR (ATR) Unfunctionalised: ν (cm^{-1}) = 3435; 2944; 1724; 1449; 1148; 907; 695; 634.

3.2.4 Elemental Analysis

Due to the industrial supply of the MIEXTM substrate, elemental analysis comparison of carbon and oxygen was not possible.

3.2.5 Trimethylamine (TMA)



Trimethylamine hydrochloride was used for initial resin synthesis, both as a mimic of the Orica MIEX-DOC resin and as a test for resin viability.

3.2.5.1 Preparation 1

Cyclohexanol ($\text{C}_6\text{H}_5\text{OH}$; 2.41 g; 99%; *Merck*) and trimethylamine hydrochloride ($(\text{CH}_3)_3\text{N.HCl}$; 2.471 g; >98%; *Fluka*) were dissolved in 13.4 mL of MilliQ water in a 100mL reagent bottle containing 5.104 g of dry unfunctionalised MIEX resin. This flask was then suspended in an oil bath and heated to 80°C on a magnetic stirrer/heater for 3 h with the resin being suspended by a rapid movement of the magnetic field from the stirrer. After cooling, the resin beads were then removed by magnetic separation and decantation of the reaction mixture followed by rinsing with ethanol (3x50 mL), acetone (1x50 mL), ethanol (1x50 mL) and then water (3x50 mL). Resins were subsequently characterised by ion-exchange analysis yielding a capacity in the range of 1.93 and 2.51 mmol/g.

IR (ATR): ν (cm^{-1}) = 3360 (OH str.); 2944 (CH_3 str.); 1719 (C=O str.); 1478 (CH_2 sym. def in amine; CH_2 sym. def in epoxide); 1350 (OH str.); 1157 (C-O-C asym. str.); 964; 695; 634

EA: Carbon (38.05%); Hydrogen (5.60%); Nitrogen (2.96%) Other (53.39%) ; Calculated for 1.9mmol/g ion-exchange capacity: Nitrogen (2.72%)

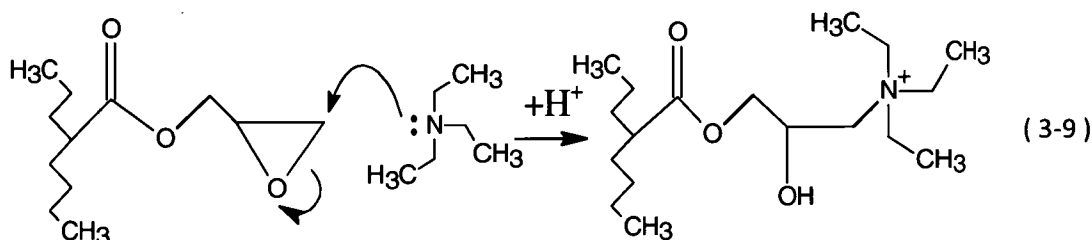
3.2.5.2 Preparation 2

Settled MIEX resin (37 mL) was added to 65 mL of MilliQ water and stirred in Resin Reactor 1. Trimethylamine hydrochloride ((CH₃)₃N.HCl; 13.43 g; >98%; *Fluka*) was then dissolved in the minimum volume of water and added. The reactor was then heated to 80°C for 3 h with constant stirring. The resin beads were then collected and rinsed as per Preparation 1 and stored for further analysis.

Further syntheses were performed as above and gave ion-exchange capacities in the range between 1.93 and 2.51 mmol/g of capacity.

IR data were identical to that for Preparation 1.

3.2.6 Triethylamine (TEA)



Settled MIEX resin (38mL) was added to 65mL of MilliQ water in Resin Reactor 1.

Triethylamine hydrochloride ((CH₃CH₂)₃N.HCl; 13.46g; ≥99%; *Fluka*) was dissolved in the minimum volume of water and added to the reactor. The reactor was then heated to 80°C for 3 h with constant stirring. The resin beads were then magnetically separated from the cooled reaction mixture before rinsing with ethanol (3x 50mL), acetone (1x 50mL), ethanol (1x 50ml) and then water (3x50 mL). Resins were then stored for further analysis.

Repeated syntheses gave ion-exchange capacities in the range of 0.46 and 0.76 mmol/g.

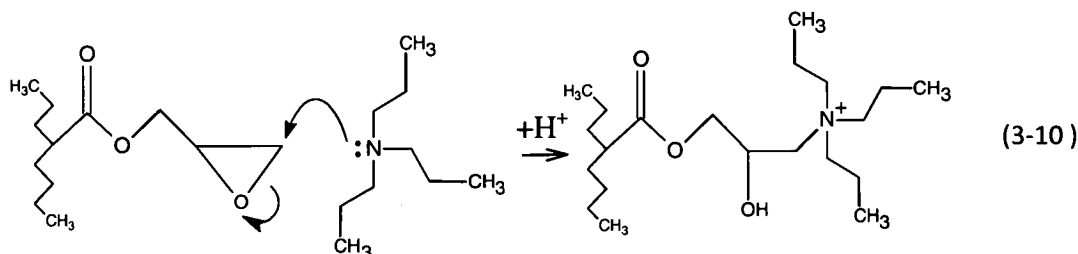
Syntheses were also repeated on Fe-free MIEX for comparison and for quantification of the amount of iron present.

IR MIEX (ATR): ν (cm⁻¹) = 3426 (OH str.); 1720 (C=O str.); 1158; 693; 633

IR Fe-Free MIEX (ATR): ν (cm^{-1}) = 3400 (OH str.); 1716 (C=O str.); 1455 (CH_2 def.); 1393; 1159 (C-N str.); 710

EA: Carbon (41.51%); Hydrogen (5.60%); Nitrogen (0.40%) Other (53.10%); Calculated for 0.219mmol/g ion-exchange capacity: Nitrogen (0.31%)

3.2.7 Tributylamine (TBA)

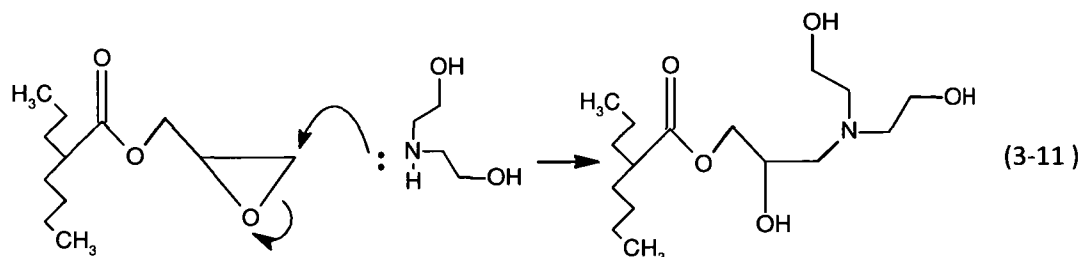


Cyclohexanol (2.47g) and tributylamine ($(\text{CH}_3\text{CH}_2\text{CH}_2)_3\text{N}$; 2.34 g; 97%; *Fluka*) were dissolved in 13.4 mL of MilliQ water in a 100 mL reagent bottle containing 5.005 g of dry unfunctionalised MIEX resin. This flask was then suspended in an oil bath and heated to 80°C on a magnetic stirrer/hotplate for 3 h with the resin being suspended by a rapid movement of the magnetic field from the stirrer. The resin beads were then removed by magnetic separation and decantation of the reaction mixture, followed by rinsing with ethanol (3x50 mL), acetone (1x50 mL), ethanol (1x50 mL) and then water (3x 50mL).

As the ion-exchange capacity of the resin was 0.16 mmol/g, this synthesis was deemed unsuccessful.

IR (ATR): ν (cm^{-1}) = 3400(OH str.); 2933 (CH_2 def.); 1722 (C=O str.); 1454 (CH_2 def.); 1386; 1154 (C-N str.) 695; 634

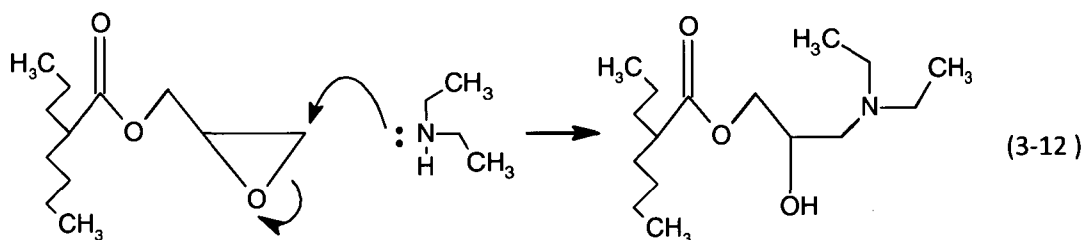
3.2.8 Diethanolamine (DAM)



Cyclohexanol (5.18 g) and diethanolamine ($\text{HOCH}_2\text{CH}_2)_2\text{NH}$; 2.499g; 98%; *May and Baker*) were dissolved in 14.48 mL of MilliQ water in a 100mL reagent bottle containing 5.472 g of dry unfunctionalised MIEX resin. This was then suspended in an oil bath and heated to 80°C on a magnetic stirrer/heater for 3 h with the resin being suspended by a rapid movement of the magnetic field from the stirrer. The resin beads were then removed by magnetic separation and decantation of the reaction mixture followed by rinsing with ethanol (3x50 mL), acetone (1x50 mL), ethanol (1x50 mL) and then water (3x50 mL).

IR (ATR): ν (cm^{-1}) = 3371 (OH str.); 2932 (CH_2 def.); 1722 (C=O str.); 1451 (CH_2 def.); 1154 (C-N str.); 635

3.2.9 Diethylamine (DEA)



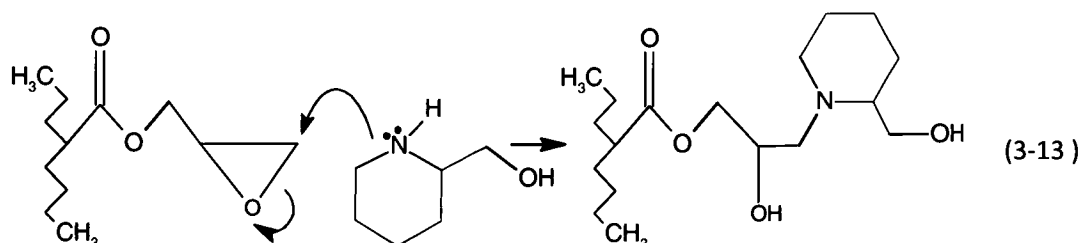
Settled MIEX resin (75.0mL) was added to 135.0mL of MilliQ water in Resin Reactor 1.

Diethylamine ($(\text{CH}_3\text{CH}_2)_2\text{NH}$; 15.06g; 98%; *Aldrich*) was dissolved in the minimum amount of water and added to the reactor. The reactor was then heated to 80°C for 3 h with constant stirring. The resin beads were then magnetically separated from the cooled reaction mixture

before rinsing with ethanol (3x50 mL), acetone (1x50 mL), ethanol (1x50 mL) and then water (3x50 mL). Resins were then stored for further analysis.

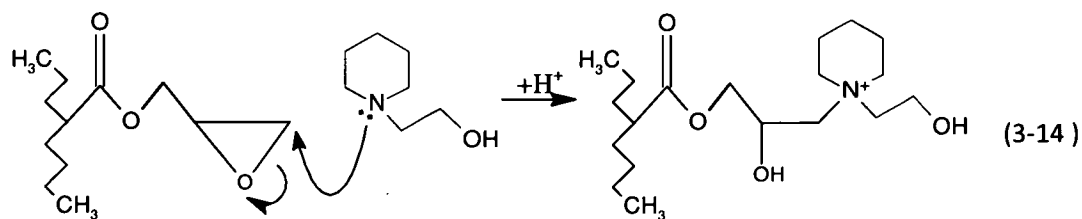
Repeated syntheses yielded an ion-exchange capacity of 0.14mmol/g.

3.2.10 2-Piperidine-methanol (2PM)



Settled resin (37.5mL) and MilliQ water (70mL) were mixed and stirred at 300 rpm in Resin Reactor 1. 2-piperidinemethanol (2(hydroxymethyl)piperidine; 11.85g; 97%; *Aldrich*) was dissolved in the minimum amount of water and added to the reactor. The reactor was then heated to 80°C for 3 h with constant stirring. The resin beads were then magnetically separated from the cooled reaction mixture and rinsed with ethanol (3x50 mL), acetone (1x50 mL), ethanol (1x50 mL) and then water (3x50 mL). Resins were then stored wet for further analysis.

3.2.11 Piperidine-ethanol (PET)



Settled MIEX resin (37.4 mL) was added to 65.0 mL of MilliQ water and stirred at 300rpm in Resin Reactor 1. 1-piperidine ethanol (N-(2hydroxyethyl)piperidine; 19.75 mL; 99%; *Aldrich*) was then added to the resin reactor and the resultant reaction mixture was then heated to 80°C for 3 h with constant stirring. The resin beads were then magnetically

Chapter 3 – Resin Synthesis and Characterisation

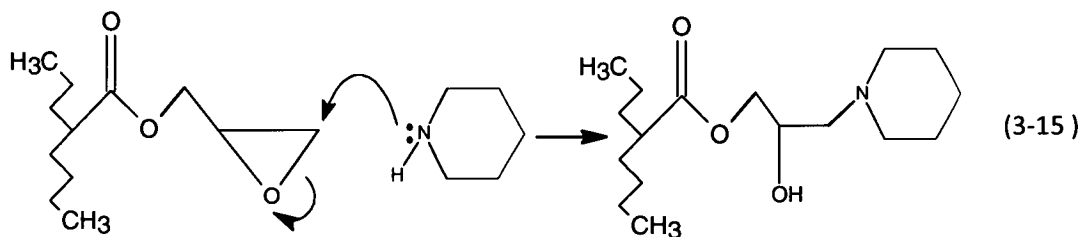
separated from the reaction mixture and rinsed with ethanol (3x50 mL), acetone (1x50 mL), ethanol (1x50 mL) and then water (3x50 mL). Resins were then stored wet for further analysis.

Syntheses were repeated several times as above and yielded ion-exchange capacities ranging between 0.4 and 0.7 mmol/g.

IR (ATR): ν (cm^{-1}) = 3365 (OH str.); 2941 (CH_2 def.); 1451 (CH_2 def.); 1387 (OH coupled CH_2 wag); 1243 & 1151 (CH_2 wag); 1048 (C-O str.); 941 (w); 879 (w) NR_4^+

EA: Carbon (41.28%); Hydrogen (5.18%); Nitrogen (0.82%) Other (52.72%) ; Calculated for 0.34mmol/g ion-exchange capacity: Nitrogen (0.47%)

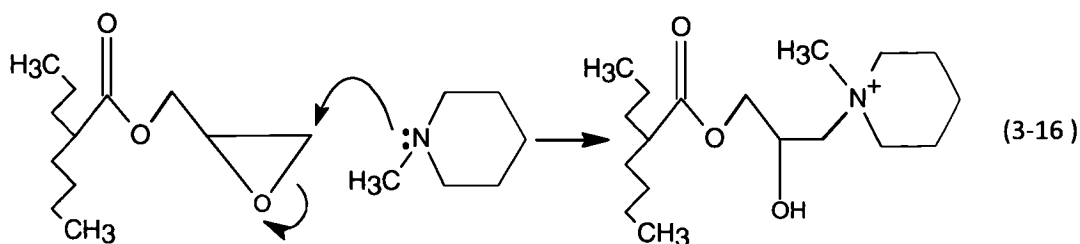
3.2.12 Piperidine (PIP)



Settled MIEX resin (73.0mL) was added to 200mL of MilliQ water and stirred at 300rpm in Resin Reactor 1. Piperidine ($\text{C}_5\text{H}_5\text{NH}$; 17.19g; $\geq 99.5\%$; Aldrich) was dissolved in the minimum amount of water and added to the resin reactor and the resultant reaction mixture was then heated to 80°C with constant stirring. The resin beads were then magnetically separated from the cooled reaction mixture and rinsed with ethanol (3x50 mL), acetone (1x50 mL), ethanol (1x50 mL) and then water (3x50 mL). Resins were then stored wet for further analysis and functionalisation.

IR (ATR): ν (cm^{-1}) = 3418 (OH str.); 2935 (CH_2 str.); 1722 (C=O str.); 1445 (CH_2 str); 1154 (CH_2 wag.);

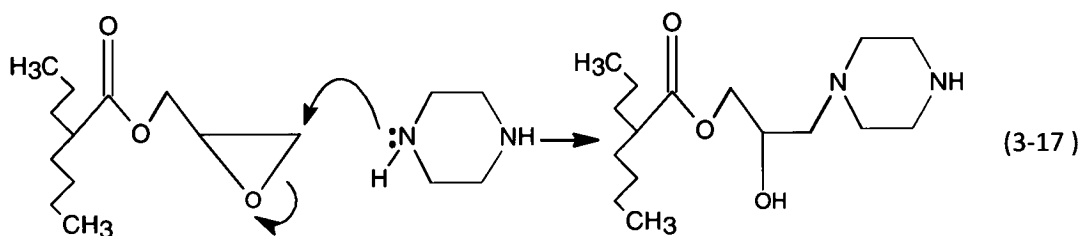
3.2.13 N-methyl piperidine (NIP)



Settled resin (75.0mL) was added to 135mL of MilliQ water and stirred at 300rpm in Resin Reactor 1. N-methyl piperidine ($C_5H_{10}NCH_3$; 19.99g; 24.50mL; 99%; *Aldrich*) was added to the resin reactor and the resultant reaction mixture was then heated to 80°C for 3 h with constant stirring. The resin beads were then magnetically separated from the cooled reaction mixture and rinsed with ethanol (3x50 mL), acetone (1x50 mL), ethanol (1x50 mL) and then water (3x50 mL). Resins were then stored wet for further analysis and functionalisation.

IR (ATR): ν (cm^{-1}) = 3371 (OH str.); 2937 (CH_2 def.); 1718 (C=O str.); 1560; 1454 (CH_2 def.); 1388 (OH coupled CH_2 wag); 1157 (CH_2 wag.); 695 (C-H out of plane def.); 634

3.2.14 Piperazine (PAZ)

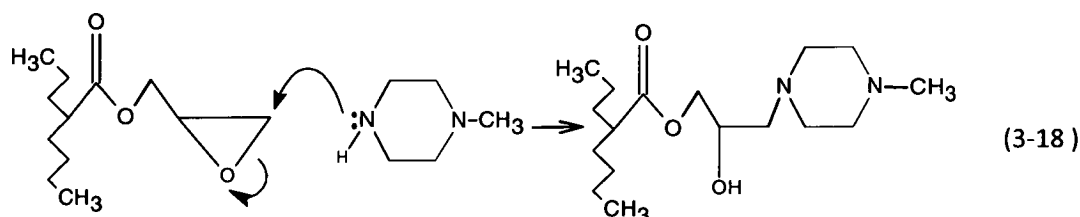


Settled MIEX resin (70mL) was added to 135mL of MilliQ water and stirred at 300rpm in Resin Reactor 1. Piperazine hexahydrate (1,4-Diazacyclohexane; 39.99g; >98%; *BDH*) was dissolved in the minimum amount of water and added to the resin reactor and the resultant reaction mixture was then heated to 80°C for 3 h with constant stirring. The resin beads were then magnetically separated from the cooled reaction mixture and rinsed with ethanol

(3x50 mL), acetone (1x50 mL), ethanol (1x50 mL) and then water (3x 50mL). Resins were then stored wet for further analysis and functionalisation.

IR (ATR): ν (cm^{-1}) = 3398 (OH str.); 2939 (CH_2 def.); 1722 (C=O str.); 1455 (CH_2 str.); 1152; 695; 635

3.2.15 N-methyl piperazine (NAZ)

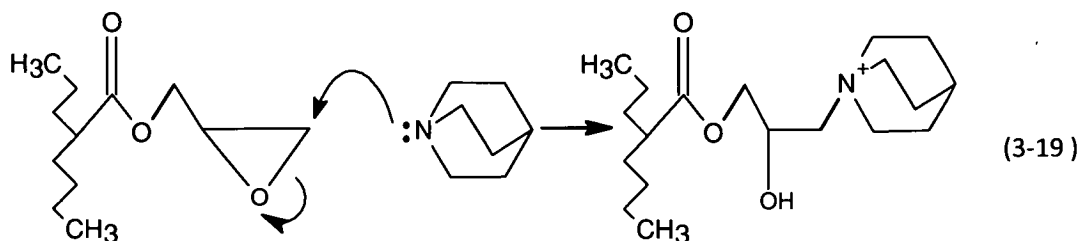


Settled MIEX resin (75.0mL) was added to 150mL of MilliQ water and stirred at 300rpm in Resin Reactor 1. N-methyl piperazine (17.8mL; >97%; *Fluka*) was added to the resin reactor and the resultant reaction mixture was then heated to 80°C for 3 h with constant stirring. The resin beads were then magnetically separated from the cooled reaction mixture and rinsed with ethanol (3x50 mL), acetone (1x50 mL), ethanol (1x50 mL) and then water (3x50 mL). Resins were then stored wet for further analysis and functionalisation.

Resins were subsequently characterised for ion-exchange capacity and yielded between 0.9 and 1.1 mmol/g for repeated syntheses.

IR (ATR): ν (cm^{-1}) = 3371 (N-H str; OH str.); 2940 (CH_3 str.); 1718 (C=O str.); 1559 (C-N str.); 1389 (CH_3 str.); 1149; 695(C-H out of plane def.); 635

3.2.16 Quinuclidine (QNU)



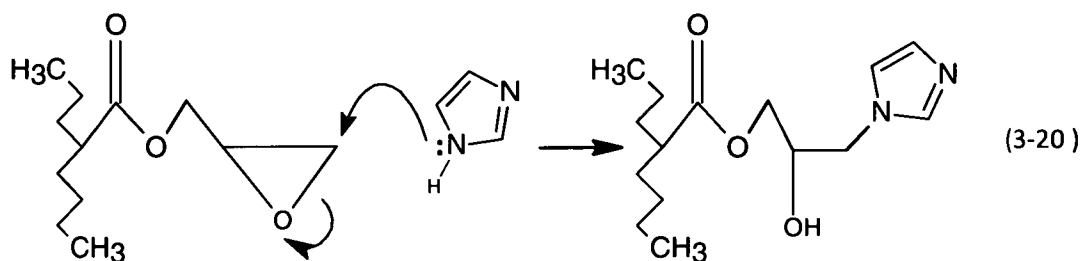
Settled MIEX resin (72.0mL) was added to 150mL of MilliQ water and stirred at 300rpm in Resin Reactor 1. Quinuclidine (1-Azabicyclo[2.2.2]octane; 22.72g; >97%; *Fluka*) was dissolved in the minimum amount of water and was added to the resin reactor. The resultant reaction mixture was then heated to 80°C for 3 h with constant stirring. The resin beads were then magnetically separated from the cooled reaction mixture and rinsed with ethanol (3x50 mL), acetone (1x50 mL), ethanol (1x50 mL) and then water (3x50 mL). Resins were then stored wet for further analysis and functionalisation.

Resins were subsequently characterised for ion-exchange capacity and yielded between 0.9 and 1.1 mmol/g for repeated syntheses.

IR (ATR): ν (cm⁻¹) = 3372 (OH str.); 2944 (CH₃ str.); 1715 (C=O str.); 1557 (C-N str.); 1465 (CH₃ str.); 1389 (OH str.); 1160; 982; 694(C-H out of plane def.); 634

EA: Carbon (39.62%); Hydrogen (5.25%); Nitrogen (1.69%) Other (53.44%) ; Calculated for 1.03mmol/g ion-exchange capacity: Nitrogen (1.44%)

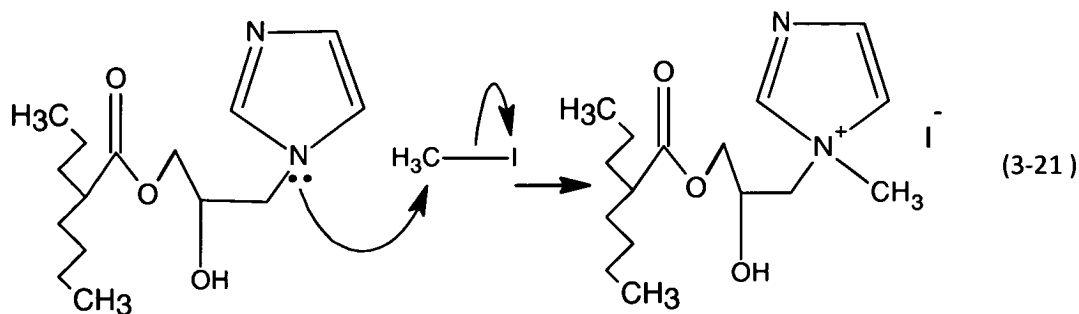
3.2.17 Imidazole (IMZ)



Settled MIEX resin (73.0mL) was added to 130mL of MilliQ water and stirred at 300rpm in Resin Reactor 1. Imidazole (1,3-Diaza-2,4-cyclopentadiene; 23.11g; 99%; *Aldrich*) was dissolved in the minimum amount of water with heating and was added to the resin reactor. The resultant reaction mixture was then heated to 80°C for 3 h with constant stirring. The resin beads were then magnetically separated from the cooled reaction mixture and rinsed with ethanol (3x50 mL), acetone (1x50 mL), ethanol (1x50 mL) and then water (3x50 mL). Resins were then stored wet for further analysis and functionalisation.

IR (ATR): ν (cm⁻¹) = 3152 (OH str.); 2934 (CH₂ str.); 1721 (C=O str.); 1559 (C=N str.); 1448 (CH₂ str.); 1388 (CH₃ str.); 1154; 695 (C-H out of plane def.); 634 (C=C-H vibration)

3.2.18 Methyl-imidazole (MIM)



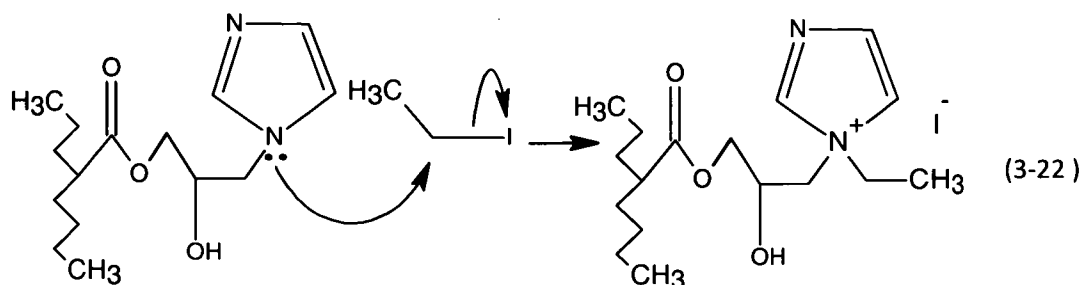
Dry imidazole functionalised MIEX resin (12.62g) was added to 150mL of dry DMF in Resin Reactor 2, which was then purged with dry nitrogen. The resin-DMF slurry was then stirred at 300rpm for 30 min to allow the resin to swell. Iodomethane (CH_3I ; 46.39g; GPR; BDH) was dissolved in 30mL dry DMF and added to the reactor dropwise over a 15 minute period. Residual iodomethane was then washed into the reactor with a 10mL aliquot of dry DMF. After addition of the iodomethane, the resin was then allowed to stir for ~20 h at room temperature followed by heating in an oil bath to 45°C for 4 h. The resin beads were then magnetically separated from the cooled alkylation mixture and rinsed with ethanol (3x50 mL), acetone (1x50 mL), ethanol (1x50 mL) and then water (3x50 mL). Resins were then stored wet for further analysis.

Ion-exchange capacities ranged between 0.7 and 1.2mmol/g for repeated syntheses.

IR (ATR): ν (cm^{-1}) = 3422 (OH str.); 1715(C=O str.); 1164(C-N str.);

EA: Carbon (39.21%); Hydrogen (4.71%); Nitrogen (3.31%) Other (SSSS%) ; Calculated for 1.01mmol/g ion-exchange capacity: Nitrogen (2.83%)

3.2.19 Ethyl-imidazole (EIM)



Imidazole functionalised resin (15.04g) was added to 150mL dry DMF in Resin Reactor 2, which was then purged with dry nitrogen. The resin-DMF slurry was then stirred at 300rpm for 30 min to allow the resin to swell. Dry iodoethane ($\text{CH}_3\text{CH}_2\text{I}$; 26.0mL; >99%; *Sigma-Aldrich*) was then added dropwise from a 100mL pressure equalising dropping funnel over a 10 minute period. Residual iodoethane was then washed into the reactor with a 10mL aliquot of dry DMF. After the addition of iodoethane, the resin was allowed to stir for ~20 h at room temperature followed by heating in an oil bath to 45°C for 4 h. The resin beads were then magnetically separated from the cooled reaction mixture and rinsed with ethanol (3x50 mL), acetone (1x50 mL), ethanol (1x50 mL) and then water (3x50 mL). Resins were then stored wet for further analysis.

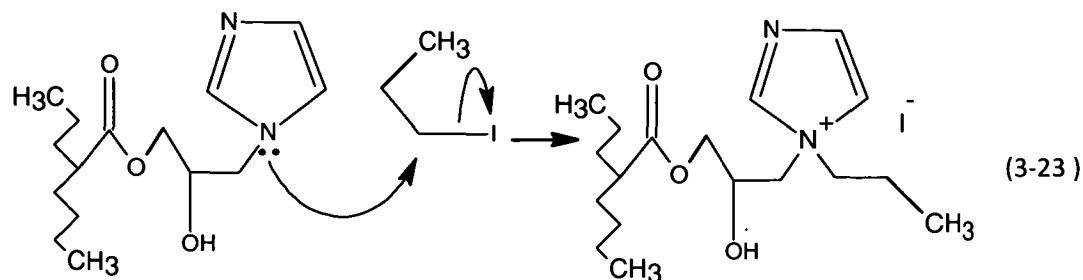
Ion-exchange capacities of functionalised resins ranged between 0.7 and 1.1 mmol/g.

IR (ATR): ν (cm^{-1}) = 3417 (OH str.); 1717 (C=O str.); 1449 (CH_2 def.); 1163(C-N str.); 879 (w)

NR_4^+

EA: Carbon (39.83%); Hydrogen (4.63%); Nitrogen (3.92%) Other (51.62%) ; Calculated for 1.08mmol/g ion-exchange capacity: Nitrogen (3.02%)

3.2.20 1-propyl-imidazole (1PIM)



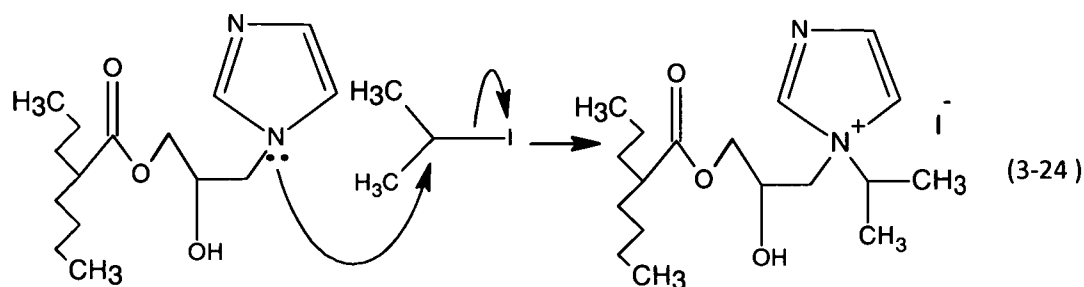
Imidazole functionalised resin (15.05g) was added to 150mL of dry DMF in Resin Reactor 2, which was then purged with dry nitrogen. The resin-DMF slurry was then stirred at 300rpm under a nitrogen atmosphere for 30 min to allow the resin to swell. 1-iodopropane ($\text{CH}_3\text{CH}_2\text{CH}_2\text{I}$; 20.0mL; 99% Aldrich) was then added dropwise from a 100mL pressure equalising dropping funnel over a 10 minute period and residual iodopropane was washed into the reactor with a 10mL aliquot of dry DMF. After addition of the iodopropane the resin was allowed to stir at room temperature for ~20 h followed by heating in an oil bath at 45°C for 4 h. The resin beads were then magnetically separated from the cooled mixture and then rinsed with ethanol (3x50 mL), acetone (1x50 mL), ethanol (1x50 mL) and then water (3x50 mL). Resins were then stored wet for further analysis.

Ion-exchange capacities ranged between 0.55 and 1.1mmol/g for repeated syntheses.

IR (ATR): ν (cm^{-1}) = 3410 (OH str.); 2977 (CH_2 def.); 1717 (C=O str.); 1449 (CH_2 def.); 1046 (CH_2 def.); 879 (w) NR_4^+

EA: Carbon (39.98%); Hydrogen (4.48%); Nitrogen (4.06%) Other (51.48%) ; Calculated for 1.07mmol/g ion-exchange capacity: Nitrogen (3.00%)

3.2.21 2-propyl-imidazole (2PIM)



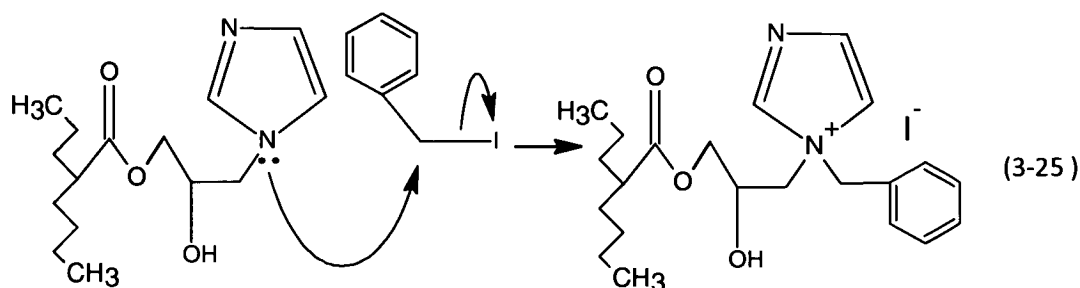
Dry imidazole functionalised resin (15.00g) was added to 150mL of dry DMF in Resin Reactor 2 which was then purged with dry nitrogen. The resin-DMF slurry was then stirred at 300rpm under a nitrogen atmosphere for 30 min to allow the resin to swell. 2-iodopropane ($\text{CH}_3\text{CHICH}_3$; 20.00mL; 99%; *Aldrich*) was then added dropwise from a 100mL pressure equalising dropping funnel over 10 min and residual iodopropane was washed into the reactor with a 10mL aliquot of dry DMF. After addition of the alkyl halide, the resin was allowed to stir at room temperature for ~20 h followed by heating in an oil bath at 45°C for 4 h. The resin beads were then magnetically separated from the cooled mixture and rinsed with ethanol (3x50 mL), acetone (1x50 mL), ethanol (1x50 mL) and then water (3x50 mL). Resins were then stored wet for further analysis.

Ion-exchange capacities ranged between 0.7 and 1.1 mmol/g.

IR (ATR): ν (cm^{-1}) = 3355 (OH str.); 2973 (CH_2 def.); 1720 (C=O str.); 1448 (CH_2 def.); 1159 (C-N str.); 1047 (CH_2 def.); 879 (w) NR_4^+ ; 695

EA: Carbon (40.31%); Hydrogen (4.79%); Nitrogen (4.03%) Other (50.87%) ; Calculated for 1.10mmol/g ion-exchange capacity: Nitrogen (3.11%)

3.2.22 Benzyl-imidazole (BIM)



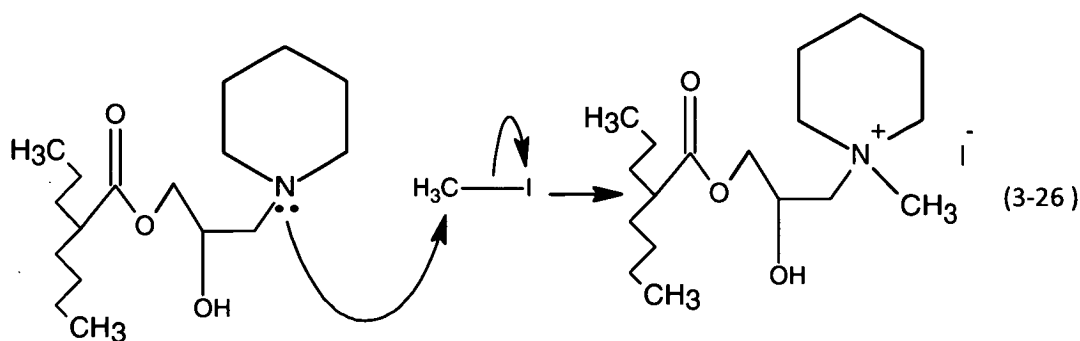
Dry imidazole functionalised resin (15.02g) was added to 150mL dry DMF in Resin Reactor 2 which was then purged with dry nitrogen. This was then stirred for 30 min at 300rpm under a nitrogen atmosphere to allow the resin to swell. Dry benzyl chloride ($\text{C}_6\text{H}_5\text{CH}_2\text{Cl}$; 45.0mL; $\geq 99\%$; *Fluka*) was then added dropwise over a 10 minute period from a pressure equalising dropping funnel and residual benzyl chloride was rinsed in with a 10mL aliquot of dry DMF. After the addition of the alkyl halide, the resin was then allowed to stir for ~ 20 h at room temperature then in an oil bath at 45°C for four h. The resin beads were then magnetically separated from the functionalisation mixture and rinsed with ethanol (3x50 mL), acetone (1x50 mL), ethanol (1x50 mL) and then water (3x50 mL). Resins were then stored wet for further analysis.

Ion-exchange capacities ranged between 0.7 and 1.1 mmol/g for successful syntheses.

IR (ATR): ν (cm^{-1}) = 3335 (OH str.); 2974 (CH_2 def.); 2885; 1721 ($\text{C}=\text{O}$ str.); 1560; 1449 (CH_2 def.); 1157 ($\text{C}-\text{N}$ str.); 879 (w) NR_4^+ ; 708; 632

EA: Carbon (39.94%); Hydrogen (4.66%); Nitrogen (5.07%) Other (50.33%) ; Calculated for 1.10mmol/g ion-exchange capacity: Nitrogen (3.08%)

3.2.23 Methyl-piperidine (MIP)



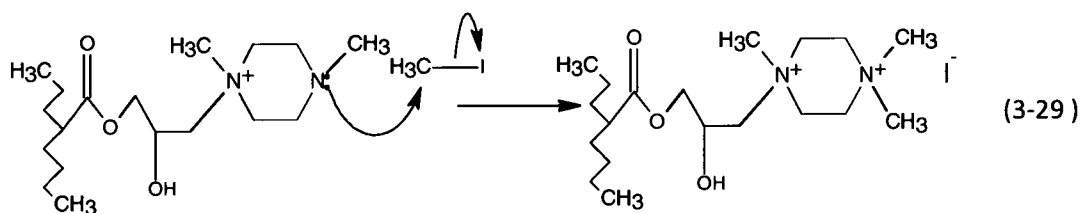
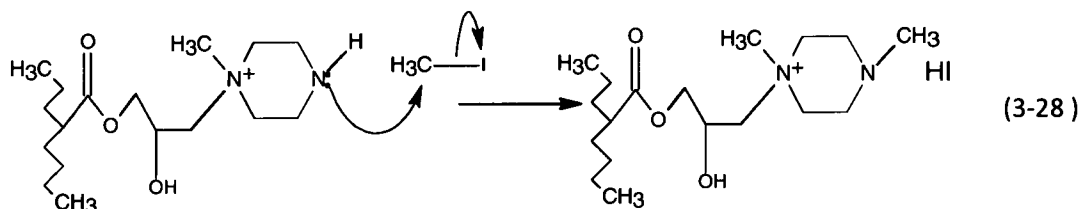
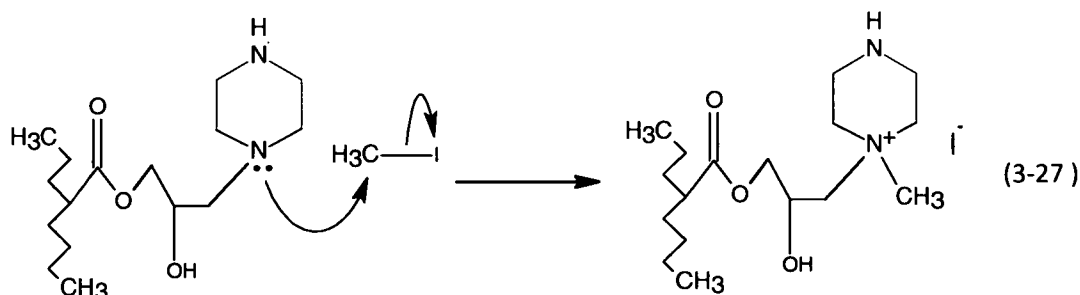
Dry piperidine functionalised resin (8.1g) was added to 150mL of dry DMF in Resin Reactor 2, which was then purged with dry nitrogen. The resin-DMF slurry was then stirred under a nitrogen atmosphere for 30 min at 300rpm to allow the resin to swell. Methyl iodide (CH_3I ; 21.5mL; GPR; BDH) was then added dropwise from a 100mL pressure equalising dropping funnel over a 10 minute period. The residual methyl iodide was then rinsed into the reactor with a 10mL aliquot of DMF and the mixture was allowed to stir for ~20 h at room temperature followed by heating in an oil bath at 45°C for 4 h. The resin beads were then magnetically separated from the cooled mixture and rinsed with ethanol (3x50 mL), acetone (1x50 mL), ethanol (1x50 mL) and then water (3x50 mL). Resins were then stored wet for further analysis

Syntheses were repeated several times as above and gave ion-exchange capacities of approximately 0.7 mmol/g.

IR (ATR): ν (cm^{-1}) = 3391 (OH str.); 2975 (CH_2 def.); 1719 ($\text{C}=\text{O}$ str.); 1450 (CH_2 def.); 1047 (CH_2 def.); 879 (w) NR_4^+

3.2.24 N,N dimethyl-piperazine (MAZ)

3.2.24.1 Preparation 1



Dry piperazine functionalised resin (15.05g) was added to 150mL of dry DMF in Resin

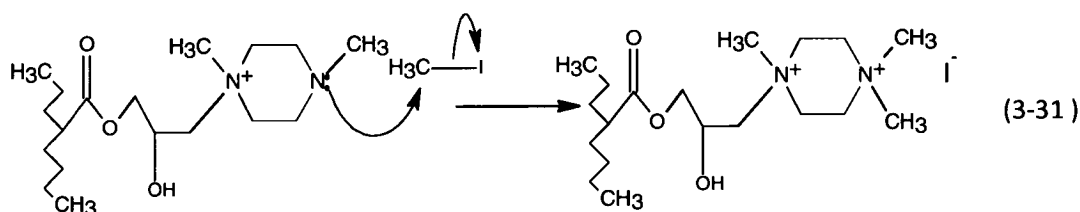
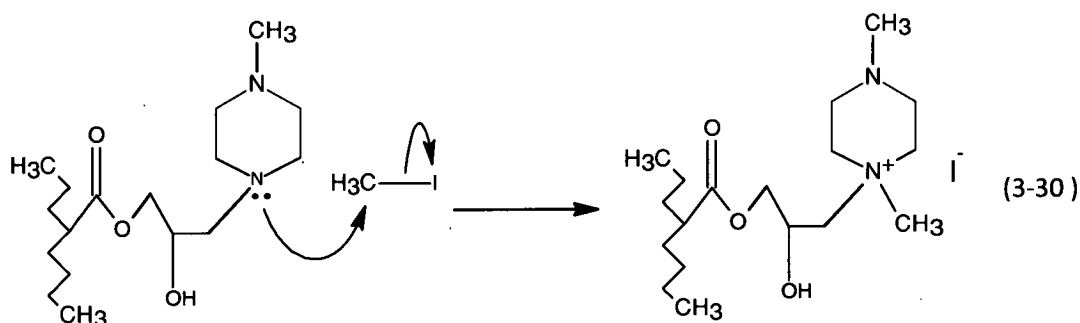
Reactor 2 which was then purged with dry nitrogen. The resin-DMF slurry was stirred under dry a nitrogen atmosphere for 30 min at 300rpm to allow the resin to swell. Methyl iodide (CH_3I ; 131.10g; 57.0mL; GPR; BDH) was added dropwise from a 100mL pressure equalising dropping funnel over a 10 minute period. Residual iodomethane was rinsed into the reactor with a 10mL aliquot of dry DMF and the mixture was then allowed to stir for ~20 h at room temperature followed by heating in an oil bath at 45°C for 4 h. The resin beads were then magnetically separated from the cooled mixture and rinsed with ethanol (3x50 mL), acetone (1x50 mL), ethanol (1x50 mL) and then water (3x50 mL). Resins were then stored wet for further analysis

Syntheses were repeated several times as above and gave ion-exchange capacities of approximately 0.7 mmol/g.

IR (ATR): ν (cm^{-1}) = 3406 (OH str.); 2976; 1717 (C=O str.); 1452(CH_2 def.); 1046; 879 (w) NR_4^+

EA: Carbon (28.87%); Hydrogen (3.71%); Nitrogen (1.61%) Other (65.80%) ; Calculated for 0.74mmol/g ion-exchange capacity: Nitrogen (2.08%)

3.2.24.2 Preparation 2

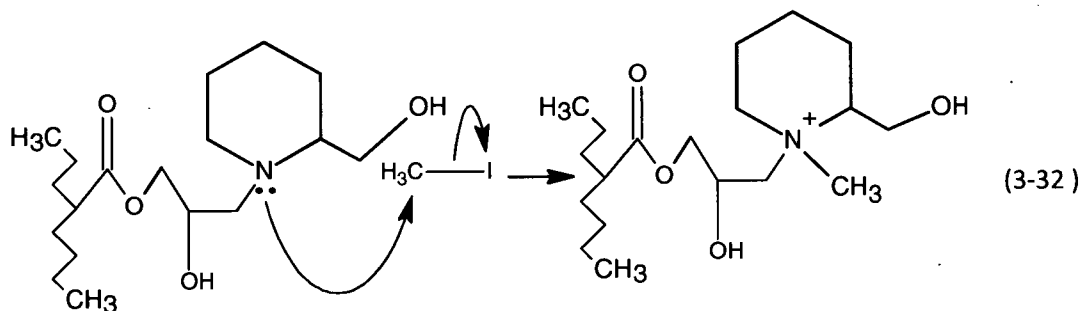


Dry N-methyl piperazine functionalised resin (7.10g) was added to 150mL of dry DMF in Resin Reactor 2 which was then purged with dry nitrogen. The resin-DMF slurry was then stirred under a dry nitrogen atmosphere for 30 min to allow the resins to swell. Dry iodomethane (CH_3I ; 42.0mL; 95.772g; GPR; BDH) was then added dropwise from a 100mL pressure equalising dropping funnel over a 10 minute period. Residual iodomethane was then rinsed into the reactor with a 10mL aliquot of dry DMF and the alkylation mixture was then allowed to stir for ~20 h at room temperature followed by heating in an oil bath at 45°C for 4 h. The resin beads were magnetically separated from the cooled mixture and then rinsed with ethanol (3x50 mL), acetone (1x50 mL), ethanol (1 x 50mL) and then water (3x50 mL). Resins were then stored wet for further analysis

Syntheses were repeated several times as above and gave a range of ion-exchange capacities between 1.3 and 1.8mmol/g.

IR (ATR): ν (cm^{-1}) = 3406 (OH str.); 2976; 1717 (C=O str.); 1452(CH_2 def.); 1046(C-N str.); 879 (w) NR_4^+

3.2.25 Methyl 2 piperidine methanol (M2PM)



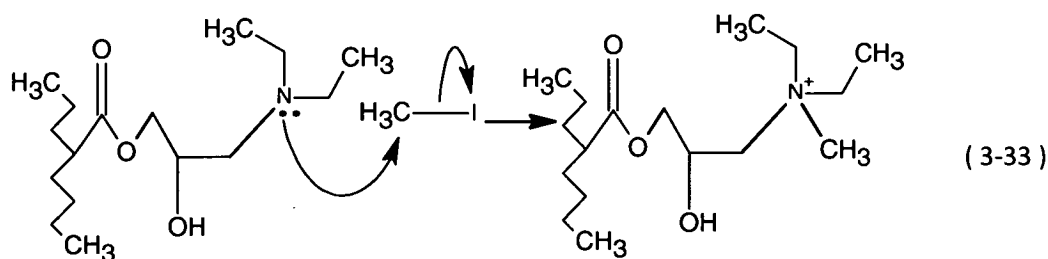
Dry 2-piperidine-methanol functionalised resin (13.37g) was added to 150mL of dry DMF in Resin Reactor 2 which was then purged with dry nitrogen. This was then stirred for 30 min at 300rpm under a nitrogen atmosphere to allow the resin to swell. Dry iodomethane (CH_3I ; 20.5mL; 46.745g; GPR; BDH) was then added dropwise from a 100mL pressure equalising dropping funnel over a 10 minute period. Any residual iodomethane present was rinsed into the reactor with a 10mL aliquot of dry DMF and the mixture was allowed to stir for ~20 h at room temperature followed by heating in an oil bath for 4 h at 45°C. The resin beads were magnetically separated from the cooled alkylation mixture and rinsed with ethanol (3x50 mL), acetone (1x50 mL), ethanol (1x50 mL) and then water (3x 50mL). Resins were then stored wet for further analysis.

Ion-exchange capacities of repeated functionalisation reactions were in the range of 0.4 to 0.5 mmol/g.

IR (ATR): ν (cm^{-1}) = 3368 (OH str.); 2974 (CH_2 def.); 1722 (C=O str.); 1450 (CH_2 def.); 1088; 1048 (CH_2 def.); 880 NR_4^+ ;

EA: Carbon (37.37%); Hydrogen (4.88%); Nitrogen (1.18%) Other (56.57%) ; Calculated for 0.56mmol/g ion-exchange capacity: Nitrogen (1.56%)

3.2.26 Methyl-diethylamine (MDM)



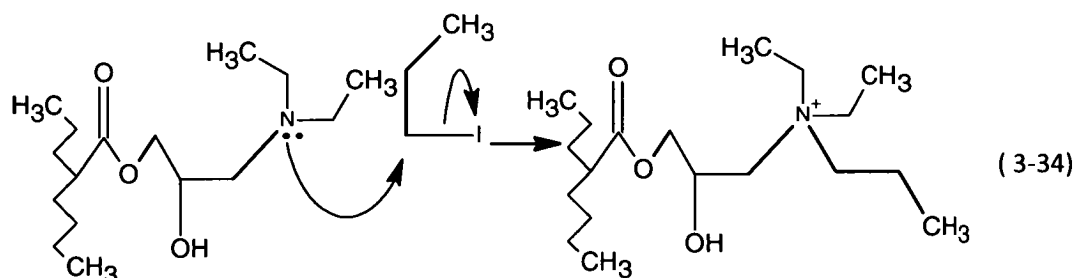
Dry diethylamine functionalised resin (10.94g) was added to 150mL dry DMF in Resin Reactor 2, which was then purged with dry nitrogen. This resin-DMF slurry was then stirred for 30 min at 300rpm under a nitrogen atmosphere to allow the resin to swell. Dry iodomethane (CH_3I ; 21mL; GPR; *BDH*) was then added dropwise over a 10 minute period from a pressure equalising dropping funnel and any residual iodomethane was rinsed into the reactor with a 10mL aliquot of dry DMF. The reaction mixture was then allowed to stir for ~20 h at room temperature followed by heating in an oil bath at 45°C for four h. The resin beads were magnetically separated from the functionalisation mixture and then rinsed with ethanol (3x50 mL), acetone (1x50 mL), ethanol (1 x 50 ml) and then water (3x50 mL). Resins were then stored wet for further analysis.

Ion-exchange capacities ranged between 1.2 and 1.6 mmol/g for successful syntheses.

IR (ATR): ν (cm^{-1}) = 3364 (OH str.); 2984 (CH_2 def.); 1720 (C=O str.); 1455 (CH_2 def.); 1157

EA: Carbon (40.46%); Hydrogen (5.61%); Nitrogen (2.27%) Other (51.66%) ; Calculated for 1.61mmol/g ion-exchange capacity: Nitrogen (2.25%)

3.2.27 1-propyl-diethylamine (1PDM)



Dry diethylamine functionalised resin (8.9g) was added to 150mL dry DMF in Resin Reactor 2, which was then purged with dry nitrogen. This mixture was then stirred for 30 min at 300rpm under a nitrogen atmosphere to allow the resin to swell. Dry 1-iodopropane ($\text{CH}_3\text{CH}_2\text{I}$; 24mL; 99%; Aldrich) was then added dropwise over a 10 minute period from a pressure equalising dropping funnel and any residual iodopropane was rinsed into the reactor with a 10mL aliquot of dry DMF. The reaction mixture was allowed to stir for ~20 h at room temperature followed by heating in an oil bath at 45°C for four h. The resin beads were magnetically separated from the functionalisation mixture and then rinsed with ethanol (3x50 mL), acetone (1x50 mL), ethanol (1x50 mL) and then water (3x50 mL). Resins were then stored wet for further analysis.

Ion-exchange capacities ranged between 0.8 and 1.2 mmol/g.

IR (ATR): ν (cm^{-1}) = 3404 (OH str.); 2976 (CH_2 def.); 1452 (CH_2 def.); 1047 (CH_2 def.); 879 (w)

NR_4^+

EA: Carbon (42.27%); Hydrogen (5.66%); Nitrogen (2.53%) Other (49.54%) ; Calculated for 1.47mmol/g ion-exchange capacity: Nitrogen (2.05%)

3.3 Resin characterisation

Due to difficulties in resin synthesis, further analyses were performed on the resin substrate provided by Orica Watercare in an attempt to rationalise inconsistencies in results. Initial research was focussed on resin bead surface area measurements as processes such as

drying, re-wetting and change of solvents are known to cause expansion and contraction of beads with permanent change a possibility. Once trends on solvation of the resin beads had been established, analyses by scanning electron microscopy were performed to characterise the surface of the resin bead and indicate the sites of functionality.

3.3.1 Surface area and porosimetry analysis

In an attempt to analyse changes in bead surface area and porosity, surface area and porosimetry analyses were performed. An initial volume of fresh resin as supplied by Orica Watercare was magnetically separated from overlying water and dried under vacuum overnight at 70°C. As initial resin functionalisation was performed at 80°C in water, this temperature was deemed sufficient to allow for rapid drying of the resin beads without altering the resin in a manner different to normal functionalisation. A sub-sample of the dried resin beads was then re-wetted in water for 60 min followed by magnetic separation of the overlying water and drying under vacuum overnight at 70°C. Subsampling and re-wetting was repeated three more times producing five stages of increasing resin degradation. A sample of imidazole-functionalised and benzyl-imidazole-functionalised resins were also dried at 70°C overnight and analysed to ascertain any changes in resin bead characteristics during the functionalisation and alkylation processes.

A known mass of dried resin (~0.1g) was added to a glass sample tube and degassed under vacuum at 50°C overnight on a Micromeritics Instrument Corporation VacPrep™ 061 degasser followed by analysis on a Micromeritics Instrument Corporation TriStar II 3020 porosity and surface area analyser running TriStar II 3020 v1.01 software. BET isotherms were calculated over 12 data points and are summarised in Table 3-3¹.

Table 3-3 BET surface area data for repeated drying of resins

Resin	BET surface area (m ² /g)
MIEX cycle 1	47.2±0.4
MIEX cycle 2	22.5±0.1
MIEX cycle 3	21.2±0.2
MIEX cycle 4	19.3±0.1
MIEX cycle 5	15.8±0.1
IMZ	28.0±0.2
BIM	40.5±0.3

As indicated in Table 3-3, 52% of the available surface area on the resin beads is lost with one attempt at drying and re-wetting with 66% lost over 5 cycles of drying and re-wetting. This loss of surface area would have a major effect on the functionalisation of the resin. Functionalisation reactions also show a loss of surface area, with 41% of the surface area lost post-functionalisation. Alteration of the solvent from water to dimethylformamide (DMF) to allow alkylation of the imidazole functional groups present on the resin beads altered the resin morphology, increasing the degree of swelling and regaining some of the lost surface area due to dimethylformamide being a resin swelling solvent.

3.3.2 Scanning electron microscopy

Dried samples of the resins studied in Section 3.3.1 were mounted on aluminium SEM stubs using double-sided tape followed by sputter coated with gold using a Bal-Tec SCD 050 Sputter Coater for 220 seconds at 40 milliamps and photographed at high magnification using an Environmental Scanning Electron Microscope (ESEM), Electroscan Corporation, Wilmington, Massachusetts, U.S.A located in the Central Science Laboratory of the University of Tasmania. Examples of the resin bead microphotographs are given in Figure 3.3 to Figure 3.8. Few morphological changes are seen with increased resin drying and re-wetting, however the change of solvent from water to dimethylformamide alters the bead morphology from spherical to oval. Resin degradation products are also more frequently observed as the resins are dried and re-wetted as beads fracture, exposing the inner

macroporous structure of the beads. The complete set of scanning electron microphotographs can be found in Appendix C.

3.3.3 Particle size analysis

Small amounts of the commercial MIEX-DOC resin and the unfunctionalised resin as received from Orica Watercare were analysed for particle size using a Micromeritics Instrument Co. Saturn Digisizer 5200 coupled to a Sonics and Materials Inc. Vibra-Cell VC130PB-2 ultrasonic processor. The Saturn Digisizer was running Saturn Digisizer 5200 v1.09 software. The samples were suspended in the centrifugally pumped 600mL sample cell of the instrument in deionised water at a flow rate of 12.0L/min. Sonication was used during the testing with 40% of the 130W total power of the ultrasonic probe being used to suspend the sample. The samples were allowed to circulate for 120 sec before analysis was performed. The particle size analyses were performed through exposures of the 658nm diode laser at ten different angular positions between 0 and 45°. The 16mm parallel laser beam was passed through the sample cell followed by focussing on a Fourier lens onto a ~1.3M element CCD. Data deconvolution was performed by Mie theory² using a refractive index of 2.420/2.500 and a density of 5.180g/cm³. The analyses were repeated three times with the results illustrated in Figure 3.1 and Figure 3.2. Based upon these analyses, the mean particle size of the MIEX resin as supplied by Orica Watercare is 250±20 micron.

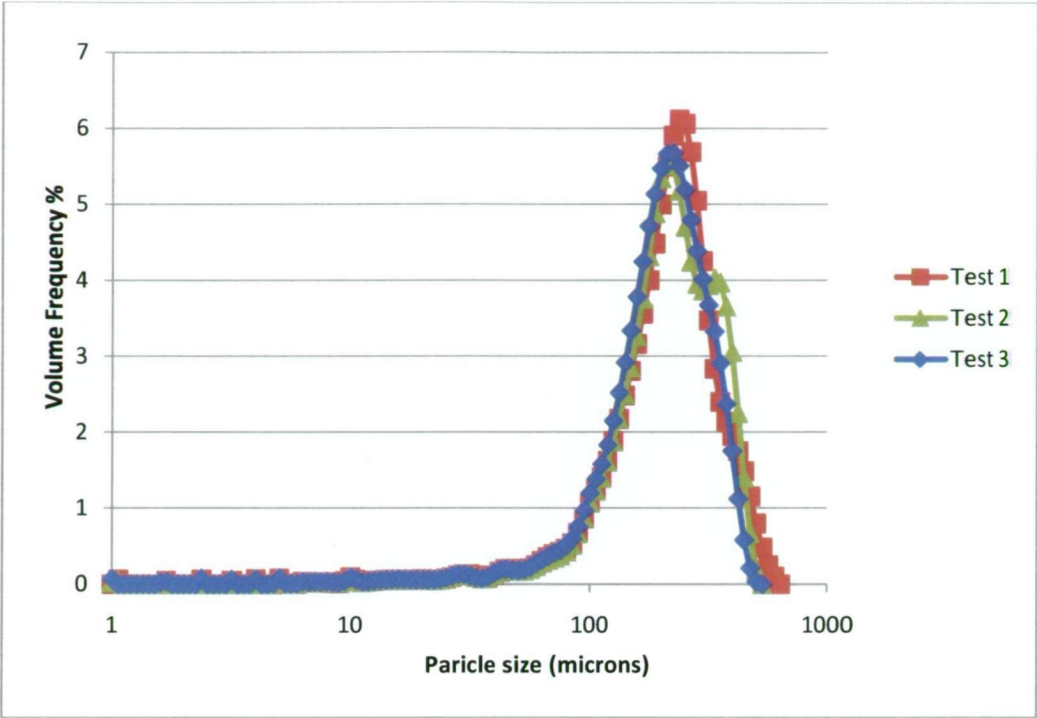


Figure 3.1 Particle size analysis of MIEX-DOC resin

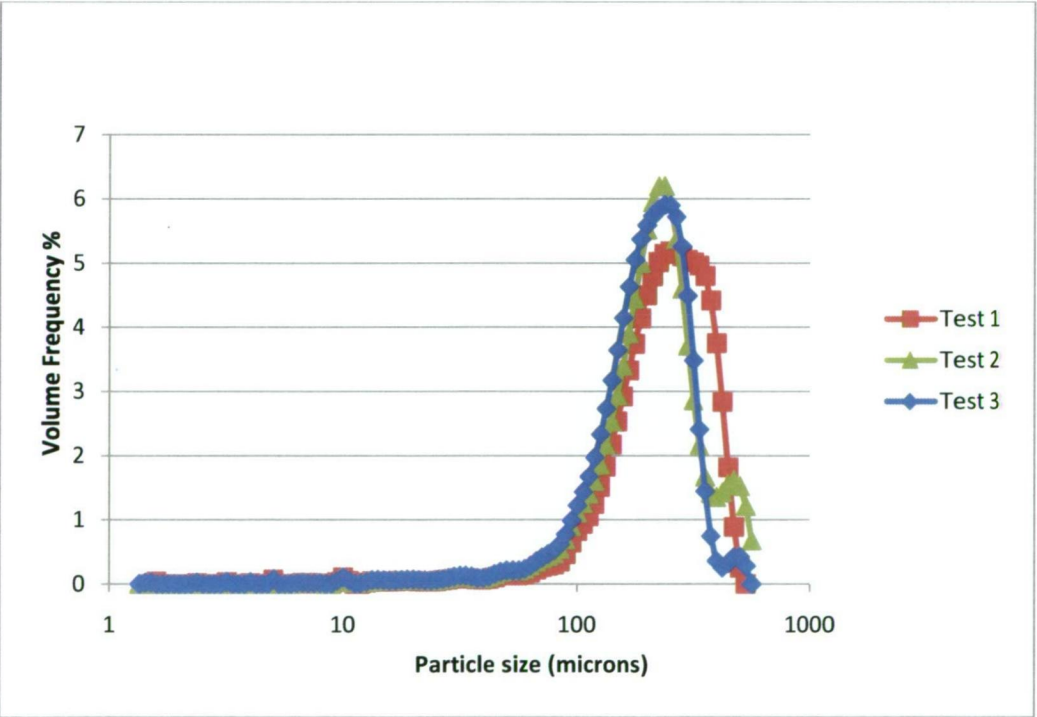
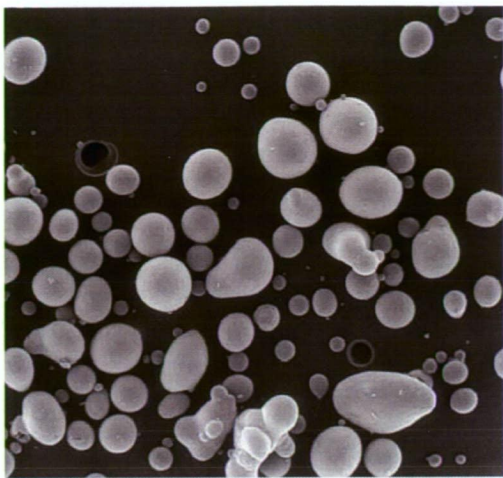
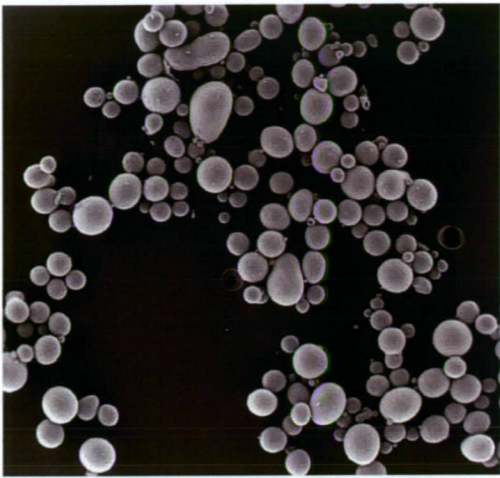


Figure 3.2 Particle size analysis of unfunctionalised resin



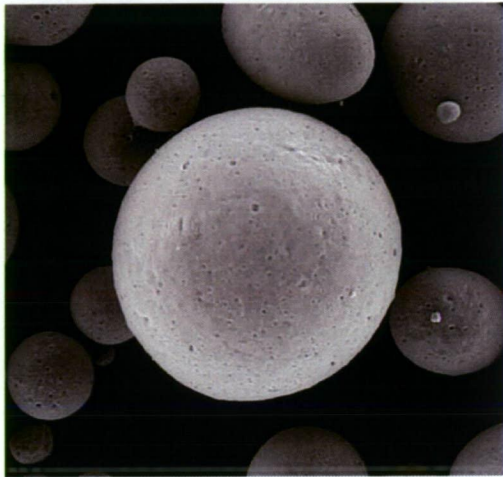
500 μm

Figure 3.3 EIM overall view of resins



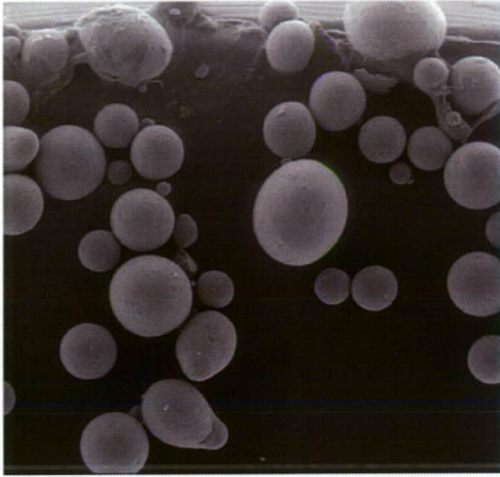
500 μm

Figure 3.4 MIEX Dry 1 overall view



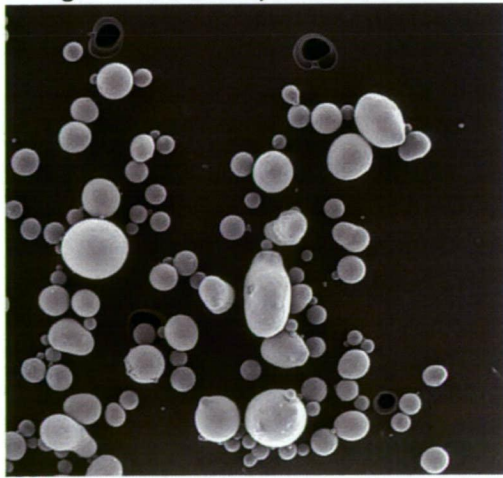
100 μm

Figure 3.5 MIEX Dry 2 overall view



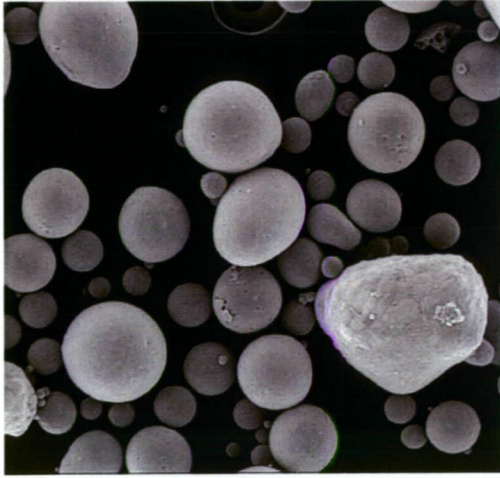
200 μm

Figure 3.6 MIEX Dry 3 overall view



500 μm

Figure 3.7 MIEX Dry 4 overall view



200 μm

Figure 3.8 MIEX Dry 5 overall view

3.4 Conclusions

Based upon the research aims detailed in Chapter 1, resins should allow a rapid and large uptake of aurothiosulfate from a synthetic leach solution. With this aim in mind, resins with very low ion-exchange capacities were not deemed suitable for further research. Ion exchange capacities are summarised in Table 3-4. These were the tributylamine- (TBA) and diethanolamine-functionalised (DEA) resins, despite literature suggestion that tributylamine-based resins have gold cyanide selectivity^{3,4}. Further, the N-methyl-piperidine- (NIP) and N-methyl-piperazine-functionalised (NAZ) resins were shown to be similar to the resins synthesised by alkylation of the base heterocyclic amine, i.e. N-methyl-piperidine- (MIP) and N,N-dimethyl-piperazine-functionalised (MAZ) resins but showed lower ion-exchange capacities. These resins were also deemed not suitable for further research.

Table 3-4 Resin ion-exchange summary

Resin	Abbreviation	Ion-exchange capacity (meq/g)
Trimethylamine	TMA	1.939
Triethylamine	TEA	0.746
Tributylamine	TBA	0.0873
Diethanolamine	DEM	WB
Diethylamine	DEA	WB
2-Piperidine-methanol	2PM	WB
Piperidine-ethanol	PET	0.682
Piperidine	PIP	WB
N-methyl-piperidine	NIP	0.3889
Piperazine	PAZ	WB
N-methyl-piperazine	NAZ	1.052
Quinuclidine	QNU	1.0306
Imidazole	IMZ	WB
Methyl-imidazole	MIM	1.01
Ethyl-imidazole	EIM	1.036
1-propyl-imidazole	1PIM	1.0694
2-propyl-imidazole	2PIM	1.1014
Benzyl-imidazole	BIM	1.1004
Methyl-piperidine	MIP	0.7246
N,N-dimethyl-piperazine	MAZ	1.52
Methyl-diethylamine	MDM	1.6132
1-propyl-diethylamine	1PDM	1.469
Methyl-2-piperidine-methanol	M2PM	0.558

3.5 References

1. Brunauer, S.; Emmett, P. H.; Teller, E. *Journal of the American Chemical Society* **1938**, *60*, 309-319.
2. Mie, G. *Annalen der Physik* **1908**, *330*, 377-445.
3. Dicoski, G. W. S. *Afr. J. Chem.* **2000**, *53*, 33-43.
4. Kotze, M. H.; Green, B. R.; Steinbach, G. In *Hydrometallurgy: Fundamentals, Technology and Innovation.*; Hiskey, J. B., Warren, J. W., Eds.; Society for Mining, Metallurgy and Exploration: Lyttleton, Colorado, USA, 1993.

4 Screening of resins

4.1 Introduction

This chapter serves to establish the basic ability of the novel functionalised resins to selectively uptake the target aurothiosulfate complex and to release this analyte when required.

Once resins these had been characterised and their ion-exchange capabilities established, they were assessed for their efficacy in relation to gold extraction. Initial studies focussed on the ability of the resin to uptake aurothiosulfate from water, followed by uptake from a synthetic leach solution. Once the uptake ability of the resin had been assessed, elution of the adsorbed aurothiosulfate complex was then investigated employing three separate elution systems. Further testing included the investigation of the selectivity of the resins for the target aurothiosulfate complex over its major competitor, the trithionate ion. Resins were then selected for further characterisation and testing based on the outcomes these parameters.

4.2 Gold uptake testing of resins

Initial studies related to aurothiosulfate uptake were performed as per Sections 2.2.9.1 and 2.2.9.2 whereby a known mass of resin was contacted with a known concentration of aurothiosulfate in either MilliQ water or in a synthetic leach solution. Samples were taken at regular intervals and assayed for gold concentration against standards prepared from either a gold AAS standard containing gold tetrachloride ($[\text{AuCl}_4]^-$) in 5% HCl or as sodium aurothiosulfate ($\text{Na}_3[\text{Au}(\text{S}_2\text{O}_3)_2] \cdot 2\text{H}_2\text{O}$) in synthetic leach solution. In the former case, a matrix correction factor was applied for correlation as per Section 2.2.6.3.

4.2.1 Gold uptake results in varying matrices

4.2.1.1 *Gold uptake in water*

Initial testing focussed on resin aurothiosulfate uptake in MilliQ water. Resins unable to remove aurothiosulfate from this simple matrix were deemed unsuitable for further testing.

For all the following uptake tests, a small mass of resin (~0.1g) was suspended in 500.0mL of a aurothiosulfate solution of known gold concentration by means of either by bottle roll or overhead stirrer. Resins were then allowed to adsorb aurothiosulfate from the solution for 24 h with sampling times as per Section 2.2.9. The samples were then analysed for gold content using AAS after calibration using known concentrations of either gold tetrachloride ($[\text{AuCl}_4^-]$) in 5% HCl or sodium aurothiosulfate ($\text{Na}_3[\text{Au}(\text{S}_2\text{O}_3)_2] \cdot 2\text{H}_2\text{O}$) in synthetic leach solution.

4.2.1.1.1 Resin gold uptake for alkylamine resins

The novel ion-exchange resins used for this test were based on N-piperidine ethanol (PET), trimethylamine (TMA) and triethylamine (TEA) amines. A sample of unfunctionalised resin (UNF) was also included in these tests in order to assess the ability of the blank resin substrate to uptake the aurothiosulfate complex.

No matrix correction was applied as the standards were in 5% HCl and the samples were in water.

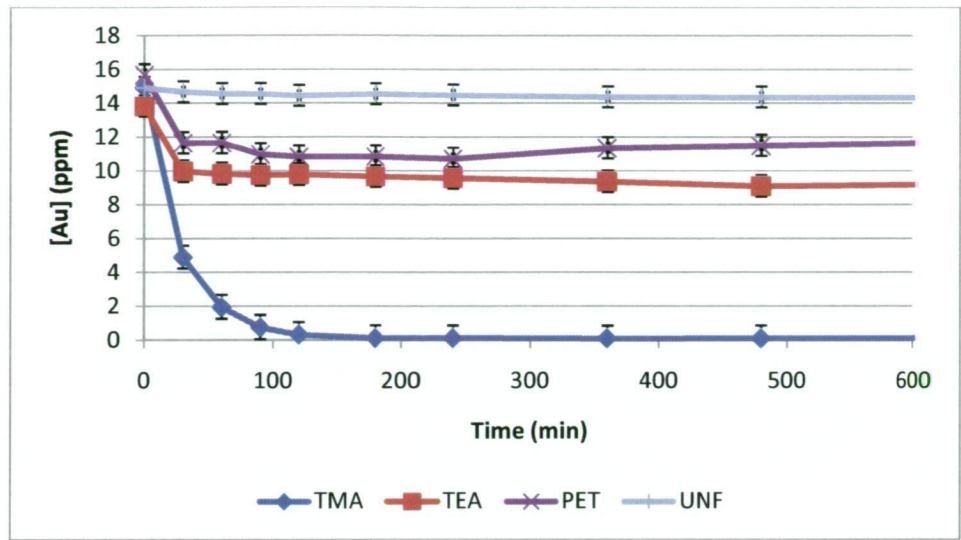


Figure 4.1 Gold uptake over 24 h for initial resins at room temperature (~23°C)

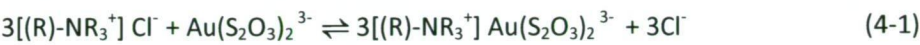
As can be seen from Figure 4.1, gold uptake was initially rapid until resin saturation, which occurred after approximately 3 h. Of further note is the weak uptake of the target aurothiosulfate complex by the unfunctionalised resin. This was added to the test as a control to ascertain physical non ion-exchange adsorption of the aurothiosulfate complex onto the resin. The uptake for the unfunctionalised resin has been corrected to account for the tenfold excess in mass of the unfunctionalised resin when compared to other resins in solution.

Based upon these results, a gold mass-balance calculation can be performed with the results summarised in Table 4-1.

Table 4-1 Resin gold uptake mass balance summary 1 after 600 min

Resin	Ion-exchange capacity (mmol/g)	Mass in solution (g)	Capacity in solution (eq)	Gold adsorbed (mg/g)	Gold adsorbed (eq)	$eq_{Au}/eq_{capacity}$ (%)
PET	0.62	0.1005	0.062	27.7 ± 4.4	0.024 ± 0.002	67.5 ± 0.01
TMA	2.23	0.1001	0.223	82.6 ± 4.4	0.125 ± 0.002	56.4 ± 0.04
TEA	0.46	0.1001	0.046	29.1 ± 4.7	0.044 ± 0.002	96.3 ± 0.09
UNF	0	1.0008	0.000	$0.315\pm.045$	0.016 ± 0.002	-

Typical results show a strong relationship between the amount of gold adsorbed by the resin and the number of ion-exchange sites present on the resin surface with the number of mmol of gold in solution being approximately 33% of the total ion-exchange capacity. This is expected due to the stoichiometric ratio between the singly valent positive charges present on the resin and the triply valent anionic aurothiosulfate complex as detailed in Equation (4-1).



where (R) is the resin polymer backbone and R is an alkyl substituent.

4.2.1.1.2 Resin gold uptake in water for ring and cage alkylamines

Further initial uptake results were obtained for quinuclidine (QNU), methyl diethylamine (MDM), 1-propyl diethylamine (1PDM), methyl piperidine (MIP) and N,N dimethyl piperazine (MAZ), as shown in Figure 4.2.

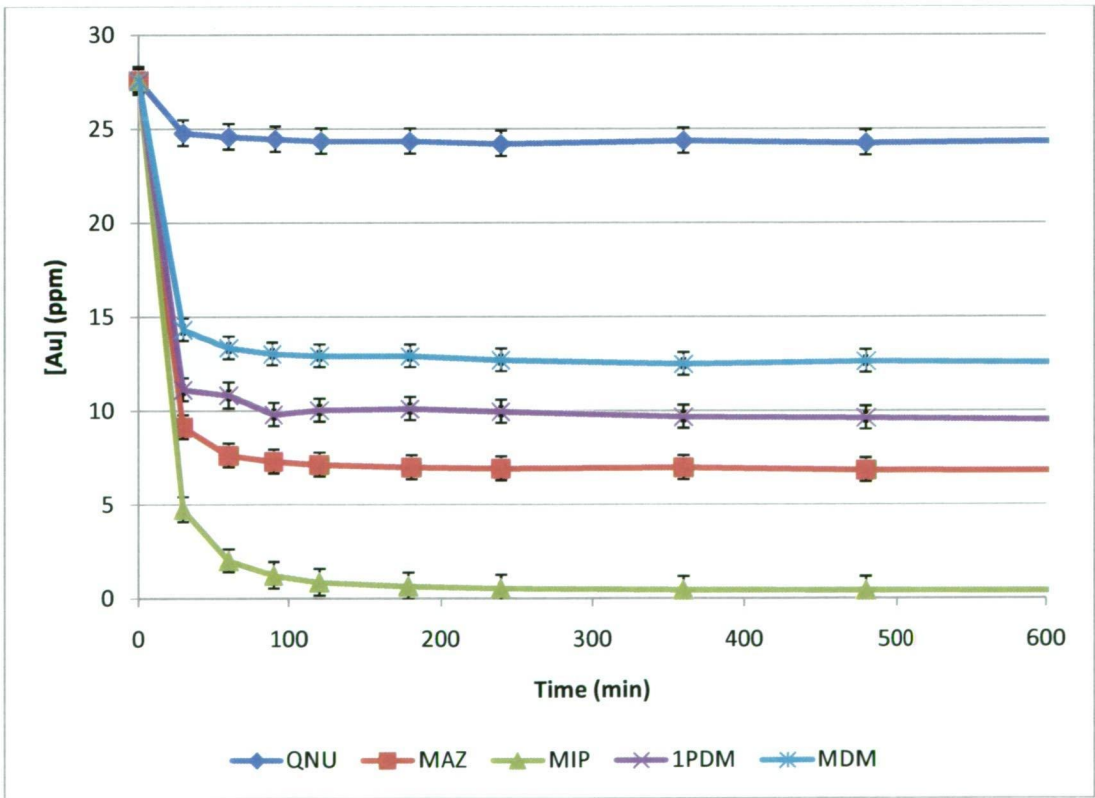


Figure 4.2 Gold uptake over 24 h for extended resins at 30°C

Again, these results indicate a rapid removal of aurothiosulfate from the solution, followed by equilibration of the resin with the aurothiosulfate complex.

From these results a gold mass balance can be calculated, with the results summarised in Table 4-2.

Table 4-2 Resin gold uptake mass balance summary 2 after 600 min

Resin	Ion-exchange capacity (mmol/g)	Mass in solution (g)	Capacity in solution (eq)	Gold adsorbed (mg/g)	Gold adsorbed (eq)	eq _{Au} /eq _{capacity} (%)
QNU	0.342	0.1058	3.62×10^{-5}	14.3±2.7	$2.57 \times 10^{-5} \pm 4.8 \times 10^{-6}$	63±12
MAZ	1.356	0.1105	1.50×10^{-4}	88.3±2.60	$1.59 \times 10^{-4} \pm 4.6 \times 10^{-6}$	99±3
MIP	1.511	0.1170	1.77×10^{-4}	124.5±3.1	$2.07 \times 10^{-4} \pm 5.1 \times 10^{-6}$	125±3
1PDM	1.469	0.1155	1.70×10^{-4}	80.8±2.6	$1.39 \times 10^{-4} \pm 4.5 \times 10^{-6}$	84±3
MDM	1.078	0.1051	1.13×10^{-4}	68.3±2.5	$1.17 \times 10^{-4} \pm 4.4 \times 10^{-6}$	97±4

As can be seen from these results, the molar amount of gold adsorbed is again approximately 33% of the molar ion-exchange capacity of the resin. This result is expected again due to the relationship between the triply valent negative charge present on the aurothiosulfate complex and the monovalent positive charge present on the ion-exchange sites. Some values are higher than expected and are represented as >100% adsorption of gold onto the ion-exchange resins. A partial explanation would be that the aurothiosulfate complex is adsorbing onto the surface of the resin bead. This has been observed in literature for silver thiosulfate by degradation and precipitation of silver sulfide¹, however this form of gold complex degradation and adsorption would be indicated as a rapid decrease in the gold concentration shown in the blank test in Figure 4.1. Other studies have shown that aurothiosulfate breakdown increases both with respect to temperature and in lower concentrations² and that the solubility of the aurothiosulfate complex is dependent on the oxidation state of the thiosulfate ligand³ with oxidation of the thiosulfate ligand causing reduction and deposition of gold as micron-sized metallic particles or as an AuS monolayer⁴.

4.2.1.1.3 Resin gold uptake in water for imidazole resins

Results shown in Figure 4.3 for benzyl-imidazole (BIM), methyl-imidazole (MIM) and ethyl-imidazole (EIM) also show similar trends to those already observed for other resins.

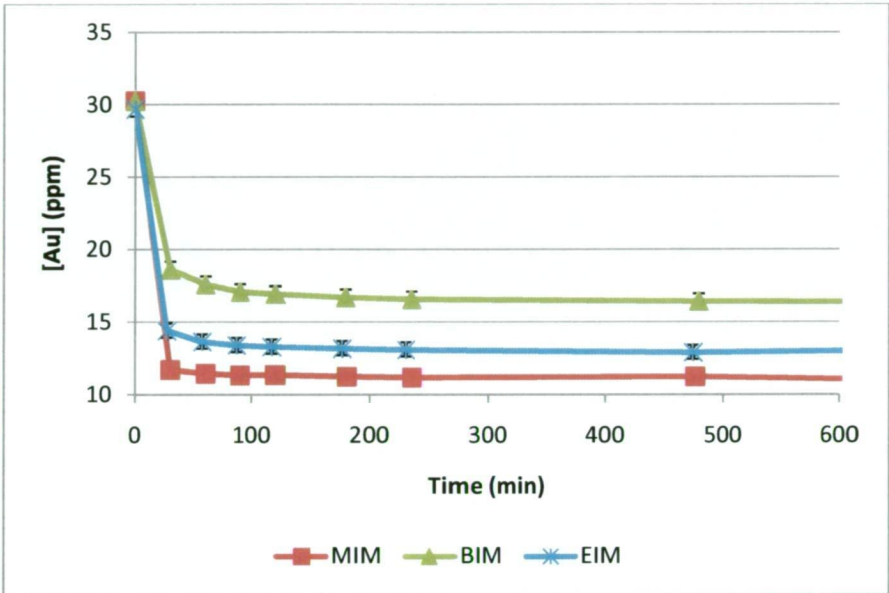


Figure 4.3 Gold uptake for extended resins at 30°C

Table 4-3 Resin gold uptake mass balance summary 3 after 600 min

Resin	Ion-exchange capacity (mmol/g)	Mass in solution (g)	Capacity in solution (eq)	Gold adsorbed (mg/g)	Gold adsorbed (eq)	eq _{Au} /eq _{capacity} (%)
MIM	1.01	0.1183	1.20x10 ⁻⁴	81.0±1.9	1.45x10 ⁻⁴ ± 3.5x10 ⁻⁶	122±3
BIM	0.991	0.1088	1.08x10 ⁻⁴	63.5±2.3	1.05x10 ⁻⁴ ± 3.7x10 ⁻⁶	97±3
EIM	1.036	0.1127	1.17x10 ⁻⁴	76.7±2.1	1.32x10 ⁻⁴ ± 3.5x10 ⁻⁶	113±3

4.2.1.2 Gold uptake in synthetic leach

Once the efficacy of the novel ion-exchange resins to extract the aurothiosulfate complex from a water matrix had been established, aurothiosulfate uptake from a synthetic leach solution was investigated. This allows quantification of resin uptake in a solution similar to that encountered industrially to be determined. Aurothiosulfate uptake is expected to be as rapid as that observed in water, however polythionate species (in particular trithionate) produced due to the degradation of thiosulfate ions in the presence of copper and air are

known to compete for ion-exchange sites on the resin surface. The results from this testing formed the basis upon which it was decided if a resin passed on for the further testing detailed in Chapter 5. Resins that were unable to adsorb sufficient aurothiosulfate complex from a synthetic leach solution would not be considered viable candidates for the extended competition and elution studies detailed in Chapter 5.

Polythionate production due to thiosulfate breakdown was quantified over the 24-hour period by ion chromatographic analysis of three identical samples of piperidine-ethanol resin utilising the same synthetic leach solution for each resin sample. The analyses were performed according to Section 2.2.7.2 and were performed in triplicate to allow for quantification of the errors associated with the sampling regime used. Tetrathionate production was below the detection limits of the instrumentation used, a result consistent with literature⁶. As can be seen in Figure 4.4, trithionate production was initially rapid followed by a linear increase in concentration to approximately 30mM.

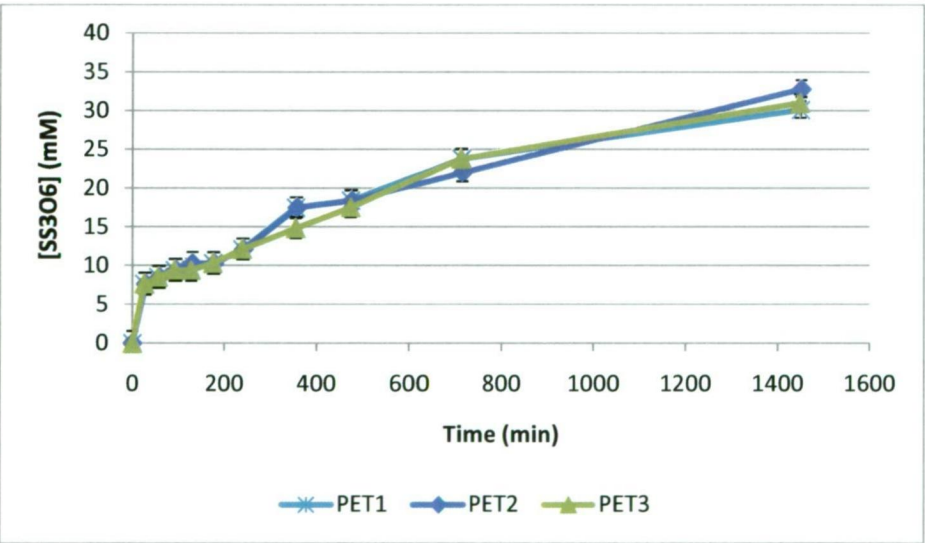


Figure 4.4 Trithionate production over 24 hours for synthetic leach solutions

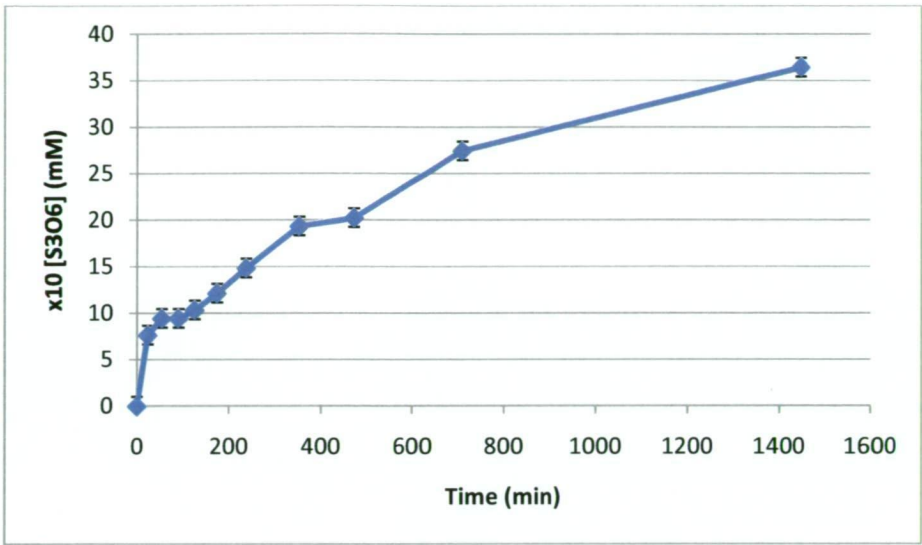


Figure 4.5 Polythionate production in blank solution

The effect of resin catalysis on polythionate production was quantified by analysis of the polythionate content of a resin-free batch of synthetic leach solution identical to that used for Figure 4.4. Comparison of Figure 4.4 and Figure 4.5 indicate that the presence of the resin beads in solution has little or no effect on the rate of trithionate production.

4.2.1.2.1 Resin gold uptake in synthetic leach for imidazole-based resins

Initial resin testing focused on ethyl-imidazole (EIM), 1- and 2-propyl-imidazole (1PIM and 2PIM), N-N dimethyl piperazine (MAZ), methyl-imidazole (MIM) and benzyl-imidazole (BIM). Resin leach concentrations were 31.84ppm aurothiosulfate dissolved in 250.0mL synthetic leach solution, prepared in accordance with Section 2.2.8. No matrix effect correction was applied in this instance as all AAS standards were prepared by using aurothiosulfate in synthetic leach solution. An aliquot removal correction was applied to each sample as outlined in Section 2.2.6.3.

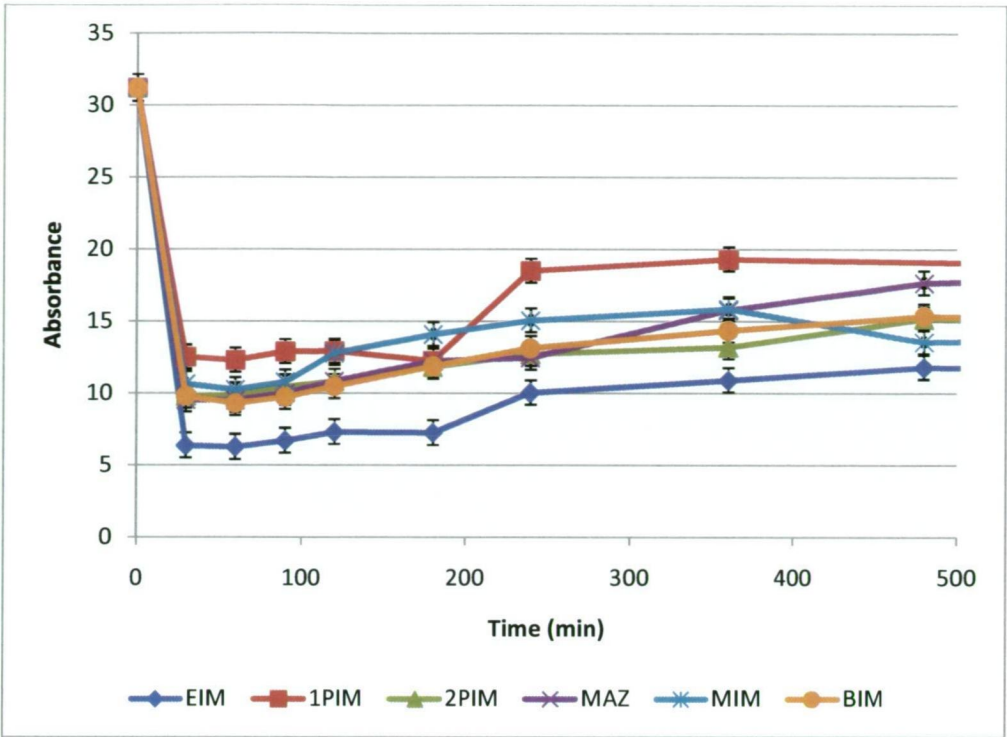


Figure 4.6 Gold uptake in synthetic leach at room temperature

Several trends can be seen in the results in Figure 4.6. Initial uptake of gold is quite rapid and equilibrium is established within 3 h. However, degradation of the thiosulfate ion in the presence of copper and atmospheric oxygen produces several different polythionate species, most notably the trithionate ion. This ion is the major competitor for ion-exchange sites on the resin surface and results in the adsorbed aurothiosulfate complex being desorbed. Differences between the amounts of aurothiosulfate adsorbed from the leach are related to both ion-exchange capacity and the selectivity of the functional groups attached to the resins.

Resin aurothiosulfate uptake results from this testing are summarised in Table 4-4. The low percentage coverage in comparison to previous results is to be expected due to an increase in concentration of counter-ions present in the system but in comparison to the low molar percentage of aurothiosulfate in solution in Table 4-5, these equate to a 300- to 900-fold enrichment factor.

Table 4-4 Leach gold uptake mass balance summary 1

Resin	Ion-exchange capacity (mmol/g)	Mass in solution (g)	Capacity in solution (eq)	Gold adsorbed (mg/g)	Gold adsorbed (eq)	eq _{Au} /eq _{capacity} (%)
EIM	1.08	5.01	5.39×10^{-3}	2.41±0.09	$1.84 \times 10^{-4} \pm 6.49 \times 10^{-6}$	3.42±0.12
1PIM	1.07	5.00	5.35×10^{-3}	1.78±0.08	$1.36 \times 10^{-4} \pm 6.24 \times 10^{-6}$	2.54±0.12
2PIM	1.10	4.40	4.84×10^{-3}	2.32±0.10	$1.55 \times 10^{-4} \pm 6.38 \times 10^{-6}$	3.20±0.13
MAZ	1.36	5.03	6.82×10^{-3}	2.05±0.08	$1.57 \times 10^{-4} \pm 6.33 \times 10^{-6}$	2.31±0.09
MIM	1.08	1.45	1.57×10^{-3}	6.89±0.29	$1.52 \times 10^{-4} \pm 6.30 \times 10^{-6}$	9.68±0.40
BIM	0.76	2.91	2.21×10^{-3}	3.61±0.14	$1.59 \times 10^{-4} \pm 6.34 \times 10^{-6}$	7.20±0.29

Gold uptake results are normally decreased when compared to these in water for most resins such as N,N-dimethyl-piperazine (MAZ; 99% to 2.31%), due to the high concentrations of competing ions present in a leach. However, the imidazole-based resins showed an increase in percentage adsorption(e.g. N-methyl-imidazole (MIM) when compared to the other resins tested. As can be seen in Table 4-5, aurothiosulfate is present at much smaller concentrations in a leach than all other ions.

Table 4-5 Standard bottle roll artificial leach concentrations and molar ratios

Name	Formula	Concentration (M)	Molar ratio	Molar %
Ammonium hydroxide	NH ₄ OH	0.42	4158	67
Ammonium chloride	NH ₄ Cl	0.1	990	16
Ammonium thiosulfate	(NH ₄) ₂ S ₂ O ₃	0.1	990	16
Cupric sulfate	CuSO ₄ .5H ₂ O	3.15×10^{-3}	34	0.55
Sodium aurothiosulfate	Na ₃ [Au(S ₂ O ₃) ₂].2H ₂ O	1.01×10^{-4}	1	0.0162

4.2.1.2.2 Resin gold uptake in synthetic leach for alkylamine resins

Further resin testing focused on trimethylamine (TMA), triethylamine (TEA), quinuclidine (QNU) and N-piperidine ethanol (PET) functionalised resins based upon their good adsorption performance in water. Resin leach concentrations were 20.45ppm of aurothiosulfate in a synthetic leach prepared in accordance with Section 2.2.8. A matrix

effect correction and gold aliquot removal correction were then applied as per Section 2.2.6.3.

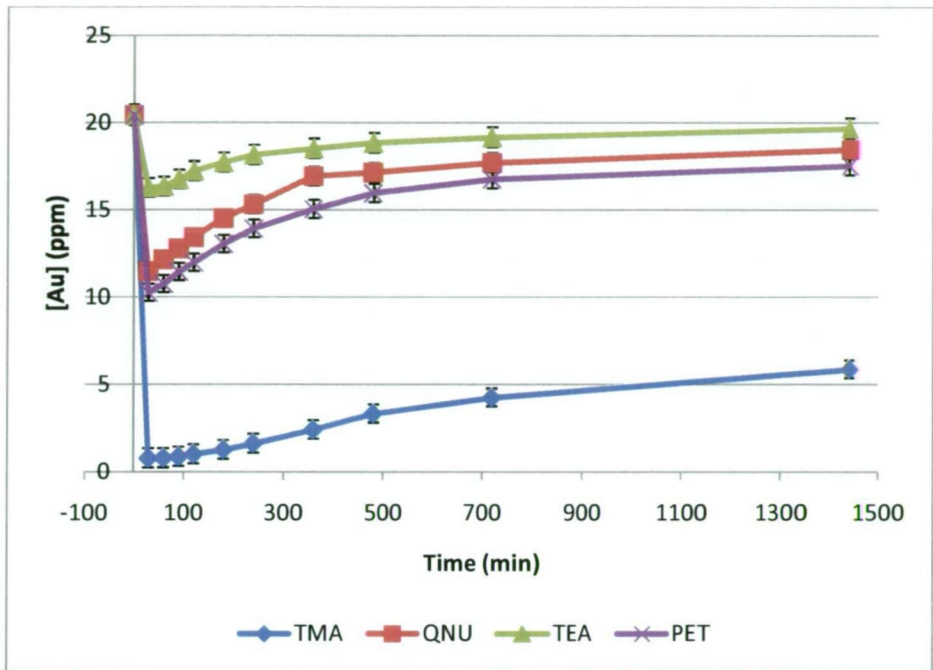


Figure 4.7 Gold uptake in synthetic leach at room temperature

Again, similar trends to Figure 4.6 can be seen in Figure 4.7 where initial gold uptake is quite rapid, with initial equilibrium with the leach being established within the first 3 h. The amount of gold adsorbed by the resin from solution is related to the ion-exchange capacity of that resin in solution. Desorption of the gold occurs due to degradation of the thiosulfate present in the leach to trithionate which successfully competes with the aurothiosulfate complex for ion-exchange sites present on the resin. The effect of the polythionates on the desorption of aurothiosulfate from the resins is related to the selectivity of the ion-exchange functionalities on the resin. As can be seen in Table 4-6, trimethylamine has a relatively large ion-exchange capacity and adsorbed a relatively large amount of aurothiosulfate but a relatively small amount of gold was adsorbed per equivalent. This is due to trimethylamine being the least selective of the functional groups tested for both aurothiosulfate and polythionate species. This means the resin has unoccupied sites available to adsorb greater

amounts of both aurothiosulfate and the polythionate species before ion-exchange competition begins to take effect, releasing aurothiosulfate. Quinuclidine has a relatively low ion-exchange capacity but a higher selectivity for both aurothiosulfate and polythionate species. Therefore, uptake of both aurothiosulfate and trithionate will be more rapid and therefore will show as a faster elution of gold with respect to time. This conclusion is supported by the comparison between triethylamine and quinuclidine-based resins. As seen in Table 4-6, triethylamine shows similar levels of functionalisation and capacity in solution to quinuclidine. However, the percentage adsorption per equivalent for quinuclidine is approximately 2.5 times that of triethylamine, due to the selectivity of the quinuclidine functional group.

Table 4-6 Leach gold uptake mass balance summary 2 after 600 minutes

Resin	Ion-exchange capacity (mmol/g)	Mass in solution (g)	Capacity in solution (eq)	Gold adsorbed (mg/g)	Gold adsorbed (mol)	$n_{Au}/n_{capacity}$ (%)
TMA	2.23	2.5110	5.60×10^{-3}	1.92 ± 0.05	$7.35 \times 10^{-5} \pm 2.08 \times 10^{-6}$	1.31 ± 0.03
QNU	0.2305	2.1787	5.02×10^{-4}	0.90 ± 0.06	$3.00 \times 10^{-5} \pm 1.86 \times 10^{-6}$	5.97 ± 0.37
TEA	0.219	2.5214	5.52×10^{-4}	0.34 ± 0.05	$1.32 \times 10^{-5} \pm 2.00 \times 10^{-6}$	2.39 ± 0.36
PET	0.342	2.5122	8.59×10^{-4}	0.90 ± 0.05	$3.45 \times 10^{-5} \pm 1.85 \times 10^{-6}$	4.03 ± 0.21

4.3 Gold elution testing of resins

Once resin gold uptake from both water and a synthetic leach solution had been established, elution of the adsorbed aurothiosulfate was investigated. Elution of adsorbed ions is possible through three mechanisms. Firstly, the ion-exchange groups present on the resin can be modified such that the selectivity for the adsorbed aurothiosulfate complex is changed. This is usually performed by using a pH gradient on the resin column to alter the ionisation of the weak-base ion-exchange functional groups. However, as all resins prepared are strong-base quaternary ammonium moieties, this particular method was not possible.

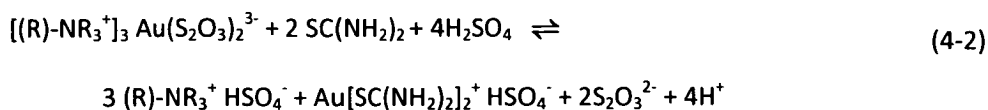
Secondly, the adsorbed aurothiosulfate complex can be altered to a different complex that has lower selectivity for the ion-exchange groups present on the resin. This forms the basis of elution mechanisms involving the use of thiourea in acidic media and thiocyanate in basic media. In the first case, the adsorbed negatively charged aurothiosulfate complex is transformed to a positively charged aurothiourea complex, $[\text{Au}(\text{CS}(\text{NH}_2)_2)_2]^+$, which therefore has no affinity with the cationic resin functional groups. In the second case, a minor part of the elution mechanism is due to the conversion of the aurothiosulfate complex to a similar gold thiocyanate complex, $[\text{Au}(\text{SCN})_2]^-$. The decrease in the charge present on the complex limits the interaction between complex and the sites present on the resin. Furthermore, the change in ligand present on the complex converts it to a form which has lower ion-exchange selectivity of the functional groups present on the resin surface.

The final method for the elution of adsorbed aurothiosulfate from ion-exchange resins is to use a large concentration of an ion that has a smaller ion-exchange selectivity for the resin sites than the adsorbed complex. Ion-exchange displacement via mass action will then elute the adsorbed complex from the resin, concentrating it into a form that allows easier recovery. In the case of the basic thiocyanate elution regime, the thiocyanate ion has the effect of displacing the adsorbed aurothiosulfate from the resin surface. The elution mechanism trialled for this study was to use a large concentration of sodium nitrate for the elution of the adsorbed aurothiosulfate.

4.3.1 Elution using acidic thiourea

Thiourea in acidic solutions has been shown to elute gold cyanide^{7,8} and aurothiosulfate^{9,10} from strong-base ion exchange resins having similar structural features to those in this study.

The reaction can be summarised by the equation (4-2).



The elution mechanism in the case of aurothiosulfate is a combination of ion-exchange displacement by the sulfate ion and the alteration of the gold complex from aurothiosulfate to aurothiourea. Use of moderate acid concentrations causes degradation of the thiosulfate ligands on the gold complex. Complexation of the gold by thiourea then follows and as the aurothiourea complex is positively charged, there is no coulombic interaction present between the ion-exchange functional groups and the complex.

Initial testing focussed on the imidazole-based functionalities, as these showed increased selectivity for aurothiosulfate in synthetic leach solutions. A known mass of 1-propyl- (1PIM), 2-propyl- (2PIM), methyl- (MIM), ethyl- (EIM) and benzyl-imidazole (BIM) and methyl-diethylamine (MDM) functionalised resins (2.500g) was added to 250mL of the synthetic leach containing 20.3ppm gold as sodium aurothiosulfate, prepared according to the procedure detailed in Section 2.2.8. In order to load the resins with a known amount of the aurothiosulfate complex, the resins were allowed to equilibrate with the solution for 2 h followed by magnetic separation of the resin beads from the leach solution.

The resins were then rinsed with MilliQ water (~15mL) to remove the bulk of the leach solution and loaded into glass ion-exchange columns (25mL capacity, 10mL diameter) with a porosity #3 sintered frit at the base and allowed to settle for 5 to 10 min. Analysis of the leach solution before and after contact with the resin beads allowed quantification of the amount of aurothiosulfate adsorbed by the resins through gold mass-balance calculations.

The adsorbed aurothiosulfate was then eluted by passing a solution of 0.5M thiourea in 0.25M sulfuric acid through the column and collecting fractions of the effluent for AAS analysis for dissolved gold.

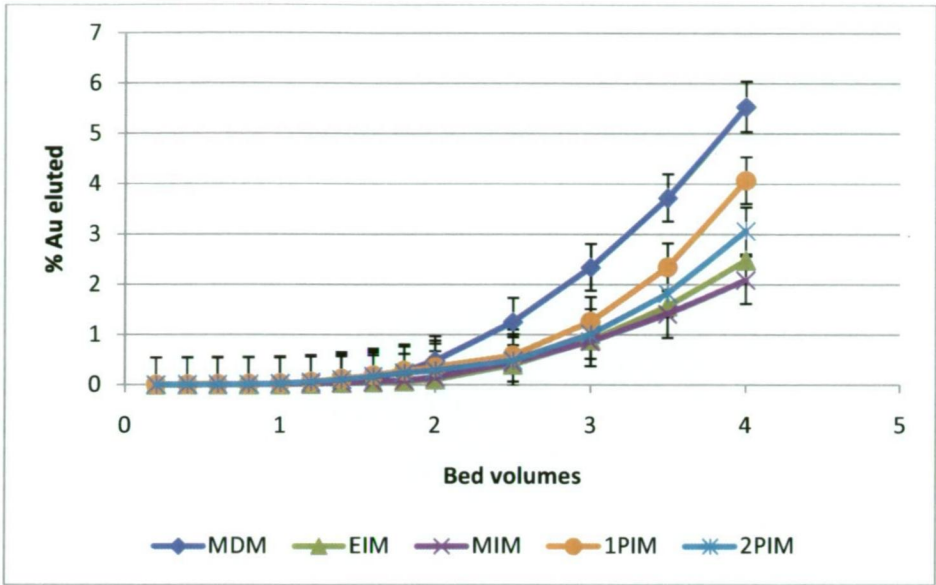


Figure 4.8 Acidic thiourea elution profile for imidazole and methyl-diethylamine resins

Figure 4.8 shows a very slow elution of aurothiosulfate from the resins. After 4 bed-volumes (40mL), elution of the imidazole resins was incomplete, as reflected in the percentage elution of gold shown in Table 4-7.

Table 4-7 Elution results for imidazole and methyl-diethylamine resins

Resin	[Au] leach (ppm)	Au uptake (mg)	Au eluted (mg)	% elution
1PIM	12.06	3.02±0.17	0.122±0.004	4.1±0.07
2PIM	13.71	3.43±0.17	0.105±0.004	3.1±0.06
MIM	18.95	4.74±0.18	0.099±0.004	2.1±0.05
EIM	18.09	4.52±0.18	0.112±0.004	2.5±0.05
MDM	18.74	4.69±0.18	0.259±0.004	5.5±0.04

From these results, it can be concluded that whilst imidazole-based resin functionalities are very selective for aurothiosulfate over all other leach species, the selectivity constant is too high to allow elution of the adsorbed aurothiosulfate complex by the 0.5M thiourea/0.25M H₂SO₄ eluent.

Further results focused on alkylamine-functionalised resins. A known mass of quinuclidine (QNU), 1-propyl-diethylamine (1PDM), N,N-dimethyl-piperazine (MAZ), N-methyl-2-

piperidine-methanol (M2PM) or piperidine-ethanol (PET) functionalised resins (2.500g) was added to a synthetic leach prepared according to Section 2.2.8 containing 20.8ppm gold as aurothiosulfate. The resins were then allowed to contact the synthetic leach for 2 h followed by magnetic separation of the resins from the leach. Elution of the adsorbed gold complex was performed in an identical manner to that used for the imidazole-based resin systems.

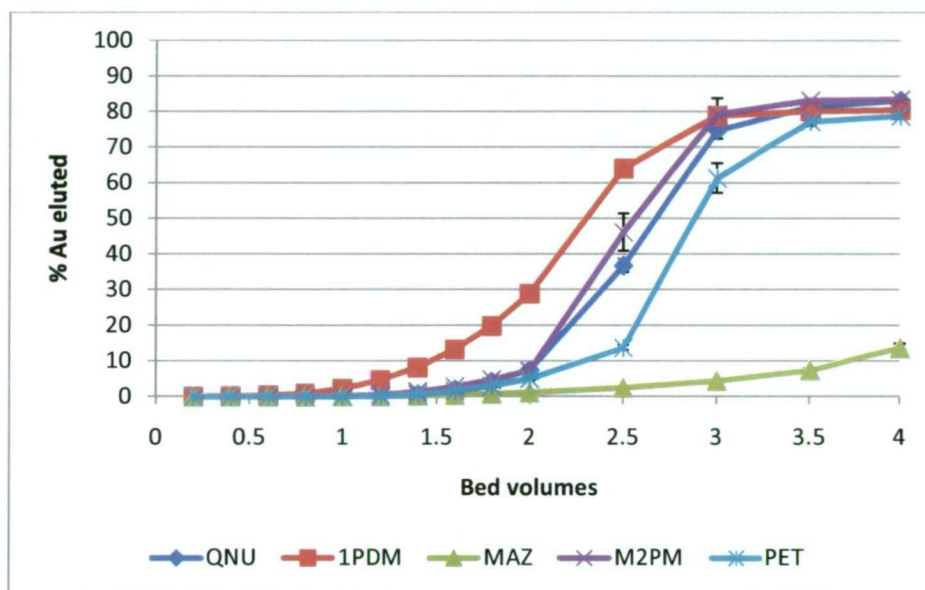


Figure 4.9 Acidic thiourea elution profile for ring and cage alkylamines

In comparison to imidazole based functionalities, Figure 4.9 shows a distinct completion of elution between 2.5 and 3.5 bed volumes or 25 to 35mL. The poor elution characteristics displayed by the N,N-dimethyl-piperazine (MAZ) resin could be due to the increased charge present on the functional group, requiring a higher concentration of eluent for more efficient elution. Comparison between Table 4-7 and Table 4-8 indicates relatively efficient elution of aurothiosulfate from the alkylamine-based functional groups using the acidic thiourea eluent. Unlike imidazole-based resin functional groups, the ion-exchange selectivity coefficients for aurothiosulfate on these alkylamine functionalities were high enough to allow selective uptake of the aurothiosulfate complex, but also low enough to allow elution of the target analyte.

Table 4-8 Elution results for ring and cage alkylamines

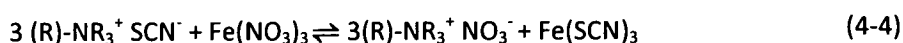
Resin	[Au] leach (ppm)	Au uptake (mg)	Au eluted (mg)	% elution
QNU	5.74±0.67	1.435±0.17	1.194±0.007	83.2±0.04
1PDM	4.08±0.68	1.020±0.17	0.821±0.005	80.5±0.06
MAZ	18.04±0.70	4.510±0.17	0.617±0.004	13.7±0.05
M2PM	11.73±0.67	2.932±0.17	2.448±0.01	83.5±0.05
PET	7.62±0.67	1.906±0.17	1.502±0.009	78.8±0.04

With the exception of N,N-dimethyl-piperazine (MAZ), all resins in this class showed good elution results.

4.3.2 Elution using basic thiocyanate

Thiocyanate elution of adsorbed aurothiosulfate relies on displacement of the adsorbed aurothiosulfate by the thiocyanate ion^{8,11}. The elution step was followed by regeneration of the resins by flushing with a solution of ferric nitrate¹². The adsorbed thiocyanate is then stripped from the resin by the formation of ferric thiocyanate, leaving the column in the nitrate form.

These mechanisms are summarised in Equations (4-3) and (4-4).



Initial elution testing focused on methyl-imidazole (MIM), 1-propyl-imidazole (1PIM), 2-propyl-imidazole (2PIM), N-methyl-piperidine (MIP), quinuclidine (QNU) and 1-propyl-diethylamine (1PDM) functionalised resins due to both an the strong adsorption of aurothiosulfate from solution for these resins and a low elution rate with acidic thiourea elution.

Resins were allowed to contact a synthetic leach prepared according to Section 2.2.8 containing 5ppm gold as aurothiosulfate for MIP, 1PDM, QNU and 2PIM and 20.2ppm for

MIM and 1PIM resins. The resins were allowed to contact the synthetic leach for 2 h followed by magnetic separation of the resin beads from the leach. Sampling of the leach before and after contact allowed quantification of the amount of aurothiosulfate adsorbed by the resins. The resins were then rinsed with MilliQ water (~15mL) to remove the bulk of the leach solution and loaded into glass ion-exchange columns (25mL capacity, 10mL diameter) with a porosity #3 sintered frit at the base and allowed to settle for 5 to 10 min. The adsorbed aurothiosulfate was then eluted by passing a solution of 1M sodium thiocyanate in 0.25M sodium hydroxide through the column and collecting fractions of the effluent for AAS analysis for dissolved gold.

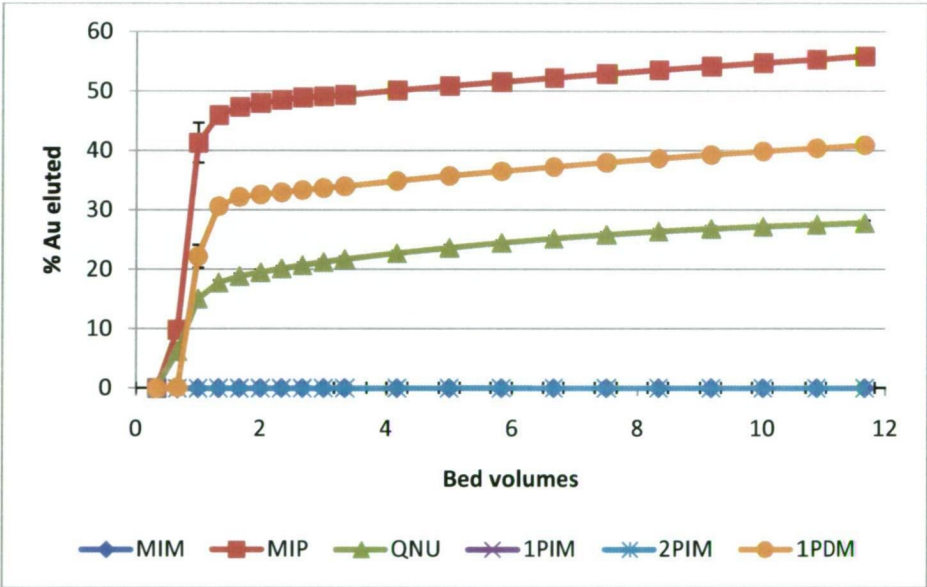


Figure 4.10 Basic thiocyanate elution profile 1

As seen in Figure 4.10, thiocyanate elution efficiently removed the adsorbed aurothiosulfate complex from the ion-exchange resins tested, with 99% of the eluted aurothiosulfate was obtained in the first 20mL or 2 bed volumes of eluent. Table 4-9 indicates that imidazole-based resins showed very little elution of adsorbed aurothiosulfate using this elution system, unlike the alkylamine-based resins which showed much higher recoveries.

Table 4-9 Basic thiocyanate elution results 1

Resin	[Au] leach (ppm)	Au uptake (mg)	Au eluted (mg)	% elution
MIM	7.18±0.43	2.71±0.11	7.642 x10 ⁻⁴ ±0.004	<1±0.04
MIP	0.94±0.51	1.08±0.13	0.602±0.008	55.9±0.11
QNU	3.43±0.47	0.46±0.12	0.127±0.004	27.9±0.25
1PIM	12.93±0.41	1.27±0.10	1.718 x10 ⁻⁴ ±0.004	<1±0.08
2PIM	9.59±0.41	2.40±0.10	3.576 x10 ⁻⁴ ±0.004	<1±0.004
1PDM	1.62±0.50	0.91±0.13	0.371±0.005	40.9±0.137

Further comparison results for similar systems were obtained using N,N-dimethyl-piperazine (MAZ), benzyl-imidazole (BIM), ethyl-imidazole (EIM), N-methyl-2-piperidine-methanol (M2PM) and piperidine-ethanol (PET) functionalised resins. These resins were allowed to contact a synthetic leach prepared according to Section 2.2.8 containing 20.2ppm gold as aurothiosulfate. After 2 h contact, the resins were magnetically separated from the leach and then eluted in an identical manner to that performed for the first set of thiocyanate elution results.

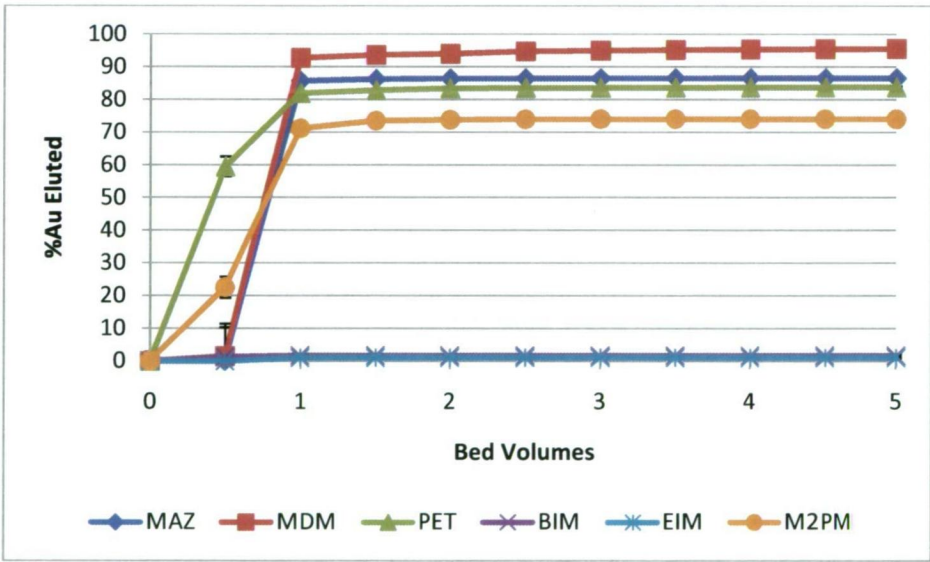


Figure 4.11 Basic thiocyanate elution profile 2

As seen in Figure 4.11, the majority of eluted gold was removed within the first 20mL or 2 bed volumes. Table 4-10 shows similar elution results as described previously for both

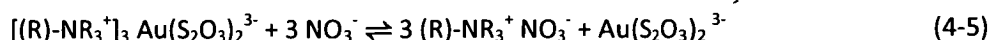
alkylamine- and imidazole-based resin systems in that this elution method is successful for alkylamine resins but unsuccessful for imidazole-based resin systems.

Table 4-10 Basic thiocyanate elution results 2

Resin	[Au] leach (ppm)	Au uptake (mg)	Au eluted (mg)	% elution
MAZ	1.01±0.51	4.28±0.13	3.74±0.10	88.1±0.04
BIM	4.64±0.46	3.34±0.11	0.06±0.10	2.0±1.53
PET	13.22±0.41	1.19±0.10	1.00±0.05	84.1±0.09
MDM	3.24±0.48	3.69±0.12	3.53±0.02	95.8±0.03
EIM	4.64±0.46	3.34±0.11	0.04±0.02	1.1±0.49
M2PM	9.18±0.42	2.21±0.10	1.64±0.05	74.1±0.06

4.3.3 Elution using nitrate

Nitrate elution relies on the mass action of a large concentration of a less selective species to displace the adsorbed aurothiosulfate complex. This is summarised by Equation (4-5) and has been the focus of several studies within the literature as an eluent for thiosulfate¹³⁻¹⁵ and cyanide¹⁶ complexes of gold.



where (R) is the resin backbone and R is an alkyl substituent.

Elution was performed by allowing a known sample of resin to contact a known volume of synthetic leach solution for 2-3 h. Sampling of the leach before and after this period allowed quantification of the amount of gold adsorbed by the resin. The loaded resins were then magnetically removed from the leach solution, rinsed with MilliQ water and slurry-loaded into glass ion-exchange columns (25mL capacity, 10mL diameter) with a porosity #3 sintered frit at the base and allowed to settle for 5 to 10 min. The adsorbed aurothiosulfate was then eluted by passing a solution of 2M sodium nitrate through the column at a flow rate of 1mL min⁻¹ at room temperature and collecting 2mL fractions of the effluent for AAS analysis for dissolved gold.

Initial results were obtained using methyl-, 1-propyl-, 2-propyl-, ethyl- and benzyl-imidazole functionalised resins, labelled MIM, 1PIM, 2PIM, EIM and BIM respectively.

Resins were allowed to contact a synthetic leach solution containing 20.3ppm gold as the aurothiosulfate complex for 2 h. This timeframe was deemed to be the point at which maximum adsorption occurred in a synthetic leach. A 2M sodium nitrate solution was then flushed through the column and 2mL fractions were collected for the first 20mL, followed by 5mL fractions for the remaining 20mL and analysed by AAS against standards diluted from AuCl_4^- in 5% HCl. A matrix correction was applied to leach solutions to enable accurate gold concentrations to be recorded.

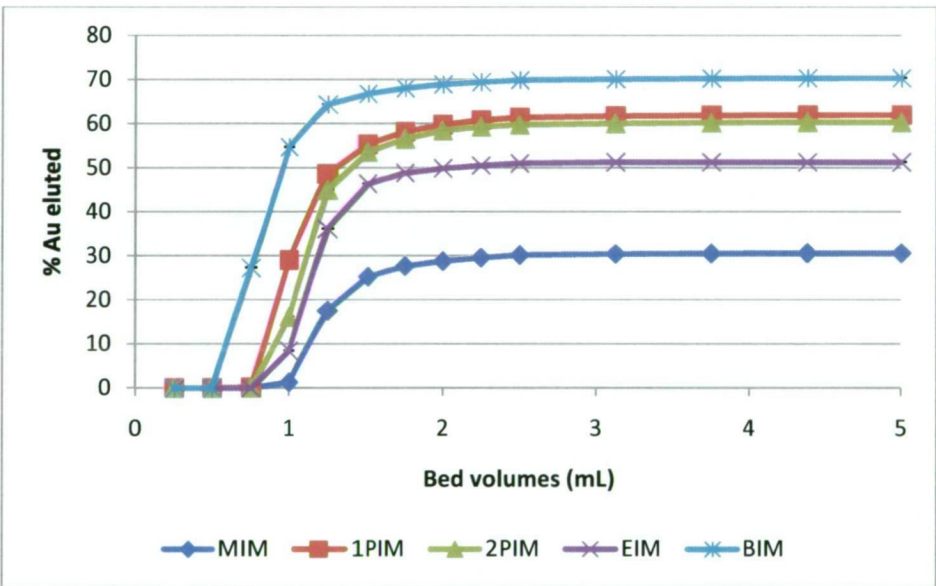


Figure 4.12 2M sodium nitrate elution for imidazole resins at room temperature

As can be seen from Figure 4.12, nitrate elution rapidly removed the adsorbed aurothiosulfate complex from the ion-exchange resins tested, with gold elution reaching a plateau within 20mL or 2 bed volumes. Similar results were obtained for thiocyanate elution, as can be seen in Figures 4-8 and 4-9. Although the elution is rapid, 100% recovery of the adsorbed gold was not achieved due to the high ion-exchange selectivity of the imidazole-

based resin systems for the aurothiosulfate complex . This can be seen in Table 4-11 where the resins have retained between 70 and 40% of the adsorbed aurothiosulfate.

Table 4-11 2M nitrate elution results for imidazole resins

Resin	[Au] leach (ppm)	Au uptake (mg)	Au eluted (mg)	% elution
MIM	18.47±0.753	4.617±0.18	1.417±0.0002	30.7±0.188
1PIM	12.04±0.759	3.009±0.19	1.866±0.0004	62.0±0.189
2PIM	13.33±0.757	3.333±0.19	2.012±0.0004	60.4±0.189
EIM	17.66±0.753	4.414±0.19	2.265±0.0006	51.3±0.188
BIM	10.58±0.762	2.644±0.19	1.861±0.0004	70.4±0.19

Further resin screening focused on alkylamine resins, as opposed to imidazole-based ring structures due to the high retention of aurothiosulfate on the resin functional groups. Quinuclidine (QNU), N,N-dimethyl-piperazine (MAZ), N-methyl-piperidine (MIP), 1-propyl-diethylamine (1PDM), methyl-diethylamine (MDM) and piperidine ethanol (PET) functionalised resins were contacted with a synthetic leach solution prepared as per Section 2.2.8 containing 20.0ppm gold as aurothiosulfate for 2 h. The resins were then eluted in an identical manner to the imidazole-based resin systems.

Similar results were obtained to the imidazole-based resin systems. Figure 4.13 shows that the majority of eluted gold was removed within 20mL or 2 bed volumes. Recovery of aurothiosulfate was greater for this resin system as the ion-exchange selectivity coefficients between aurothiosulfate and these resin functional groups are less than those of the imidazole-based resin functional groups. Comparing Table 4-11 to Table 4-12 shows that although higher loadings of aurothiosulfate were achieved for imidazole based resin systems, much greater recoveries of adsorbed gold were achieved for alkylamine resins, whilst these adsorbents still showed high selectivity for aurothiosulfate over all other leach competitor species.

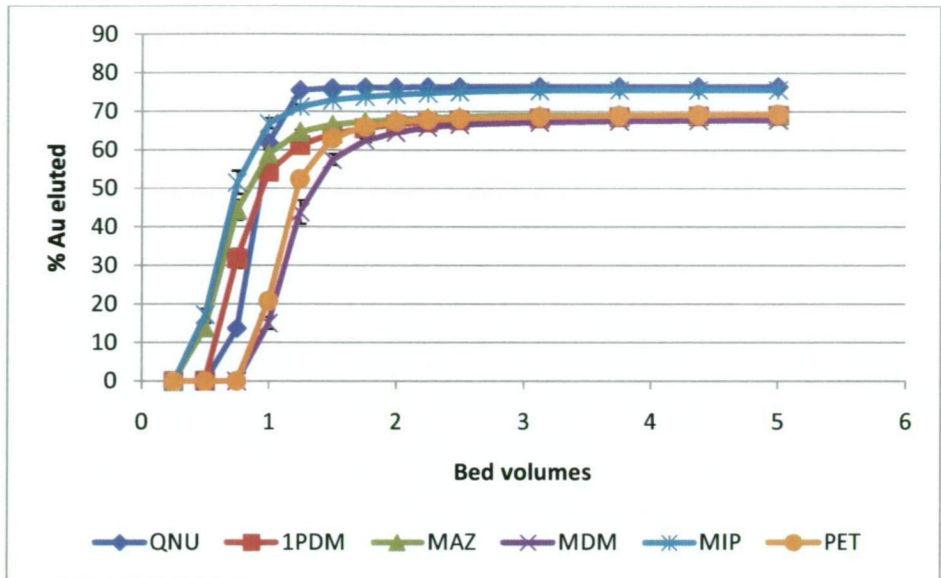


Figure 4.13 2M sodium nitrate elution for alkylamine resins at room temperature

Table 4-12 2M nitrate elution results for alkylamine resins

Resin	[Au] leach (ppm)	Au uptake (mg)	Au eluted (mg)	% elution
QNU	5.51±0.90	1.378±0.22	1.055±0.005	76.5±0.16
1PDM	12.87±0.90	3.218±0.22	2.220±0.01	69.0±0.07
MAZ	14.38±0.91	3.596±0.23	2.492±0.01	69.3±0.06
MDM	17.81±0.94	4.453±0.24	3.02±0.13	67.8±0.05
MIP	14.68±0.92	3.670±0.23	2.78±0.13	75.6±0.06
PET	7.62±0.90	1.904±0.22	1.320±0.006	69.4±0.11

4.3.4 Conclusions

The criteria for the selection of the resins most likely to perform adequately in a synthetic leach are summarised below:

- Rapid and large uptake of aurothiosulfate from synthetic leach solutions
- Little or no susceptibility to elution of gold by trithionate ions
- Maximum elution of adsorbed aurothiosulfate by the chosen elution
- Minimum amount of aurothiosulfate retained by the resin after elution/regeneration

Chapter 4 – Screening of resins

In conclusion, all resins have shown uptake of the aurothiosulfate complex in water and a good correlation between the ion-exchange capacity of the resins and the amount of gold adsorbed was observed.

All resins tested showed uptake of aurothiosulfate from synthetic leach solutions, with most showing considerable enrichment factors when compared with the percentage of aurothiosulfate present in the leach solution. Resins that showed high ion-exchange selectivity for aurothiosulfate also tended to show greater selectivity for trithionate and other leach degradation products, thus making them more susceptible to desorption of the aurothiosulfate complex with increased leach degradation. This was indicated by a rapid decrease in gold concentration in solution and therefore a rapid adsorption of aurothiosulfate onto the resin surface. This initial adsorption is followed by a gradual increase in gold concentration as the increased concentration of trithionate in solution begins to compete with the aurothiosulfate complex for the ion-exchange sites on the resin surface. This susceptibility to trithionate competition also allows for the possibility of utilising trithionate as an eluting ion followed by sulfite regeneration of the trithionate adsorbed to the ion-exchange sites on the resin surface¹⁷. This elution method would prevent the use of leach recycling due to contamination of the leach solution by trithionate and other higher polythionate species. High-capacity resins also contained enough capacity to adsorb trithionate ions before selective elution of aurothiosulfate.

Resin elution methods were successful depending on the type of functionality used. Nitrate was successful for all resin types, showing good elution of adsorbed gold, even for the imidazole-based resins. Acidic thiourea and basic thiocyanate elution schemes showed adequate elution of adsorbed aurothiosulfate on alkylamine-based resins, but were unsuccessful for the elution of aurothiosulfate from imidazole-based resin systems.

Chapter 4 – Screening of resins

Resins were passed onto further testing based on these results and based on structural features of interest. Although 2M nitrate elution was the most successful eluent system, it has not been used commercially, whereas thiocyanate elution has been proven in industrial situations employing cyanide for gold extraction. Recovery of gold from concentrated solutions is also easier for the thiocyanate elution system than 2M nitrate¹⁸.

The resins passed on for further testing are detailed in Chapter 5, however some preliminary rankings can be performed at this stage. Imidazole-based resin functionalities were passed onto further testing due to rapid and highly selective uptake of the aurothiosulfate complex and functionalities exhibiting a range of alkyl group chain length and steric bulk were used. As there was very little difference in uptake between the ethyl-, 1-propyl- and 2-propyl-imidazole resin systems, the 1- and 2-propyl-imidazole resin systems were not selected for further screening experiments. Methyl-, ethyl- and benzyl-imidazole were selected for further testing based upon aurothiosulfate loading.

Linear trialkylamine species showed good uptake and elution characteristics and several were submitted for further screening experimentation. These were selected to allow comparison between three identical alkyl substituents and a variation on a single alkyl group. The resins used were triethylamine, methyl-diethylamine and 1-propyl-diethylamine functionalised resins.

The resins having cyclic functional groups which were selected were archetypes of piperidine- and piperazine-based functionalities and were N-methyl-piperidine, N,N-dimethyl-piperazine, piperidine-ethanol, quinuclidine and N-methyl-2-piperidine-methanol. The piperidine-ethanol and N-methyl-2-piperidine-methanol resins were selected based upon their Type 2 functionality, i.e. the pendant hydroxide group present near the charged site on the functional group would allow some steric/colombic interaction with the target aurothiosulfate complex. Piperidine resins were selected as a comparison to the imidazole

resins, allowing observation of the effect of the delocalisation present in fully-alkylated imidazole-based resin systems.

Literature has suggested that a combination of eluting ions has greater elution recovery^{13, 14, 19}, in particular the combination of sulfite and nitrate/chloride. The presence of sulfite in the elution stream regenerates any polythionates produced by oxidation of thiosulfate, thus preventing the formation of trithionate and higher polythionates. This elution scheme has been shown to be very effective in the elution of aurothiosulfate from Purolite A500/2788 macroporous strong-base resins and it is an acknowledged deficiency of the experimental work performed that this elution scheme was not applied to the ion-exchange resins synthesised.

4.4 References

1. Hubin, A.; Vereecken, J., Electrochemical reduction of silver thiosulfate complexes. Part 2: Mechanism and Kinetics. *Journal of Applied Electrochemistry* **1994**, *24*, 396-403.
2. Skoog, D. A.; Holler, F. J.; West, D. M., *Fundamentals of analytical chemistry*. 7th ed.; Saunders College Pub.: Fort Worth, 1996; p 1 v. (various pagings).
3. Benedetti, M.; Boulegue, J., Mechanism of gold transfer and deposition in a supergene environment. *Geochim. Cosmochim. Acta* **1991**, *55*, (6), 1539-1547.
4. Woods, R.; Hope, G. A.; Watling, K. M.; Jeffrey, M. I., A Spectroelectrochemical Study of Surface Species Formed in the Gold/Thiosulfate System. *Journal of the Electrochemical Society* **2006**, *153*, (7), D105-D113.
5. Woods, R.; Hope, G. A.; Watling, K.; Jeffrey, M. I. In *Raman spectroelectrochemical investigations of the leaching of gold in chloride and thiosulfate media*, Proceedings of the Jan D. Miller Symposium - Innovations in Natural Resource Processing, Salt Lake City, UT, 2005; Salt Lake City, UT, 2005; pp 245-259.
6. Jeffrey, M. I.; Brunt, S. D., The quantification of thiosulfate and polythionates in gold leach solutions and on anion exchange resins. *Hydrometallurgy* **2007**, *89*, (1-2), 52-60.
7. Groenewald, T., The dissolution of gold in acidic solutions of thiourea. *Hydrometallurgy* **1976**, *1*, (3), 277-290.
8. Fleming, C. A.; Cromberge, G., The elution of aurocyanide from strong- and weak-base resins. *Journal of the South African Institute of Mining & Metallurgy* **1984**, *84*, (9), 269-80.
9. Kononova, O. N.; Kholmogorov, A. G.; Kononov, Y. S.; Pashkov, G. L.; Kachin, S. V.; Zotova, S. V., Sorption recovery of gold from thiosulfate solutions after leaching of products of chemical preparation of hard concentrates. *Hydrometallurgy* **2001**, *59*, 115-123.
10. Kholmogorov, A. G.; Kononova, O. N.; Pashkov, G. L.; Kononov, Y. S., Sorption recovery of gold thiosulphate complexes. *Chinese J. Chem. Eng.* **2002**, *10*, (1), 123-127.
11. Nicol, M. J.; O'Malley, G., Recovering Gold from Thiosulfate Leach Pulps via Ion Exchange. *JOM* **2002**, (October), 44-46.
12. Fleming, C. A. Regeneration of Thiocyanate Resins. U.S. patent US4608176, August 6, 1986, 1986.

13. Jeffrey, M. I.; Brunt, S., Loading and elution of gold thiosulfate from anion exchange resins. *Publications of the Australasian Institute of Mining and Metallurgy* **2007**, 9/2007, (World Gold 2007), 239-243.
14. Jeffrey, M. I.; Hewitt, D. M.; Dai, X.; Brunt, S. D., Ion exchange adsorption and elution for recovering gold thiosulfate from leach solutions. *Hydrometallurgy* **2010**, 100, (3-4), 136-143.
15. O'Malley, G. P. The Elution of Gold from Anion Exchange Resins. International patent WO 01/23626 A1, 5 April 2001, 2001.
16. Oliveira, A. M.; Leao, V. A.; da Silva, C. A., A proposed mechanism for nitrate and thiocyanate elution of strong-base ion exchange resins loaded with copper and gold cyano complexes. *Reactive & Functional Polymers* **2008**, 68, (1), 141-152.
17. Fleming, C. A.; McMullen, J.; Thomas, K. G.; Wells, J. A., Recent Advances in the Development of an alternative to the cyanidation process: Thiosulfate leaching and resin in pulp. *Minerals & Metallurgical Processing* **2002**, 20, (1), 1-9.
18. Marsden, J.; House, I., *The Chemistry of Gold Extraction*. Second Edition ed.; Society for Mining, Metallurgy and Exploration 2006; p 650.
19. Jeffrey, M. I. Recovery of metals from ion-exchange resins. International patent WO 2007/137325 A1, 20070522., 2007.

5 Further resin evaluation

5.1 Introduction

Once gold uptake and elution performance of the novel resins had been established, study was commenced into the performance of those resins in simulated industrial situations.

The two areas of interest for industrial applications of aurothiosulfate-selective ion-exchange resins are the ability of adsorbents to load aurothiosulfate in the presence of species known to compete for ion-exchange sites with the aurothiosulfate complex and the performance of the resins over repeated loading/elution/regeneration cycles.

Resins that performed well in the previous screening tests were selected for further analysis and the following resin functionalities were used: methyl-imidazole, ethyl-imidazole, 1-propyl-imidazole, 2-propyl-imidazole, benzyl-imidazole, methyl-diethylamine, 1-propyl-diethylamine, N-methyl-piperidine, N,N-dimethyl-piperazine, piperidine-ethanol, quinuclidine and N-methyl-2-piperidine-methanol. These were either archetype resins containing structural features of interest or resins that performed very well in screening tests.

5.1.1 Trithionate competition testing results

Degradation of thiosulfate to polythionates is one of the drawbacks to industrial use of thiosulfate as a lixiviant for gold. Polythionates are formed by the degradation of thiosulfate in the presence of oxidising species according to the equations detailed in Chapter 1. Although literature suggests that tetrathionate has the greatest detrimental effect on aurothiosulfate adsorption onto ion-exchange resins¹, more recent research has shown that trithionate is the predominant thiosulfate degradation species produced at the pH values of the synthetic leach used in this study².

To ascertain the effect that increasing concentrations of trithionate would have on the concentration of adsorbed aurothiosulfate, the candidate resins were allowed to adsorb aurothiosulfate from a synthetic leach solution, followed by the sequential additions of small aliquots of a concentrated solution of in-house prepared trithionate and sampling of the liquor for gold analysis using AAS.

A known mass of each novel ion-exchange resin (2.500g) was suspended in 250.00mL of synthetic leach solution prepared according to the method detailed in Section 2.2.82.2.8, using an orbital shaker at 200rpm. The synthetic leach solution contained 19.99ppm gold as aurothiosulfate. The resin was allowed to equilibrate with the synthetic leach solution for 2h after which a 2.50mL sample was taken for AAS and IC analysis to allow quantification of resin gold uptake and polythionate content respectively.

Immediately following this sample, 2.50mL of 100mM sodium trithionate was then added to the mixture and allowed to equilibrate for 30 min. This yielded a final trithionate concentration in the leach solution of 1mM. However, this value does not include any trithionate formed from the degradation of the thiosulfate present in the leach solution. This process was repeated for 10 additions, giving a total concentration of added trithionate of 10mM. The resins were then magnetically separated from the synthetic leach solution and stored.

Ion chromatographic analysis of the polythionate content of the leach during testing was performed according to Section 2.2.7.2 with analyses performed on three identical samples of benzyl-imidazole resin utilising the same synthetic leach solution in each. This was to allow for quantification of the errors associated with the analysis of the polythionate species produced by breakdown of the leach solution. Tetrathionate production was below the detection limit of the instrumentation used. The high levels of trithionate initially present in the leach are due to the 2 hour delay in measurement to allow for leach equilibration.

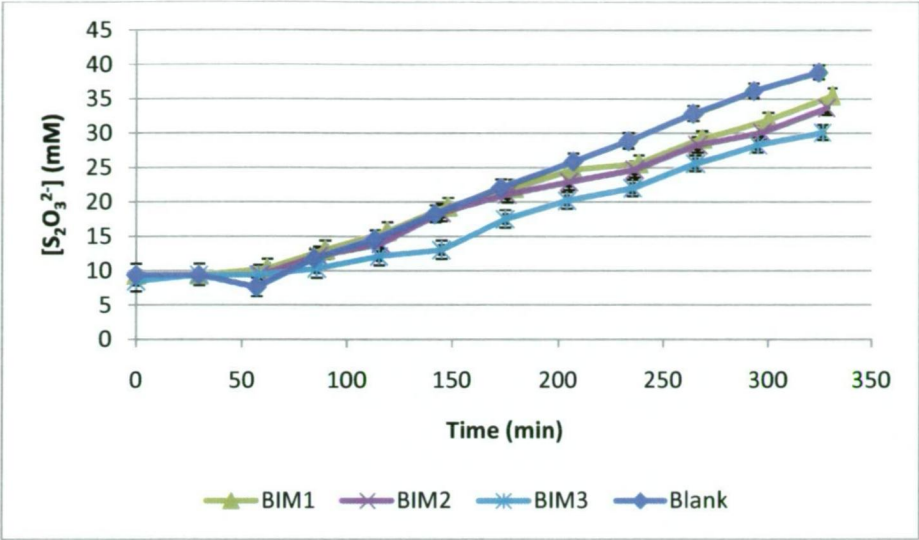


Figure 5.1 Trithionate analysis of synthetic leach solution

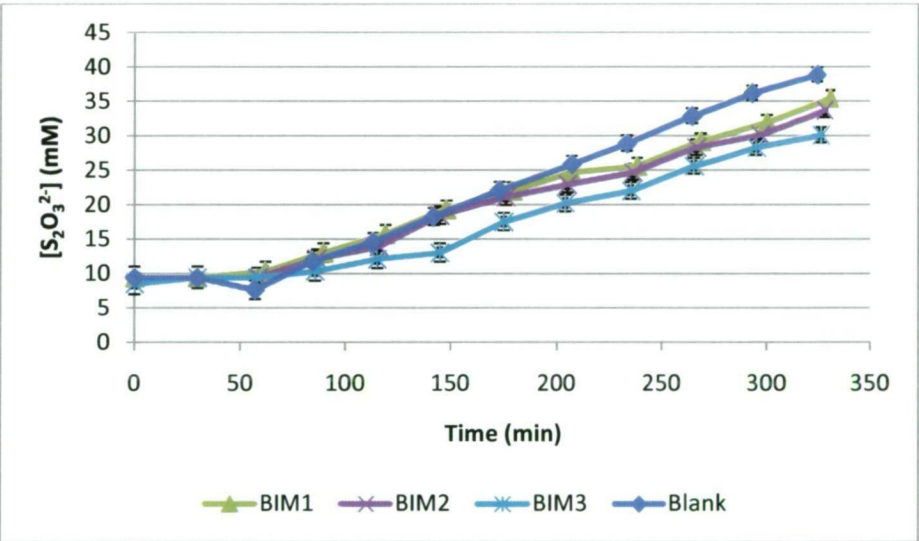


Figure 5.1 indicates that the final concentration of trithionate is similar to that shown in Section 4.2.1.2 for a 24 hour period. Furthermore, the final concentration of trithionate in the leach is consistent with both the timeframe of analysis and the concentration of added trithionate.

Results were obtained for a set of 10 resins that had performed successfully during screening testing. The resins selected were methyl-imidazole (MIM), ethyl-imidazole (EIM), 1-propyl-imidazole(1PIM), 2-propyl-imidazole(2PIM), benzyl-imidazole (BIM), methyl-diethylamine (MDM), 1-propyl-diethylamine (1PDM), quinuclidine (QNU), N-methyl-2-

piperidine-methanol (M2PM), N,N-dimethyl-piperazine (MAZ), N-methyl-piperidine (MIP) and piperidine-ethanol (PET).

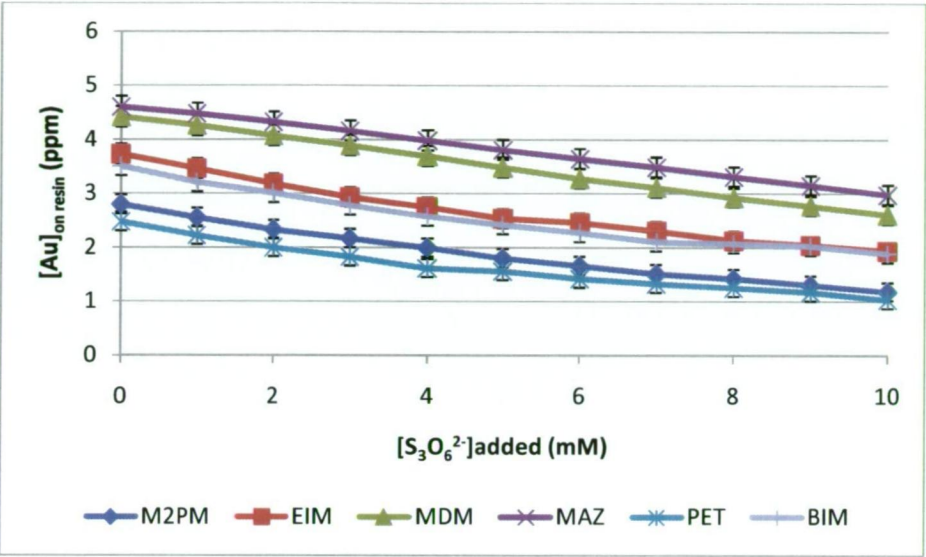


Figure 5.2 Trithionate competition testing results 1

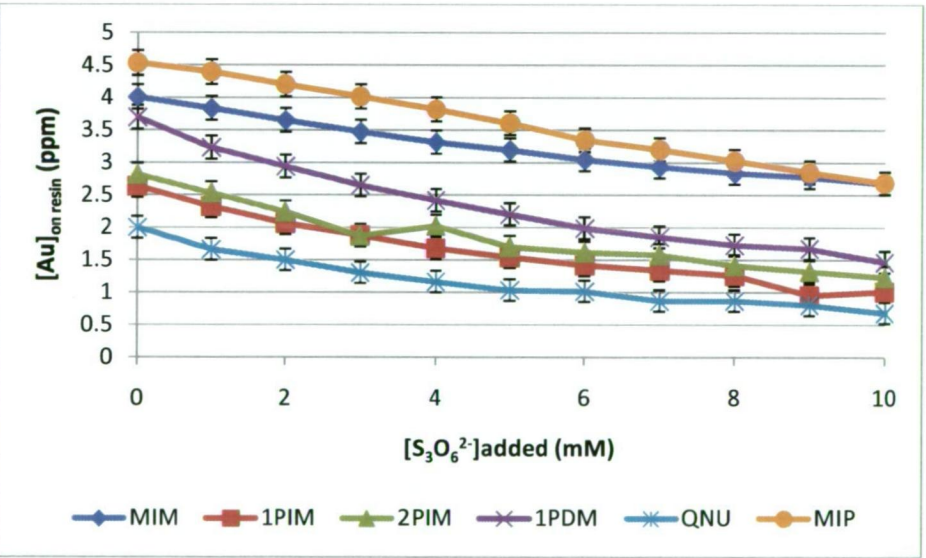


Figure 5.3 Trithionate competition testing results 2

Figure 5.2 and Figure 5.3 show similar trends in that as the concentration of added trithionate in the leach solution increases there is a corresponding decrease in the concentration of adsorbed aurothiosulfate, resulting in an increase in the solution concentration of gold. This is due to increased competition for ion-exchange sites between

the adsorbed aurothiosulfate complex and the trithionate ion. Results from this testing are summarised below in Table 5-1.

Table 5-1 Trithionate uptake and elution results

Resin	Mass (g)	Capacity (mmol/g)	Capacity in leach (mmol)	Mass Au at 0mM (mg)	Mass Au at 10mM (mg)	% Au removed at 10mM added $S_3O_6^{2-}$
MIM	2.5097	1.14	2.86	4.01±0.19	2.68±0.35	33±0.14
EIM	2.4995	1.08	2.69	3.73±0.18	1.94±0.34	48±0.18
1PIM	2.5034	1.07	2.68	2.64±0.17	1.02±0.31	61±0.31
2PIM	2.5073	1.10	2.76	2.82±0.17	1.24±0.31	56±0.26
BIM	2.5608	1.10	2.82	3.51±0.18	1.89±0.33	46±0.18
MDM	2.5024	1.61	4.04	4.42±0.19	2.61±0.37	41±0.14
1PDM	2.5039	1.47	3.68	3.70±0.18	1.47±0.33	60±0.23
MIP	2.5151	0.73	1.82	4.53±0.19	2.69±0.37	41±0.41
MAZ	2.5013	1.36	3.39	4.61±0.19	2.98±0.38	35±0.10
PET	2.5049	0.34	0.86	2.48±0.17	1.04±0.31	58±0.30
QNU	2.5041	1.03	2.58	2.00±0.17	0.69±0.30	66±0.45
M2PM	2.5082	0.56	1.40	2.80±0.17	1.18±0.32	58±0.27

Data in Table 5-1 have been sorted such that imidazole-based resins are listed in order of increasing alkyl chain bulk. Initially, as the length of the alkyl chain increases from methyl- to propyl-imidazole, the percentage of gold displaced increases as a result of trithionate competition. However, as the size of the functional groups increases, e.g. for benzyl- and 2-propyl-imidazole, the increased steric bulk reduces the extent of the trithionate competition. Also of particular interest are those resins that show low ion-exchange capacities yet have adsorbed comparable amounts of aurothiosulfate. The three piperidine derivatives, PET, M2PM and MIP, all show comparatively large masses of gold extracted, and in the case of MIP a very high tolerance for competition by trithionate. Further, as shown in Figure 5.1, the concentration of polythionates produced by leach degradation indicates a greater than expected tolerance for all resins to competition by trithionate.

5.1.2 Gold saturation testing results

The maximum capacity of the ion-exchange resins for the target aurothiosulfate complex is one of the key indicators of resin performance. Ideally, resins should be able to adsorb gold to the limit imposed by the stoichiometry of the Equation 5-1.



where (R) is the resin backbone and R is an alkyl substituent.

Resins that deviate from this ideal behaviour are suspect and should be discarded from further consideration as adsorption greater than that suggested by the stoichiometry of the adsorption mechanism indicates either an adsorption mechanism other than ion-exchange or penetration and entrapment of the aurothiosulfate complex in pore spaces within the resin and therefore would cause issues with elution and recovery of adsorbed aurothiosulfate. An adsorption of aurothiosulfate less than that suggested by the stoichiometry of the adsorption mechanism indicates either the presence of hindered ion-exchange sites inaccessible to the aurothiosulfate complex or inaccuracies in the initial ion-exchange capacity estimation.

A small mass (0.100g) of each of the resins of interest was suspended in 500mL of a solution containing 30ppm of gold as sodium aurothiosulfate using an overhead stirrer. The reaction vessels were suspended in a water bath thermostatically controlled at 30°C. Resins were allowed to adsorb aurothiosulfate from solution for 24 h with sampling performed in a similar manner to that described in Section 2.2.9.1. The removed aliquots were then analysed for gold content by atomic AAS against known concentrations of gold tetrachloride ($[AuCl_4^-]$) in 5% HCl.

Initial testing focussed on methyl-imidazole (MIM), ethyl-imidazole (EIM), benzyl-imidazole (BIM), piperidine ethanol (PET) and triethylamine (TEA) functionalised resin systems due to

good results shown in the previous chapter. As can be seen in Figure 5.4, initial uptake of aurothiosulfate was rapid, followed by saturation of the resin functional groups at equilibrium.

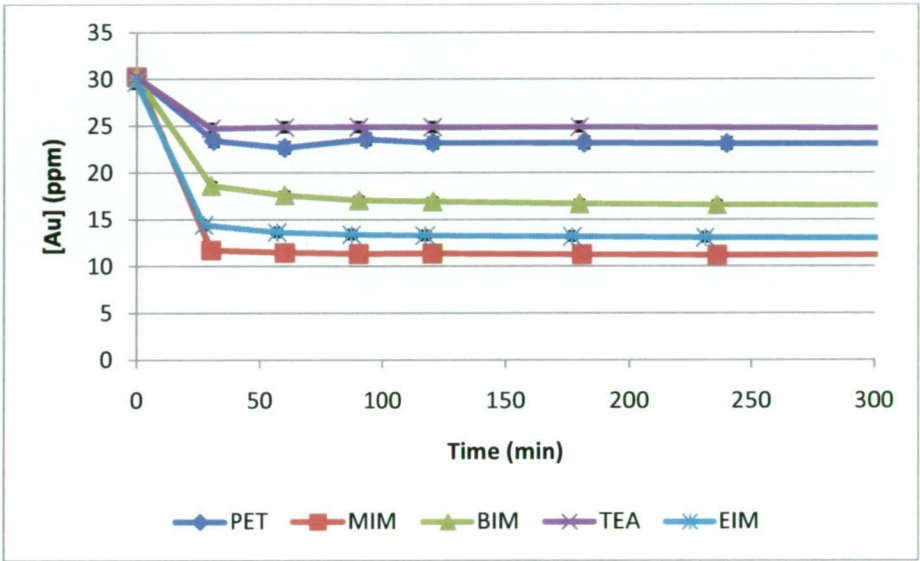


Figure 5.4 Aurothiosulfate uptake results for selected resins at 30°C

Table 5-2 shows that all resin systems tested had reached equilibrium and all available ion-exchange sites had been saturated with aurothiosulfate. Given the stoichiometry shown in Equation 4-1, a 1:3 relationship should be shown between the adsorbed aurothiosulfate complex and the ion-exchange functional groups present on the surface of the resin. Therefore the relationship between the two was calculated according to Equation 5-2 with a value of 100% indicating complete coverage.

$$\% \text{ coverage} = \frac{[Au]_{\text{adsorbed}}}{3 \times [\text{Ion exchange groups}]_{\text{resin}}} \times 100 \quad (5-2)$$

Table 5-2 Gold mass balance calculations for selected resins at 30°C

Resin	Ion-exchange capacity (mmol/g)	Mass (g)	Capacity in solution (eq)	Gold adsorbed (mg/g)	Gold adsorbed (eq)	eq _{Au} /eq _{capacity} (%)
PET	0.342	0.1175	4.018 x10 ⁻⁵	30.1±2.0	5.40 x10 ⁻⁵ ±1.2x10 ⁻⁶	134±3
MIM	1.01	0.1183	1.195 x10 ⁻⁴	81.0±2.8	1.46 x10 ⁻⁴ ±1.7x10 ⁻⁶	122±1
BIM	0.991	0.1088	1.079 x10 ⁻⁴	63.4±1.4	1.10 x10 ⁻⁴ ±7.8x10 ⁻⁷	97±0.7
TEA	0.219	0.1127	2.467 x10 ⁻⁵	24.4±1.3	4.11 x10 ⁻⁵ ±7.7x10 ⁻⁷	170±3
EIM	1.036	0.1127	1.167 x10 ⁻⁴	76.7±1.3	1.32 x10 ⁻⁴ ±7.6x10 ⁻⁷	113±0.7

Similar results were obtained for quinuclidine (QNU), methyl diethylamine (MDM), 1-propyl diethylamine (1PDM), methyl piperidine (MIP) and N,N dimethyl piperazine (MAZ) functionalised resin systems. Figure 5.5 illustrates a similar uptake curve to that shown in Figure 5.4 as uptake of aurothiosulfate was rapid with equilibrium being established within 2h for most resins.

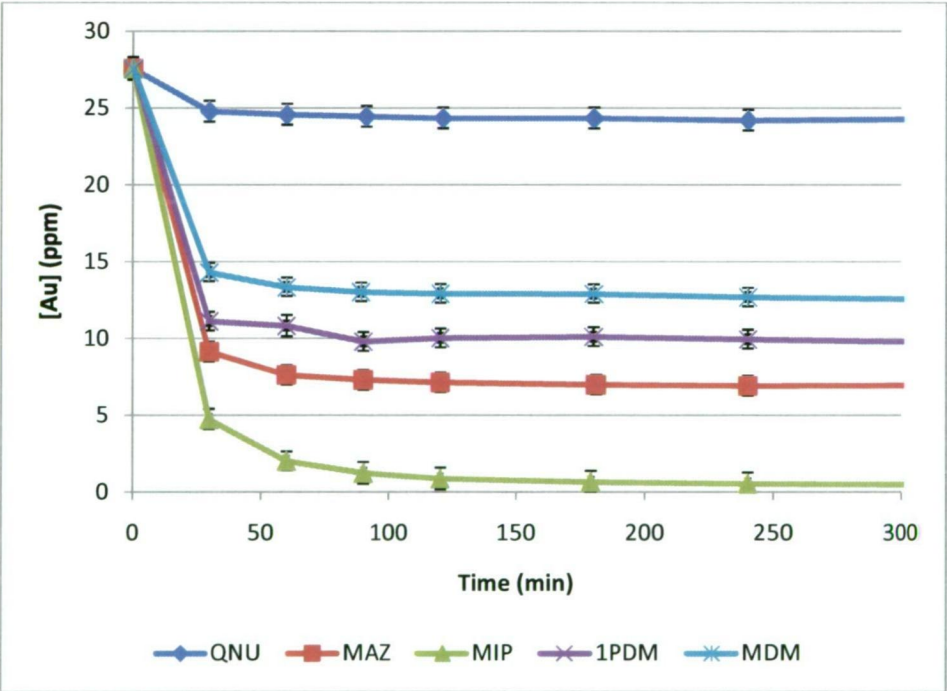


Figure 5.5 Aurothiosulfate uptake results for selected resins at 30°C

As seen in previous results, the aurothiosulfate concentration in solution had stabilised, indicating that all resins had reached equilibrium. A mass balance was performed with the

results provided in Table 5-3. Of note is the low aurothiosulfate loading of quinuclidine and 1-propyl-diethylamine functionalised resins in comparison to their ion-exchange capacities. This can be attributed to either inaccurate ion-exchange capacity measurements or loss of aurothiosulfate to other surfaces within the reactor system. However, each of these explanations does not account for the small coverage of these resins.

Adsorption values being greater than 100% of the available ion-exchange coverage are discussed in Section 4.2.1.1.2.

Table 5-3 Gold mass balance calculations for selected resins at 30°C

Resin	Ion-exchange capacity (mmol/g)	Mass (g)	Capacity in solution (eq)	Gold adsorbed (mg/g)	Gold adsorbed (eq)	$eq_{Au}/eq_{capacity}$ (%)
QNU	0.342	0.1175	4.02×10^{-5}	14.4 ± 2.7	$2.56 \times 10^{-5} \pm 4.8 \times 10^{-6}$	64 ± 12
MAZ	1.356	0.1183	1.60×10^{-4}	88.3 ± 2.6	$1.59 \times 10^{-4} \pm 4.6 \times 10^{-6}$	99 ± 3
MIP	1.511	0.1089	1.64×10^{-4}	124.5 ± 3.1	$2.06 \times 10^{-4} \pm 5.2 \times 10^{-6}$	126 ± 3
1PDM	1.469	0.1127	1.65×10^{-4}	80.8 ± 2.6	$1.39 \times 10^{-4} \pm 4.5 \times 10^{-6}$	84 ± 3
MDM	1.078	0.1127	1.21×10^{-4}	68.4 ± 2.5	$1.17 \times 10^{-4} \pm 4.4 \times 10^{-6}$	97 ± 4

5.2 Resin cycling results

The ability of a resin to adsorb and release aurothiosulfate over several uptake/elution/regeneration cycles is an essential factor for industrial operational viability. As seen in Section 4.3, several elution systems were shown to be effective for the elution of aurothiosulfate. Although the nitrate elution scheme was shown to be more effective at eluting gold from imidazole based resins, the thiocyanate elution regime followed by ferric nitrate regeneration was shown to be effective for the elution of aurothiosulfate from most resin functional groups studied. Another important factor in the choice of the eluent system is the ease with which it can be employed in an industrial application. The nitrate elution regime has been used in industrial applications for the selective elution of copper from Dowex-Minix resins³ at Murantau mine, Uzbekistan. Elution employing the thiocyanate ion

Chapter 5 – Further resin evaluation

has been shown to elute both gold cyanide and aurothiosulfate species from ion-exchange resins⁴ and has been shown in this work to be a more effective eluent for selected resins than nitrate⁵.

An adsorption/elution/regeneration cycle was performed in a similar manner to that described in Section 2.2.9 and 2.2.10. A known mass of resin was loaded into a glass ion-exchange column as detailed in Section 2.2.4 and flushed with 50mL of 1M sodium chloride solution at a flow rate of 1mL/min followed by 50mL of MilliQ water at the same flow-rate. This ensured all ion-exchange groups were present in the chloride form. The resins were then removed from the ion-exchange columns by flushing with water and magnetically separated from the overlying supernatant water. The resin slurry was then rinsed into 500mL polypropylene bottles with aliquots of a synthetic leach solution containing 20ppm gold as the aurothiosulfate complex prepared as per Section 2.2.8. A 5mL aliquot of the synthetic leach solution was taken to determine the initial gold concentration. The resins were then agitated on an orbital shaker at 200rpm and allowed to adsorb gold for 2h after which a 5mL aliquot of the leach solution was taken for solution gold mass-balance calculations. The resins were then magnetically separated from the leach solution, loaded into the glass ion-exchange columns and elution performed as described in Section 2.2.10.3. Following elution of the adsorbed aurothiosulfate complex and regeneration of the resin beads, the eluted resin was then flushed with MilliQ water at 2mL/min until the eluent was clear and colourless. This procedure was then repeated four times allowing quantification of resin performance for 5 uptake/elution/regeneration cycles.

5.2.1 Basic thiocyanate elution cycling results

Figure 5.6 illustrates an elution profile typical to all resin functional groups in that 100% of the aurothiosulfate that will be eluted is achieved within 3 bed volumes, or 30mL. Further resin elution profiles are provided in Appendix B.

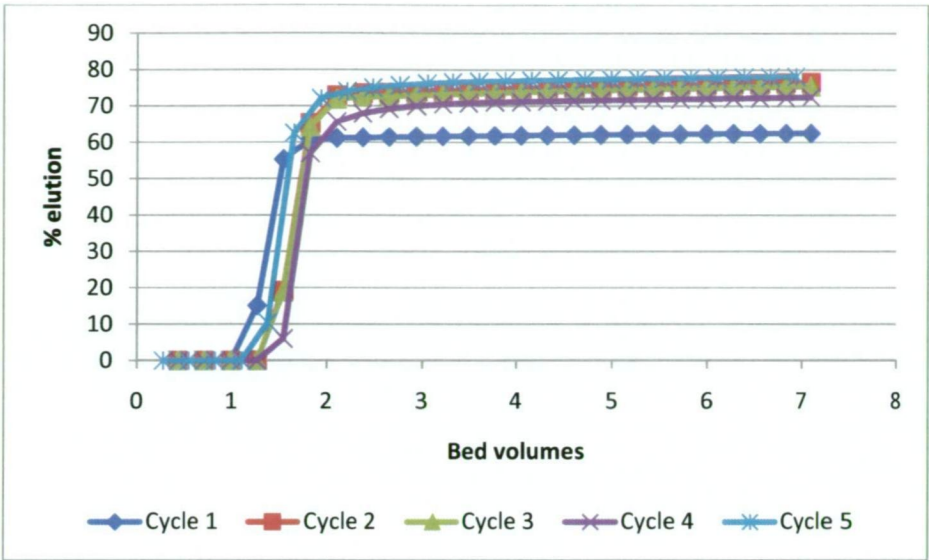


Figure 5.6 MIP 5 cycle elution profile

Table 5-4 Resin cycling results

Resin	Cycle #	mg Au uptake	mg Au eluted	% elution	Resin	Cycle #	mg Au uptake	mg Au eluted	% elution
PET	1	5.19±0.23	2.75±0.008	53±4	QNU	1	1.03±0.23	0.68±0.008	66±23
	2	1.73±0.14	1.16±0.06	67±10		2	1.58±0.24	0.50±0.008	32±15
	3	3.06±0.21	1.08±0.007	35±7		3	3.02±0.19	0.59±0.011	20±6
	4	2.33±0.21	1.16±0.007	50±9		4	0.91±0.19	0.55±0.007	60±21
	5	1.56±0.22	0.97±0.008	62±14		5	1.01±0.19	0.65±0.006	64±19
BIM	1	6.66±0.19	4.23±0.008	64±3	1PDM	1	2.47±0.24	1.50±0.009	61±9
	2	4.04±0.15	1.80±0.06	45±5		2	2.68±0.24	1.07±0.008	40±8
	3	3.96±0.21	1.72±0.007	43±0.5		3	1.63±0.19	1.24±0.017	76±11
	4	3.97±0.22	2.24±0.008	57±6		4	1.91±0.19	1.25±0.007	65±10
	5	3.82±0.23	1.71±0.008	45±6		5	2.10±0.19	1.36±0.007	65±9
EIM	1	7.53±0.19	4.88±0.008	65±3	MAZ	1	4.74±0.25	3.23±0.009	68±5
	2	4.32±0.16	1.73±0.06	40±5		2	4.60±0.24	2.92±0.009	63±5
	3	4.13±0.21	1.83±0.007	44±5		3	4.58±0.20	3.67±0.055	80±5
	4	4.16±0.22	2.40±0.008	58±0.5		4	4.64±0.20	3.68±0.007	79±5
	5	4.01±0.23	1.84±0.008	46±6		5	4.78±0.20	3.73±0.008	78±0.4
TEA	1	4.63±0.24	1.08±0.007	23±5	MDM	1	4.59±0.25	3.06±0.009	67±5
	2	0.64±0.15	0.38±0.05	59±27		2	4.45±0.25	3.13±0.009	70±6
	3	0.93±0.21	0.26±0.007	28±23		3	4.44±0.20	3.43±0.05	77±5
	4	0.86±0.22	0.27±0.007	31±25		4	4.47±0.20	3.53±0.007	79±4
	5	0.87±0.23	0.23±0.007	26±26		5	4.64±0.20	3.81±0.008	82±4
MIM	1	7.60±0.19	3.55±0.012	47±2	MIP	1	4.67±0.25	2.93±0.008	63±5
	2	4.72±0.16	1.42±0.05	30±5		2	4.64±0.25	3.55±0.009	77±5
	3	4.47±0.21	1.63±0.008	37±5		3	4.71±0.19	3.49±0.05	74±5
	4	4.51±0.23	2.29±0.008	51±5		4	4.71±0.20	3.42±0.007	72±4
	5	4.45±0.23	1.29±0.008	29±5		5	4.88±0.20	3.81±0.007	78±4

Data in Table 5-4 shows that the behaviour seen in resin uptake and elution studies performed for initial screening is maintained over multiple adsorption/elution/regeneration cycles. Imidazole based resins, such as methyl-, ethyl- and benzyl-imidazole (MIM, EIM and BIM respectively) show comparatively large amounts of aurothiosulfate being adsorbed onto the resin ion-exchange sites, but low percentages of gold being eluted. In comparison, the alkylamine resins show lesser amounts of aurothiosulfate being adsorbed but higher amounts of gold being eluted. None of the resins tested show greater than 80% elution. This indicates that even though thiocyanate was the most viable elution mechanism for these resins, further elution system optimisation is required.

Most of the resins in Table 5-4 show similarities in uptake and elution performance between cycles. If aurothiosulfate was being retained by the resin between cycles, then ion-exchange capacity would be being diminished between cycles as sites are occupied by uneluted gold complexes. This would be indicated by a decline in the adsorption of aurothiosulfate with successive cycles. This behaviour is shown in Table 5-4 for imidazole-based resin systems, however the trialkylamine-based resin systems show very little retention of aurothiosulfate between cycles due to incomplete elution of the aurothiosulfate complex by the thiocyanate elution system.

To determine the amount of adsorbed gold that the resins retained, 0.500g of cycled resin was digested in a similar manner to the method detailed in Section 2.2.14 by charring the resin in 10mL of concentrated sulfuric acid followed by clarification with concentrated nitric acid. Both acids were certified to contain less than 0.05ppm total gold. The resultant clarified solutions were then made to 100.00mL and analysed for gold content using AAS with calibration against known concentrations of gold tetrachloride ($[\text{AuCl}_4]^-$) in 5% HCl.

Data in Table 5-5 shows large discrepancies between the mass of gold theoretically uneluted from the resin beads according to mass-balance from the elution results and from that

calculated by the digestion of a sample of the eluted resins. The imidazole-based resins have retained a larger proportion of the adsorbed aurothiosulfate complex when compared to the alkylamine-based resin systems. A possibility for the adsorbed aurothiosulfate to have been removed from the resin is during the testing cycles is during the regeneration portion of the elution system. This is unlikely, as the concentrations of ferric nitrate used for that step are a tenth of that used in Section 2.2.10.3 for the elution of adsorbed aurothiosulfate. However, literature has shown that a mixed-mode elution system^{6,7} shows greater gold recovery than with single eluents alone and as such it is possible that aurothiosulfate has been eluted in the regeneration step. Further suggestions in the literature for the possible loss of aurothiosulfate during testing is due to oxidation of the thiosulfate ligand and consequent reduction and precipitation of the gold as micron-sized particles⁸.

Table 5-5 Resin digestion results

Resin	Total mass Au adsorbed (mg)	Total mass Au eluted (mg)	Theoretical mass Au on resin (mg)	Mass Au from digestion (mg)
PET	13.87±0.45	7.125±0.06	6.747±0.45	0.89±0.51
BIM	22.45±0.45	11.72±0.06	10.73±0.45	5.45±2.86
EIM	24.16±0.46	12.69±0.06	11.47±0.46	4.32±2.25
TEA	7.935±0.47	2.217±0.05	5.718±0.47	1.85±1.01
MIM	25.76±0.46	10.18±0.05	15.58±0.45	11.0±7.27
QNU	7.541±0.46	2.968±0.08	4.573±0.47	0.55±0.31
1PDM	10.78±0.47	6.426±0.02	4.359±0.47	1.13±0.62
MAZ	23.35±0.48	17.23±0.06	6.112±0.48	0.56±0.31
MDM	22.59±0.49	16.96±0.06	5.630±0.49	0.05±0.02
MIP	23.62±0.49	17.20±0.05	6.419±0.49	0.053±0.05

5.3 Kinetic studies

5.3.1 Resin preparation and temperature selection

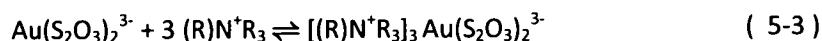
Ion-exchange resins were initially prepared for kinetic studies by loading resins into ion-exchange columns in a similar manner to that employed in Section 2.2.4. A 50mL aliquot of a 1M solution of sodium chloride was then flushed through the column at a flow-rate of 1mL min⁻¹ at room temperature, followed by 50mL of MilliQ water at room temperature at the same flow-rate. This ensured that all functional groups present on the resin were in the chloride form. The resins were then flushed from the ion-exchange columns and magnetically separated from the overlying supernatant water, followed by drying as described in Section 2.2.2. A known mass of resin was wetted in 30mL of MilliQ water for 30 min. A solution containing 30ppm gold as sodium aurothiosulfate was then prepared and once the resin beads had been adequately wetted, the beads were magnetically separated from the overlying solution and transferred to 500mL glass reaction vessels using aliquots of this solution. The glass reaction vessels were then suspended in a water bath at temperatures of 30, 40 and 50°C for 24 h. Aliquots of the solutions were taken at intervals as described in Section 2.2.9.1 for AAS analysis for gold against known concentrations of gold tetrachloride ([AuCl₄]⁻) in 5% HCl.

5.3.2 Results, analysis and discussion

5.3.2.1 Rate of aurothiosulfate adsorption approximation

As gold uptake results were obtained from solutions containing only sodium aurothiosulfate, it is theoretically possible to fit the adsorption data to standard reaction kinetics equations and derive a reaction order with respect to gold.

The reaction is of the type:



where (R) is the stationary phase and R is an alkyl substituent.

Chapter 5 – Further resin evaluation

If the reaction displays first order kinetics with respect to both components, then the rate equation is given by

$$v = k \cdot [A]_t \cdot [B]_t \quad (5-4)^9$$

where $[X]_t$ denotes the concentration of component X in solution at time t .

Given a large excess of reagent B relative to reagent A, i.e $B \gg A$, then the rate equation can be approximated by

$$v = k' \cdot [A] \quad (5-5)^9$$

$$k' = k \cdot [B]_0 \quad (5-6)^9$$

Integration of the approximated rate equation gives

$$\ln \frac{[A]_t}{[A]_0} = -k't \quad (5-7)^9$$

Hence, a plot of $\ln[Au]_t$ against time will have a slope of $-k'$.

Alternatively, if the reaction is second order with respect to A, then the rate of reaction is given by

$$v = \frac{k \cdot [A]_t^2 \cdot [B]_t}{3} \quad (5-8)$$

and if the same approximation as before is used, i.e $B \gg A$, then we can make the approximation that $k = (k' \cdot [B]_0)$.

Integration of the second order approximation is given by

$$\frac{1}{[A]_t} - \frac{1}{[A]_0} = -kt \quad (5-9)$$

Hence a plot of $1/[Au]_t$ against time will have a slope of $-k$.

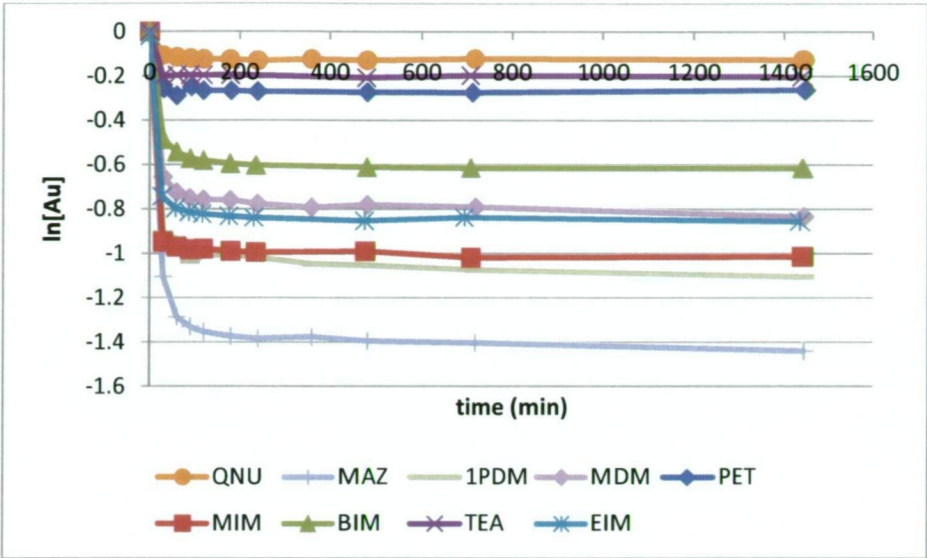


Figure 5.7 Plot of $\ln [Au]$ vs time (min) for resins studied

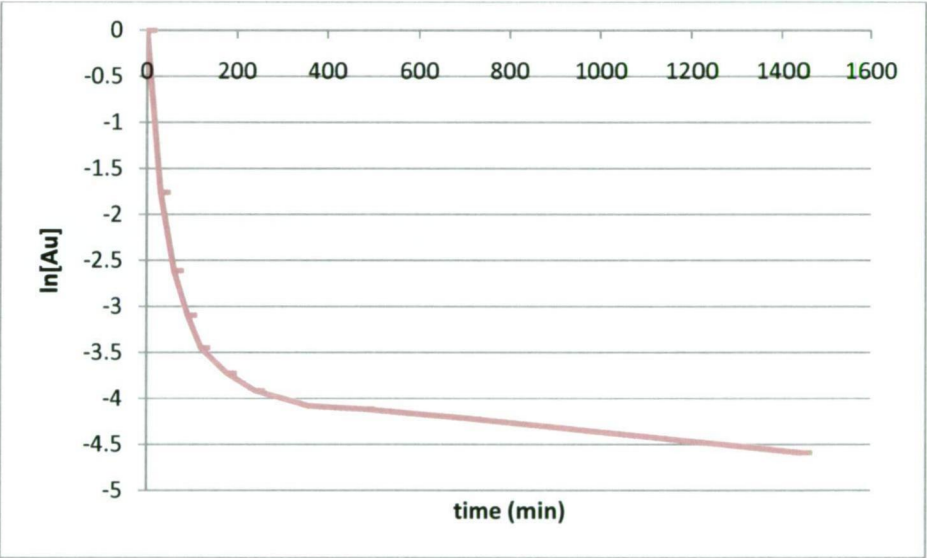


Figure 5.8 Plot of $\ln [Au]$ vs time (min) for N-methyl-piperidine (MIP)

Figure 5.7 displays linear behaviour after 200 min at which point equilibrium is established. Before this time, adsorption is exponential. Data in Figure 5.8 indicates that for the N-methyl-piperidine resin, initial adsorption was exponential until approximately 400 min. This was followed by a period of linear adsorption by the resin. Similar behaviour is indicated by Figure 5.9 below. For most resins, a short period of exponential adsorption was followed by equilibrium. Data in Figure 5.10 indicates a similar trend to Figure 5.8 in that N-methyl-piperidine shows rapid exponential adsorption followed by a linear period of adsorption.

Due to the non-linear results shown by these plots, first or second order kinetics cannot be assumed for any of the resins studied.

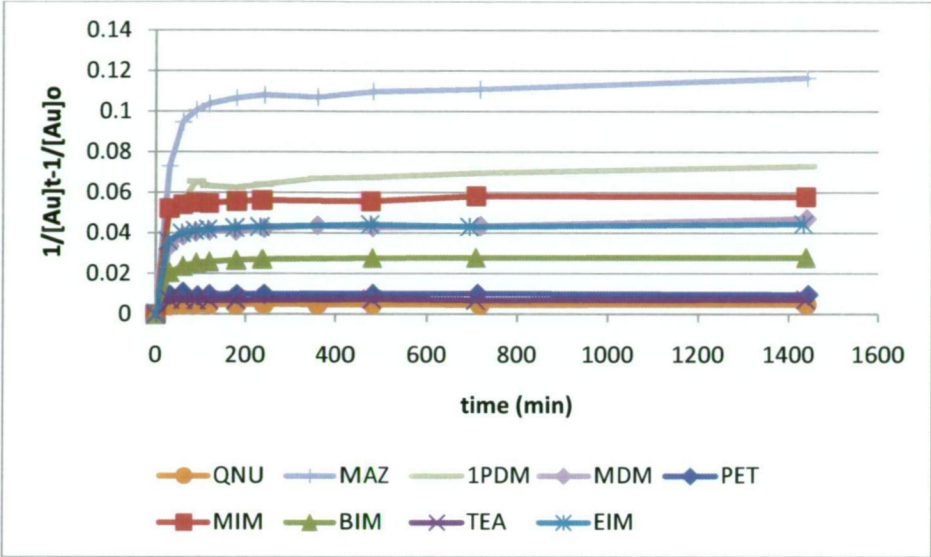


Figure 5.9 Plot of $1/[Au]_t - 1/[Au]_0$ vs time (min) for selected resins

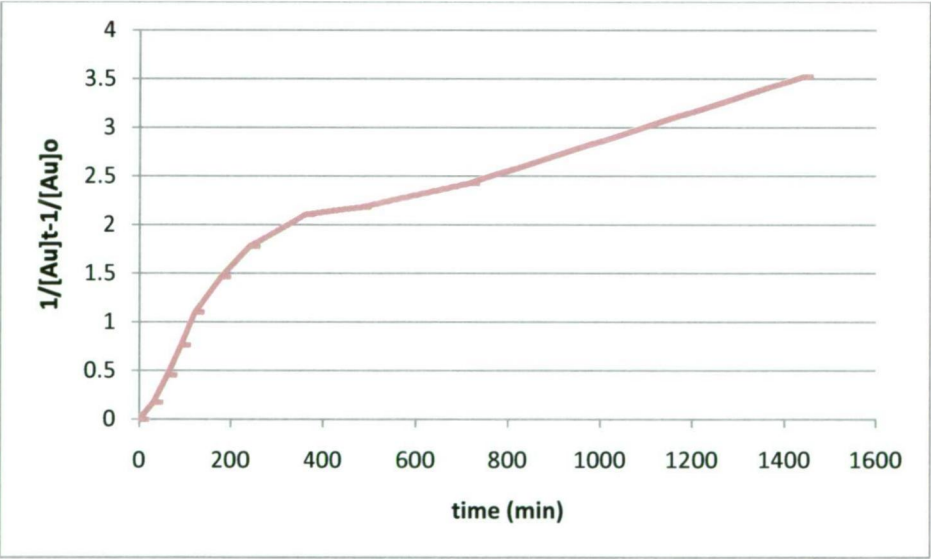


Figure 5.10 Plot of $1/[Au]_t - 1/[Au]_0$ vs time (min) for N-methyl-piperidine (MIP)

5.4 Thermodynamic studies

5.4.1.1 Estimation of enthalpy of extraction

To allow the enthalpy of extraction to be calculated, the distribution coefficient (D) for aurothiosulfate is defined according to

$$D = \frac{\text{mg Au} / \text{g adsorbent}}{\text{mg Au} / \text{L solution}} \quad (5-10)^{10-12}$$

The loading of the aurothiosulfate complex onto the ion-exchange resins studied is shown to be exothermic. For confirmation, the enthalpy of extraction was calculated by graphical analysis.

According to (5-11), a plot of $\log D$ vs. $1/T$ will have a slope of $-\Delta H/2.303R$.

$$\log D = \frac{-\Delta H}{2.303 RT} \quad (5-11)$$

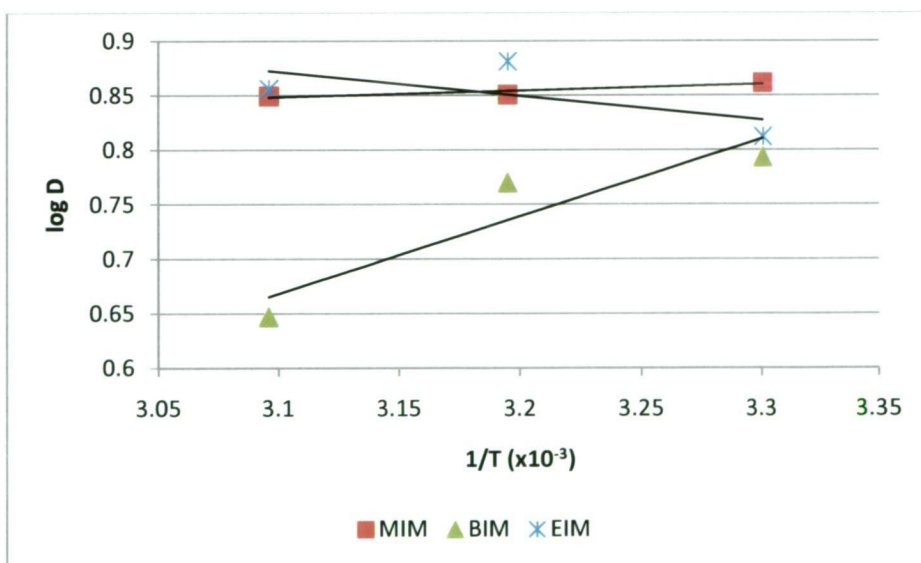


Figure 5.11 Initial enthalpy of adsorption results for MIM, BIM and EIM

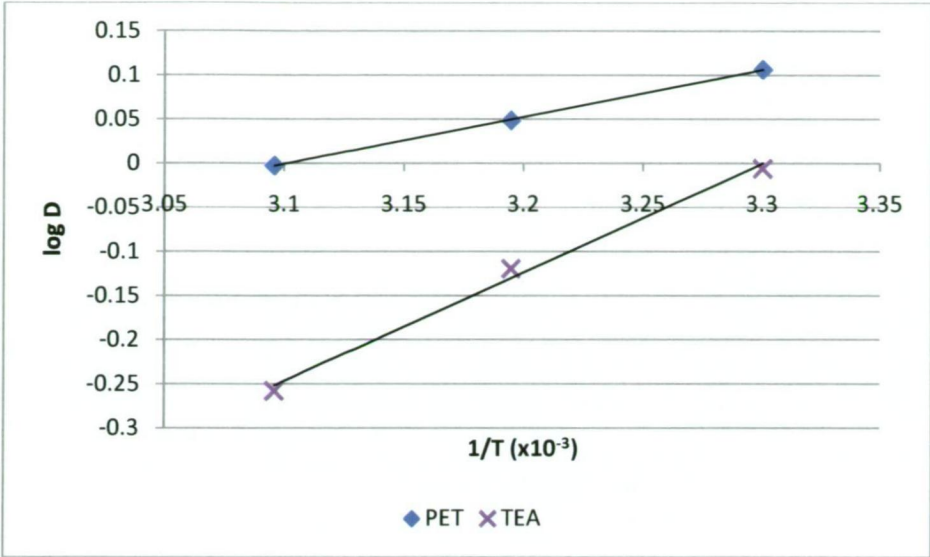


Figure 5.12 Enthalpy of adsorption results for PET and TEA

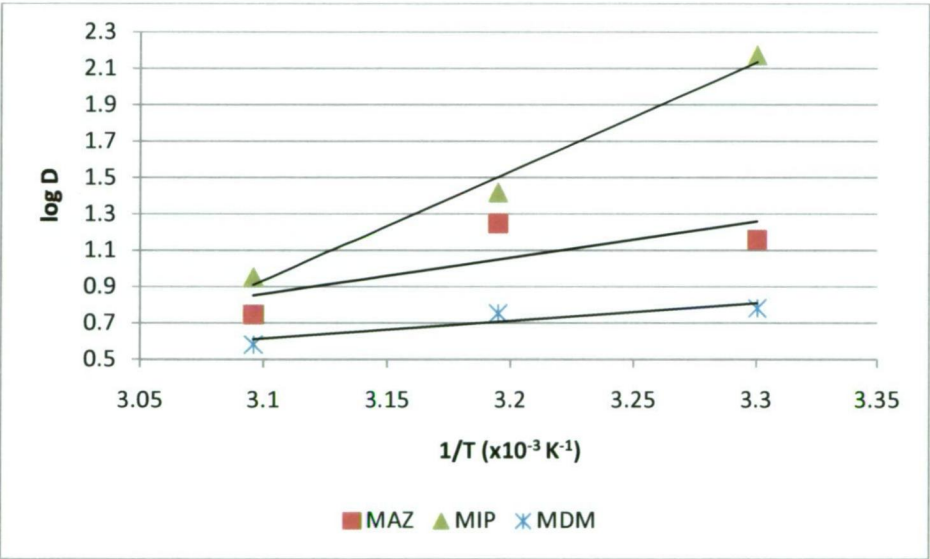


Figure 5.13 Enthalpy of adsorption results for MAZ, MIP and MDM

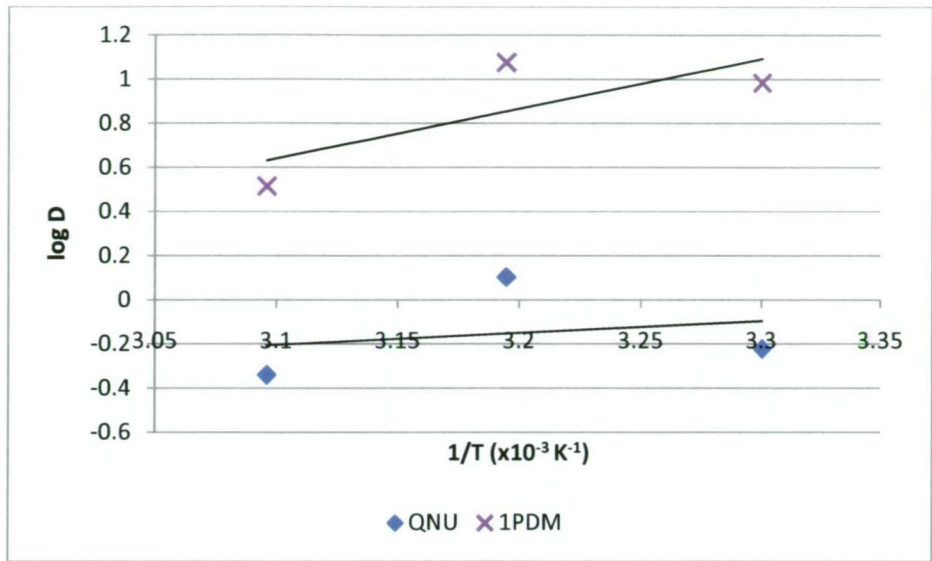


Figure 5.14 Enthalpy of adsorption results for QNU and 1PDM

Deviation from linearity may be due to degradation of the aurothiosulfate complex at high temperatures or an adsorption mechanism other than ion-exchange. This hypothesis is supported by the ratio between the amount of adsorbed gold and the number of available ion-exchange functional groups.

Table 5-6 Resin gold stoichiometry at 50°C

Resin	Ion-exchange capacity (mmol/g)	Mass in solution (g)	Capacity in solution (eq)	Gold adsorbed (mg/g)	Gold adsorbed (eq)	eq _{Au} /eq _{capacity} (%)
PET	0.342	0.1175	4.02 x10 ⁻⁵	31.2	5.58 x10 ⁻⁵	139
MIM	1.01	0.1106	11.2 x10 ⁻⁵	105.8	1.78 x10 ⁻⁴	159
BIM	0.991	0.1160	11.5 x10 ⁻⁵	96.5	1.71 x10 ⁻⁴	150
TEA	0.219	0.1117	2.45 x10 ⁻⁵	21.1	3.60 x10 ⁻⁵	147
EIM	1.036	0.1012	10.5 x10 ⁻⁵	99.8	1.54 x10 ⁻⁴	147
QNU	0.342	0.1153	1.31 x10 ⁻⁵	17.7	1.04 x10 ⁻⁵	79
MAZ	1.36	0.1055	4.77 x10 ⁻⁵	94.4	5.06 x10 ⁻⁵	106
MIP	0.725	0.1045	2.52 x10 ⁻⁵	108.4	5.76 x10 ⁻⁵	228
1PDM	1.47	0.1051	5.15 x10 ⁻⁵	69.4	3.71 x10 ⁻⁵	72
MDM	1.61	0.1167	6.27 x10 ⁻⁵	75.5	4.47 x10 ⁻⁵	71

Table 5-6 indicates that more aurothiosulfate has been adsorbed than can be accounted for by ion-exchange adsorption. This is discussed in Section 4.2.1.1.2 and indicates that some

form of aurothiosulfate adsorption or degradation is taking place at higher temperatures.

Whether this is due to increased access to hindered ion-exchange sites within the resin beads due to swelling at temperature or by degradation of thiosulfate species at higher temperatures remains to be ascertained. Previous studies have shown that thiosulfate degradation is increased with respect to temperature and in smaller concentrations¹³ and that the stability of the aurothiosulfate complex is dependent on oxidation of the thiosulfate ligand⁸.

Table 5-7 Resin enthalpy calculation results

Resin	ΔH (kJ/mol)	Resin	ΔH (kJ/mol)
TEA	-23.6	MIM	-1.12
MDM	-18.7	EIM	4.22
1PDM	-43.3	BIM	-13.6
MIP	-114	QNU	-10.3
PET	-10.2	MAZ	-38.1

Table 5-7 shows resin enthalpy data for each resin functional group. Most are exothermic and with the exceptions of MIP and MAZ, are comparable with values of -17.00kJ/mol obtained for the extraction of gold cyanide with IRA 400¹⁰. Increased steric bulk and asymmetry alters the enthalpy of extraction as seen in the enthalpy results for triethylamine (TEA), methyl-diethylamine (MDM) and 1-propyl-diethylamine (1PDM) functionalised resins.

The large exothermic value obtained for MIP was related to the complete extraction of aurothiosulfate in Section 5.1.2.

5.5 Conclusions

5.5.1 Resin cycling results

All resins were able to repeatedly uptake and elute the target aurothiosulfate complex using the thiocyanate elution regime followed by ferric nitrate regeneration. The imidazole-based resins demonstrated a large uptake of the aurothiosulfate complex but poor elution,

Chapter 5 – Further resin evaluation

whereas alkylamine-based resins showed lesser aurothiosulfate uptake but more efficient elution of the aurothiosulfate complex from the ion-exchange resins tested.

The criteria for the selection of the resins most likely to be adequate industrial performers in a synthetic leach solution are summarised below:

- Rapid and large uptake of aurothiosulfate from synthetic leach solutions
- Little or no susceptibility to elution of gold by trithionate ions
- Maximum elution of adsorbed aurothiosulfate by elution method chosen
- Minimum amount of aurothiosulfate retained by resin after elution/regeneration

As seen in Chapter 4, all resins show rapid uptake of aurothiosulfate in both synthetic leach solutions and in water, whilst most resin systems show some small susceptibility to added trithionate ions.

To quantitatively rank each resin and thereby determine the most viable resin system for industrial application, Table 5-8 and Table 5-9 were prepared.

Table 5-8 Maximum elution of adsorbed aurothiosulfate

Resin	Total mass Au adsorbed (mg)	Total mass Au eluted (mg)	Mass Au on resin (mg)	% elution
MDM	22.59±0.49	16.96±0.05	5.630±0.49	75±2
MAZ	23.35±0.48	17.23±0.06	6.112±0.48	74±2
MIP	23.62±0.49	17.20±0.05	6.419±0.49	73±2
1PDM	10.78±0.47	6.426±0.02	4.359±0.47	60±4
EIM	24.16±0.46	12.69±0.06	11.47±0.46	53±2
BIM	22.45±0.45	11.72±0.06	10.73±0.45	52±2
PET	13.87±0.45	7.125±0.06	6.747±0.45	51±3
MIM	25.76±0.46	10.18±0.05	15.58±0.46	40±2
QNU	7.541±0.46	2.968±0.08	4.573±0.47	39±7
TEA	7.935±0.47	2.217±0.05	5.718±0.47	27±6

Table 5-8 indicates that the best performing resin would be the methyl-diethylamine resin, which is similar in structure to the trimethylamine resins used commercially. An interesting result is that for triethylamine (TEA) which demonstrated a strong aurothiosulfate retention

behaviour as seen in Table 5-4. The initial uptake and elution for this resin is quite large, however performance over subsequent cycles is greatly reduced. Similar behaviour is seen for quinuclidine (QNU).

Table 5-9 Minimum retention of adsorbed aurothiosulfate after 5 uptake/elution cycles

Resin	Total mass Au adsorbed (mg)	Total mass Au eluted (mg)	Mass Au on resin (mg)	Mass Au from digestion (mg)
MDM	22.6±0.49	16.9±0.05	5.63±0.49	0.05±0.02
MIP	23.6±0.49	17.2±0.05	6.42±0.49	0.05±0.05
QNU	7.54±0.46	2.97±0.08	4.57±0.47	1.13±0.62
MAZ	23.4±0.48	17.2±0.06	6.11±0.48	0.56±0.31
PET	13.9±0.45	7.13±0.06	6.75±0.45	0.89±0.51
1PDM	10.8±0.47	6.43±0.02	4.36±0.47	1.13±0.62
TEA	7.94±0.47	2.22±0.05	5.72±0.47	1.85±1.01
EIM	24.2±0.46	12.7±0.06	11.5±0.46	4.32±2.25
BIM	22.5±0.45	11.7±0.06	10.7±0.45	5.45±2.86
MIM	25.8±0.46	10.2±0.05	15.58±0.45	11.0±7.27

Table 5-9 is similar to Table 5-8 but the data have been sorted with respect to the amount of gold remaining within the resin, as determined by resin digestion. In this case, most of the alkylamine-based resins show very little gold retained within the resin beads. A common thread through Table 5-8 and Table 5-9 is the presence of N-methyl-piperidine (MIP) near the top of each table. This particular resin shows good uptake and elution of aurothiosulfate in leach conditions, along with low concentrations of aurothiosulfate retained after cycling.

5.5.2 Kinetics and thermodynamics studies

Resin kinetics were evaluated at constant temperature by correlating decrease in gold concentration in solution to resin aurothiosulfate loadings. First order or second order kinetics were unable to be confirmed due to a lack of linearity in either plot.

Enthalpy of extraction was able to be estimated and most resins showed exothermic enthalpies of extraction for aurothiosulfate. With a few notable exceptions, values for the enthalpy of extraction of aurothiosulfate onto the ion-exchange resins studied were comparable to those for gold cyanide onto commercial ion-exchange resins. This indicates

that the MIEX^(R) resins developed in this study can be integrated into an operational mill flow sheet without major modification.

Further studies that may be performed would determine whether the rate of adsorption of aurothiosulfate onto the ion-exchange resins tested was limited by diffusion of the complex to the resin surface through a hypothetical hydrodynamic boundary layer (the linear film diffusion model¹⁴), mass-transport of the dissolved species in the filled pores of the resin (the pore diffusion model¹⁴) or migration along internal pore walls (the surface diffusion model¹⁴). Whilst this work has shown that aurothiosulfate is readily adsorbed onto the ion-exchange resins tested, it is an acknowledged deficiency of the work that the mechanism behind that adsorption was unable to be determined.

5.5.3 Resin selection

As shown in Chapter 1, resins should be highly selective for aurothiosulfate over both the copper thiosulfate complexes and polythionate species present in a synthetic leach solution, allow a rapid and large uptake of aurothiosulfate from a synthetic leach solution, allow for rapid and efficient elution of the adsorbed aurothiosulfate complex and retain a minimum of aurothiosulfate after elution. Due to similarities to other imidazole-based resins present in the study, the 1-propyl- and 2-propyl-imidazole functionalised resins were deemed to be unsuitable for further study after trithionate testing. Based upon high retention of aurothiosulfate after 5 uptake/elution/regeneration cycles, the quinuclidine-, 1-propyl-diethylamine and imidazole-based resins were deemed to be unsuitable for industrial application.

5.6 References

1. West-Sells, P. G.; Ji, J.; Hackl, R. P., A process for counteracting the detrimental effect of tetrathionate on resin gold adsorption from thiosulfate leachates. *Hydrometallurgy* 2003, *Proceedings of the International Symposium honoring Professor Ian M. Ritchie, 5th, Vancouver, BC, Canada, Aug. 24-27, 2003* **2003**, 1, 245-256.
2. Jeffrey, M. I.; Brunt, S. D., The quantification of thiosulfate and polythionates in gold leach solutions and on anion exchange resins. *Hydrometallurgy* **2007**, 89, (1-2), 52-60.
3. Marsden, J.; House, I., *The Chemistry of Gold Extraction*. Second Edition ed.; Society for Mining, Metallurgy and Exploration 2006; p 650.
4. Fleming, C. A.; Cromberge, G., The elution of aurocyanide from strong- and weak-base resins. *Journal of the South African Institute of Mining & Metallurgy* **1984**, 84, (9), 269-80.
5. Oliveira, A. M.; Leao, V. A.; da Silva, C. A., A proposed mechanism for nitrate and thiocyanate elution of strong-base ion exchange resins loaded with copper and gold cyano complexes. *Reactive & Functional Polymers* **2008**, 68, (1), 141-152.
6. Jeffrey, M. I.; Brunt, S., Loading and elution of gold thiosulfate from anion exchange resins. *Publications of the Australasian Institute of Mining and Metallurgy* **2007**, 9/2007, (World Gold 2007), 239-243.
7. Jeffrey, M. I. Recovery of metals from ion-exchange resins. International patent WO 2007/137325 A1, 20070522., 2007.
8. Benedetti, M.; Boulegue, J., Mechanism of gold transfer and deposition in a supergene environment. *Geochim. Cosmochim. Acta* **1991**, 55, (6), 1539-1547.
9. Atkins, P.; De Paula, J., *Physical Chemistry*. 8th ed.; Oxford University Press: New York, 2006; Vol. 1, p 1064.
10. Adams, M. D.; McDougall, G. J.; Hancock, R. D., Models for the absorption of aurocyanide onto activated carbon. Part II: Extraction of aurocyanide ion pairs by polymeric adsorbents. *Hydrometallurgy* **1987**, 18, (2), 139-54.
11. McDougall, G. J.; Adams, M. D.; Hancock, R. D., Models for the adsorption of aurocyanide onto activated carbon. Part I: Solvent extraction of aurocyanide ion pairs by 1-pentanol. *Hydrometallurgy* **1987**, 18, (2), 125-38.
12. Adams, M. D.; McDougall, G. J.; Hancock, R. D., Models for the adsorption of aurocyanide onto activated carbon. Part III: Comparison between the extraction of aurocyanide by activated carbon, polymeric adsorbents and 1-pentanol. *Hydrometallurgy* **1987**, 19, (1), 95-115.
13. Skoog, D. A.; Holler, F. J.; West, D. M., *Fundamentals of analytical chemistry*. 7th ed.; Saunders College Pub.: Fort Worth, 1996; p 1 v. (various pagings).
14. Dai, X.; Breuer, P. L.; Jeffrey, M. I. In *Microtomography based identification of the mechanisms of gold adsorption onto activated carbon and modelling*, *Hydrometallurgy* 2008: Proceedings of the 6th International Symposium, Phoenix, AZ, 2008; Phoenix, AZ, 2008; pp 696-705.

6 Conclusions

6.1 Introduction

This chapter serves to summarise the work in this project with a critical analysis of the final results and recommendations for further research.

6.2 Resin recommendations and proposals

6.2.1 Problematic resin syntheses

This work has demonstrated the preparation and characterisation of a series of magnetic, aurothiosulfate selective ion-exchange resins that have been tested in simulated thiosulfate leach environments. These novel resins were synthesised by the attachment of secondary or tertiary amines to the epoxide functional groups present on the MIEX™ magnetic resin substrate supplied by Orica Watercare. This resin caused some of the issues with resin functionalisation as the epoxide functional groups degraded over time via mechanisms illustrated in Scheme 3.1. As a result, this caused major difficulties with the attachment of amine functionalities to the resin substrate. This has resulted in abandonment of several promising functionalities suggested from prior work¹⁻³ due to inability to attach larger quaternary and tertiary amines to the solid support as degradation had caused the epoxide groups present on the resin surface to open, forming vicinal diols. Once this had occurred, any attempt at resin functionalisation with amines would fail.

Furthermore, the supplied functionalisation method developed by CSIRO and licensed to Orica Watercare employed water as a solvent. The use of water as a solvent complicated the resin functionalisation procedure as to alkylate the amine functional groups attached to the resin surface, alkyl halides were required. The use of these reagents demanded that the resins had to be dried and then re-wetted in the organic solvent of choice as these reagents would degrade in the presence of water, forming the alcohol and halide ions. This

Chapter 6 - Conclusions

drying/solvation/drying cycle caused resin beads to swell and contract, resulting in the loss of pore structure within the resin bead as a result of osmotic shock, along with cracking and deformation of the resin surface as seen in Section 3.3.

Despite these issues, most of the resins employed in the further testing category detailed in Chapter 5 exhibited functionalisation greater than 1mmol/g, which is comparable to similar ion-exchange resins reported in literature for this application^{4,5}. Resins also demonstrated good correlations between the amount of gold present on the ion-exchange resin and the number of functional groups present when the resins were suspended in water, indicating attainment of equilibrium and confirming ion-exchange capacity measurements. When the resins were suspended in a synthetic leach solution, strong competition from the other ions present in the leach solution prevented complete adsorption of aurothiosulfate, as the resin was saturated with other ions from the synthetic leach solution. Despite this, uptake of aurothiosulfate from solution reached equilibrium rapidly. Resin systems were also subjected to elution performance using three elution systems currently in commercial use.

The novel resins that displayed good aurothiosulfate uptake and elution characteristics were then employed in cycling and kinetic experimentation. Cycling experiments were designed to ascertain resin performance with repeated uptake/elution/regeneration cycles using the thiocyanate/ferric nitrate elution/regeneration system. Several resins performed very well, however a discrepancy was noted between the total amount of gold adsorbed by the resin and the total amount eluted. Upon digestion of a small sample of the cycled resin, the unaccounted aurothiosulfate was deemed to have been removed in the regeneration step.

Kinetic analysis was performed at three temperatures to ascertain the reaction order and if possible the rate constant of the reaction. Unfortunately, first- and second-order kinetic plots were shown to be non-linear, suggesting that the reaction order is either a non-integer

or higher than second-order. As such, the rate constant for the reaction was unable to be determined.

The enthalpy of the adsorption reaction was also able to be determined, with most resins exhibiting exothermic reaction enthalpies and therefore showing that uptake of the target aurothiosulfate species is thermodynamically preferred. The amount of energy released by the adsorption reaction was consistent with similar testing performed on commercial ion-exchange resins in the literature^{6, 7}.

6.2.2 Possible correlations between structural characteristics of resins and performance

A strong trend throughout all the data gathered in both testing regimes was the high ion-exchange selectivity coefficients shown by the imidazole-based resins.

As can be seen in the initial screening and further resin selection testing, imidazole-based resins showed the highest uptake of aurothiosulfate from the leach solutions of all the resins tested. However, due to the high ion-exchange selectivity of these resin functional groups for aurothiosulfate, elution of the gold complex from these resin systems was much more inefficient than that for the alkylamine-based resin functionalities.

6.2.3 Selection of optimal resin systems from uptake/elution/regeneration testing and kinetic experimentation

The criteria for the selection of the resins most likely to be adequate industrial performers in a synthetic leach are summarised below:

1. Rapid and large uptake of aurothiosulfate in synthetic leach solutions
2. Little or no susceptibility to elution of gold by trithionate ions
3. Maximum and efficient elution of the adsorbed aurothiosulfate by the chosen elution method

4. Minimum amount of aurothiosulfate retained by resin after elution/regeneration

As resins are required to have a large and rapid uptake of aurothiosulfate in leach solutions, tributylamine- and diethanolamine-based resins were deemed unsuitable for further study based upon very low ion-exchange capacities. This was unfortunate, as tributylamine-based resins have been shown to be gold cyanide-specific ².

As observed in Chapter 4, all resins tested show rapid uptake of aurothiosulfate from both synthetic leach solutions and from water. In synthetic leach solutions, despite the large concentrations of competing ions present, all resin systems were able to remove a large proportion of the aurothiosulfate in solution, relative to the ion-exchange capacity of the resin used.

Similarly, Chapter 4 also demonstrates that most resins show some susceptibility to trithionate when it was introduced into the leach system, however these results are based upon resins being left in a synthetic leach for over 12h. Experimentation in Chapter 4 has also shown that complete elution of the adsorbed aurothiosulfate was unable to be achieved. Based upon the results from Chapter 4 and the criteria listed above, the trimethylamine-based resin (TMA) was deemed unsuitable for further study, due to the unselective nature of the trimethylamine functional group. This was despite the large uptake and elution of aurothiosulfate by this functional group. Due to similarities in performance between piperidine-ethanol- (PET) and methyl-2-piperidine-methanol-functionalised resins (M2PM), the M2PM resin was deemed unsuitable for further study.

Chapter 5 has shown that despite high uptake and retention of aurothiosulfate, the imidazole-based resins retain the target analyte too strongly to allow easy elution of the adsorbed aurothiosulfate employing the elution regimes tested in this work. Hence, these resin systems are not suitable for industrial application. Thus, the viable resin systems as

Chapter 6 - Conclusions

indicated by Table 6-1 are the piperidine-ethanol-, methyl-piperidine-, N,N-dimethyl-piperazine- and methyl-diethylamine-based resin systems.

Table 6-1 Selection of industrially applicable resins

Resin	Abbreviation	Ion-exchange capacity	Capacity testing	Aurothiosulfate testing			Trithionate competition	Uptake/elution/regeneration testing
				Uptake from Water	Elution	Uptake from leach		
Trimethylamine	TMA	1.94	Passed	Passed	Passed	Rejected - unselective however still largest Au uptake/elution		
Triethylamine	TEA	0.75	Passed	Passed	Passed	Passed	Passed	Rejected - Strong Au retention between cycles
Tributylamine	TBA	0.08	Rejected - too low capacity					
Diethanolamine	DEM	WB	Rejected - too low capacity					
Diethylamine	DEA	WB	<i>Alkylated – formed MDM and 1PDM</i>					
2-Piperidine-methanol	2PM	WB	<i>Alkylated – formed M2PM</i>					
Piperidine-ethanol	PET	0.68	Passed	Passed	Passed	Passed	Passed	Passed
Piperidine	PIP	WB	<i>Alkylated – formed MIP</i>					
N-methyl-piperidine	NIP	0.39	Rejected - Similar to MIP					
Piperazine	PAZ	WB	<i>Alkylated – formed MAZ</i>					
N-methyl-piperazine	NAZ	1.05	Rejected - Similar to MAZ					
Quinuclidine	QNU	1.03	Passed	Passed	Passed	Passed	Passed	Rejected - Strong Au retention between cycles
Imidazole	IMZ	WB	Alkylated – formed MIM, EIM, 1PIM, 2PIM, BIM					
Methyl-imidazole	MIM	1.01	Passed	Passed	Passed	Passed	Passed	Rejected - Strong Au retention between cycles
Ethyl-imidazole	EIM	1.04	Passed	Passed	Passed	Passed	Passed	Rejected - Strong Au retention between cycles
1-propyl-imidazole	1PIM	1.06	Passed	Passed	Passed	Passed	Rejected - Similar to other imidazoles	
2-propyl-imidazole	2PIM	1.10	Passed	Passed	Passed	Passed	Rejected - Similar to other imidazoles	

Benzyl-imidazole	BIM	1.10	Passed	Passed	Passed	Passed	Passed	Rejected - Strong Au retention between cycles
Methyl-piperidine	MIP	0.73	Passed	Passed	Passed	Passed	Passed	Passed
N,N-dimethyl- piperazine	MAZ	1.52	Passed	Passed	Passed	Passed	Passed	Passed
Methyl- diethylamine	MDM	1.61	Passed	Passed	Passed	Passed	Passed	Passed
1-propyl- diethylamine	1PDM	1.47	Passed	Passed	Passed	Passed	Passed	Rejected - Strong Au retention between cycles
Methyl-2- piperidine- methanol	M2PM	0.56	Passed	Passed	Passed	Rejected - Similar to PET		

6.3 Possible further work and development

6.3.1 Optimisation of the synthetic method

One of the resins excluded from the study was the commercial MIEX-DOC trimethylamine-functionalised resin, due to unselective adsorption of the aurothiosulfate complex. This was despite good aurothiosulfate uptake and elution performance, due to the relatively high capacity of the resin in question. This is directly related to the size of the amine used in the functionalisation reaction. Further research is therefore required to refine and develop the functionalisation reaction and methodologies further, thus allowing the synthesis of the aurothiosulfate-selective functional groups selected in this study with capacities similar to the trimethylamine-based resins tested.

6.3.2 Resin strengthening and use in actual leach environments

The MIEX substrate has been optimised for the removal of dissolved organic carbon components from potable water. As such, it has not been optimised to perform in harsher and abrasive environments, such as those present in unclarified leach solutions containing up to 50% solids. The MIEXTM resin beads as supplied are resilient, however they do not tolerate shear forces well, fragmenting and powdering when these forces are applied. Furthermore, the mean bead size is around 260 micron and as such the resin beads are too small to use effectively in a leach environment⁸, despite excellent uptake and elution kinetics at this size. As such, resin beads would require an increase in size along with a degree of strengthening by increasing the amount of cross-linking present and to allow easier separation of the loaded beads from the pulp/leach and the required level of robustness in the leach-pulp environment.

6.3.3 Development and optimisation of elution/regeneration process

Due to incomplete elution profiles during resin cycling, further development and optimisation of the elution/regeneration process needs to be undertaken. From ion-

exchange principles, a simple method of accomplishing this would be to increase the concentration of sodium thiocyanate used as this would increase the interaction of the eluting ion with the resin functional groups, forcing more of the adsorbed aurothiosulfate into solution. A second method would be to use a combination elution method, initially with a low concentration of sodium nitrate followed by sodium thiocyanate. This would preferentially elute the copper compounds from the resin first and then produce a concentrated aurothiosulfate solution for further refining⁹. Literature has suggested that a combination of two or more eluting ions would give a greater elution recovery¹⁰⁻¹² and this process is also applicable in this case. This particular elution system utilises sulfite in combination with a separate eluting ion such as nitrate or chloride. The presence of sulfite in the elution stream prevents degradation of the aurothiosulfate complex and regenerates any trithionate or higher polythionates to thiosulfate. This elution scheme has been shown to be very effective in the elution of aurothiosulfate from Purolite A500/2788 macroporous strong-base ion-exchange resin. The sulfite/chloride elution system has been effectively applied to a complete gold recovery system utilising pressure oxidation, thiosulfate leaching, resin-in-pulp aurothiosulfate adsorption onto Purolite A500/2788 resin followed by sulfite/chloride elution and electrowinning of the gold credits produced¹³. Each of these alterations would need to be considered once the resin substrate optimisation had been completed.

6.3.4 Development of single solvent synthetic method

The current synthetic method for the production of the MIEX resin is to use water as the solvent for all stages of manufacture. This choice of solvent is essential for bead formation, but limits the range of amines that can be used to functionalise the resin beads for aurothiosulfate selectivity. This limitation is driven by those amines that can be protonated to form an ammonium salt and thus are somewhat water-soluble. Several of the amines

used in this work are only slightly soluble in water as the ammonium salt and thus this becomes a limiting factor in the amount of functionalisation that can be attached to the resin beads. Furthermore, most of the amine systems that showed good aurothiosulfate selectivity were those that required a second alkylation step. Due to the nature of the alkylation reagents, the resins required drying to remove any traces of water before this could take place. The use of a single organic solvent for functionalisation would allow a broader range of amines to be attached to the MIEX substrate and therefore would allow further scope for optimisation of the functional group for selective extraction of aurothiosulfate.

6.3.5 Integration of MIEX-Au resins into working RIP/RIL process

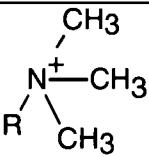
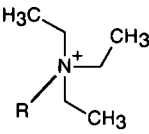
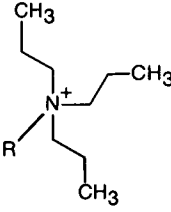
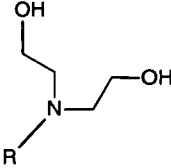
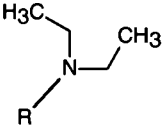
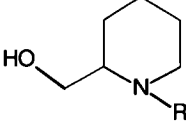
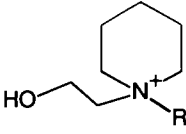
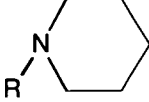
Once resin beads have been strengthened and the elution system optimised, the resin synthesis needs to be scaled up to suitable levels to generate quantities sufficient for industrial application and the resin system integrated into the flow sheet of a working gold plant. This will require scaling of the resin synthesis from the bench-top to pilot-scale amounts followed by tonnes-per-run levels of resin production. The use of a single solvent for resin manufacture will streamline this process, eliminating the need for resin drying prior to alkylation. Once resin manufacture has been optimised, the leaching regime for a particular gold-bearing ore needs to be analysed to ascertain whether it would be suitable for trial of the resin system as a viable solution concentration and recovery mechanism for gold. This would require attempting to leach gold from ore using ammoniacal thiosulfate followed by uptake of the formed aurothiosulfate complex by the ion-exchange resin. Elution and regeneration of the resin would then follow, producing a concentrated aurothiosulfate solution suitable for electrowinning or Merrill-Crowe precipitation of gold. This process would also recover thiosulfate, suitable for recycling into the leaching process.

6.4 References

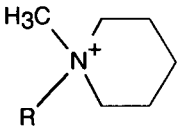
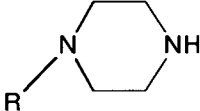
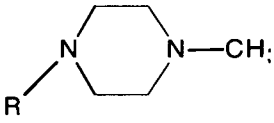
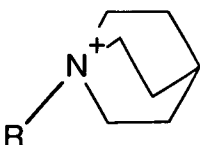
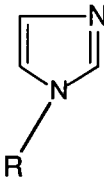
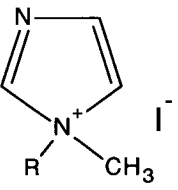
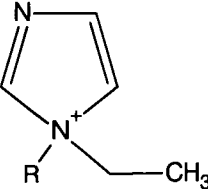
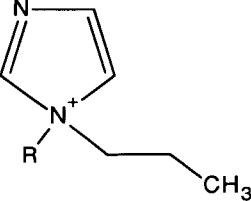
1. Grosse, A. C. The development of Resin Sorbents for Gold in Ammoniacal Thiosulfate Leach Liquors. PhD, University of Tasmania, Hobart 2006.
2. Dicoski, G. W., Novel Resins for the Selective Extraction of Gold from Copper Rich Ores. *S. Afr. J. Chem.* **2000**, 53, (1), 33-43.
3. Kotze, M. H.; Green, B. R.; Steinbach, G., Progress in the Development of the Minix Gold-selective Strong-base Resin. In *Hydrometallurgy: Fundamentals, Technology and Innovation.*, Hiskey, J. B.; Warren, J. W., Eds. Society for Mining, Metallurgy and Exploration: Littleton, Colorado, USA, 1993.
4. Riveros, P. A., Selectivity aspects of the extraction of gold from cyanide solutions with ion exchange resins. *Hydrometallurgy* **1993**, 33, (1-2), 43-58.
5. Warshawsky, A.; Kahana, N.; Kampel, V.; Rogachev, I.; Meinhardt, E.; Kautzmann, R.; Cortina, J. L.; Sampaio, C., Ion exchange resins for gold cyanide extraction containing a piperazine functionality. 1. Synthesis and physico-chemical properties. *Macromol. Mater. Eng.* **2000**, (283), 103-114.
6. Adams, M. D.; McDougall, G. J.; Hancock, R. D., Models for the absorption of aurocyanide onto activated carbon. Part II: Extraction of aurocyanide ion pairs by polymeric adsorbents. *Hydrometallurgy* **1987**, 18, (2), 139-54.
7. Adams, M. D.; McDougall, G. J.; Hancock, R. D., Models for the adsorption of aurocyanide onto activated carbon. Part III: Comparison between the extraction of aurocyanide by activated carbon, polymeric adsorbents and 1-pentanol. *Hydrometallurgy* **1987**, 19, (1), 95-115.
8. Marsden, J.; House, I., *The Chemistry of Gold Extraction*. Second Edition ed.; Society for Mining, Metallurgy and Exploration 2006; p 650.
9. Oliveira, A. M.; Leao, V. A.; da Silva, C. A., A proposed mechanism for nitrate and thiocyanate elution of strong-base ion exchange resins loaded with copper and gold cyano complexes. *Reactive & Functional Polymers* **2008**, 68, (1), 141-152.
10. Jeffrey, M. I. Recovery of metals from ion-exchange resins. International Patent 2007137325, 20070522., 2007.
11. Jeffrey, M. I.; Brunt, S., Loading and elution of gold thiosulfate from anion exchange resins. *Publications of the Australasian Institute of Mining and Metallurgy* **2007**, 9/2007, (World Gold 2007), 239-243.
12. Jeffrey, M. I.; Hewitt, D. M.; Dai, X.; Brunt, S. D., Ion exchange adsorption and elution for recovering gold thiosulfate from leach solutions. *Hydrometallurgy* **2010**, 100, (3-4), 136-143.
13. Jeffrey, M.; Heath, J.; Hewitt, D.; Brunt, S.; Dai, X. In *A thiosulfate process for recovering gold from refractory ores which encompasses pressure oxidation, leaching, resin adsorption, elution, and electrowinning*, Hydrometallurgy 2008: Proceedings of the 6th International Symposium, Phoenix, AZ, 2008; Phoenix, AZ, 2008; pp 791-800.

Appendix A Resin correlation table

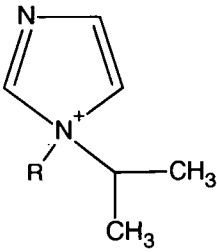
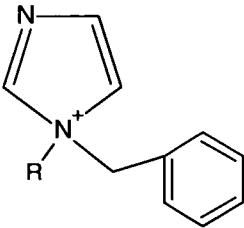
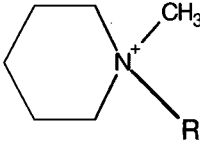
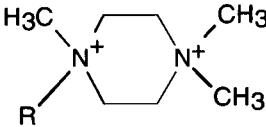
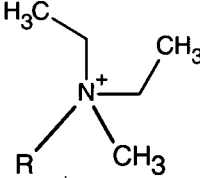
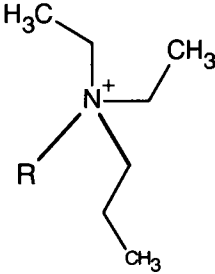
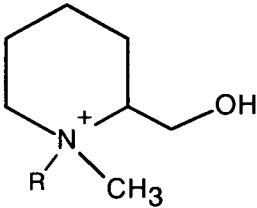
Table A-1 Resin abbreviation/structure correlation table

Resin	Abbreviation	Structure	Strong base ion-exchange capacity (meq/g)
Trimethylamine	TMA		1.939
Triethylamine	TEA		0.746
Tributylamine	TBA		0.0873
Diethanolamine	DEM		WB
Diethylamine	DEA		WB
2-Piperidine-methanol	2PM		WB
Piperidine-ethanol	PET		0.682
Piperidine	PIP		WB

Appendix A – Resin correlation table

N-methyl-piperidine	NIP		0.3889
Piperazine	PAZ		WB
N-methyl-piperazine	NAZ		1.052
Quinuclidine	QNU		1.0306
Imidazole	IMZ		WB
Methyl-imidazole	MIM		1.01
Ethyl-imidazole	EIM		1.036
1-propyl-imidazole	1PIM		1.0694

Appendix A – Resin correlation table

2-propyl-imidazole	2PIM		1.1014
Benzyl-imidazole	BIM		1.1004
Methyl-piperidine	MIP		0.7246
N,N-dimethyl-piperazine	MAZ		1.52
Methyl-diethylamine	MDM		1.6132
1-propyl-diethylamine	1PDM		1.469
Methyl-2-piperidine-methanol	M2PM		0.558

Appendix A – Resin correlation table

Where R is the resin stationary support and WB indicates that a strong-base ion-exchange capacity was not measured.

Appendix B Elution performances of all resins

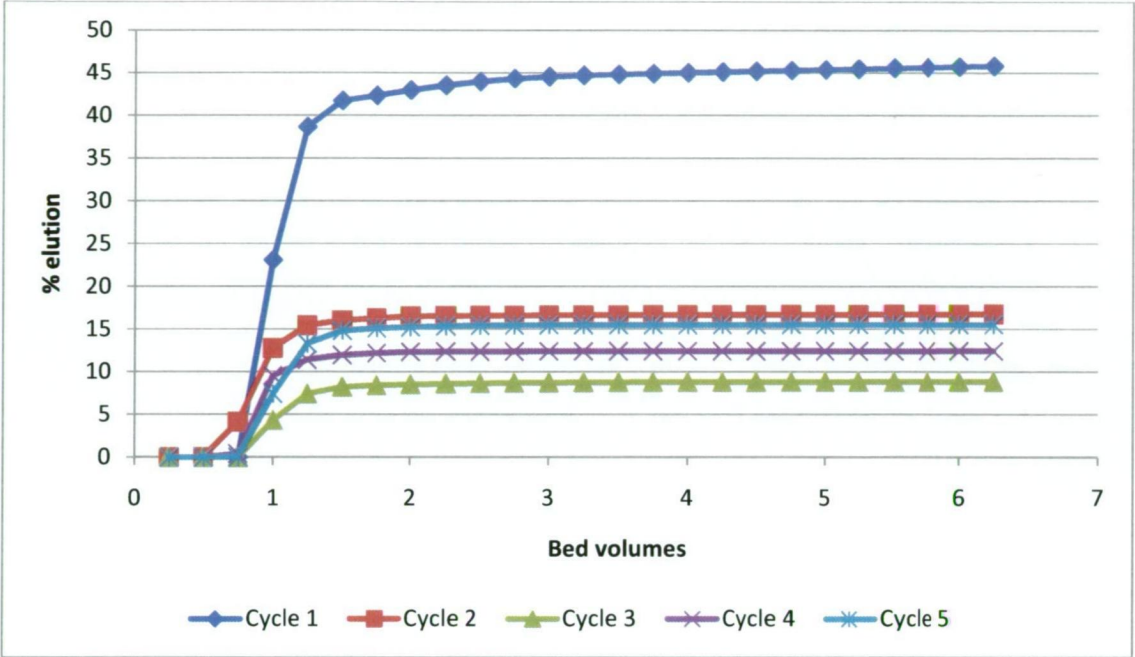


Figure B-1 PET Elution performance over 5 cycles

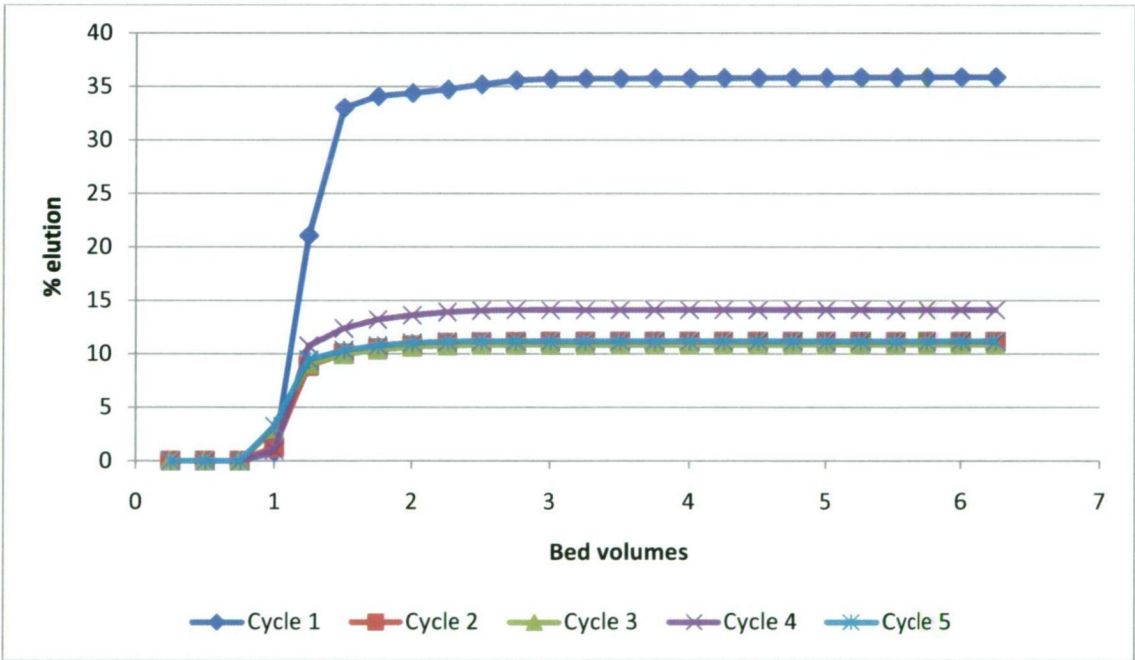


Figure B-2 BIM Elution performance over 5 cycles

Appendix B – Elution performances over 5 cycles

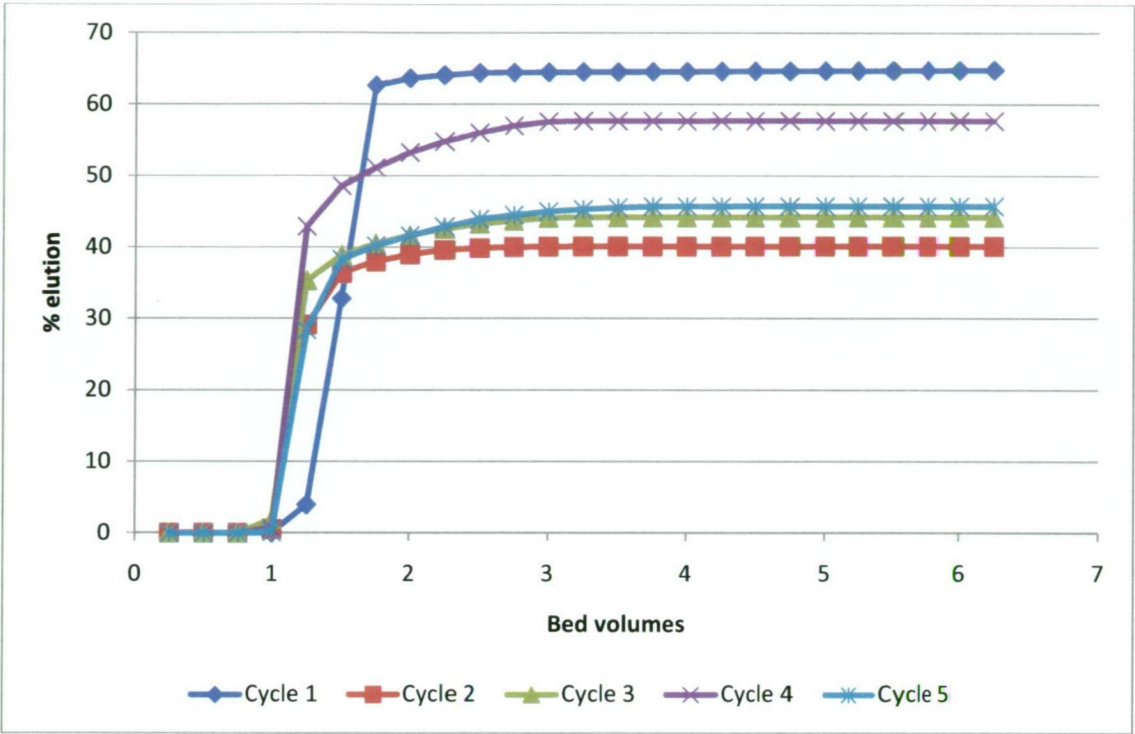


Figure B-3 EIM Elution performance over 5 cycles

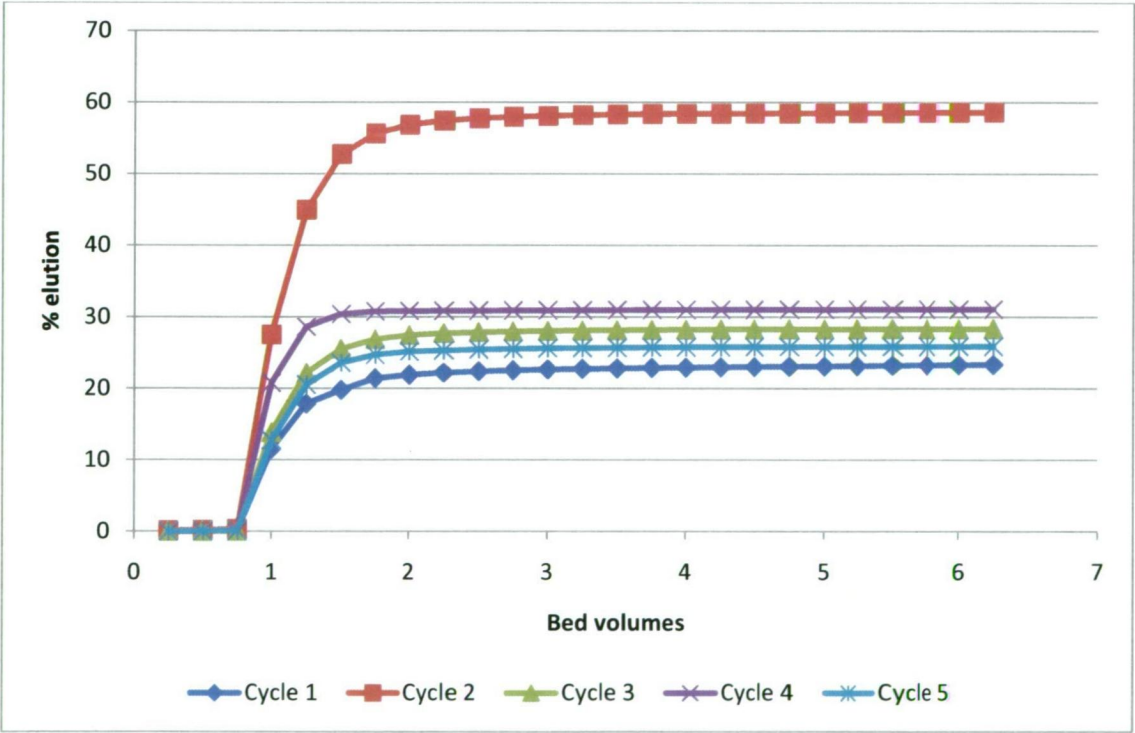


Figure B-4 TEA Elution performance over 5 cycles

Appendix B – Elution performances over 5 cycles

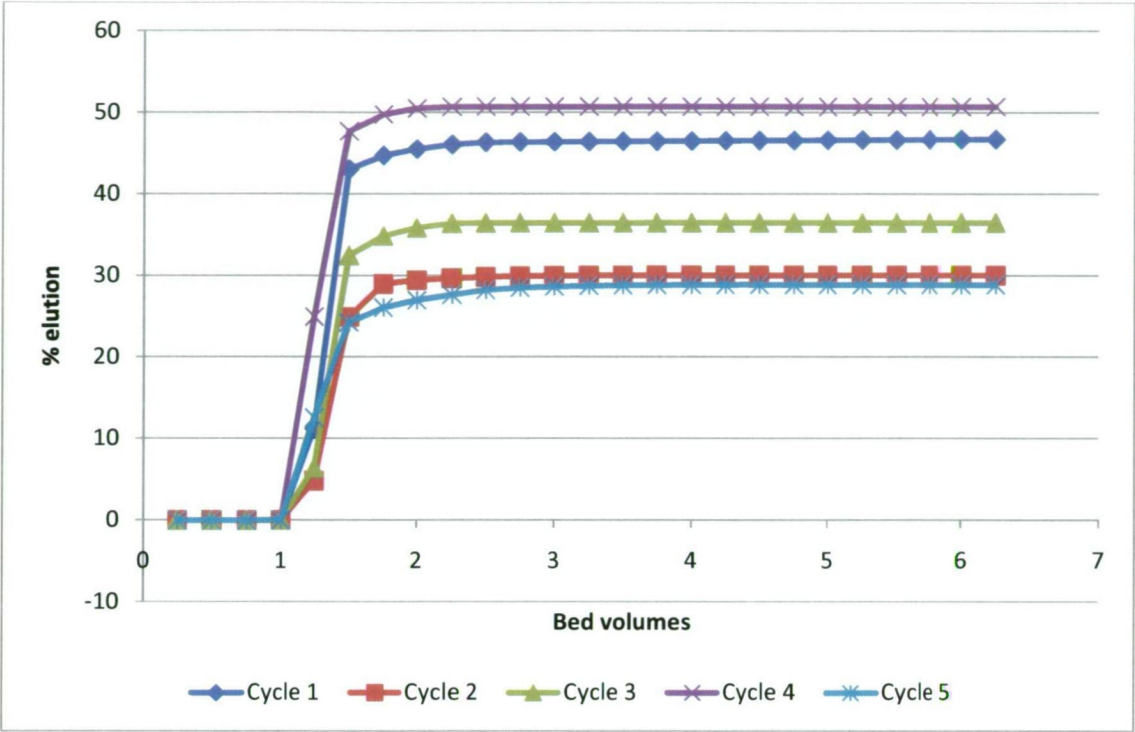


Figure B-5 MIM Elution performance over 5 cycles

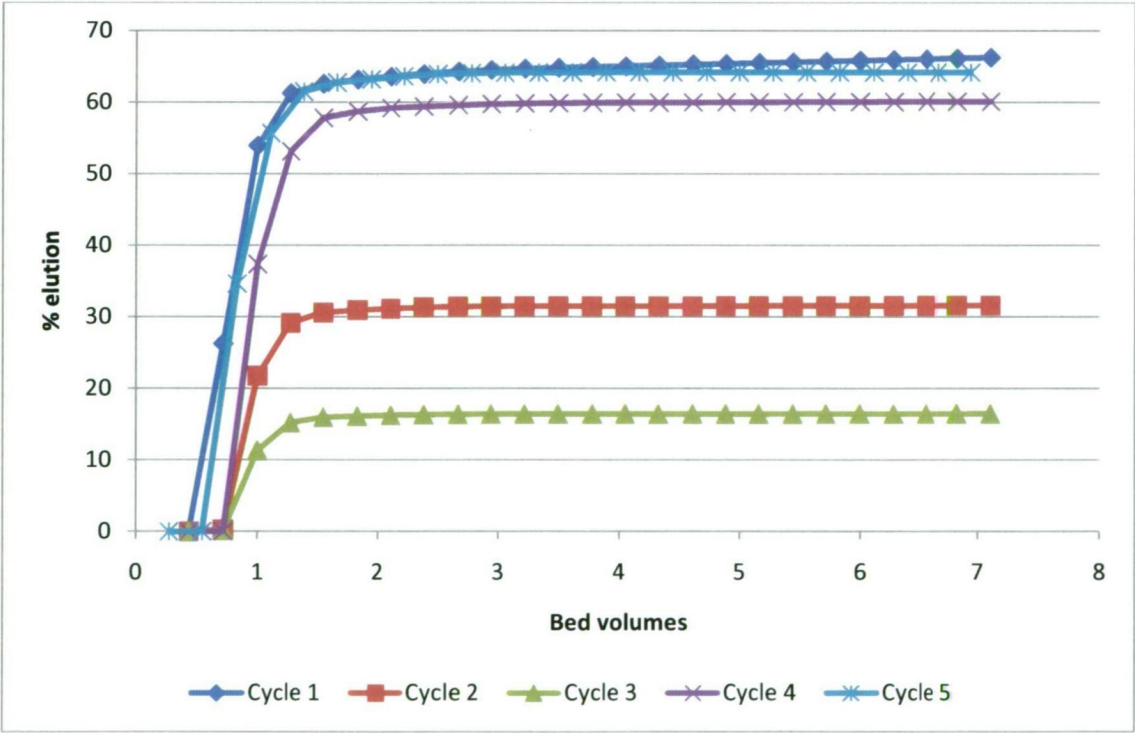


Figure B-6 QNU Elution performance over 5 cycles

Appendix B – Elution performances over 5 cycles

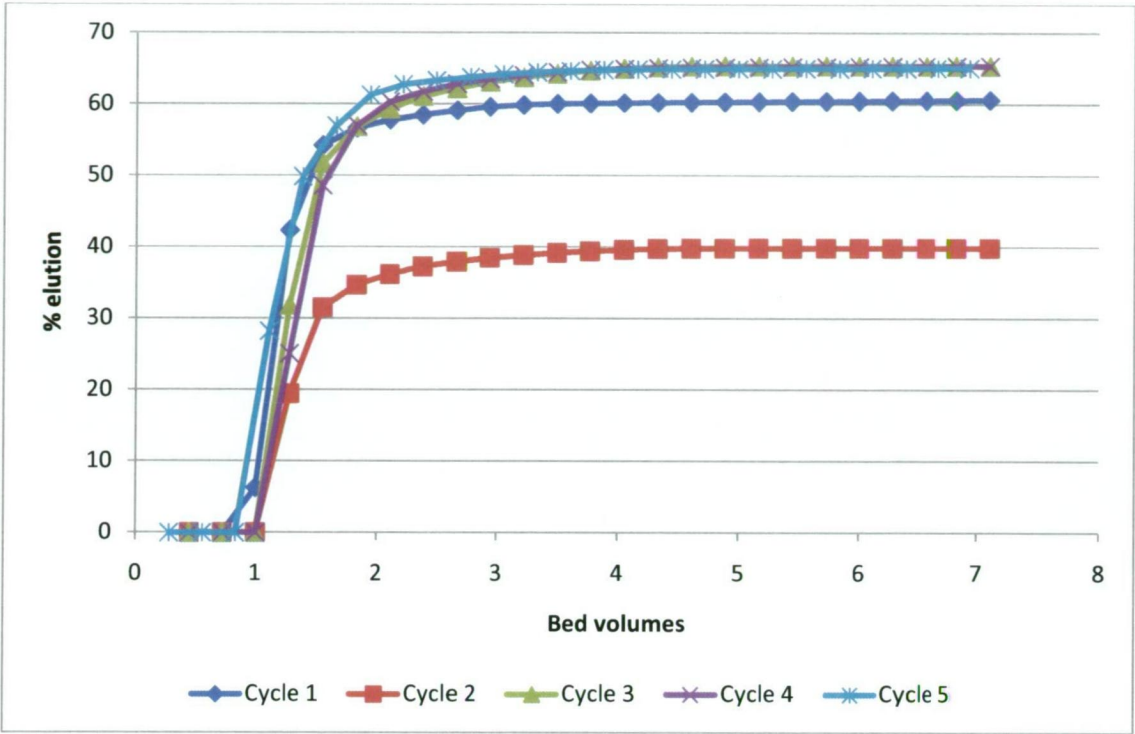


Figure B-7 1PDM Elution performance over 5 cycles

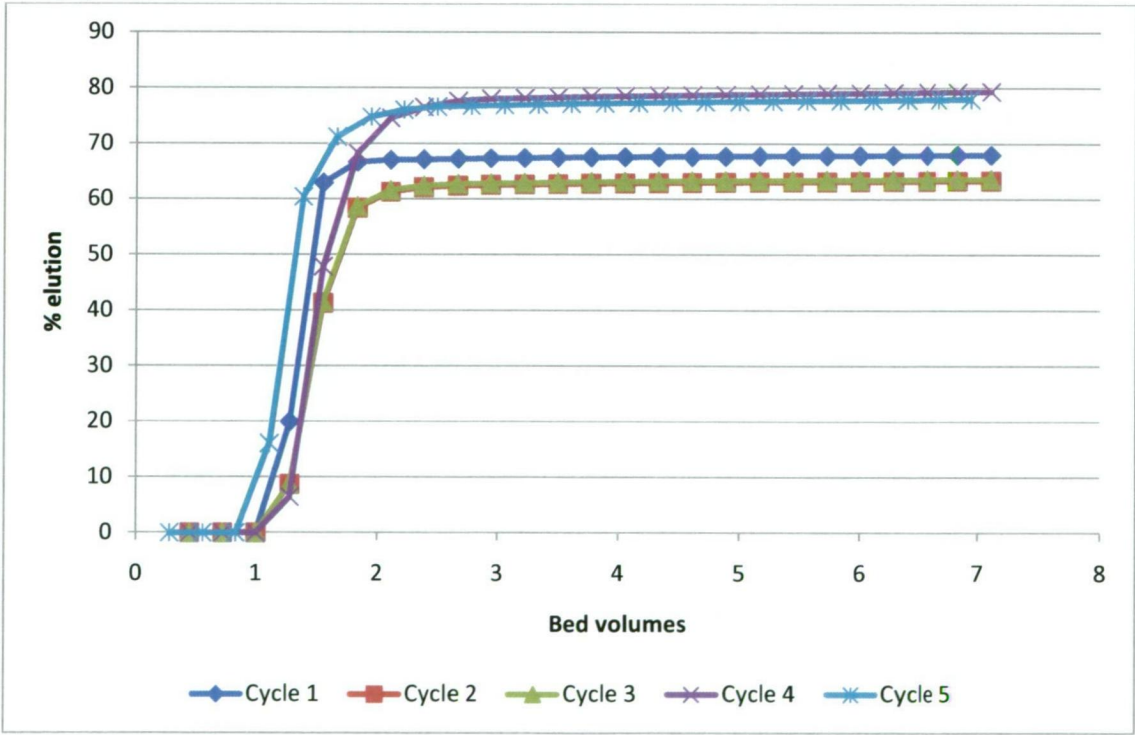


Figure B-8 MAZ Elution performance over 5 cycles

Appendix B – Elution performances over 5 cycles

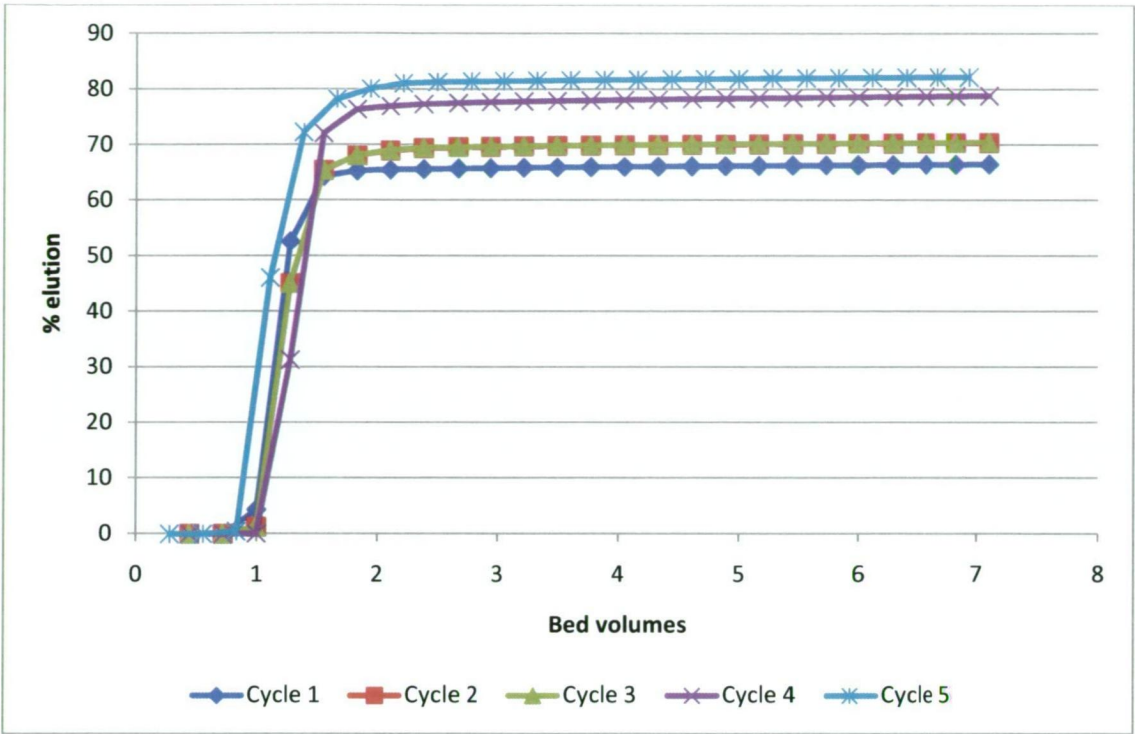


Figure B-9 MDM Elution performance over 5 cycles

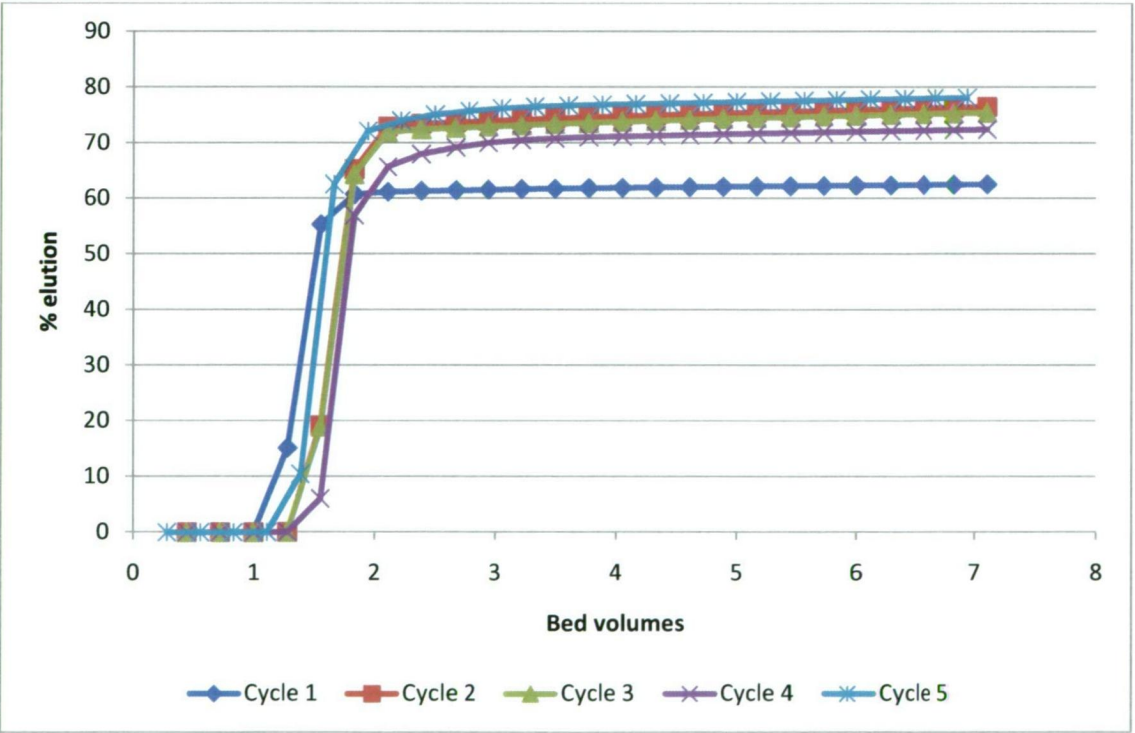
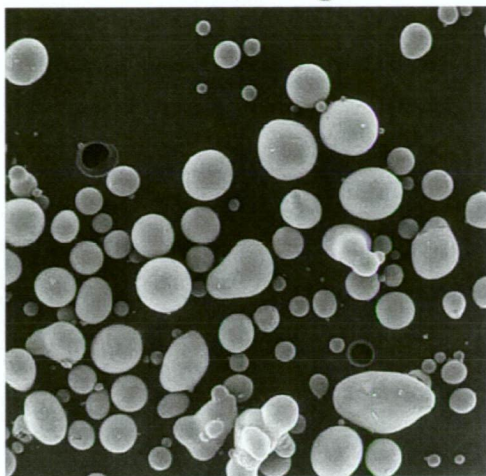


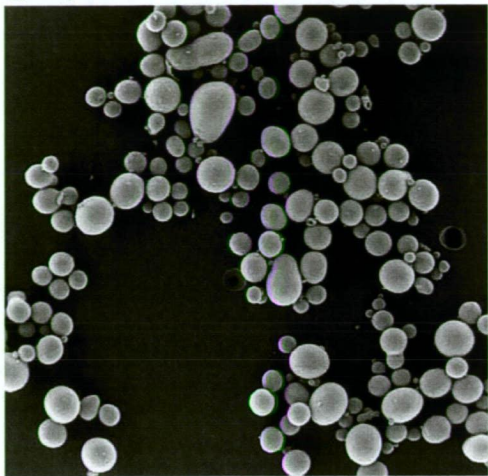
Figure B-10 MIP Elution performance over 5 cycles

Appendix C Scanning electron micrographs of resin beads



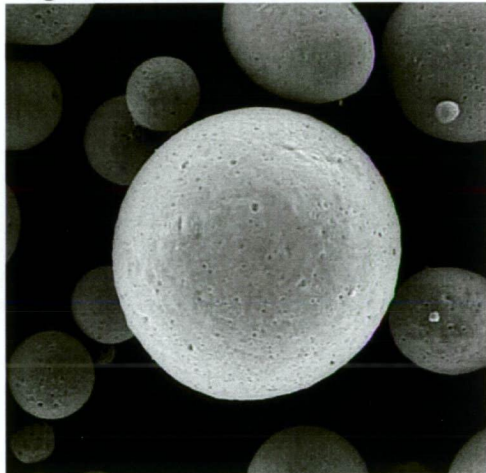
500 μm

Figure C-1 EIM overall view of resins



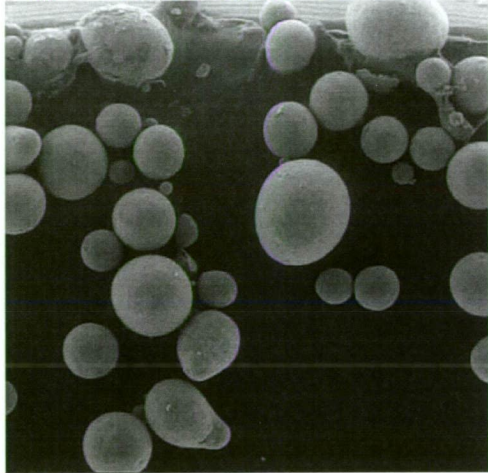
500 μm

Figure C-2 MIEX Drying 1 overall view



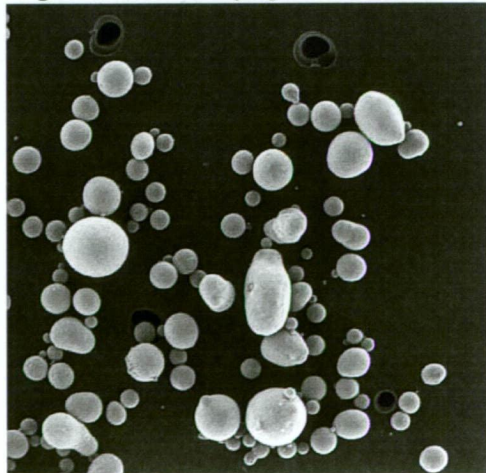
100 μm

Figure C-3 MIEX Drying 2 overall view



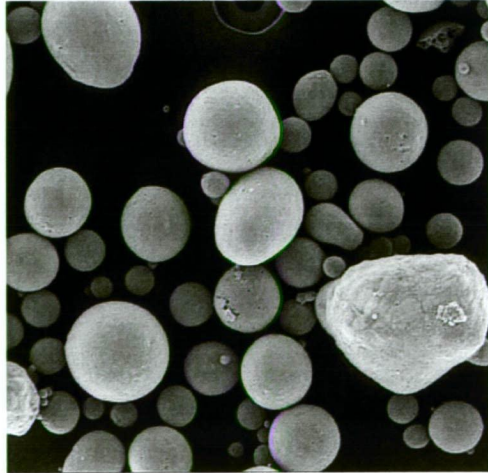
200 μm

Figure C-4 MIEX Drying 3 overall view



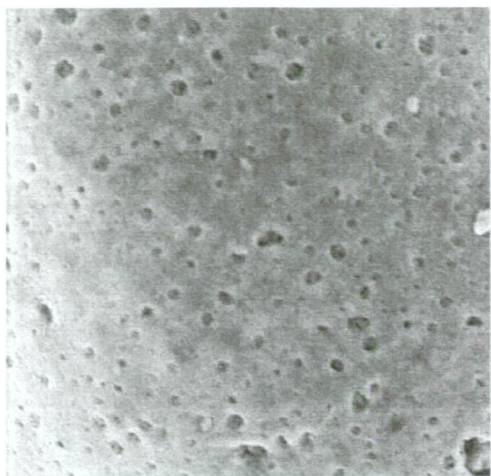
500 μm

Figure C-5 MIEX Drying 4 overall view



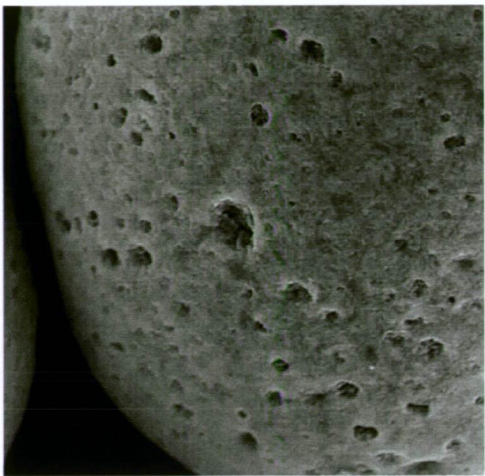
200 μm

Figure C-6 MIEX Drying 5 overall view



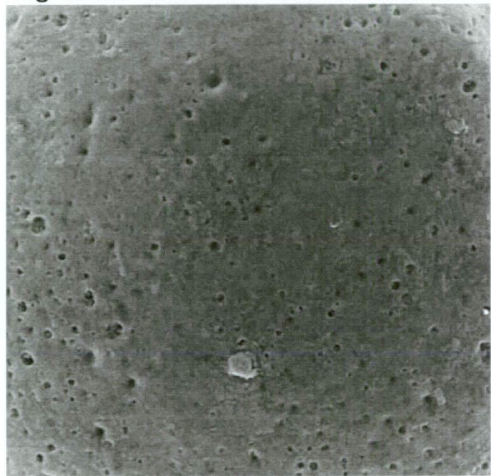
20 μm

Figure C-7 EIM detail of bead surface



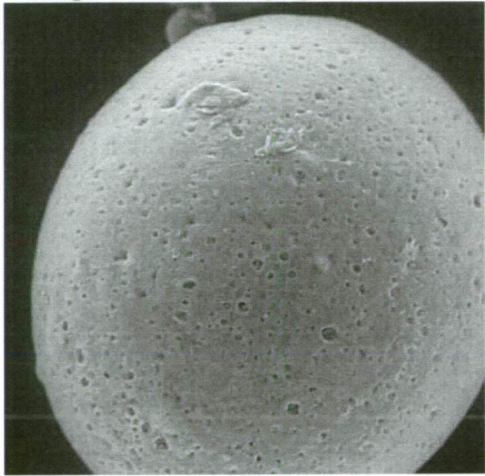
1 μm

Figure C-8 MIEX Drying 1 detail



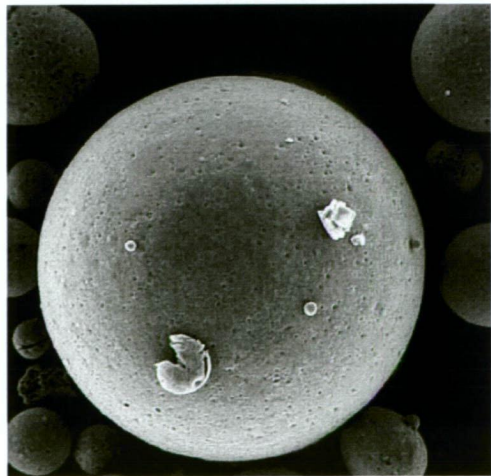
20 μm

Figure C-9 MIEX Drying 2 detail of bead surface



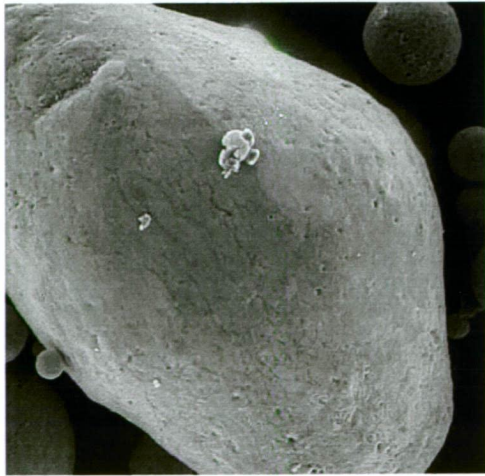
50 μm

Figure C-10 MIEX Drying 3 detail of bead surface



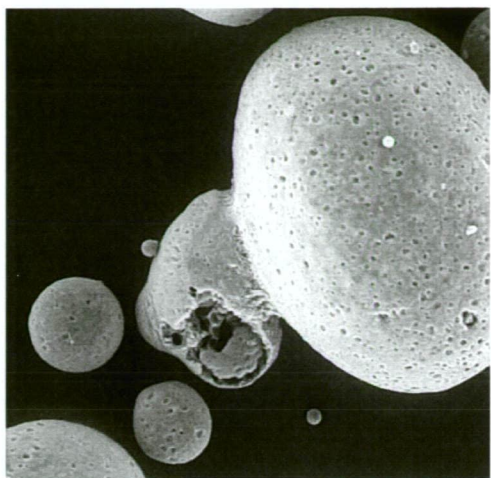
100 μm

Figure C-11 MIEX Drying 4 large bead



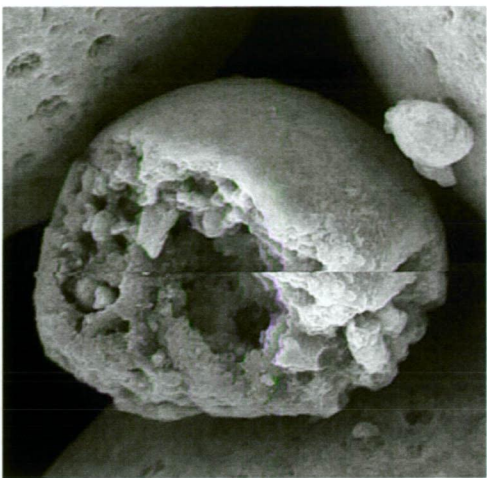
50 μm

Figure C-12 MIEX Drying 5 large bead



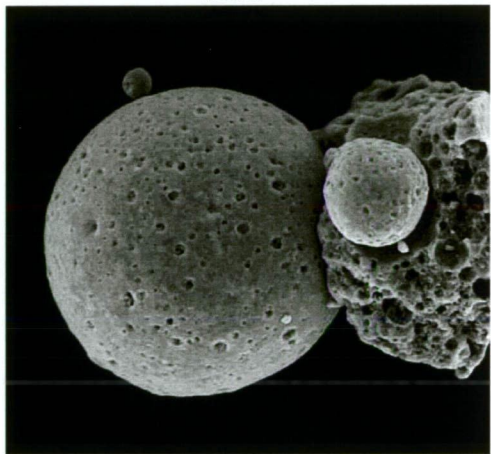
50 μ m

Figure C-13 EIM cracked conjoined bead



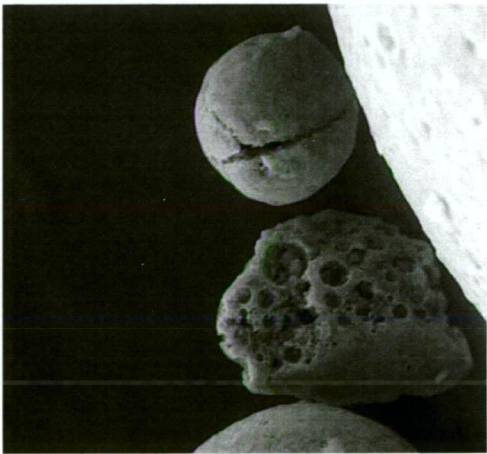
10 μ m

Figure C-14 MIEX Drying 1 cracked bead



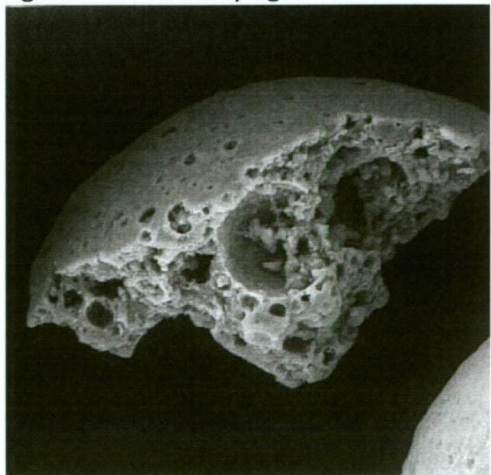
20 μ m

Figure C-15 MIEX Drying 3 cracked bead



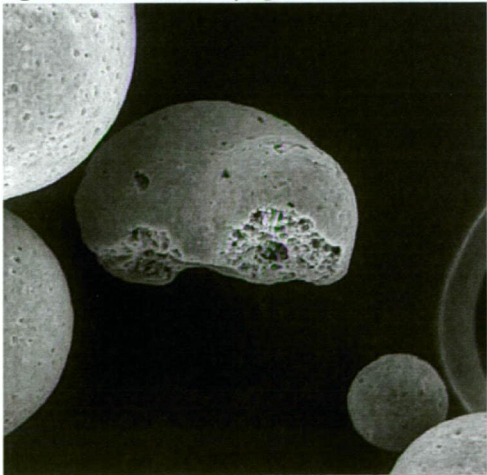
20 μ m

Figure C-16 MIEX Drying 4 cracked bead



20 μ m

Figure C-17 MIEX Drying 5 bead fragments



50 μ m

Figure C-18 MIEX Drying 5 bead fragments

Appendix C – Resin scanning electron micrographs

All scanning electron micrographs were prepared using an accelerating voltage of 15kV, an electron spot diameter of 3.0nm and at a pressure of 0.98 Torr.